The Role of Plasma Gelsolin in Epithelial Ovarian Cancer Chemoresistance

Meshach Asare-Werehene

This thesis is submitted as a partial fulfilment of the Ph.D. program
in Cellular and Molecular Medicine, Faculty of Medicine,
University of Ottawa, Ottawa, Canada

Cellular and Molecular Medicine
Faculty of Medicine
University of Ottawa

Abstract

Ovarian cancer (OVCA) is the most lethal gynecological cancer with a 5-year survival rate less than 50%. Despite new therapeutic strategies, such as targeted therapies and immune checkpoint blockers (ICBs), tumor recurrence and drug resistance remain key obstacles in achieving long term therapeutic success. Therefore, there is an urgent need to understand the cellular and molecular mechanisms of immune dysregulation in chemoresistant ovarian cancer in order to harness the host's immune system to improve cancer survival. Early diagnosis and residual disease are key determinants of favorable survival in OVCA; however, CA125 which is the conventional marker is not reliable and has modest diagnostic accuracy. There is therefore an urgent need to discover reliable biomarkers to optimize individualized treatment and diagnostic recommendations. Plasma gelsolin (pGSN; an actin binding protein) is the secreted isoform of the gelsolin (GSN) gene implicated in inflammatory disorders, colon cancer and prostate cancer. Increased expression of total GSN is associated with poor survival of patients with gynecological cancers. As to whether this is due to pGSN is yet to be investigated. Increased expression of pGSN is significantly associated with the down-regulation of immune cell markers; however, the exact mechanism has not been explored. If and how pGSN is involved in the cellular and molecular mechanisms of OVCA remains to be determined. In our current research, we have demonstrated that pGSN is involved in the regulation of immune cells, early diagnosis, tumor recurrence and chemoresistance in OVCA, using standard *in vitro* techniques and human clinical samples (North America, Asia and public datasets).

We have shown that pGSN is highly expressed and secreted in chemoresistant OVCA cells than their chemosensitive counterparts. pGSN, secreted and transported via exosomes, upregulated HIF1α–mediated pGSN expression in chemoresistant OVCA cells in an autocrine

manner as well as conferred cisplatin resistance in otherwise chemosensitive OVCA cells. pGSN also induced the OVCA expression of the antioxidant and tumor growth promoter, glutathione (GSH), by activating Nuclear factor erythroid 2-related factor 2 (NRF2), a response that attenuated cisplatin (CDDP)-induced apoptosis. In human tumor tissues, increased pGSN mRNA and protein expressions were significantly associated with advanced tumor stage, suboptimal residual disease, tumor recurrence, chemoresistance and poor survival regardless of patients' ethnic background and histologic subtypes. Increased Infiltration of CD8+ T cells was significantly associated with favorable patient survival; however, increased pGSN hindered the survival impact of these infiltrated CD8+ T cells. Further investigation revealed that pGSN induced CD8+ T cell death via caspase-3 activation, an action that resulted in decreased IFNγ levels. Increased epithelial pGSN expression was significantly associated with reduced survival benefits of infiltrated M1 macrophages, through caspase-3-dependent apoptosis as well as reduced production of TNFα and iNOS. The clinical application of circulatory pGSN as a biomarker for early detection and patients' survival was investigated. Pre-operative circulating pGSN presented as a favorable and independent biomarker for early disease detection and residual disease prediction compared with CA125. The test accuracy of pGSN was significantly enhanced when combined with CA125 in multianalyte index assay.

The findings suggest that pGSN is a potential target for chemoresistant OVCA and presents as a diagnostic marker for early stage disease and surgical outcomes, interventions that could maximize the therapeutic success of immunotherapies.

Table of Contents

Abstract ii
List of Figures vi
List of Tables ix
List of Supplementary Figures x
List of Supplementary Tables xii
List of Abbreviations xiv
Acknowledgment xxxi
CHAPTER 1 – INTRODUCTION 1
1.0 Ovarian Cancer 1
1.1 Epidemiology and etiology of ovarian cancer 1
1.2 Risk factors of ovarian cancer 4
1.2.1 High-risk genetic alterations in ovarian cancer 5
1.2.2 BRCA1/2 mutations 5
1.2.3 Mismatch repair genes 6
1.2.4 Homologous Recombination Deficiency (HRD)-Related Genes 9
1.3 EPITHELIAL OVARIAN CANCER (EOC) 9
1.3.1 High grade serous carcinomas (HGSC) 10
1.3.2 Low grade serous carcinomas (LGSC) 12
1.3.3 Endometrioid carcinomas (ECs) 13
1.3.4 Clear cell carcinomas (CCCs) 13
1.3.5 Mucinous carcinomas (MCs) 14
1.4 STAGES AND GRADES OF OVARIAN CANCER 15
1.4.1 Ovarian cancer staging 15
1.4.2 Ovarian cancer grading 16
1.5 OVARIAN CANCER SCREENING AND DIAGNOSIS 18
1.5.1 CA125 18
1.5.2 Transvaginal sonography (TVS) 19
1.5.3 Combining CA125 with TVS in ovarian cancer screening 19
1.6 TREATMENT STRATEGIES FOR OVARIAN CANCER 20
1.6.1 Surgical intervention 20
1.6.2 Frontline chemotherapy 21
1.6.2.1 Standard chemotherapy 21
1.6.2.2 Intraperitoneal chemotherapy 22
1.6.3 Targeted molecular therapy and chemotherapy 22
1.6.4 Immunotherapy of ovarian cancer 24
1.7 CHEMORESISTANCE IN OVARIAN CANCER 24
1.7.1 Mechanism of cisplatin action and chemoresistance 26
1.7.2 Multidrug resistance ‘pumps’ (MDRs) 29
1.7.3 Drug detoxification 30
1.7.4 DNA damage repair 31
1.7.5 Signalling cascades involved in ovarian cancer cell chemoresistance 32
1.7.5.1 The PI3K/Akt signalling and chemoresistance 32
1.7.5.2 p53 and chemoresistance 33
1.8 TUMOR MICROENVIRONMENT AND CHEMORESISTANCE 35

1.8.1 Tumour infiltrated lymphocytes (TILs) 38
1.8.2 Tumour-associated marcophages (TAMs) 38
1.9 CROSS-TALK MOLECULES IN THE TUMOUR MICROENVIRONMENT AND CHEMORESISTANCE 39
1.9.1 Characteristics of extracellular vesicles 40
1.9.2 Small extracellular vesicles (exosomes) 40
1.9.3 Large extracelluar vesicles (Microparticles) 41
1.9.4 Cancer cell-derived extracellular vesicles (EVs) and chemoresistance 41
1.10 GELSOLIN AND CHEMORESISTANCE 42
1.10.1 Gelsolin biology and function 42
1.10.2 Plasma gelsolin (pGSN) and chemoresistance 44
CHAPTER 2 – RATIONALE, HYPOTHESIS AND OBJECTIVES 46
2.0 Rationale and background 46
2.1 Overall objective 47
2.2 Overall hypothesis 48
2.3 Specific hypothesis 48
2.3 Specific objectives 48
CHAPTER 3 – ONCOGENE 39, 1600-1616 (2019) 50
CHAPTER 4 – CANCER RESEARCH 10.1158/0008-5472.CAN-20-0788 (2020) 104
CHAPTER 5 – MANUSCRIPT TO BE SUBMITTED 159
CHAPTER 6 – SCIENTIFIC REPORTS 9, 13924 (2019) 216
CHAPTER 7 – ADDITIONAL RESEARCH FINDINGS 246
7.0 Preview 246
7.1 Specificity of antibody used for assessment of pGSN expression in OVCA cells 246
7.2 Specificity of siRNA for pGSN knockdown in OVCA cells 248
7.3 pGSN-mediated induction of stem-like features in OVCA cells 250
7.4 Exosomal pGSN is present in human plasma and urine 252
CHAPTER 8 – DISCUSSION 256
8.0 Overview and significance 256
8.1 Experimental significance for using isogenic paired cancer cell lines 260
8.2 Experimental significance of the use of clinical samples 261
8.3 Antioxidant regulation in ovarian cancer chemoresistance 261
8.4 Clinical relevance of tissue pGSN expression and OVCA chemoresistance 262
8.5 Immuno-regulatory role of pGSN in the ovarian tumour microenvironment 263
8.6 Early diagnosis and residual disease in ovarian cancer 266
CHAPTER 9 – FUTURE RESEARCH DIRECTIONS 267
CHAPTER 10 – CONCLUSION 281
CHAPTER 11 – REFERENCES 283

List of Figures

Figure 1.1 Schematic diagram of obstacles to epithelial ovarian cancer treatment success....2

Figure 1.2 Schematic diagram of histologic subtypes of epithelial ovarian cancer (EOC)….7

Figure 1.3 Schematic diagram of contributing factors of epithelial ovarian cancer chemoresistance ……25

Figure 1.4 Chemical structure of platinum ……27

Figure 1.5 Schematic diagram of multifactorial roles of the tumour microenvironment on epithelial ovarian cancer chemoresistance ……...36

Figure 1.6 Schematic diagram of cancer immuno-editing ……37

Figure 1.7 Schematic diagram of the structure of gelsolin ……43

Figure 3.1 High pGSN expression is associated with tumor recurrence in patients with ovarian cancer ……..62

Figure 3.2 pGSN regulates CDDP-induced apoptosis in OVCA cells ……..67

Figure 3.3 Extracellular vesicle characterization and CDDP effect on vesicle size distribution……73

Figure 3.4 The integrin signaling pathway is involved in the autocrine up-regulation of pGSN content by pGSN ……..78

Figure 3.5 pGSN-mediated OVCA chemoresistance involves HIF1α modulation by Akt ……..80

Figure 3.6 Chemoresistant cells-derived exosomes enhance HIF1α binding to pGSN promoter region and induces CDDP resistance in chemosensitive OVCA cells ……..84

Figure 3.7 Hypothetical models illustrating the autocrine and paracrine mechanisms of Ex-pGSN in OVCA chemoresistance ……...94

Figure 4.1 pGSN expression and CD8+ T cell infiltration in normal fallopian tube and HGS OVCA tissues ……121

Figure 4.2 Increased pGSN expression is associated with reduced survival impact of tumor infiltrated CD8+ T cells ……128

Figure 4.3 sEV-pGSN induces CD8+ T cell death via FLIP down-regulation and caspase-3 activation ……137

Figure 4.4 Increased pGSN expression promotes NRF2-dependent GSH production ……141

Figure 4.5 IFNγ-mediated suppression of GSH production is via STAT1 phosphorylation ……147

Figure 4.6 A Hypothetical model illustrating the expression and role of pGSN in the regulation of chemoresistance in OVCA ……...155

Figure 5.1 Increased epithelial pGSN expression is associated with suppressed survival benefits of infiltrated M1 macrophages in OVCA patients ……...185

Figure 5.2 Chemoresistance is associated with increased epithelial pGSN expression and M2 infiltration ……..187

Figure 5.3 Chemoresistant cells-derived sEV attenuates the anti-tumor function of M1 macrophages by increased caspase-3-dependent apoptosis and decreased secretion of iNOS and TNFα ……201

Figure 5.4 pGSN is directly involved with M1 macrophages apoptosis and anti-tumor suppression ……203

Figure 5.5 pGSN is directly involved with M1 macrophages apoptosis and anti-tumor suppression ……212

Figure 6.1 Ovarian cancer patients with high residual disease (RD) have significantly high levels of circulating pGSN ……223

Figure 6.2 Receiving operating characteristic (ROC) curves for pGSN and CA-125 in detection of residual disease (RD) in ovarian cancer patients ……...227

Figure 6.3 Circulating pGSN is highly detected in ovarian cancer patients with stage 1 disease ……231

Figure 6.4 Receiving operating characteristic (ROC) curves for pGSN, CA125 and ISO1 index in the detection of stage 1 disease in ovarian cancer patients ……..233

Figure 6.5 Hypothetical models illustrating how pre-treatment levels of pGSN could predict stage 1 ovarian cancer and residual disease (RD) ……241

Figure 7.1 pGSN antibody (ABIN1019662) specifically targets the N-terminal region of pGSN but not cGSN ……..247

Figure 7.2 pGSN siRNA 1 and 2 specifically target pGSN without affecting cGSN …...249

Figure 7.3 pGSN-mediated OVCA chemoresistance induces stem-like features ……251

Figure 7.4 pGSN and β-actin levels are detectable in the urine …….254

Figure 7.5 Exosomal pGSN is detectable in the plasma of HGS ovarian cancer patients ……...255

Figure 8.1 Schematic diagram of the role of pGSN in epithelial OVCA chemoresistance ……...259

Figure 9.1 pGSN up-regulation in murine ID8 cells attenuated CDDP-induced apoptosis ……..270

Figure 9.2 pGSN mRNA expression is inversely correlated with miR-200a expression ……..273

Figure 9.3 Schematic diagram of therapeutic targeting nanoformulation with GSN sub-fragment ……..279

List of Tables

Table 1.1 Risk factors for EOCs …….....3

Table 1.2 Genetic alterations in epithelial ovarian cancer …….….8

Table 1.3 Stages of epithelial ovarian cancer ……...17

Table 5.1 Univariate Cox regression analysis for PFS and OS ……..194

Table 5.2 Multivariate Cox regression analysis for PFS and OS ……...195

List of Supplementary Figures

Figure 3.S1 CDDP decreases pGSN content in the chemosensitive cells but not their resistant counterparts ……..….69

Figure 3.S2 Higher levels of pGSN are secreted than retained in OVCA cells *in vitro*……..70

Figure 3.S3 GSN knock-down sensitizes chemoresistant cells to CDDP-induced apoptosis ……71

Figure 3.S4 pGSN is detectable in both chemosensitive and chemoresistant OVCA cell lines and could be successfully knocked-down (KD) in exosomes from chemoresistant cells ……75

Figure 3.S5 Chemoresistant cells-derived exosomes induce CDDP resistance to pGSN-KD-chemosensitive OVCA cells ……87

Figure 4.S1 pGSN expression was validated in HGS OVCA cell pellets, tissues and normal fallopian tube tissues ……123

Figure 4.S2 pGSN mRNA is barely expressed in CD8+ T cells ……..130

Figure 4.S3 pGSN knock down and over-expression in sEVs ……136

Figure 4.S4 pGSN induces CD8+ T cell death whereas sEV-pGSN polarizes naïve CD4+ T cells towards type 2 helper cells ……139

Figure 4.S5 pGSN positively correlate with NRF2-dependent genes ……..143

Figure 4.S6 pGSN expression negatively correlates with CD8+ T cell anti-tumor factors ……...……146

Figure 5.S1 pGSN expression and infiltrated TAMs in OVCA tissues ……...……178

Figure 5.S2 Epithelial pGSN expression, M1/M2 density and survival in OVCA histologic subtypes ……...180

Figure 5.S3 Higher infiltration of M1 but not M2 macrophages is associated with improved survival ……191

Figure 5.S4 Epithelial pGSN expression is significantly correlated with M1/M2 macrophage ratio ……..192

Figure 5.S5 M1 macrophage differentiation and polarization ……199

Figure 5.S6 pGSN knockdown and overexpression confirmation in sEVs and rhpGSN-induced apoptosis in M1 macrophages ……205

Figure 5.S7 Epithelial pGSN expression increases with increased tumor stage and suboptimal residual disease ……210

List of Supplementary Tables

Supplementary Table 3.1 Target sequences for 200696_s_at probe and GSN transcript variant 1; mRNA (Isoform a; pGSN) sequence ……58

Supplementary Table 3.2 Target sequences for 214040_s_at probe and GSN transcript variant 4; mRNA (Isoform f) sequence ……60

Supplementary Table 3.3 Information on OVCA cell lines ……..64

Supplementary Table 3.4 Antibodies used in the present studies ……..…….100

Supplementary Table 3.5 Customized siRNA oligonucleotide duplexes ……101

Supplementary Table 3.6 Primer sequences for amplifying the gelsolin promoter ……102

Supplementary Table 4.1 Epithelial expressions of markers in OVCA patients ……111

Supplementary Table 4.2 Information on antibodies and reagents ……117

Supplementary Table 4.3 Information on OVCA cell lines ……119

Supplementary Table 4.4 Epithelial expressions of markers in OVCA patients ……125

Supplementary Table 4.5 Univariate Cox regression analysis for progression-free and overall survival ……...132

Supplementary Table 4.6 Multivariate Cox regression analysis for progression-free and overall survival ……...133

Supplementary Table 5.1 Patient demographics ……167

Supplementary Table 5.2 Information on antibodies and Reagents ……162

Supplementary Table 5.3 Information on OVCA cell lines ……169

Supplementary Table 5.4 pGSN expression and TAMs infiltration in OVCA tissue compartments ……179

Supplementary Table 6.1 Characteristics of patients ……222

Supplementary Table 6.2 Correlation between plasma pGSN and CA-125 levels and ovarian cancer residual disease and stage ……..225

Supplementary Table 6.3 The sensitivities and specificities of OVCA plasma biomarkers ……...228

Supplementary Table 6.4 Univariate Cox regression analysis for disease-free and overall survival ……..234

Supplementary Table 6.5 Multivariate Cox regression analysis for disease-free and overall survival ……..235

List of Abbreviations

ABC	ATP binding cassette family
ABCB1	ATP Binding Cassette Subfamily B Member 1
ABCC1	ATP Binding Cassette Subfamily C Member 1
ABCG2	ATP Binding Cassette Subfamily G Member 2
AIF	Apoptosis inducing factor
α5β1	Alpha-5 beta-1
Akt	aka Protein Kinase B, PKB
A-Akt	Activated Akt
ALDH1	Aldehyde Dehydrogenase 1 Family Member
ALG-2	Apoptosis-linked-gene 2
Alix2	ALG-2-Interacting Protein X 2
Apaf-1	Apoptotic protease activating factor-1
APC	Antigen presenting cells
APE1	Apurinic/apyrimidinic endonuclease 1
ARF	Alternate open reading frame
ARID1A	AT-rich interactive domain-containing protein 1A
ATM	Ataxia telangiectasia mutated
ATR	Ataxia telangiectasia mutated and Rad3-Related

ATRIP	ATR interacting protein
ATP	Adenosine triphosphate
ATP7A	ATPase Copper Transporting Alpha
ATP7B	ATPase Copper Transporting Beta
AUC	Area under curve
bAb	Blocking antibody
BAD	Bcl-2 antagonist of cell death
BaK	Bcl-2 antagonist killer
Bax	Bcl-2-associated X protein
Bcl-2	B-cell lymphoma-2
Bcl-xL	B-cell lymphoma-extra large
BER	Base excision repair
BH3	Bcl-2 homology domain 3
Bid	BH3-interacting domain death agonist
Bim	Bcl-2 interacting mediator of cell death
BRAF	B-raf murine sarcoma viral oncogene homolog
BRCA	Breast cancer susceptibility gene
BRIP1	BRCA1-interacting protein 1

BSO	Buthionine sulfoximine
CA125	Cancer antigen 125
CA-153	Cancer antigen 153
CCC	Clear cell carcinoma
CCK-8	Cell Counting Kit-8
CCL22	C-C Motif Chemokine Ligand 22
CCNE	Cyclin E
CDDP	Cis-diamminedichloroplatinum (II) or cisplatin
CDK1	Cyclin dependent kinase 1
CDKN2A	Cyclin dependent kinase inhibitor 2A
cDNA	Complementary deoxyribonucleic acid
CDX	Caudal-type homeobox
cGSN	Cytoplasmic gelsolin
Chk1	Checkpoint kinase 1
CHEK2	Checkpoint kinase 2
CI	Confidence Interval
CK	Cytokeratin
CL	Chloride ion

CKI	Cyclin-dependent kinase inhibitor
CM	Conditioned media
CREB	cAMP-response element binding protein
CRISPR	Clustered regularly interspaced short palindromic repeats
CRK	CRK Proto-Oncogene, Adaptor Protein
CTLA4	Cytotoxic T-lymphocyte associated protein 4
Ctr1	Copper transporter homolog 1
CTNNB1	Catenin (cadherin-associated protein) beta 1
Cyt c	Cytochrome complex
DAPI	4′,6-diamidino-2-phenylindole
DC	Dendritic cell
DDR	DNA damage response
DFS	Disease free survival
DIABLO	Direct IAP binding protein with low pI
DMEM	Dulbecco's modified Eagle Medium
DMSO	Dimethyl sulfoxide
DNA	Deoxyribonucleic acid
DN-Akt	Dominant negative Akt

DR4	Death Receptor 4
DR5	Death Receptor 5
2-DG	2-Deoxy-D-Glucose
EC	Endometrioid carcinoma
EM	Epithelial-mesenchymal
EOC	Epithelial ovarian carcinoma
Epcam	Epithelial cellular adhesion molecule
ER	Endoplasmic reticulum
ERBB2	Erythroblastic oncogene B2
ERCC1	Excision repair cross-complementing rodent repair deficiency, complementation group 1
ERK	Extracellular-signal-regulated kinase
ESCRT	Endosomal sorting complexes required for transport
Ex	Exosome
Ex/Em	Excitation/Emission
Ex-pGSN	Exosomal pGSN
FADD	Fas-associated protein with death domain
FAK	Focal adhesion kinase
Fas L	Fas ligand

FBS	Fetal bovine serum
FDA	Food and drug authority
FIGO	International Federation of Gynecology and Obstetrics
FITC	Fluorescein isothiocyanate
FLICE	Fas-associated death domain-like interleukin 1 β-converting enzyme
FLIP	FLICE-like inhibitory protein
FOXO	Forkhead Box O
FoxP3	Forkhead Box P3
GAPDH	Glyceraldehyde phosphate dehydrogenase
GB	Grade borderline
GCML	Glutamate-Cysteine Ligase Modifier Subunit
GFP	Green fluorescent protein
GSH	Glutathione
GSN	Gelsolin
GSK3β	Glycogen Synthase Kinase 3 Beta
GST	Glutathione S-transferase
GX	Grade of tumor cannot be assessed
G1	Grade 1

G2	Grade 2
G3	Grade 3
G4	Grade 4
GZMB	Granzyme B
γH2AX	Phosphorylated H2AX
H2AX	H2A histone family member X
HE4	Human epididymis protein 4
HGS	High grade serous
HGSC	High grade serous carcinoma
HIF1	Hypoxia inducible factor
HKII	Hexokinase II
HLA-DR	Human leukocyte antigen – DR isotype
HNF-1β	Hepatocyte nuclear factor 1-beta
HR	Hazard Ratio
HR	Homologous recombination
HRD	Homologous recombinant deficiency
HRP	Horseradish peroxidase
Hsp	Heat shock protein

HtrA2/Omi	Human high temperature requirement protein A2
IDS	Interval debulking surgery
iEM	Immuno-gold electron microscopy
IF	Immunofluorescence
IFNα	Interferon alpha
IFNGR1	Interferon gamma receptor 1
IgG	Immunoglobulin G
IHC	Immunohistochemistry
IL	Interleukin
ILK	Integrin-linked kinase
iNOS	Inducible nitric oxide synthase
IRB	Institutional Review Board
IRS	Immunoreactive score
IP	Intraperitoneal
ISO1	Indicator of stage 1
i.v	Intravenous
JAK	Janus tyrosine kinase
Jnk	c-Jun N-terminal kinase

LEVs	Large extracellular vesicles
LPA	Lipoprotein A
LPS	Lipopolysaccharide
KD	Knock down
kDa	Kilodalton
KRT	Keratin
KRAS	Kirsten rat sarcoma viral oncogene homolog
LGALS4	Lectin galactoside-binding soluble 4
LGS	Low grade serous
LGSC	Low grade serous carcinoma
M1/M2	M1 macrophage to M2 macrophage ratio
MAPK	Mitogen-activated protein kinase
MAPKAPK2	MAPK Activated Protein Kinase 2
MC	Mucinous carcinoma
MDM2	Mouse double minute 2 homolog
MDMX	a.k.a MDM4 (Mouse double minute 4 homolog)
MDR	Multi drug resistance
MDSCs	Myeloid-derived suppressor cells

MECOM	MDS1 and EVI1 complex locus
MEK	Mitogen-activated protein kinase kinase
MFI	Mean fluorescent intensity
MHCII	Major Histocompatibility Complex class II
MiR-34a	MicroRNA 34a
MLH1	Human mutL homolog 1
MLH3	Human mutL homolog 3
MMR	Mismatch repair
MPs	Microparticles
Mre11	Meiotic recombination 11
MRP	Multi drug resistance protein
mRNA	Messenger ribonucleic Acid
MSH2	MutS homolog 2
MSH6	MutS homolog 6
MSI	Microsatellite instability
mTOR	Mammalian target of rapamycin complex
MUC2	Mucin 2
MUC3	Mucin 3

MUC16	Mucin 16
MUC17	Mucin 17
MVB	Multivesicular bodies
MVs	Microvesicles
MYC	Myelocytomatosis oncogene
NAC	N-Acetyl-L-Cysteine
NAV3	Neuron Navigator 3
NBS1	Nijmegen breakage syndrome 1
NER	Nucleotide excision repair
NF1	Neurofibromin 1
NFE2L2	Nuclear factor erythroid 2 like 2
NF- κB	Nuclear factor kappa B
NH_2	Amino group
NHEJ	Non-homologous end joining
NK	Natural killer
NLS	Nuclear localization signal
NOXA	A.k.a Phorbol-12-myristate-13-acetate-induced protein 1 (PMAIP1)
NPV	Negative predictive value

NRF2	Nuclear factor erythroid 2-related factor 2
NTA	Nanoparticle tracking analyser
OD	Optical density
OPA1	Optic atrophy 1
OS	Overall Survival
OSE	Ovarian surface epithelium
OVA1	OVA1 Biomarkers: CA-125 II, Apoliproprotein A1 (Apo A-1), Beta-2 Microglobulin (B2M), Transferrin, and Prealbumin
OVCA	Ovarian cancer
OVERA	OVERA Biomarkers: Apolipoprotein A1 (Apo A-1), HE4 (Human Epididymis protein 4), CA-125 II, FSH (Follicle Stimulating Hormone), and Transferrin
OX	Overexpression
P-Akt	Phosphorylated Akt
PALB2	Partner and localizer of BRCA2
PARP	Poly (adenosine diphosphate) polymerase
PAX8	Paired box gene 8
PBS	Phosphate buffered saline
PD1	Programmed cell death protein 1
PDL1	Programmed death-ligand 1

PDK1	Pyruvate dehydrogenase kinase 1
PDS	Primary debulking surgery
PFI	Progression free Interval
PFS	Progression free Survival
PGE2	Prostaglandin E2
pGSN	Plasma gelsolin
PI3K	Phosphoinositide-3 kinase
PIK3CA	Phosphatidylinositol-4, 5-bisphosphate 3-kinase catalytic subunit alpha
PIP2	Phosphatidylinositol-4, 5-bisphosphate
PIP3	Phosphatidylinositol-3, 4, 5-trisphosphate
PKA	Protein kinase A
PKB	Protein kinase B
PKBβ	Protein kinase B beta
PMA	Phosphomolybdic acid
PMS2	Postmeiotic segregation increased 2
PMSF	Phenylmethylsulfonyl fluoride
PPP2R1A	Protein phosphatase 2 scaffold subunit A alpha
PPV	Positive predictive value

PPM1D	Protein Phosphatase, Mg2+/Mn2+ Dependent 1D
PRF1	Perforin 1
pSTAT1	Phosphorylated STAT1
PTEN	Phosphatase and tensin homolog
PUMA	p53-upregulated mediator of apoptosis
RAD50	Radiation repair gene 50
RAD51C	Radiation repair gene 51 paralog C
RAD51D	Radiation repair gene 51 paralog D
RAF	Rapidly Accelerated Fibrosarcoma
RAS	Rat sarcoma
RB1	retinoblastoma 1
RD	Residual disease
RNF43	Ring finger protein 43
ROC	Receiving operating curve
ROI	Region of interest
ROMA	Risk of ovarian malignancy algorithm
ROS	Reactive oxygen species
RPMI	Roswell Park Memorial Institute

RR	Response rate
SBT	Serous borderline tumor
SD	Standard deviation
SDS	Sodium dodecyl sulfate
SEM	Standard error of the mean
Ser	Serine
SEVs	Small extracellular vesicles
SHIP	Src homology 2 (SH2) domain containing inositol polyphosphate 5-phosphatase
siRNA	small interfering RNA
SLC7A11	Solute carrier family 7 member 11
Smac	Second mitochondria derived activator of caspases
SMARCA4	SWI/SNF related matrix associated actin dependent regulator of chromatin subfamily A member 4
SMAD4	Mothers against decapentaplegic homolog 4
SOX2	SRY-Box Transcription Factor 2
SPP1	Secreted phosphoprotein 1
STAT1	Signal transducer and activator of transcription 1
STAT3	Signal transducer and activator of transcription 3
STIC	Serous tubal intraepithelial carcinoma

TAM	Tumor-associated macrophage
TBS	Tris-buffered saline
TC	Taxotere and Cyclophosphamide
TCGA	The Cancer Genome Atlas
TGFβ	Transforming growth factor beta
Thr	Threonine
TFPI2	Tissue factor pathway inhibitor 2
TIL	Tumor infiltrating lymphocytes
TKI	Tyrosine kinase inhibitor
TMA	Tissue microarray
TME	Tumor microenvironment
TNF	Tumor necrosis factor
TP53	Tumor protein p53
TSG101	Tumor susceptibility gene 101
TTBS	Tris-Tween Buffered Saline
TVS	Transvaginal ultrasound
UT	Untranslated region
VDAC	Voltage-dependent anion channel

VEGF	Vascular endothelial growth factor
VEGFR	Vascular endothelial growth factor receptor
WB	Western blotting
Wt	Wild type
xCT	Cystine/glutamate transporter
XIAP	X-linked inhibitor of apoptosis protein
ZNF217	Zinc finger protein 217

Acknowledgment

To God be the glory for His abundant grace upon my life. I am highly indebted to God for granting me the strength and endurance through my doctoral studies.

My sincere gratitude goes to my research mentor, Professor Benjamin K. Tsang for his enormous support, intellectual guidance and advice which enabled me to complete my doctoral studies. His love and passion for science is exceptional, an attribute that encouraged me to strive for the best. He was there for me when I was emotionally drained and was always ready to talk over coffee. I also appreciate his financial generosity and career guidance. Professor Tsang was not just a mentor to me, but a father on a foreign land who took risk and gave me the opportunity to be in his lab. I am forever grateful.

I would like to appreciate my committee members: Dr. Dylan Burger, Dr. Rebecca Auer and Dr. Chantal Matar for their intellectual and scientific guidance. I would not have made it this far without your support. My appreciation once again goes to Dr. Dylan Burger for his collaboration on extracellular vesicles.

A special thank you to all my collaborators both locally and internationally especially Dr. Anne-Marie Mes-Masson for providing me clinical samples for my studies as well as granting me the opportunity to undertake research training in her lab at Centre de recherche du CHUM et Institut du cancer de Montréal. Also, I am grateful to Dr. Yoshio Yoshida and his team for granting me the opportunity to visit and work in their laboratory at University of Fukui as well as provide me with clinical samples for my studies. Dr. Tien Le was also generous with his clinical knowledge and expertise which significantly helped me in my clinical sample investigations. I am very grateful. I also appreciate the collaborations of Drs. Yong Sang Song and Dar-Bin Shieh as well as their scientific contributions to my training.

Many thanks to all past and present members of Dr. Tsang lab, for their emotional support and intellectual stimulations during lab meetings. This has gone a long way to shape me into a competitive researcher.

A big thank you to the funding agencies that made my studies possible: the Canadian Institute of Health Research (CIHR; MOP-126144), Destination 2020 Faculty of Medicine Scholarship, OHRI matching fund, Ovarian Cancer Canada (OCC), Mitacs Globalink Research Award, International Doctoral Student Scholarships, CUPE, financial aid bursaries and BMO Financial Group Bursaries.

I bless God for my wonderful and sweet wife, Dr. Afrakoma Afriyie-Asante, who motivated, prayed and supported me throughout my doctoral studies. Her love and prayers were the fuel that drove me through my doctoral studies. A special thank you to my parents and siblings for their continuous support and love. Although you are far away, your frequent calls, prayers and concerns encouraged me to sail through my training. God richly bless you.

And to Terri Van Gulik, I am grateful for all the administrative support you provided for me in the course of my training. It enabled me focus primarily on my training without bothering about paper-work. To Mrs. Janet Tsang, your wonderful Christmas gifts will be cherished forever. God bless you for your beautiful and kind heart.

CHAPTER 1 – INTRODUCTION

1 Ovarian Cancer

1.1 Epidemiology and etiology of ovarian cancer

Ovarian cancer (OVCA) comprises of tumours that originate from the ovaries, endometium and fallopian tubes. It is estimated that over 200,000 women worldwide are diagnosed with OVCA yearly, of which 152,000 die from the disease[1]. In the United States of America, 22,000 new cases were diagnosed in 2016 with 14,240 cases of death[1,2]. In Canada, 3,000 new cases were diagnosed with 1,900 recorded deaths[3]. Despite advances in diagnosis and treatment in the last 30 years, the 5-year survival rate of OVCA patients in the US and Canada is considerably lower (45 - 47%) compared with that of breast cancer (85%)[3,4]. OVCA, based on their origin are categorized into epithelial, sex-cord stromal, germ cell and non-specific mesenchymal tumours. Epithelial tumours are the most commonly diagnosed OVCA which account for nearly 85-95% of all cases[5-7]. These tumours are derived from surface epithelial tissues. The nonepithelial tumours account for approximately 5% of all OVCA and are derived from germ cells and sex cord-stromal cells differentiating from the interstitium[5]. 3-5% of all OVCA are made up of germ cell tumours which originate from germ cells or extraembryonic tissues[5]. Interestingly, the histology of OVCA is dependent on age factor[5]. For example, women aged 20 years or below stand a higher risk of malignant germ cell tumours whereas malignant epithelial tumours are mostly found in women 50 years and above.

OVCA prevalence increases with increase in age with the median age ranging from 55 – 64 years[1-3,5]. The incidence rate of OVCA per 100,000 persons is higher in whites and non-Hispanics compared with Asians and Blacks[1,5]. This phenomenon is same for the mortality rate although Asians have the lowest compared with other races or ethnic groups[1,5].

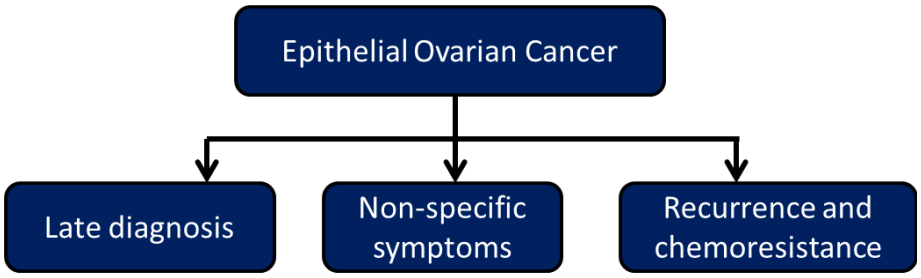

Fig. 1.1 Schematic diagram of obstacles to epithelial ovarian cancer treatment success. Over two (2) decades now, the 5-year survival rate of ovarian cancer patients is still less than 50%. This is primarily due to late diagnosis, non-specific symptoms, recurrence and chemoresistance.

Table 1.1 Risk factors for EOCs

Increased	Decreased	Indeterminate
Hereditary •Family history of ovarian cancer •Personal history of breast cancer •Alteration in BRCA1/2 •Lynch syndrome	**Reproductive** •Multiparity •Breastfeeding	Fertility drugs
Reproductive • Advanced age • Nulligravida • Infertility	**Hormonal** •Oral contraceptives •Progestrins	Exercise
Hormonal •Early age at menarche •Late age at natural menopause •Hormone replacement therapy •Estrogen •Androgens	**Surgery** •Hysterectomy •Tubal ligation	Cigarette smoking
Inflammatory •Perineal talc exposure •Endometriosis •Pelvic inflammatory disease		
Lifestyle •Obesity		
Geography •Extremes in latitude		

Cited and modified from Hidetaka Katabuchi, *Frontiers in Ovarian Cancer Science*, 2017, Springer.

In approximately 60% of all cases, the cancer would have metastasized to other organ sites[1,5]. In 15% of all patients, the cancer is confined to the ovary or primary site although in 19% and 6% of all cases, the cancer would have spread to regional lymph nodes or remains unstaged (not enough information to indicate a stage) respectively[1,5]. This is as a result of non-specific symptoms presented by the disease which are difficult to detect at an early stage hence, most cancer metastasize by the time patients are diagnosed[8,9] **(Fig. 1.1)**. Symptoms may present as unexplained fatigue, increased abdominal size and pain, eating disorders, bowel inconsistencies as well as urinary disorders[9]. The five year survival rate for patients with localized, regional, distant and unstaged diseases are 92.1%, 73.1%, 28.8% and 24.2% respectively[1,5]. Thus, the more localized the tumour, the more likely the survival of the patient will be prolonged.

1.2 Risk factors of ovarian cancer

The risk factors for OVCA are multi-factorial. These include genetic, biological and environmental factors[10] **(Table 1.1)**. These factors could have a decreased, increased or intermediary effect on the development of OVCA. Factors that increase the risk of tumour development include hereditary [breast cancer susceptibility gene (BRCA) 1/2 mutation, history of breast cancer, familial OVCA], hormonal (Increased levels of estrogen and androgen, early age at menarche, hormonal replacement therapy, late age at menarche), lifestyle (increased cholesterol intake, obesity), inflammatory (endometriosis and pelvic inflammatory disease), reproductive (advanced age and infertility), geographic locations (extremes in latitude) and increased exposure to carcinogens (talc and asbestos)[10,11]. Hysterectomy, breastfeeding, multiparity, intake of oral contraceptives and tubal ligations contribute to the reduction of OVCA

risk[10,11]. Intake of fertility drugs and cigarette smoking moderately affect the risk of OVCA development[10,11].

1.2.1 High-risk genetic alterations in ovarian cancer

A family history of the disease presents as a strong risk to developing OVCA, suggesting the presence of a hereditary components[12,13]. In all OVCA cases reported, genetic inheritance accounts for approximately 20%[12-14]. Although more than 20 tumour suppressor and oncogenes are implicated in hereditary OVCA, mutations of the BRCA1/2 genes account for 65 – 75% of all cases[14,15].

1.2.2 BRCA1/2 mutations

BRCA1 and 2 genes are tumour suppressor genes located on chromosomes 17 and 13 respectively and are involved in the repair of double-stranded DNA damages and the regulation of cell cycle checkpoints[16,17]. There are mutations that are specific to various ethnic populations. 187delAG and 5385insC mutations in BRCA1 and 617delT mutations in BRCA2 are predominantly found in the Ashkenazi Jewish population whereas the L63X and Q934X mutations in BRCA1 are mostly found in the Japanese population. Women who inherit a BRCA1 mutation (72%) and BRCA2 mutation (69%) will develop breast cancer by the age of 80. By contrast, it is 44% of women who inherit a BRCA1 mutation and about 17% of women who inherit a BRCA2 mutation will develop ovarian cancer by the age of 80 [18-20].

BRCA1/2 mutations in OVCA are mostly associated with high grade serous carcinoma, although other histologic subtypes such as clear cell and endometrioid carcinomas have been reported to have BRCA1/2 related mutations[21-24]. In rare cases, the mucinous

histologic subtypes might also contain BRCA1/2 mutations[22,23]. However, borderline epithelial and non-epithelial OVCAs are not significantly associated with BRCA1/2 mutations[24]. OVCA patients with higher BRCA1/2 mutational loads [BRCA1, HR = 0.78 (95% CI, 0.68 – 0.89), P < 0.001 and BRCA2, HR = 0.61 (95% CI, 0.50-0.76), P < 0.001] have prolonged survival compared with BRCA1/2 mutation-negative patients with BRCA2 mutations, having the best survival impact[25]. The prolonged survival impact of BRCA mutation carriers is as a result of increased sensitivity to platinum-based cytotoxic chemotherapy compared with non-carrier patients[26]. This is due to the inability of tumours with BRCA mutations to repair double-stranded DNA breaks caused by platinum-based cytotoxic drugs; a process that is fully functional in the non-carrier patients[27-29]. The homologous recombination repair deficiency makes BRCA1 mutation carriers more sensitive to poly (ADP-ribose) polymerase (PARP) inhibitors and other DNA-damaging chemotherapeutic agents[26,29].

1.2.3 Mismatch repair genes

Other than BRCA1/2 mutations, germline mutations of mismatch repair genes [Lynch syndrome; human mutL homolog (MLH) 1, MLH3, mutS homolog (MSH) 2, MSH6 and postmeiotic segregation increased (PMS2)] are also involved in hereditary OVCA[30]. Lynch syndrome increases the risk of OVCA by 24% and accounts for approximately 10-15% of all hereditary OVCA[31,32]. Mutation of the mismatch repair (MMR) genes results in the formation of microsatellite instability (MSI) which could be accumulated in both oncogenes and tumour suppressor genes, a condition that drives ovarian tumorigenesis[33]. Lynch syndrome are mostly associated with endometrioid and clear cell carcinoma with better prognosis since most tumors are diagnosed with low grade and at an early stage[34].

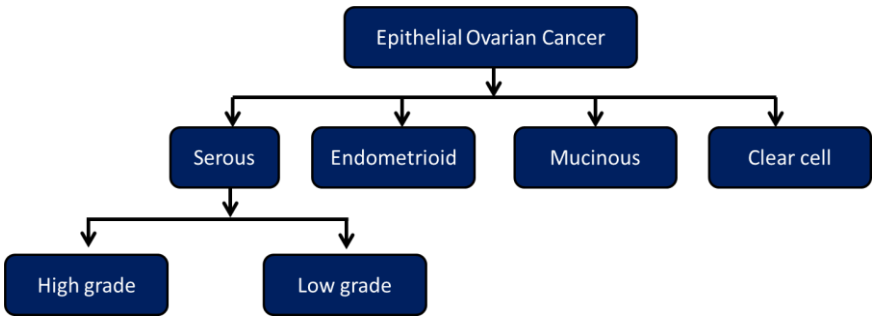

Fig. 1.2 Histologic subtypes of epithelial ovarian cancer (EOC). EOCs are categorized based on their histologic subtypes. There are serous (low grade and high grade), endometrioid, mucinous and clear cell histologic subtypes of EOCs.

Table 1.2 Genetic alterations in epithelial ovarian cancer

	Gene mutation	Copy number amplification	Copy number loss	OVCA Type	Histologic representation
High-grade serous (HGS)	*TP53*, *BRCA1/2*	*CCNE1*, *MYC*, *MECOM*	*PTEN*, *RB1*, *NF1*	Type II	Solid growth with slit-like spaces, abnormal cell nuclei and hyper-proliferation of the cells.
Clear cell carcinoma (CCC)	*ARID1A*, *PIK3CA*	*MYC*, *ZNF217*, *ERBB2*, *STAT3*, *HNF1B*, *PPM1D*	*SMARCA4*, *RB1*, *SMAD4*	Type I	Hyaline bodies, densely hyaline basement membrane and multiple complex papillae.
Endometrioid carcinoma (EC)	*CTNNB1*, *PIK3CA*, *KRAS*, *PTEN*			Low grade - Type I High grade - Type II	Glandular formations
Mucinous carcinoma (MC)	*KRAS*, *TP53*, *BRAF*, *RNF43*, *CDKN2A*	*ERBB2*		Type I	Atypia, stratification, papillae, loss of glandular architecture, necrosis. Loss of mucin staining in the cytoplasm.
Low-grade serous (LGS)	*KRAS*, *BRAF*		*CDKN2A/2B*, miR-34a	Type I	Low mitotic activity, papillary structures and relatively uniform and small nuclei in the tumor cells.

TP53; Tumour protein p53, *CCNE1*; Cyclin E1, *MYC*; Myelocytomatosis oncogene, *MECOM*; MDS1 and EVI1 complex locus, *RB1*; Retinoblastoma 1, *NF1*; Neurofibromin 1, *ARID1A*; AT-rich interactive domain-containing protein 1A, *ZNF217*; Zinc finger protein 217, *STAT3*; Signal transducer and activator of transcription 3, *HNF1B*; Hepatocyte nuclear factor 1-beta, *PPM1D*; Protein Phosphatase Mg2+/Mn2+ Dependent 1D, *SMARCA4*; SWI/SNF related matrix associated actin dependent regulator of chromatin subfamily A member 4, *SMAD4*; Mothers against decapentaplegic homolog 4, *RNF43*; Ring finger protein 43, *CDKN2A/2B*; Cyclin dependent kinase inhibitor 2A/2B

1.2.4 Homologous recombination deficiency (HRD)-related genes

HRD-related proteins interact with BRCA1/2 to repair double-stranded DNA damages as well as maintain genomic stability[35]. Examples of these proteins include Checkpoint kinase 2 (CHEK2), radiation repair gene 51 paralog C (RAD51C), radiation repair gene 51 paralog D (RAD51D), meiotic recombination 11 (Mre11), BRCA1/2, ataxia telangiectasia mutated (ATM), partner and localizer of BRCA2 (PALB2), radiation repair gene 50 (RAD50), Nijmegen breakage syndrome 1 (NBS1) and BRCA1-interacting protein 1 (BRIP1)[14,35]. Alterations of these genes could be detected in approximately half of all high grade serous OVCAs and increases the risk of OVCA[36,37]. OVCA patients with mutations in HRD-related proteins have improved survival rates due to their increased sensitivity to chemotherapeutic agents, responses similar to that of BRCA1/2 mutation carriers[29,38].

1.3 Epithelial ovarian cancer (EOC)

Epithelial OVCAs comprise of approximately 95% of all OVCA cases[5,6]. Using molecular, morphological and genetic profiling, EOC is classified into five (5) histologic subtypes **(Fig. 1.2; Table 1.2)**: high grade serous (70-74%), low grade serous (10%), clear cell (10-26%), endometrioid (10%) and mucinous (2-3%) carcinomas[6,7]. EOCs are categorized into two main types based on clinical, morphological and molecular pathogenesis: type I and II[39]. Type I EOCs are genetically stable, share lineages with benign precursors and borderline-malignant tumours, slow growing tumours that are detected mostly at early stages and include low grade serous, low grade endometrioid, mucinous and clear cells carcinomas[39]. In Low grade serous carcinomas (LGSCs), B-raf murine sarcoma viral oncogene homolog (BRAF), Kirsten rat sarcoma viral oncogene homolog (KRAS) and erythroblastic oncogene B2 (ERBB2) are

predominantly altered whereas low grade endometrioid carcinomas (ECs) harbour mutations in phosphatase and tensin homolog (PTEN), phosphatidylinositol-4, 5-bisphosphate 3-kinase catalytic subunit alpha (PIK3CA) and catenin (cadherin-associated protein) beta 1 (CTNNB1)[39]. Clear cell carcinomas (CCCs) harbour PIK3CA-activating mutations while most of the mutations in mucinous carcinomas (MCs) are related to KRAS. The Type I carcinomas rarely contain TP 53 mutations[39].

In contrast, the type II are very invasive, fast growing, detected at advanced stages, genetically unstable compared with the type I and do not have defined precursors[39]. These include, high grade serous, high grade endometrioid, carcino-sarcomas and undifferentiated carcinomas[39]. The Type II EOCs especially high grade serous carcinomas (HGSC) are characterized by mutations in TP53 and BRCA1/2 tumour suppressor genes[39]. TP53 mutations are detected in about 90% of all Type II carcinoma cases and are also significantly associated with chromosomal instability[39].

1.3.1 High grade serous carcinomas (HGSC)

HGSC accounts for approximately 70-74% of all EOCs and is the most fatal of all subtypes[6,7]. HGSC are very invasive and are predominantly diagnosed in advanced stages where the tumour would have metastasized to distant organs with or without ascites[6,7]. Most of the HGSC cases are detected in post-menopausal women with few cases identified in pre-menopausal women[40]. Histologically, HGSCs are characterized by solid growth with slit-like spaces, abnormal cell nuclei and hyper-proliferation of cells[41]. TP53 is frequently mutated in more than 95% of HGSCs cases with BRCA1 mutations and chromosomal instability representing 30-45% and 100%, respectively[6,42]. Although other tumour suppressor genes and

oncogenes such as RB1, BRIP1, RAD51, PALB2, CDK12 and NF1 are also mutated in HGSCs, their mutation frequencies are considered low[37,42]. Genetic alterations in PT53 and BRCA1/2 result in the deficiency of the homologous DNA damage repairing system leading to chromosomal instability and copy number changes[37,43,44]. CCNE, MYC and MECOM are each amplified in 20% of all HGSCs although MYC is the most frequently amplified[37,45] **(Table 1.2)**.

Until 2001, HGSC was considered to solely originate from the ovarian surface epithelial (OSE)[40,46]. There is however, increasing evidence to demonstrate that the secretory cells of the mucosa of fallopian tubes significantly contribute to the pathogenesis of HGSC[40,46]. Small non-invasive lesions in the oviductal fimbrial mucosa of BRCA1 mutation carriers share similar characteristics with serous carcinomas[46]. The lesions developed in the oviductal fimbrial mucosa are termed as serous tubal intraepithelial carcinomas (STICs)[47,48]. Cells released from the STICs during ovulation are deposited on the ovarian surface epithelium (OSE) and form the precursors for the development of serous ovarian carcinomas[47,49]. Genetic screening and mutational profiling have indicated that approximately 60% of all HGSCs are derived from STICs[47,49]

Since STICs are not found in 100% of all HGSCs, it suggestive that other alternative mechanisms are involved[49]. The importation of fimbrial epithelium fragments into the ovarian stroma, a process called endosalpingiosis is considered as a likely source due to the detection of benign tubal-type epithelium cysts in the ovarian stroma[49]. As to whether and how this ectopic tubal epithelium was imported remain to be determined. Also, it is yet to be determined if these ectopic tubal epithelia undergo neoplastic transformations. However, there are increasing evidence that ectopic OSE-lined cysts in the ovarian stroma could undergo neoplastic transformation and become positive for paired box gene 8 (PAX8), oviduct-specific glycoprotein

1, cilia and epithelial cell adhesion molecule (Epcam) as well as co-express calretinin and PAX8[50,51].

1.3.2 Low grade serous carcinoma (LGSC)

LGSCs are Type I EOCs which are not frequently diagnosed as HGSCs. They are slow growing and rarely diagnosed at early stage with poor overall survival. LGSCs are mostly chemoresistant when diagnosed at advanced stages and typically express the transcription factor PAX8[52,53]. LGSCs account for about 3-5% of all EOCs and are derived via a stepwise transformation from benign serous cystadenomas to serous borderline tumors (SBTs), serous tumours of low malignant potential (LMP serous tumours) and then to LGSCs[54]. LGSCs are genetically stable and histologically characterized by low mitotic activity, papillary structures and relatively uniform and small nuclei in the tumour cells[41,55]. There are frequent mutations of KRAS (19%), BRAF (38%) and ERBB2 but not TP53 and BRCA1/2[56]. The activating mutations of KRAS (codon 12 or less frequently codon 13) or BRAF (codons 599 and 600) result in hyper-activation and the transmission of growth signals via the rat sarcoma (RAS)/ rapidly accelerated fibrosarcoma (RAF)/ mitogen-activated protein kinase kinase (MEK)/ extracellular-signal-regulated kinase (ERK)/ mitogen-activated protein kinase (MAPK) signalling cascade leading to neoplastic transformation and tumorigenesis[56,57]. Interestingly, mutations in LGSCs are mutually exclusive; tumours with KRAS mutations do not have mutations in BRAF and vice versa[56,57] **(Table 1.2)**.

1.3.3 Endometrioid carcinomas (ECs)

ECs are derived from the malignant transformation of ovarian endometriosis or endometriotic cysts and account for 10% of all EOCs[6,41]. Although patients diagnosed at an early stage have better survival, those diagnosed at advanced stages have poor 5-year survival outcomes[6,41]. Increasing evidence suggest endometriosis as a significant risk factor for developing ECs[58,59]. Endometriosis is caused by retrograde menstruation where epithelial and stromal cells from the endometrium are transported from the uterus via the oviduct to the ovary, leading to the formation of an endometriotic cyst[60]. The iron-rich cystic fluid causes oxidative stress and hypoxia leading to DNA damage and the accumulation of mutations, a phenomenon that serves as a driving force for ovarian endometrioid cancers[61,62]. Histologically, ovarian ECs are characterized by glandular formations[41]. Increased risk of ECs is significantly associated with Lynch syndrome, microsatellite instability and mutations in the following genes: PTEN (16%), KRAS (30%), ARID1A (30%), PIK3CA (40%) and protein phosphatase 2 scaffold subunit A alpha (PPP2R1A) (16%)[63]. Unlike ARID1A and PIK3CA that are mutated in both ECs and clear cell carcinomas (CCCs), CTNNB1 is predominantly mutated in ECs but rare in other subtypes[63,64]. Endometriotic lesions may occur in various sites in the pelvis, however, those resident on the ovaries are likely to progress to carcinoma[60] **(Table 1.2)**.

1.3.4 Clear cell carcinomas (CCCs)

CCCs are the second most abundant OVCA cases after HGSCs and with a higher frequency in Asian population compared with Caucasians as well as account for approximately 5-26% of all EOCs[65,66]. The cells of CCC have clear cytoplasms due to the upregulation of hepatocyte nuclear factor-1 beta (HNF-1β) which regulates the glucose and glycogen

metabolism; a process that leads to the accumulation of glycogen and the clear appearance in the cells[67,68]. CCCs are characterized by hyaline bodies, densely hyaline basement membrane and multiple complex papillae[67,68]. CCCs patients in advanced stages have the worst prognosis compared with other EOCs of similar stages due to chemoresistance and tumour recurrence[7,41]. Like ECs, CCCs have a significant association with endometriosis[69,70]. Aside endometriosis being a causal factor of CCCs, there are significant evidence showing the co-existence of CCCs with benign tumours known as adenofibromas[71,72]. Molecular profiling has demonstrated that CCCs are negative for BRCA1/2 mutations but positive for ARID1A and PIK3CA mutations[73-75]. Alterations in PPP2R1A, KRAS, TP53 and PTEN have also been identified in CCCs but with lower frequencies compared with ECs[73-75]. Increased PIK3CA mutations lead to hyper-activation of the phosphoinositide-3 kinase (PI3K)/ protein kinase B (PKB; AKT)/ mammalian target of rapamycin complex (mTOR) signalling cascade, resulting in malignant transformation[73-75] **(Table 1.2)**.

1.3.5 Mucinous carcinomas (MCs)

MCs represent about 2-3% of all EOCs[76,77]. Most MC cases diagnosed are benign with a few being borderline malignancies[76,77]. The overall prognosis of patients at all stages is relatively good; however, patients with advanced stages have very poor overall survival compared with advanced serous carcinomas[41]. Studies have indicated that MCs are not primary to the ovary but rather metastasized from the gastrointestinal (GI) tract, endometrium and endocervix[78]. However, differentiating between primary MCs from metastatic MCs is not clearly demonstrated. Primary (ovarian) MCs are cytokeratin (CK) 7 positive whereas metastatic MCs from colorectal adenocarcinoma sites are CK7 negative but CK20 positive[79]. Regardless of the

tissue of origin, MCs express mucin genes such as MUC2, MUC3 and MUC17 as well as intestinal differentiation markers such as caudal-type homeobox transcription factors CDX1 and CDX2 and Lectin galactoside-binding soluble 4 (LGALS4; an intestinal surface adhesion molecule)[80]. Cells in MCs have pale-staining of mucin in the cytoplasm which increasingly depletes with tumour advancement[79]. In MCs, there are mutations in KRAS, TP53 and ERBB2 although the alterations in KRAS and ERBB2 are mutually exclusive[81-83] **(Table 1.2)**.

1.4 STAGES AND GRADES OF OVARIAN CANCER

1.4.1 Ovarian cancer staging

Staging describes the amount of tumour present and how far it has spread in an individual. This is done after surgical resection of the tumour. Tumour staging provides useful information which is able to guide physicians in planning patients' treatment and management, an intervention that could hugely impact the survival of patients. Ovarian cancer is primarily staged using the guidelines provided by the International Federation of Gynecology and Obstetrics (FIGO) using physical examination and clinical tests[84,85]. The FIGO system of staging uses information regarding the size of the tumour, how localized the tumour is in the ovaries as well as metastasis to distant organs. OVCA could be classified under 4 main stages[84,85] **(Table 1.3)**:

Stage 1: the tumour is localized in one or two ovaries without any spread outside the ovaries. These patients have the best prognosis of all stages with a 5-year survival rate of 90%. Patients diagnosed with stage 1 respond very well to treatment; however, only 15% of OVCA patients are diagnosed at this stage.

Stage 2: the tumour is found in one or two ovaries and has extended to the pelvis. About 19% of all cases are diagnosed with stage 2 and these patients have a 5-year survival rate of 70%. Patients generally have good prognosis compared with those with advanced stages of the disease.

Stage 3: the tumour is found in one or two ovaries, has spread beyond the pelvis to other parts of the abdomen and lymph nodes. Stage 3 patients represent 60% of all cased diagnosed and have poor survival with a 5-year survival rate of 39%.

Stage 4: this is the most advanced form of OVCA. This is when the tumour spreads beyond the abdominal cavity to distant organs such as the lungs, skin, brain and liver. These patients have the worst survival with a 5-year survival rate of 17%.

1.4.2 Ovarian cancer grading

Tumour grading describes how healthy the cells in the tumour are compared with the cancerous cells. Unlike staging which is judged macroscopically, grading is defined under the microscope as to whether a tumour is well or poorly differentiated, a condition that could determine how aggressive a cancer could be[86,87]. This could inform the physician as to whether a cancer is likely to spread as well as guide treatment plan. Tumours could be graded as follows:

GX: this is when the tumour cannot be evaluated or graded.

GB: tumours that have low malignant potential (LMP) as well as borderline are graded as GB.

G1: this is when a tumour is well differentiated and with large proportion of healthy-looking cells.

G2: tumours graded as G2 have moderately differentiated cells with few healthy-looking cells.

G3 and G4: these tumours are poorly differentiated with no healthy-looking cells present.

Table 1.3 FIGO Stages of epithelial ovarian cancer

	Stages		
Stage I	IA – The cancer is confined to one ovary only.	IB – The cancer is found in the two ovaries.	IC – The cancer spreads outside the ovaries.
Stage II	IIA – Cancer extends to the uterus or fallopian tube.	IIB – Cancer extends to the pelvis.	
Stage III	IIIA – Cancer cells are detected in the upper abdominal cavity or lymph nodes.	IIIB – Cancer in upper abdominal cavity measures less than 2 cm in size.	IIIC – Cancer in upper abdominal cavity measures above 2 cm and also present on the liver surface.
Stage IV	IVA – Cancer metatasized to the lungs and found in fluids around the lungs.	IVB – Cancer present in lung tissues and spleen.	

1.5 OVARIAN CANCER SCREENING AND DIAGNOSIS

Ovarian cancer screening is key to determining high-risk patients as well as early stage disease patients even before they exhibit symptoms. Effective screening ensures cost-effective treatment and management of patients leading to the improvement in the overall survival of patients. Ovarian cancer screening is mostly tailored for postmenopausal women who are mostly considered high risk[9]. Up-to-date, serum marker cancer antigen 125 (CA125) and transvaginal sonography (TVS) still present as the conventional strategies for screening the general population[9].

1.5.1 CA125

CA125, a high molecular weight transmembrane mucin (MUC16), is the most widely used tumour marker for EOC[9,88]. Serum CA125 was originally developed to monitor patients who have already being diagnosed with ovarian cancer and is elevated in the serum of about 90% of all patients with advanced EOCs[9]. Cancer cells upon stimulation by tumour necrosis factor (TNF) alpha and interferon (IFN) gamma release CA125 into the blood[88]. Although helpful, CA125 alone is not recommended as a screening test in asymptomatic patients due to its low test accuracy[9]. CA125 has been shown to be elevated in about 50 – 60% of stage I disease, ovarian cysts, hepatic diseases, endometriosis, adenomyosis, renal dysfunction and uterine fibroids suggesting that serum CA125 is not a reliable marker for screening ovarian cancer[89-91]. Thus, multi-analyte panel of biomarkers instead of single biomarkers are recommended to ensure effective screening of ovarian cancer patients. With the exception of clear cell carcinomas, CA125 is elevated in all types of EOCs[9,92]. Instead of CA125, serum tissue factor pathway inhibitor 2 (TFPI2) is the marker elevated in patients with clear cell carcinomas[92]. With the low

sensitivity of CA125 combined with the non-specific symptoms exhibited by ovarian cancer patients[9,90,91], novel markers with reliable test accuracies are needed to improve patients screening, treatment success and overall survival.

1.5.2 Transvaginal sonography (TVS)

TVS is an imaging modality that uses pattern recognition technique and grey-scale ultrasound to detect and evaluate adnexal mass with very high specificity and sensitivity[9,93,94]. In the first Kentucky study conducted in the year 2000, involving 14,469 asymptomatic subjects, TVS achieved a sensitivity, specificity, positive predictive value (PPV) and negative predictive value (NPV) of 81%, 98.9%, 9.4% and 99.97%, respectively[95]. In 2007, a second Kentucky study was conducted with 25,327 asymptomatic women[96]. The use of TVS annually recorded a sensitivity, specificity, positive predictive value (PPV) and negative predictive value (NPV) of 85%, 98.7%, 14% and 99.9%, respectively[96]. Although the use of TVS provides promising results, its detection accuracy could be further enhanced when combined with other markers in a two-stage strategy. This will be significantly helpful in asymptomatic women with normal ovarian volume.

1.5.3 Combining CA125 with TVS in ovarian cancer screening

The sequential or concurrent use of CA125 and TVS in the screening of ovarian cancer provides enhanced diagnostic accuracy compared with individual markers[91]. This is clinically beneficial in therapeutic success and improved patients' survival. In a London study, the combination of TVS and CA125 showed a specificity of 99.8% compared with CA125 combined with pelvic examination (specificity; 99%)[97]. In a second London study by Jacobs and

colleagues, the median survival of postmenopausal women screened with the combination of TVS and CA125 was 72.9 months compared with the control groups which were 41.8%[98]. In other trials organized in the US, Japan and UK, the combination of CA125 and TVS provided enhanced test accuracy compared with the individual markers[9]. Suggesting that including more novel markers to CA125 and TVS could further increase the sensitivity and specificity of screening ovarian cancer patients.

1.6 TREATMENT STRATEGIES FOR OVARIAN CANCER

Ovarian cancer is the most lethal gynaecological cancer due to late diagnosis, tumour recurrence and chemoresistance[99]. For the past decade, the 5-year survival rate has not been more than 50% partly due to treatment non-responsiveness[1,3,5]. The primary standard of care treatment regimen for OVCA is surgical intervention to debulk the tumour, platinum-taxane-based chemotherapeutic agents and then optimal follow-up strategies[8,66]. Recently, there have been treatment revolutions where other molecular targeted therapies and immunotherapies have shown therapeutic promise in the treatment of OVCA patients[8,66].

1.6.1 Surgical intervention

In the treatment of OVCA patients, surgical intervention is crucial to debulk the tumour and provide definite staging according to the International Federation of Gynecology and Obstetrics guidelines, an intervention that is key for effective treatment[84,100]. In early staged OVCA, optimal stage laparotomy which includes total hysterectomy, bilateral salpingo-oophorectomy, peritoneal cytology, omentectomy, pelvic/para-aortic lymph node dissection

(biopsy) and abdominal cavity biopsies are needed to reveal occult advanced disease as well as provide useful information for subsequent treatment[101,102].

In advanced staged OVCA, a maximal debulking surgery is recommended to completely remove any visible residual tissue or tumour[101]. No residual tumour is significantly associated with prolonged patient survival[103]. Surgical debulking outcomes could be classified into three (3) main categories[104-106]:

I. Complete residual disease/surgery: No detectable residual tumour by macroscopic examination.
II. Optimal residual disease/surgery: maximum residual tumour with a diameter < 1 cm.
III. Suboptimal residual disease/surgery: maximum residual tumour with a diameter ≥ 1 cm.

In most cases, a primary debulking surgery (PDS) is needed to completely remove all tumours before other treatments are initiated[8,104,106]. In advanced stages, interval debulking surgery (IDS) could be recommended if there is an extensive metastasis and complete resection is almost impossible[8,104,106]. IDS is carried out after chemotherapy to remove completely the tumour as a secondary procedure[8]. Surgical debulking is therefore key to the overall survival of the patients.

1.6.2 Frontline chemotherapy

1.6.2.1 Standard chemotherapy

The standard frontline chemotherapy is administered in two main forms: conventional and dose-dense chemotherapy[8]. The conventional treatment involves the administration of paclitaxel followed by carboplatin on day 1 and then every 3 weeks for 6 cycles (TC)[107]. The dose-dense TC treatment involves the administration of paclitaxel via i.v for 1 h plus carboplatin

(i.v) for 1 h[108]. The dose-dense treatment is administered for 6 cycles every 3 weeks[108]. In a trial (JGOG3016) comparing these two forms of treatments in advanced staged OVCA patients, the dose-dense treatment was associated with significant progression-free survival (PFS) and overall survival (OS) compared with the conventional treatment regimen[108]. The setback was the higher toxicity observed with the dose-dense treatment, a potential obstacle that will warrant the discontinuation of such treatments.

1.6.2.2 Intraperitoneal chemotherapy

Intraperitoneal (IP) chemotherapy is recommended in advanced stage diseases after surgical debulking although there are associated risks involved such as abdominal pains, infections and abdominal discomfort[8,109]. Regardless of these complications, IP chemotherapy has shown a significant survival advantage with less than 1 cm residual tissue as demonstrated in the Gynecologic Oncology Group 172 (GOG172) trial[110]. Other randomized controlled trials have also observed significant survival advantages of IP chemotherapy especially in advanced stages EOCs[111]. Thus, IP chemotherapy remains promising regardless of the associated complications. Efforts in reducing these complications will be favourable for patients with advanced staged EOCs.

1.6.3 Targeted molecular therapy and chemotherapy

Targeted molecular therapy is widely used in the treatment of cancer and has also shown therapeutic promise in ovarian cancer[8]. There are two types of targeted therapy that are used in ovarian cancer: anti-angiogenic target agents and poly (ADP-ribose) polymerase (PARP) inhibitors[8]. Vascular endothelial growth factor (VEGF) and its receptor (VEGFR) are involved in

neovascularisation leading to tumour progression and metastasis[112]. Upregulation of VEGF and VEGFR is significantly associated with ovarian cancer progression, poor patient survival and development of ascites[112]. Developing monoclonal antibody (bevacizumab; BEV) to block the action of VEGF has shown therapeutic success in lung, breast, colon and ovarian cancers. In two separate clinical studies (GOG218 and ICON7), administering BEV together with TC therapy provided a significant improvement in the PFS (GOG218; 3.8 months, ICON7; 1.7 months) of the patients compared with the control group[113,114]. However, adverse side-effects were observed in the patients treated with BEV such as gastrointestinal perforation, haemorrhage, proteinuria, thromboembolism and hypertension[113,114]. Upon further investigation, it was shown that gastrointestinal perforation was significantly associated with patients who had intestinal obstruction or had been exposed to radiation at their abdomen/pelvic region[113,114]. It is therefore important to carefully select patients and scrutinize their treatment history before administering BEV. Inhibiting the action of VEGFR with tyrosine kinase inhibitor (TKI; nintedanib) has also shown therapeutic promise in the treatment of ovarian cancer in a phase III clinical study.[115].

PARP is a DNA binding protein involved with the repair of double-stranded DNA damage[116]. Thus, inhibiting the function of PARP is key to killing tumour cells and enhancing patient survival[116]. Tumours with BRCA1/2 mutation are more susceptible to PARP inhibitors compared with non-carriers[28,117]. In a randomized double-blinded clinical studies of chemosensitive ovarian cancer patients, olaparib (the first PARP inhibitor to be developed) treatment was associated with prolonged PFS compared with the placebo group (8.4 months vs. 4.8 months; 0.35)[118]. Upon further stratification, patients with BRCA1/2 mutation had a marked improvement in PFS compared with the non-carrier group (11.2 months vs. 4.3 months; HR = 0.18)[119]. Another PARP inhibitor, veliparib, has also demonstrated significant therapeutic

success in recurrent EOCs and with acceptable side-effects[120]. These suggest that the use of PARP inhibitors in combination with chemotherapy is an effective treatment option for advanced stage patients especially those carrying BRCA1/2 mutations.

1.6.4 Immunotherapy of ovarian cancer

The standard treatment of ovarian cancer for the past two decades still remains surgical debulking and cytotoxic chemotherapy (carboplatin plus paclitaxel)[8]. However, the 5-year survival rate still remains below 50%[3,5]. This has resulted in the development of novel therapies that harness the immune system to fight cancer. Examples of immunotherapies tested in ovarian cancers include peptide-based vaccines (peptides from MUC1, p53, WT-1 and CA-125)[121-124], immune checkpoint blockers [anti- cytotoxic T-lymphocyte-associated protein 4 (CTLA-4; ipilimumab and tremelimumab) and anti- programmed cell death protein 1/ programmed death-ligand 1; (PD1/PD-L1; nivolumab, pembrolizumab and atezolizumab)][125-128] and adoptive T cell therapy[129]. These treatments have achieved marginal therapeutic advantages hence; novel approaches are required to increase their treatment outcomes.

1.7 CHEMORESISTANCE IN OVARIAN CANCER

Although ovarian cancer patients initially respond to standard treatments, 55% of the patients relapse in 2 years with over 70% recurring within 5 years[3,5,99]. For two decades, the 5-year survival rate for OVCA patients still fall below 50% despite tremendous efforts in investigating the cellular and molecular basis of OVCA[3,99]. Clinically, progression-free interval (PFI) is the most reliable indicator for stratifying patients in chemosensitive or chemoresistant[130,131].

Fig. 1.3 Contributing factors of epithelial ovarian cancer chemoresistance. Chemoresistance in EOCs is multi-faceted. This could be contributed by genetic mutation of tumor suppressor genes (p53), upregulation and activation of oncogenes (AKT), BRCA1/2 mutations, increased metabolic activities (HKII), tumor microenvironment (immune cell suppression) and over-expression of gelsolin.

PFI is described as the interval between the completion of an initial treatment and the beginning of another treatment regimen due to recurrence[130,131]. Chemoresistance is classified as PFI < 6 months, partially chemosensitivity is classified as PFI within 6 – 12 months and chemosensitivity classified as PFI over 12 months[130,131]. Depending on the study, chemoresponsiveness could be defined as 6 < PFI ≥ 6 months or 12 < PFI ≥ 12 months[130,131]. The cellular and molecular basis of chemoresistance is attributed to the dysregulation of pro-survival (such as PI3K/Akt)[132-135] and pro-apoptotic (such as p53) signalling cascade[136-138], epigenetic modifications (DNA methylation and histone modification, protein ubiquitination and degradation, and microRNA regulation)[139-141], metabolic activities [hexokinase II (HKII), hypoxia-inducible factor 1-alpha (HIF1α)] [142-144], increased expression of multidrug resistance pumps[145-148] and enhanced DNA damage repair[16,149] **(Fig. 1.3)**. Also, accumulating evidence has shown that the tumour microenvironment regulates the sensitivity of OVCA cells to chemotherapy treatment[150,151]. The key players in determining the fate of ovarian cancer cells in the TME include: i) pro-apoptotic and pro-survival genes in the cancer cells ii) dysregulation of immune cells [e.g. increased expression of checkpoint proteins (PDL1 and PD-1)], and iii) soluble factors and extracellular vesicles that promote crosstalk between the OVCA cells and the neighbouring target cells. Such mechanisms could act independently or inter-dependently to orchestrate their effects.

1.7.1 Mechanism of cisplatin action and chemoresistance

Cisplatin [*cis*-Pt (II) $(NH3)_2CL_2$; *cis*-diaminodichloroplatinum; (CDDP)] consists of a central platinum ion bound to two amino groups (NH2) and two chloride ions (Cl) in the *cis* configuration **(Fig. 1.4).** The *cis* configuration is critical for the anti-tumour functions of CDDP since its *trans*-isomer does not provide any biological effects[152].

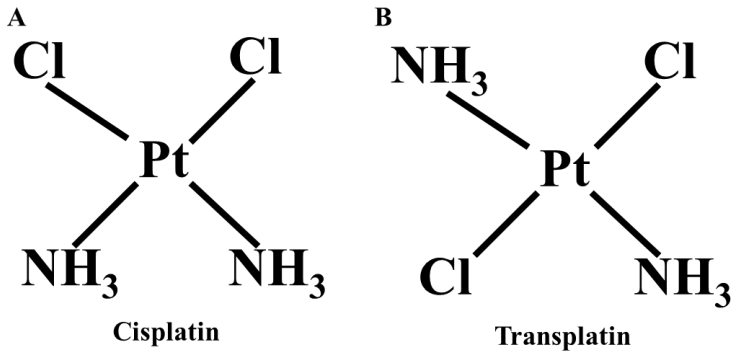

Fig. 1.4 Chemical structure of platinum. (A) Cisplatin and its *trans* stereoisomer **(B)** transplatin.

CDDP crosses the cell membrane by simple diffusion since it's non-ionized in a native state. CDDP upon entering the cell reacts with water, a reaction that leads to chloride ion loss and a positively charged electrophile.

This enables the platinum atom to bind to negatively charged molecules such as DNA to form inter and intra-strand DNA crosslinks between adjacent guanines[153-155]. Also, CDDP agents are transported into cells via active (copper transporter, CTR1) or passive transport after which they bind to the nuclear DNA forming intra-strand (most abundant ~70%) and inter-strand crosslinks[156]. These adducts result in DNA conformational changes as well as inhibit DNA unwinding and synthesis, processes that damage the DNA leading to the initiation of apoptotic signalling or DNA damage repair mechanisms[157]. Ataxia telangiectasia mutated protein (ATM), ataxia telangiectasia and Rad3 - related protein (ATR) and their downstream effector checkpoint kinases 1 and 2 (Chk1 and Chk2) act as CDDP-induced DNA damage sensors that trigger the activation of p53, leading to apoptosis[158]. Aside DNA damage, CDDP treatment also inflict deleterious damages to mitochondria, alters chemotherapeutic agent cellular transport mechanisms as well as decreases the expression of ATPase, ATPase copper transporting alpha and beta (ATP7A and ATP7B). ATPase, ATP7A and ATP7B sequester and block CDDP from interacting with the nuclear DNA[159-162]. The initial response rate (RR) to platinum-based chemotherapies is about 70%; however, 70% of the patients relapse after 5 years[110,163]. Tumour recurrence could be due to genetic modification of tumour cells to acquire a chemoresistant state[164]. The underlying mechanisms of OVCA chemoresistance could be grouped into 3 main categories: mechanisms inhibiting the formation of lethal DNA-cisplatin adduct[165], mechanisms attenuating the initiation of apoptotic signalling after DNA damage[157,165] and mechanisms involving anti-tumour cells in the TME[166-170].

1.7.2 Multidrug resistance 'pumps' (MDRs)

MDRs are proteins that are involved in the efflux of chemotherapeutic agents from cells, a mechanism that reduces drug concentration in its target cells as well as minimizes its efficacy[147]. Examples of these proteins include ATP-binding cassette sub-family B member 1 (ABCB1) or p-glycoprotein, ABC subfamily C member 1 (ABCC1/MRP1) and ABC subfamily G member 2 (ABCG2)[147,171]. The downregulation of p-glycoprotein by cisplatin renders ovarian cancer cells sensitive cisplatin-induced apoptosis[172]. Overexpression of p-glycoprotein in chemosensitive ovarian cancer cells rendered them resistant to cisplatin-induced death[173]. MRP1 shares 15% amino acid sequence with p-glycoprotein[174,175]; however, their resistance profiles overlap[146,176]. Although MRP1 is resistant to anthracyclines and methotrexate but not taxanes and CDDP, p-glycoprotein and MRP2 on the other hand are resistant to taxanes and cisplatin[147]. Thus, the type of MDR expressed on OVCA cells could also determine the type of chemotherapeutic drug the cell is resistant to. Although this information could help physicians select the appropriate chemotherapeutic agent for OVCA patients, it also addresses the point that MDRs alone are not adequate to indicate chemoresistance. MRP1 is involved in the transportation of glutathione (GSH) and glucoronate conjugates, a process that is key to phase II metabolism and cellular detoxification[177,178]. In addition to ovarian cancer, MRP1 has been reported to be highly expressed in breast cancer, prostate cancer, non-small cell lung cancer and haematological cancers[145,179,180]. MRP1 expressions in these cancers are significantly associated with poor therapeutic outcomes[145]. Murine ovarian cancer cells when cultured with ascites exhibited increased expression MRP1 and breast cancer related protein (BCRP)[148]. This attenuated the sensitivity of these cells to paclitaxel-induced death. Taken together, these results

suggest that the aberrant expression of multidrug resistant proteins plays a key role in human ovarian cancer chemoresistance.

1.7.3 Drug Detoxification

Glutathione (GSH) is an important antioxidant that is involved in the detoxification of chemotherapeutic drugs including CDDP[181,182]. GSH binds covalently with CDDP to form GSH-CDDP complex via catalytic reaction with glutathione-S-transferase (GST) or non-enzymatic reactions[178]. Upon complex formation with GSH, CDDP is refluxed from the cells by an ATP-dependent transporter GS-X, a mechanism that reduces the intracellular accumulation of CDDP[177,178,183]. Increased expression of GSH and/or GST render(s) ovarian cancer cells resistant to CDDP-induced death; however, their cellular depletion makes ovarian cancer cells more susceptible to CDDP-induced death[172,184]. Primary cells derived from ovarian cancer patients treated with chemotherapy revealed increased expression of GSH, a phenomenon that was significantly associated with multidrug resistance[185]. Taken together, these findings suggest that chemotherapeutic drug detoxification and efflux is a key determining factor of drug resistance in ovarian cancer. The role of the tumour microenvironment in the regulation of GSH and other antioxidants is not well established. Fibroblast-derived GSH confers resistance in ovarian cancer cells by reducing the intracellular accumulation of CDDP in the cells[186]. This reduces the cytotoxic effects of CDDP on the ovarian cancer cells. GSH synthesis in OVCA and its interaction with immune cells is less established. As to whether immune cells modulate the expression of antioxidants in cancer cells remains to be investigated.

1.7.4 DNA damage repair

DNA damage repair involves the use of excision damage repair mechanisms that replace damaged nucleotides with healthy nucleotides[149]. Enhanced DNA damage repair has been reported to be associated with chemoresistance[8,149]. This is as result of increased repair of DNA damages inflicted by chemotherapeutic agents. There are five (5) types of DNA repair mechanisms which include base excision repair (BER; repairs single nucleotide damages), nucleotide excision repair (NER; repairs 2 – 30 bases of nucleotide damages), mismatch repair (MMR; repairs mismatched nucleotides resulting from errors generated by DNA band recombination) and homologous recombination (HR) and non-homologous end joining (NHEJ) for double strand breaks[149].

In cancer cells, there are high replication rate and defective DNA repair mechanisms which result in genomic instability, a mechanism that is frequently observed in high grade serious ovarian cancer[149]. BRCA1 and 2 are key proteins involved in the DNA repair mechanism. Mutations of BRCA1/2 are associated with approximately 10% of all HGS EOC cases and 2.1% of all endometrioid EOC cases[187,188]. Although defective repair mechanisms promote oncogenesis due to the accumulation of mutations, they also render cancer cells sensitive to chemotherapeutic agents which are the case of BRCA1/2 mutations[117]. Increased expression of human apurinic/apyrimidinic endonuclease (APE1), a key protein of the BER complex, is associated with platinum resistance, poor surgical outcome and poor overall survival in EOC patients, gastro-oesophageal and pancreatico-biliary cancers, making it a suitable candidate for targeted therapy[189]. Increased expression of excision repair cross-complementing 1 (ERCC1) renders ovarian cancer cells resistant to chemotherapeutic agents; however, ERCC1 downregulation sensitized ovarian cancer cells to CDDP-induced cytotoxicity[190]. Understanding

the DNA damage repair mechanisms and their pathogenesis in ovarian cancer will enable the development of novel targets for effective and successful therapeutic outcomes.

1.7.5 Signalling cascades involved in ovarian cancer cell chemoresistance

Genes such as *TP53*, Akt/PI3K and gelsolin control cell cycle, proliferation, apoptosis and survival[134,138,191,192]. Alterations in these genes could potentially result in cancer cell aggressiveness and chemoresistance. Some of these gene products act in isolation or in partnership with other proteins or RNAs to execute their influence. The ovarian cancer cell develops smart mechanisms to dysregulate these genes and to favour its survival.

1.7.5.1 The PI3K/Akt signalling and chemoresistance

Phosphatidylinositol 3-kinase (PI3K)/Akt pathway is an intracellular signalling cascade that is mainly involved in the regulation of the cell cycle thus, participating in cellular quiescence, proliferation and carcinogenesis[193,194]. This pathway is mostly activated in response to growth factors and cytokines; PI3K phosphorylates and activates Akt which in turn leads to a number of downstream effects such as inhibition of p27[195] and cAMP-response element binding protein (CREB)[196]. It also affects the localisation of forkhead box O (FOXO)[195,197] in the cytoplasm and activation of mTOR[195,197]. PI3K consists of two main subunits, namely the regulatory (p85) and catalytic (p110) subunits[198]. Akt, also known as protein kinase B (PKB) is a downstream protein target of PI3K[199]. As a serine/threonine protein kinase, Akt has three isoforms (Akt/AKT1/PKBα, AKT2/PKBβ and AKT3/PKBγ) with overall homology greater than 85%[135,200,201]. Akt contains an N-terminal PH domain which binds to PI3K, a C-terminal rich in serine and threonine that is phosphorylated for kinase activation, and a central kinase domain.

Akt is phosphorylated by phosphoinositide-dependent kinase 1 (PDK-1), integrated linked kinase (ILK) and MAP kinase-associated protein kinase-2 (MAPKAPK2)[202-204], but is negatively regulated by SH2 domain-containing inositol phosphatase (SHIP)[205,206] and phosphatase and tension homolog (PTEN)[207,208] which are known tumour suppressor genes mostly mutated/down-regulated in cancers, including ovarian cancer. The PI3K/Akt signalling pathway is critical in the regulation of ovarian cancer cisplatin sensitivity[135,191]. Akt is overexpressed, activated and functionally altered at the DNA or mRNA levels in primary ovarian cancer[209]. Ovarian cancer cells overexpressing a constitutively active Akt or amplified AKT2 are resistant to cisplatin-induced apoptosis compared to cells expressing low Akt levels[133]. PI3K/Akt pathway interacts with other proteins such as HKII, X-linked inhibitor of apoptosis protein (XIAP), gelsolin and p53 to regulate ovarian cancer chemosensitivity[143,191,192]. This implies that, the mechanism of ovarian chemoresistance is multifactorial hence, a holistic approach should be considered in its strategic management.

1.7.5.2 p53 and chemoresistance

p53, a tumour suppressor, is considered the "guardian of the genome" which arrests cell replication to initiate DNA repair upon sensing DNA damage[136]. It also acts as a transcription factor involved in the expression of genes responsible for cell cycle arrest regulation and apoptosis[138,210,211]. p53 activation and upregulation is associated with the attenuation of cellular proliferation and induction of apoptosis depending on the severity of the DNA damage[212].

Murine double-minute-2 (MDM2) or it's human homologue (HDM2) ubiquitinates p53 and targets it for proteasomal degradation, a process that regulates p53 content and activity[213]. The

Serine (Ser) and Threonine (Thr) sites in the MDM2 binding pockets of p53 are phosphorylated following stress[214]. This attenuates MDM2-mediated p53 ubiquitination and proteasomal degradation, a process that leads to p53 activation, stabilization and up-regulation[214]. p53 mutation and downregulation have been recorded in a high percentage of human cancers including ovarian cancer[212]. The activation of p53 is required to sensitize cancer cells to DNA damaging chemotherapeutic agents such as CDDP. Thus, inactivation of p53 in ovarian cancer cells results in the development of resistance to cisplatin treatment[210]. p53 is activated in response to cisplatin-induced genetic insults by DNA damaging protein sensors ataxia telangiectasia mutated protein (ATM) and ataxia telangiectasia and Rad-3 related protein (ATR) and also through serine phosphorylation (S15 and S20) by the G2 checkpoint kinase 1 (Chk1), preventing its ubiquitination and proteasomal degradation while increasing its pro-apoptotic properties[215-217].

P53 is involved in the upregulation of pro-apoptotic proteins [Phorbol-12-myristate-13-acetate-induced protein 1 (NOXA), p53-upregulated mediator of apoptosis (PUMA), apoptotic protease activating factor-1 (Apaf-1), Bcl-2-associated X protein (Bax) and Bcl-2 antagonist of cell death (Bad)] and death receptors (DR4, DR5 and Fas). Cisplatin also causes p53-dependent, Itch-mediated Flice-like Inhibitory Protein (FLIP) degradation at the plasma membrane[191,192,218-222]. In addition to the transcriptional action of p53, it is also involved in mitochondria dynamics by interacting with prohibitin 1 resulting in metalloendopeptidase Oma1-mediated processing of optic atrophy 1 (OPA1) and CDDP-induced apoptosis[223]. p53 is accumulated in the mitochondria upon CDDP treatment, an action that results in the release of second mitochondria derived activator of caspases (Smac), cytochrome c (Cyt c), human high temperature requirement protein A2 (HtrA2/Omi) and apoptosis in chemosensitive OVCA cells[134]. In response to cisplatin, p53

binds to the voltage-dependent anion channel (VDAC) of the mitochondrial outer membrane in chemosensitive ovarian cancer cells to induce release of pro-apoptotic factors such as cytochrome c (cyt c), apoptosis inducing factor (AIF) and smac[211].

Protein phosphatase magnesium-dependent 1 D (PPMID) expression has been implicated in many types of cancers including ovarian cancer[224,225]. Its expression is directly correlated with poor prognosis[224,225]. PPM1D regulates p53 activation through ataxia telangiectasia mutated (ATM), Chk1 and Chk2[226,227]. It also regulates p53 stabilization through mouse double minute 2 homolog (MDM2)[213,214,228] and MDMX [a.k.a MDM4 (Mouse double minute 4 homolog)][228,229]. As a potent oncogene, the primary function of PPM1D is to inhibit cell cycle checkpoints, DNA repair and cellular apoptosis thus, leading to oncogenic transformation, cancer cell proliferation and chemoresistance[224,225,229].

1.8 TUMOUR MICROENVIRONMENT AND CHEMORESISTANCE

The tumour microenvironment (TME) modulates the responsiveness of cancer cells to treatment, a process that could result in tumour progression, chemoresistance and poor patient survival[150,167,168]. The tumour microenvironment entails a plethora of interactive cells that communicate with each other via cell-cell contact or the soluble factors that modulate the behaviour of the tumours **(Fig. 1.5)**. Although immune cells such as T cells, B cells, natural killer (NK) cells and macrophages are programmed to kill cancer cells, their anti-tumour properties could be suppressed to favour tumour growth and recurrence[169,230,231].

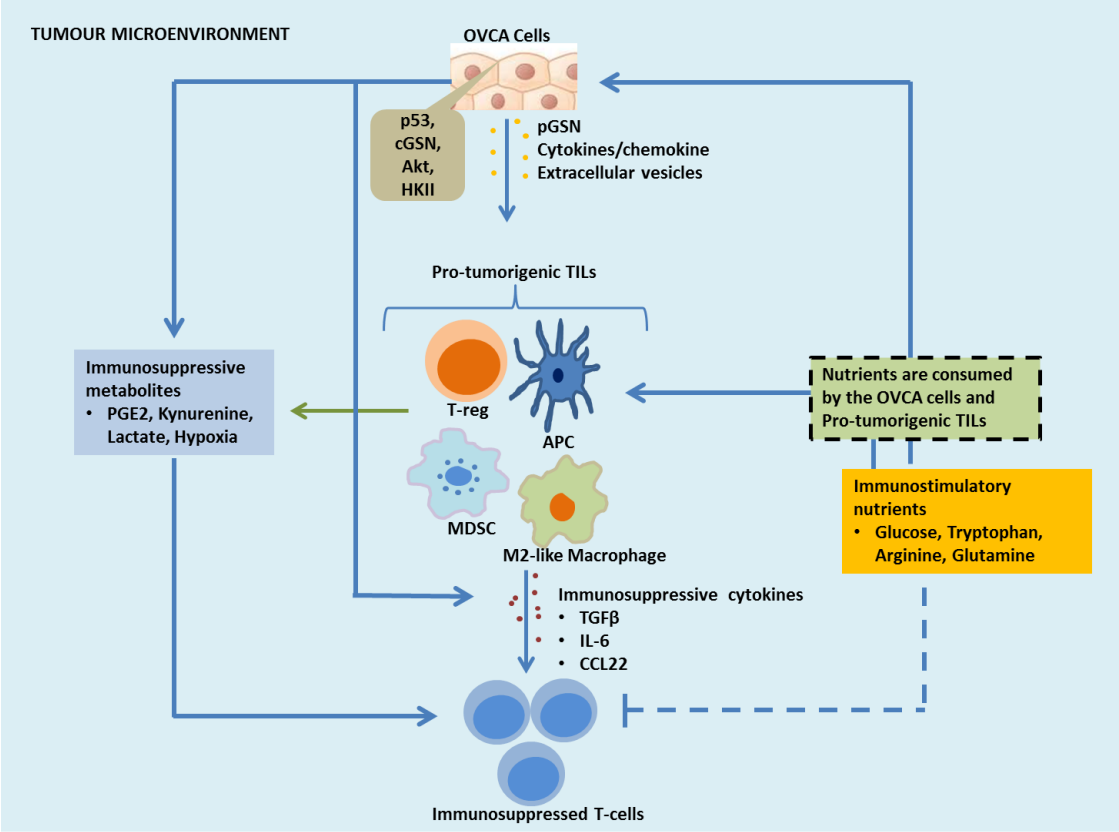

Fig. 1.5 Multifactorial roles of the tumour microenvironment on epithelial ovarian cancer chemoresistance. Immunostimulatory nutrients, immunosuppressive metabolites, pro-tumourigenic cytokine milieu and intracellular signaling proteins regulate the behavior of OVCA cells and T cells' functions contributing to chemoresistance. OVCA cells and pro-tumourigenic tumour infiltrating lymphocytes (TILs) deplete immunostimulatory nutrients meant to boost the functions of T cells. Immunosuppressive metabolites are produced by the OVCA cells and pro-tumorigenic TILs after consuming the nutrients which further promote T cell dysfunction. APC, antigen-presenting cell; MDSC, myeloid-derived suppressor cell; IL, interleukin; T reg, regulatory T cell; PGE2, prostaglandin E2; TGFβ, transforming growth factor-β. Adapted from Daniel .E. Speiser, *et al*., 2016 and modified.

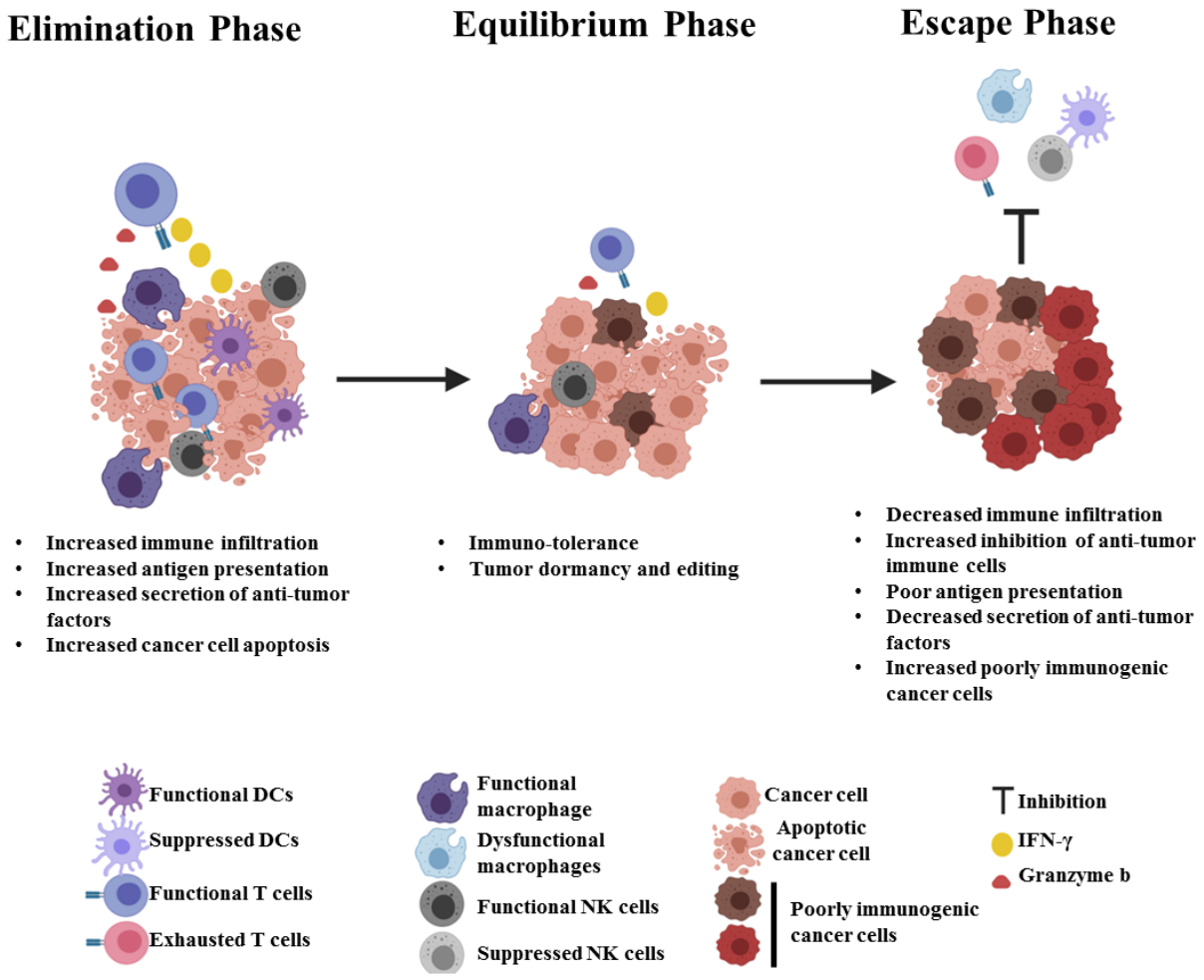

Fig. 1.6 Schematic diagram of cancer immuno-editing. There are three (3) phases of cancer immune-editing: elimination phase, equilibrium phase and the escape phase. The elimination phase is when the tumour is overwhelmed with functional immune cells leading to tumour cell death. A state of dormancy where tumour expansion is controlled is achieved when the tumour and immune cells reach a phase of dynamic equilibrium. The escape phase is when anti-tumour immune responses are curtailed leading to tumour expansion. *Diagram designed using biorender*.

1.8.1 Tumour infiltrated lymphocytes (TILs)

TILs are immune cells that home from the circulation and are presented in the tumour stroma as well as parenchyma. They consist of the members from both innate (macrophages and natural killer cells) and adaptive (T and B cells) immune systems[232]. Although the normal physiological function of these immune cells should be used to recognize and kill tumour cells, they are usually "re-engineered" to help tumour development instead[168,230,233] **(Fig. 1.6)**. In a functional immune system, tumour antigens should be sampled by antigen presenting cells (APCs) such as dendritic cell (DCs) and macrophages, after which they are processed and presented to T cells to activate cytotoxic T cells for eradication of the tumour cells. This is known in the TME as the **elimination phase**[167] **(Fig. 1.6)**. The antigens could also be presented to helper T cells to get activated for pro-inflammatory and immune-stimulatory cytokines secretion that potentiates immune response. Tumour cells in their quest to combat the immune response may secrete inhibitory cytokines (TGF-β, IL-10) and chemokine ligand 2 (CCL2) to down-regulate the cytotoxic functions of CD8+ T cells and CD4+ T helper cells. This counter-attack mounted by the tumour cells are in balance with anti-tumour attack hence, creating an **equilibrium phase**[167] **(Fig. 1.6)**. Although most tumour cells will be killed by the effector T cells, some of the antigens in the tumour cells are mutated hence acquire resistance to tumour killing. This period of evading immune attack is referred to as the **escape phase**[167] **(Fig. 1.6)**. At this phase, the tumour becomes resistant, malignant, and metastasizes easily.

1.8.2 Tumour-associated macrophages (TAMs)

TAMs are phagocytic immune cells derived from monocytes that could either stimulate anti-tumour function or promote tumour growth, depending on the local signal

networks to which they are exposed. Circulating monocytes could be committed to either M1 or M2 macrophages depending on the cytokine stimulation[234]. Upon lipopolysaccharide (LPS) and/or interferon gamma (IFN-γ) stimulation, monocytes could be differentiated into M1 macrophages that are responsible for high-level IL-12 and IL-23 secretion but low levels for IL-10[234]. On the other hand, when monocytes are stimulated by IL-4, they are differentiated into M2 macrophages, which secrete high-level IL-10, TGF-β and IL-4 but low-level IL-12[234]. TAMs are mostly M2 macrophage populations that secrete immunosuppressive cytokines to promote tumour growth, invasion, angiogenesis, metastasis and chemoresistance[168,234,235]. The immune-suppressive role of TAMs has been reported in different types of cancers including ovarian cancer, where increased TAM population is associated with poorer patient outcome, tumour aggressiveness, and chemoresistance[236].

1.9 CROSS-TALK MOLECULES IN THE TUMOUR MICROENVIRONMENT AND CHEMORESISTANCE

Intercellular communication is a fundamental process not only in the tumour microenvironment but also in the metastatic dissemination of tumour cells and chemoresistance. Cross-talk between cancer cells and neighbouring cells could be mediated through several mechanisms[237,238], namely **(Fig. 1.5)**: (1) direct cell-cell contact, (2) cytokine/receptor interaction and (3) vesicle-mediated interaction. As to whether these mechanisms act independently or dependently still remain a puzzle to be solved. Nevertheless, with the exception of the vesicle-mediated mechanism, they have been extensively studied especially in the tumour microenvironment.

1.9.1 Characteristics of extracellular vesicles

A plethora of extracellular vesicles are released by tumour cells into the TME which modulate neighbouring target cells to favour tumour growth, angiogenesis and chemoresistance[239,240]. These tumour cell secreted vesicles are heterogeneous and may include small extracellular vesicles (sEVs; mostly called exosomes), large extracellular vesicles (lEVs; mostly called microvesicles/microparticles), and apoptotic bodies. Regardless of the fact that these vesicles share some common features, they differ by their sizes, mechanism of formation, characteristic structural and molecular features, and compositions (proteins, nucleic acids and lipids, etc.)[237,238]. These distinctive features provide information about the cell of origin. Amongst these vesicles, sEVs and lEVs are the most studied in the context of tumour growth and chemoresistance[140,141,240-243].

1.9.2 Small extracellular vesicles (Exosomes)

Exosomes are vesicles measuring from 30 – 150 nm in diameter formed within endosomes by membrane invagination leading to the formation of multivesicular bodies (MVBs)[238,244]. Upon fusion with the plasma membrane, the sEVs are released into the extracellular space. Proteins such as ALG-2-interacting protein X 2 (Alix2), endosomal sorting complex required for transport (ESCRT), tumour susceptibility gene 101 (Tsg101), CD63, heat shock proteins(Hsps) and major histocompatibility complex II (MHC class II) are highly contained in exosomes hence, used as markers for detection after sedimenting at 100,000 g from appropriate samples (culture media and biological fluids)[237,238,244].

1.9.3 Large extracellular vesicles (Microparticles)

Microparticles are 150 – 1000 nm in diameter and formed by the outward blebbing of plasma membrane mostly under stress conditions[244]. LEVs sediments at 20,000 g and is positive for Annexin V and other cell-specific surface markers[237,238,244]. LEVs, just like sEVs, shuttle proteins, lipids and nucleic acids that are involved in regulating tumour proliferation, invasion and chemoresistance[242,243].

1.9.4 Cancer cell-derived extracellular vesicles (EVs) and chemoresistance

EVs-mediated drug resistance is frequently classified into three mechanisms: (1) Neutralization of antibody-based drugs, (2) export of small molecular drugs, and (3) transfer of biologically active materials (proteins, lipids and miRNAs)[141,245-248]. Exosomes released from chemoresistant OVCA cells contain approximately 3 folds more cisplatin compared to the exosomes from their sensitive counterparts, suggesting that cancer cells utilize exosome transport system for drug export[249]. It has also been demonstrated that cisplatin-resistant OVCA cells release exosomes that contain biologically active miR-21-3p which targets the neuron navigator 3 gene (NAV3) in the chemosensitive cells, rendering them resistant to cisplatin treatment[139]. In functional studies, miR-21 was observed to be carried in exosomes released from cancer associated adipocytes or cancer associated fibroblasts to ovarian cancer cells. These functional exosomes suppressed paclitaxel-induced apoptosis in OVCA through their direct interaction with Apaf1[140]. EVs derived from cisplatin resistant OVCA cells contain mutated SMAD4 that confers resistance of naïve A2780 (cisplatin-sensitive) recipient cells via endocytosis and is associated with epithelial to mesenchymal transition (EMT)[240]. The efficacy of most immunotherapy has been compromised due to the ability of cancer-derived exosomes to bind and inhibit therapeutic

antibodies such as trastuzumab and rituximab[248]. Cancer-derived EVs have also been shown to down-regulate the cytotoxic functions of immune cells thus, enabling cancer cells to evade anti-tumour response[141,250-252]. The underlying mechanism behind the transfer of EVs and selective uptake by immune cells are still largely unknown. Understanding how cancer cell-derived EVs modulate immune cells to facilitate tumour escape is key to developing novel cancer therapies.

1.10 GELSOLIN AND CHEMORESISTANCE

1.10.1 Gelsolin biology and function

Gelsolin (GSN), an 80 – 84 kDa protein, exists as both cytoplasmic (cGSN) and secretory (pGSN) isoforms[253,254]. It also has other isoforms which are less characterized and mainly expressed in the nervous system. Both isoforms are encoded by a single gene on chromosome 9 and derived from alternative splicing and different transcriptional initiation sites **(Fig. 1.7)**[253,254]. All gelsolin isoforms bind, sever and cap actin filaments[253,255]. They differ by an N-terminal 25-amino acid signaling peptide and a cystine residues disulfide bond[253,255]**.** cGSN has been implicated in cytoskeletal remodeling, cell growth and proliferation, cell motility and apoptosis[256]. cGSN also exists in the mitochondria and preserves mitochondrial integrity by blocking the loss in mitochondrial membrane potential and apoptosis[256-258].

GSN plays an important role in the regulation of gynecological cancer cell fate as reflected in dysregulating their chemosensitivity[192]. Chemoresistant cancer cells exhibit higher intact cGSN and lower cleaved cGSN contents in OVCA cell lines compared to their sensitive counterparts[192,257]. cGSN expression in high-grade serous OVCA is significantly associated with tumour progression, progression-free and overall survival[192].

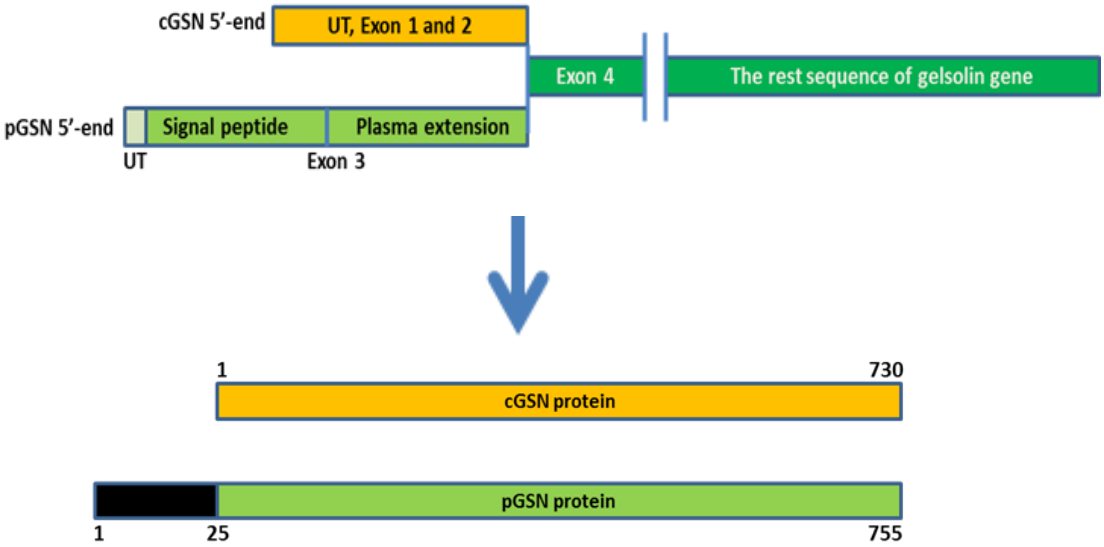

Fig. 1.7 The structure of gelsolin. Both isoforms of gelsolin (cytoplasmic; cGSN and secreted, pGSN) are encoded by a single gene on chromosome 9 in humans. Transcription at exon 1 produces cGSN mRNA whereas transcription at exon 3 produces pGSN mRNA. pGSN protein has an additional 25 amino acids sequence at its N-terminal region which is absent in the cGSN. UT, untranslated sequence; cGSN, cytoplasmic gelsolin; pGSN, plasma gelsolin.

cGSN undergoes CDDP-induced, caspase-3-mediated cleavage between residues Asp^{352} and Gly^{353}, resulting in the formation of C-terminus (C-cGSN; 41KDa) and N-terminus (N-cGSN; 39KDa) fragments and ultimately apoptosis in chemosensitive but not in chemoresistant cancer cells[192]. Forced expression of C-cGSN and its sub-fragments sensitize chemoresistant ovarian cancer to cisplatin *in vitro* through caspase-3-mediated cleavage and apoptosis[192]. CDDP down-regulates FLIP in chemosensitive OVCA cells thereby increasing apoptosis; this effect does not happen in chemoresistant OVCA cells[192]. CDDP dissociates cGSN from the GSN-FLIP-Itch complex in chemosensitive cells, thereby inducing FLIP ubiquitination and degradation, activation of caspase-8 and -3, caspase-3-mediated cleavage of cGSN, and apoptosis[192]. In the chemoresistant OVCA cells, CDDP fails to dislodge cGSN from the complex and hence CDDP-induced apoptosis is attenuated[192].

1.10.2 Plasma gelsolin (pGSN) and chemoresistance

pGSN, a secretory/soluble form of gelsolin, differs from the cGSN by a N-terminal 25-amino acid signalling peptide and a cysteine residue disulfide bond between positions 188 and 201, designated as the "plasma extension" signal[253,254] **(Fig. 1.7)**. The major sites for pGSN synthesis are the skeletal, cardiac and smooth muscles instead of the liver cells, which is a major organ that contributes to most circulating proteins[253,254]. pGSN is an extracellular actin scavenger which prevents actin toxicity and further life-threatening conditions[259]. Such risk may present in an array of clinical conditions such as acute respiratory distress syndrome[260,261], sepsis[261-263], major trauma[261,264,265], malaria[266,267] and liver injury[268]. GSN expression has been studied in breast[269], gastric[270], eosophageal[271], osteosarcoma[272] and liver[242] cancers and appeared regulated by BRCA1/2 and AKT signalling[269,272], methylation[270], and mir-200a targeting[242] and have been

implicated in TGF/EM transition[269]. Total GSN overexpression in gynaecologic cancers is significantly associated with chemoresistance, poor prognosis, aggressive behavior and cancer deaths; however, the role of pGSN (secreted form of GSN) remains elusive[192,257].

Elevated pGSN levels in the blood of colorectal patients and tissues of prostate cancer patients are significantly associated with distant organ metastasis[273] and disease progression[274] respectively. However, the mechanisms behind these phenomena have not been explored. Although pGSN is distributed by body fluids, little is known about its expression, secretion and interaction with immune cells in the tumour microenvironment. Despite the observation that pGSN interacts with cell surface proteins such as integrin[275], detail interactions and resulting effects are yet to be studied. Although the levels of pGSN are inversely proportional to T cells levels in the plasma of patients with burns, the detailed mechanism has not been demonstrated. As to whether pGSN promote OVCA cell survival and chemoresistance as well as suppress the functions of immune cells in the OVCA microenvironment remain to be determined.

CHAPTER 2 - RATIONALE, HYPOTHESIS AND OBJECTIVES

2 Rationale and background

OVCA is the most lethal gynecological cancer, due mainly to late diagnosis, recurrence and chemo-resistance[1,2]. The standard first line treatment for OVCA is a combination of surgical debulking and chemotherapy with cisplatin (CDDP) and taxane derivatives[3,4]. Although they are successful initially, chemoresistance is a major hurdle for long term therapeutic success, and there have not been significant change in the 5-year survival rate over the past 30 years[3,4]. The molecular mechanism of chemo-resistance is multi-factorial and is associated with evasion of apoptosis and impaired immunological response[5,6]. OVCA is considered a cold tumour hence, has poor immune cell infiltration[6]. Thus, immunotherapy has failed to be effective to date. There is still more to learn about the molecular contributors to chemoresistance in OVCA to afford new diagnosis and treatment.

Although gelsolin overexpression is significantly associated with chemoresistance, poor prognosis, aggressive behavior and cancer deaths, the role of pGSN (secreted form of GSN) remains elusive[7,8]. Elevated levels of pGSN in the plasma of colorectal and head-and-neck cancers are significantly correlated with tumour recurrence and poor prognosis[9]; however, the mechanism involved has not been reported. Although pGSN is distributed by body fluids, little is known about the regulation of its expression/secretion. As to whether pGSN expression is key to ovarian cancer chemoresistance remains to be determined.

TME is a strong contributing factor for chemoresistance[5]. In addition to tumour cells, the TME entails various cell types, including immune cells. Due to the coldness of OVCA (low infiltration of immune cells), patients are unresponsive to immunotherapy although melanoma, breast cancer and lung cancer patients respond well[6,10]. There is an urgent need for alternative

immunotherapies that target novel pathways responsible for the coldness of OVCA. Although pGSN is secreted into the blood during the normal physiologic state, its interaction with neighbouring immune cells remains to be examined. Whether there is a dysregulation in its interaction with cells which further contributes to OVCA progression and drug resistance is yet to be unveiled. We have yet to investigate the mechanistic role of pGSN in inhibiting the anti-tumour functions of infiltrated T cells and macrophages in OVCA chemoresistance. We expect that pGSN expression could serve as a novel target for elucidating the coldness of OVCA and also provide alternative means to improve patient survival.

Extracellular vesicles play a key role in cell-cell communication through surface interactions and transfer of proteins or nucleic acids and are involved in cancer progression, survival and metastasis[11-14]; however, their identity and precise role in OVCA chemoresistance is not well established. The secretion of extracellular vesicles from cancer cells could regulate the functions of neighboring cells, including immune cells[13,15]. We have yet to demonstrate if and how sEV-pGSN regulate immune cell functions such as T cells and macrophages *in vitro* and how this dysregulation contributes to OVCA chemoresistance

2.1 Overall objective

The **overall objective** of the proposed study is to determine if and how pGSN regulates chemosensitivity in OVCA.

2.2 Overall hypothesis

1. pGSN contributes to OVCA chemoresistance by;
    a. auto-regulating its own gene expression in an autocrine and paracrine manner;
    b. down-regulating the anti-tumor functions of immune cells
2. pGSN is a biomarker for early detection of OVCA and prognostic marker for residual disease and patient survival.

2.3 Specific Hypotheses and specific objectives

1. ***Hypothesis:*** pGSN promotes OVCA cell survival through both autocrine and paracrine mechanisms that confers CDDP resistance to chemosensitive OVCA cells.

   Objectives: To determine whether

    a. PGSN gene expression in OVCA cells is mediated via α5β1 integrin/AKT/HIF1α signaling cascade;
    b. HIF1α binds to the DNA promoter region of pGSN to prmote the endogenous expression of pGSN in OVCA cells;
    c. pGSN is secreted via small extracellular vesicles (sEVs);
    d. Chemoresistant OVCA cell-derived sEVs induce CDDP-resistance in otherwise chemosensitive OVCA cells via the activation of the α5β1 integrin/AKT/HIF1α signaling cascade.
2. ***Hypothesis:*** pGSN inhibits CD8+ T cell function and regulates GSH production to confer chemoresistance in OVCA.

   Objectives: To determine whether

a. sEVs containing pGSN induce the production of GSH which attenuate CDDP-induced death in OVCA cells;
b. Increased expression of pGSN in OVCA tissues is associated with poor anti-tumors effects of infiltrated CD8+ T cells;
c. Chemoresistant OVCA cell-derived sEVs containing pGSN induce caspase-3-dependent apoptosis in activated CD8+ T cells, a process that decreases its production of IFNγ.

3. ***Hypothesis:*** pGSN modulates ovarian inflammation and confers chemoresistance in OVCA by resetting the relative abundance and function of macrophage subtypes.

   Objectives: To determine whether

   a. Increased expression of pGSN in OVCA tissues is associated with poor anti-tumour effects of infiltrated M1 macrophages;
   b. Chemoresistant OVCA cell-derived sEVs containing pGSN induce caspase-3-dependent apoptosis in M1 macrophages as well as decrease the secretion of iNOS and TNFα.

4. ***Hypothesis:*** Pre-operative circulating pGSN is a favourable and independent biomarker for OVCA prognosis

   Objectives: To determine whether

   a. Increased levels of circulatory pGSN is indicative of early stage OVCA;
   b. Increased levels of circulating pGSN is predictive of sub-optimal residual disease.

CHAPTER 3 – ONCOGENE 39, 1600–1616 (2019)

(Formatted as per Oncogene requirements)

The Exosome-Mediated Autocrine and Paracrine Actions of Plasma Gelsolin in Ovarian Cancer Chemoresistance

Running Title: pGSN Overexpression Confers Resistance in OVCA

Meshach Asare-Werehene[1,2], Kiran Nakka[2,3], Arkadiy Reunov[4], Chen-Tzu Chiu[5], Wei-Ting Lee[5], Mohammad R. Abedini[2,7], Pei-Wen Wang[5], Dar-Bin Shieh[5,6], F. Jeffrey Dilworth[2,3], Euridice Carmona[8,9], Tien Le[1,2], Anne-Marie Mes- Masson[8,9], Dylan Burger[2,3], and Benjamin K Tsang[1,2,3]

[1]Departments of Obstetrics & Gynecology and Cellular & Molecular Medicine, University of Ottawa, Ottawa, Ontario, Canada;

[2]Chronic Disease Program and Regenerative Medicine Program, Ottawa Hospital Research Institute, Ottawa, Ontario, Canada K1H 8L6

[3]Departments of Medicine and Cellular & Molecular Medicine, University of Ottawa, Ottawa, Ontario, Canada;

[4]St. Francis Xavier University, Department of Biology, 2320 Notre Dame Avenue, Antigonish, NS, B2G 2W5, Canada;

[5]Institute of Basic Medical Science, Institute of Oral Medicine and Department of Stomatology, National Cheng Kung University Hospital, National Cheng Kung University, Tainan 704, Taiwan.

[6]Advanced Optoelectronic Technology Center and Center for Micro/Nano Science and Technology,

National Cheng Kung University, Tainan 701, Taiwan

[7]Cellular and Molecular Medicine Research Center, Department of Pharmacology, Birjand University of Medical Sciences, Birjand , 97178, Iran;

[8]Centre de recherche du CHUM et Institut du cancer de Montréal, Montréal, Québec, Canada H2X 0A9

[9]Department of Medicine, Université de Montréal, Montréal, Québec, Canada H3C 3J7

Correspondance: Dr. Benjamin K Tsang, Chronic Disease Program, Ottawa Hospital Research Institute, The Ottawa Hospital (General Campus), Ottawa, Canada K1H 8L6; Tel: 1-613-798-5555 ext 72926; Email: btsang@ohri.ca

Author Contributions: M.A.W. and B.K.T. conceived and designed the study. M.A.W. performed all experiments unless otherwise stated. K.N. and F.J.D. performed and analysed the ChIP data. M.A.W., B.K.T. and D.B. designed and performed extracellular vesicle isolation and data analysis. TEM and iEM were done by A.R. pGSN siRNA was designed and tested by C.-T.C., W.-T.L., P.-W.W and D.-B.S. M.A.W. analysed the data with scientific input from B.K.T., D.B., A.R., D.-B.S, M.R.A, E.C, T.L., A.M.M.M and F.J.D. E.C and A.M.M.M provided validated high grade serous ovarian cancer cell lines. M.A.W. wrote the paper with feedback from all authors.

SIGNIFICANCE

These findings support a novel role of pGSN in conferring platinum resistance in OVCA through autocrine and paracrine mechanisms which could help improve the design of effective therapeutics for chemoresistant OVCA patients.

Competing Interests: The authors declared no conflicts of interest.

ABSTRACT

Ovarian Cancer (OVCA) is the most lethal gynecological cancer, due predominantly to late presentation, high recurrence rate and common chemoresistance development. The expression of the actin-associated protein cytosolic gelsolin (GSN) regulates the gynaecological cancer cell fate resulting in dysregulation in chemosensitivity. In this study, we report that elevated expression of plasma gelsolin (pGSN), a secreted isoform of GSN and expressed from the same GSN gene, correlates with poorer overall survival and relapse-free survival in patients with ovarian cancer. In addition, it is highly expressed and secreted in chemoresistant OVCA cells than its chemosensitive counterparts. pGSN, secreted and transported via exosomes (Ex-pGSN), up-regulates HIF1α–mediated pGSN expression in chemoresistant OVCA cells in an autocrine manner as well as confers cisplatin resistance in otherwise chemosensitive OVCA cells. These findings support our hypothesis that exosomal pGSN promotes ovarian cancer cell survival through both autocrine and paracrine mechanisms which transform chemosensitive cells to resistant counterparts. Specifically, pGSN transported via exosomes is a determinant of chemoresistance in OVCA.

KEY WORDS

Plasma gelsolin (pGSN), ovarian cancer (OVCA), cisplatin (CDDP), chemoresistance, exosomes

INTRODUCTION

Chemoresistance is a major obstacle in the treatment of ovarian cancer, one of the most fatal gynaecological cancers. Although most patients initially respond to platinum based chemotherapy, about 70 – 80% of the tumour relapses and become resistant to treatment especially with the high grade serous (HGS) histological subtype[1]. The HGS subtype is considered the most fatal with the worst mortality compared to the other subtypes[2]. Platinum or taxane derivatives combined with cytoreduction are standard first-line treatment strategy for ovarian cancer; however, there has been no significant change in 5-year patient survival rate, due to high rate of tumour recurrence and chemoresistance[2]. It is therefore urgent to investigate novel targets and markers that are involved in OVCA recurrence and chemoresistance and how these affect patient survival. The molecular and cellular mechanisms underpinning chemoresistance is multifactorial, as it involves apoptosis evasion, aberrant expression and activation of survival factors, dysregulation of tumour suppressors and impairment of the immunological defence system[3-5].

Gelsolin (GSN), an 80 – 85KDa calcium-dependent multifunctional actin-binding protein, has two well characterized isoforms – cytoplasmic gelsolin (cGSN) and plasma gelsolin (pGSN)[6]. There are other isoforms which are less characterized. These isoforms are encoded by a single gene on chromosome 12 as a result of alternative splicing and different transcriptional initiation sites[6]. The extra 25 amino acid sequence at the N-terminal of pGSN is one of the main architectural differences that distinguish it from cGSN[7]. GSN forms a complex with FLICE-like inhibitory protein (FLIP) and Itch and stabilizes FLIP in a non-stress state, whereas cisplatin (CDDP) dissociates GSN from the complex in chemosensitive cells, thereby facilitating FLIP ubiquitination and degradation, caspase-3 activation, and GSN cleavage[8]. We have recently

shown that cGSN overexpression correlates with chemoresistance, poor prognosis, aggressive behaviour and cancer death[9], whereas the role of pGSN remains elusive.

pGSN is an extracellular actin scavenger with an average concentration at ~ 200-300 µg/ml, which is mostly produced by the muscle and distributed by body fluid[6,10-13]. pGSN has been implicated in various inflammatory disorders, injuries and bacterial infections[6,14] although its mechanistic involvement is poorly understood. High levels of pGSN have also been detected in the plasma/serum and tissues of head-and-neck, colorectal, prostate and breast cancers[13]; however, the exact mechanism is largely unknown. Although pGSN has been shown to interact with α5β1 integrin[15], the detailed interaction and its consequence on chemosensitivity in OVCA are yet to be studied. To date, there is no data on the possible role of pGSN in OVCA recurrence, suboptimal surgical debulking and chemoresistance.

Extracellular vesicles (EVs) play a key role in cell-cell communication through surface interactions and the transfer of proteins, nucleic acids and fatty acids[16-19]. Exosomes (EXs) are vesicles of approximately 30-100 nm in size and formed within endosomes by membrane invaginations, whereas microvesicles (MVs) range from 0.1 to 1.0 µm and are produced by membrane blebbing in cells under stress[17,18]. The secretion of EXs or MVs from cancer cells could regulate the functions of neighbouring cells, including non-cancerous or immune cells[17,19-21]. EVs are believed to play a role in cancer progression, survival and metastasis although their participation in cellular basis of chemoresistance in OVCA remains largely unknown[17]. Whether exosomes containing pGSN (Ex-pGSN) may be important in the regulation of chemosensitivity in neighbouring OVCA cells has not been reported. In this study, we report for the first time pGSN secretion and transport via exosomes, its functional interaction with HIF1α in an autocrine manner and conferring of cisplatin resistance in otherwise chemosensitive OVCA cells.

RESULTS

pGSN expression in ovarian cancer patients predicts clinical outcomes.

Using meta-analysis, we assessed the expression of pGSN with the 200696_s_ at probe (Supplementary Tables 1 and 2) in primary ovarian tumour (serous and endometrioid) in the context of the patient's clinical outcomes by interrogating publicly available gene expression datasets on an online Kaplan-Meier plotter ovarian cancer survival analysis (www.kmplot.com)[22]. pGSN gene expression was stratified by histological subtype (serous; serous and endometrioid), chemotherapeutic agents (platinum or platinum + taxol) and suboptimal surgical debulking (Fig. 1A) and correlated with progression free survival (PFS)[22]. In serous patients with treatments containing platinum derivatives, elevated expression of pGSN was significantly ($p = 0.044$) associated with shorter time for tumour recurrence (16.6 months) compared with patients with lower pGSN expression (18.27 months) (Fig. 1B). The tumour recurrence trend was similar in serous patients with treatments containing both platinum and taxol agents although the difference was not significant ($p = 0.069$; low pGSN, 17.38 months; high pGSN, 14.9) (Fig. 1B). Analysis of serous patients with suboptimal surgical debulking revealed that increased pGSN expression was significantly correlated with shorter time for tumour recurrence irrespective of treatment component [(platinum, $P = 0.024$; low pGSN, 15.01 months; high pGSN, 13 months), (platinum and taxol, $P = 0.0055$; low pGSN, 15.01 months; high pGSN, 11.93 months)] (Fig. 1C).

Our interrogation of both serous and endometroid datasets revealed that patients treated with platinum and taxol compounds and had elevated expression of pGSN experienced significantly shortened progression-free survival ($P = 0.015$; low pGSN, 18 months; high pGSN, 14.87 months) (Fig. 1D). However, no significant difference was observed in the same datasets

with treatments containing only platinum derivatives (P = 0.13; low pGSN, 19 months; high pGSN, 19.3 months) (Fig 1D). When the datasets (serous and endometrioid) were stratified using suboptimal surgical debulking and treatment containing platinum and taxol, there was significantly shorter time to occurence in patients with elevated levels of pGSN (P = 0.0025; low pGSN, 15.01 months; high pGSN, 11.93 months) (Fig. 1E). In the context of patients treated with platinum derivatives, we observed that elevated pGSN expression was associated with shorter PFS (14.9 months) compared to those with lower pGSN expression (PFS; 16.83 months) although the difference was not significant (P = 0.16) (Fig. 1E). The beeswarm plot further provided a visual view of the relative expression of pGSN in ovarian cancer patients dichotomized as either high or low (Fig. 1B-E; bottom panels). Although not shown by any figure, there were no significant differences between overall survival (OS) and pGSN levels irrespective of stratification. We therefore decided not to present the OS data in the current study.

pGSN content and secretion are higher in chemoresistant OVCA cells and are associated with decreased CDDP-induced apoptosis.

To examine the mechanistic action of pGSN in the regulation of chemosensitivity in OVCA cells, we compared the influence of CDDP on pGSN levels in chemosensitive and resistant OVCA cells of HGS subtype with various p53 mutational status and extended these investigations to include the OVCA of the endometrioid subtypes (see Supplementary Table 3). HGS [chemosensitive (OV2295 and OV4453) and chemoresistant (OV90, OV866 (2) and Hey] and Endometrioid [chemosensitive (A2780s and PA-1) and chemoresistant (A2780cp and SKOV-3)] OVCA cells were cultured with or without CDDP (10 μM; 24 h) and cellular and conditioned media contents of pGSN were assessed by WB and ELISA.

Supplementary Table 3.1: Target sequences for 200696_s_at probe and GSN transcript variant 1; mRNA (Isoform a; pGSN) sequence.

Probe Set Name	Probe X	Probe Y	Probe Interrogation Position	Probe Sequence	Target Strandedness
200696_s_at	310	575	2122	TGCTTCTGGACACCTGGGACCAGGT	Antisense
200696_s_at	702	477	2137	GGGACCAGGTCTTTGTCTGGGTTGG	Antisense
200696_s_at	451	343	2190	GAAGCCTTGACTTCTGCTAAGCGGT	Antisense
200696_s_at	613	621	2207	TAAGCGGTACATCGAGACGGACCCA	Antisense
200696_s_at	375	569	2266	TGAAGCAAGGCTTTGAGCCTCCCTC	Antisense
200696_s_at	509	297	2299	GCTGGTTCCTTGGCTGGGATGATGA	Antisense
200696_s_at	528	551	2321	TGATTACTGGTCTGTGGACCCCTTG	Antisense
200696_s_at	334	607	2398	TCACCGGTCAGTGCCTTTTGGAACT	Antisense
200696_s_at	611	229	2421	CTGTCCTTCCCTCAAAGAGGCCTTA	Antisense
200696_s_at	59	63	2436	AGAGGCCTTAGAGCGAGCAGAGCAG	Antisense
200696_s_at	204	381	2455	GAGCAGCTCTGCTATGAGTGTGTGT	Antisense

Homo sapiens gelsolin (GSN), transcript variant 1, mRNA (Isoform a); probe target sequences are highlighted in yellow.

```
   1 ccaccatggc tccgcaccgc cccgcgcccg cgctgctttg cgcgctgtcc ctggcgctgt
  61 gcgcgctgtc gctgcccgtc cgcgcggcca ctgcgtcgcg gggggcgtcc caggcggggg
 121 cgccccaggg gcgggtgccc gaggcgcggc ccaacagcat ggtggtggaa caccccgagt
 181 tcctcaaggc agggaaggag cctggcctgc agatctggcg tgtggagaag ttcgatctgg
 241 tgcccgtgcc caccaacctt tatggagact tcttcacggg cgacgcctac gtcatcctga
 301 agacagtgca gctgaggaac ggaaatctgc agtatgacct ccactactgg ctgggcaatg
 361 agtgcagcca ggatgagagc ggggcggccg ccatctttac cgtgcagctg gatgactacc
 421 tgaacggccg ggccgtgcag caccgtgagg tccagggctt cgagtcggcc accttcctag
 481 gctacttcaa gtctggcctg aagtacaaga aaggaggtgt ggcatcagga ttcaagcacg
 541 tggtacccaa cgaggtggtg gtgcagagac tcttccaggt caaagggcgg cgtgtggtcc
 601 gtgccaccga ggtacctgtg tcctgggaga gcttcaacaa tggcgactgc ttcatcctgg
 661 acctgggcaa caacatccac cagtggtgtg gttccaacag caatcggtat gaaagactga
 721 aggccacaca ggtgtccaag ggcatccggg acaacgagcg gagtggccgg gcccgagtgc
 781 acgtgtctga ggagggcact gagcccgagg cgatgctcca ggtgctgggc cccaagccgg
 841 ctctgcctgc aggtaccgag gacaccgcca aggaggatgc ggccaaccgc aagctggcca
 901 agctctacaa ggtctccaat ggtgcaggga ccatgtccgt ctccctcgtg gctgatgaga
 961 acccccttcgc ccaggggggcc ctgaagtcag aggactgctt catcctggac cacggcaaag
1021 atgggaaaat ctttgtctgg aaaggcaagc aggcaaacac ggaggagagg aaggctgccc
1081 tcaaaacagc ctctgacttc atcaccaaga tggactaccc caagcagact caggtctcgg
```

1141 tccttcctga gggcggtgag accccactgt tcaagcagtt cttcaagaac tggcgggacc

1201 cagaccagac agatggcctg ggcttgtcct acctttccag ccatatcgcc aacgtggagc

1261 gggtgccctt cgacgccgcc accctgcaca cctccactgc catggccgcc cagcacggca

1321 tggatgacga tggcacaggc cagaaacaga tctggagaat cgaaggttcc aacaaggtgc

1381 ccgtggaccc tgccacatat ggacagttct atggaggcga cagctacatc attctgtaca

1441 actaccgcca tggtggccgc caggggcaga taatctataa ctggcagggt gcccagtcta

1501 cccaggatga ggtcgctgca tctgccatcc tgactgctca gctggatgag gagctgggag

1561 gtacccctgt ccagagccgt gtggtccaag gcaaggagcc cgcccacctc atgagcctgt

1621 ttggtgggaa gcccatgatc atctacaagg gcggcacctc ccgcgagggc gggcagacag

1681 cccctgccag cacccgcctc ttccaggtcc gcgccaacag cgctggagcc acccgggctg

1741 ttgaggtatt gcctaaggct ggtgcactga actccaacga tgcctttgtt ctgaaaaccc

1801 cctcagccgc ctacctgtgg gtgggtacag gagccagcga ggcagagaag acgggggccc

1861 aggagctgct cagggtgctg cgggcccaac ctgtgcaggt ggcagaaggc agcgagccag

1921 atggcttctg ggaggccctg ggcgggaagg ctgcctaccg cacatcccca cggctgaagg

1981 acaagaagat ggatgcccat cctcctcgcc tctttgcctg ctccaacaag attggacgtt

2041 ttgtgatcga agaggttcct ggtgagctca tgcaggaaga cctggcaacg gatgacgtca

2101 tgcttctgga cacctgggac caggtctttg tctgggttgg aaaggattct caagaagaag

2161 aaaagacaga agccttgact tctgctaagc ggtacatcga gacggaccca gccaatcggg

2221 atcggcggac gcccatcacc gtggtgaagc aaggctttga gcctccctcc tttgtgggct

2281 ggttccttgg ctgggatgat gattactggt ctgtggaccc cttggacagg gccatggctg

2341 agctggctgc ctgaggaggg gcagggccca cccatgtcac cggtcagtgc cttttggaac

2401 tgtccttccc tcaaagaggc cttagagcga gcagagcagc tctgctatga gtgtgtgtgt

2461 gtgtgtgtgt tgtttctttt ttttttttt acagtatcca aaaatagccc tgcaaaaatt

2521 cagagtcctt gcaaaattgt ctaaaatgtc agtgtttggg aaattaaatc caataaaaac

2581 attttgaagt gtgaaaaaaa aaaaaaaaaa aaaaaaaaaa aaaaaaaaaa aaaaaaaaaa

2641 aaaaaaaaaa aaaaaaaaaa aaa

Supplementary Table 3.2: Target sequences for 214040_s_at probe and GSN transcript variant 4; mRNA (Isoform f) sequence.

Probe Set Name	Probe X	Probe Y	Probe Interrogation Position	Probe Sequence	Target Strandedness
214040_s_at	136	103	262	ACAGCATGGTGGTGGAACACCCCGA	Antisense
214040_s_at	627	313	265	GCATGGTGGTGGAACACCCCGAGTT	Antisense
214040_s_at	615	535	311	TGGCCTGCAGATCTGGCGTGTGGAG	Antisense
214040_s_at	407	319	317	GCAGATCTGGCGTGTGGAGAAGTTC	Antisense
214040_s_at	55	549	329	TGTGGAGAAGTTCGATCTGGTGCCC	Antisense
214040_s_at	360	235	353	CGTGCCCACCAACCTTTATGGAGAC	Antisense
214040_s_at	156	175	359	CACCAACCTTTATGGAGACTTCTTC	Antisense
214040_s_at	104	141	408	AAGACAGTGCAGCTGAGGAACGGAA	Antisense
214040_s_at	153	105	411	ACAGTGCAGCTGAGGAACGGAAATC	Antisense
214040_s_at	433	23	433	ATCTGCAGTATGACCTCCACTACTG	Antisense
214040_s_at	377	573	436	TGCAGTATGACCTCCACTACTGGCT	Antisense

Homo sapiens gelsolin (GSN), transcript variant 4, mRNA (Isoform f); probe target sequences are highlighted in yellow.

```
   1 ggaaccagct gagcgcagct ggacccagca gccgctgtct ccagtgccgc agcagcaggt
  61 agtgctcata gctctctttg tccagtgctt cggccttggt cccagcgcct tcccacggag
 121 cagcactctt caccctgcac agccttgtta ggagaagggg atgaatgaat acaggactta
 181 cgcgtctgct gtggcccagc tggcttccag atggtgacat gagccaccca cagccggagc
 241 tgttcctctt tcccaaagct cagcccaaca gcatggtggt ggaacacccc gagttcctca
 301 aggcagggaa ggagcctggc ctgcagatct ggcgtgtgga gaagttcgat ctggtgcccg
 361 tgcccaccaa cctttatgga gacttcttca cgggcgacgc ctacgtcatc ctgaagacag
 421 tgcagctgag gaacggaaat ctgcagtatg acctccacta ctggctgggc aatgagtgca
 481 gccaggatga gagcggggcg gccgccatct ttaccgtgca gctggatgac tacctgaacg
 541 gccgggccgt gcagcaccgt gaggtccagg gcttcgagtc ggccaccttc ctaggctact
 601 tcaagtctgg cctgaagtac aagaaaggag gtgtggcatc aggattcaag cacgtggtac
 661 ccaacgaggt ggtggtgcag agactcttcc aggtcaaagg gcggcgtgtg gtccgtgcca
 721 ccgaggtacc tgtgtcctgg gagagcttca acaatggcga ctgcttcatc ctggacctgg
 781 gcaacaacat ccaccagtgg tgtggttcca acagcaatcg gtatgaaaga ctgaaggcca
 841 cacaggtgtc caagggcatc cgggacaacg agcggagtgg ccgggcccga gtgcacgtgt
 901 ctgaggaggg cactgagccc gaggcgatgc tccaggtgct gggccccaag ccggctctgc
 961 ctgcaggtac cgaggacacc gccaaggagg atgcggccaa ccgcaagctg gccaagctct
1021 acaaggtctc caatggtgca gggaccatgt ccgtctccct cgtggctgat gagaacccct
1081 tcgcccaggg ggccctgaag tcagaggact gcttcatcct ggaccacggc aaagatggga
1141 aaatctttgt ctggaaaggc aagcaggcaa acacggagga gaggaaggct gccctcaaaa
```

1201 cagcctctga cttcatcacc aagatggact accccaagca gactcaggtc tcggtccttc

1261 ctgagggcgg tgagacccca ctgttcaagc agttcttcaa gaactggcgg gacccagacc

1321 agacagatgg cctgggcttg tcctaccttt ccagccatat cgccaacgtg gagcgggtgc

1381 ccttcgacgc cgccaccctg cacacctcca ctgccatggc cgcccagcac ggcatggatg

1441 acgatggcac aggccagaaa cagatctgga gaatcgaagg ttccaacaag gtgcccgtgg

1501 accctgccac atatggacag ttctatggag gcgacagcta catcattctg tacaactacc

1561 gccatggtgg ccgccagggg cagataatct ataactggca gggtgcccag tctacccagg

1621 atgaggtcgc tgcatctgcc atcctgactg ctcagctgga tgaggagctg ggaggtaccc

1681 ctgtccagag ccgtgtggtc caaggcaagg agcccgccca cctcatgagc ctgtttggtg

1741 ggaagcccat gatcatctac aagggcggca cctcccgcga gggcgggcag acagcccctg

1801 ccagcacccg cctcttccag gtccgcgcca acagcgctgg agccacccgg gctgttgagg

1861 tattgcctaa ggctggtgca ctgaactcca acgatgcctt tgttctgaaa acccccctcag

1921 ccgcctacct gtgggtgggt acaggagcca gcgaggcaga gaagacgggg gcccaggagc

1981 tgctcagggt gctgcgggcc caacctgtgc aggtggcaga aggcagcgag ccagatggct

2041 tctgggaggc cctgggcggg aaggctgcct accgcacatc cccacggctg aaggacaaga

2101 agatggatgc ccatcctcct cgcctctttg cctgctccaa caagattgga cgttttgtga

2161 tcgaagaggt tcctggtgag ctcatgcagg aagacctggc aacggatgac gtcatgcttc

2221 tggacacctg ggaccaggtc tttgtctggg ttggaaagga ttctcaagaa gaagaaaaga

2281 cagaagcctt gacttctgct aagcggtaca tcgagacgga cccagccaat cgggatcggc

2341 ggacgcccat caccgtggtg aagcaaggct ttgagcctcc ctcctttgtg ggctggttcc

2401 ttggctggga tgatgattac tggtctgtgg acccccttgga cagggccatg gctgagctgg

2461 ctgcctgagg aggggcaggg cccacccatg tcaccggtca gtgccttttg gaactgtcct

2521 tccctcaaag aggccttaga gcgagcagag cagctctgct atgagtgtgt gtgtgtgtgt

2581 gtgttgtttc ttttttttt ttttacagta tccaaaaata gccctgcaaa aattcagagt

2641 ccttgcaaaa ttgtctaaaa tgtcagtgtt tgggaaatta aatccaataa aaacattttg

2701 aagtgtg

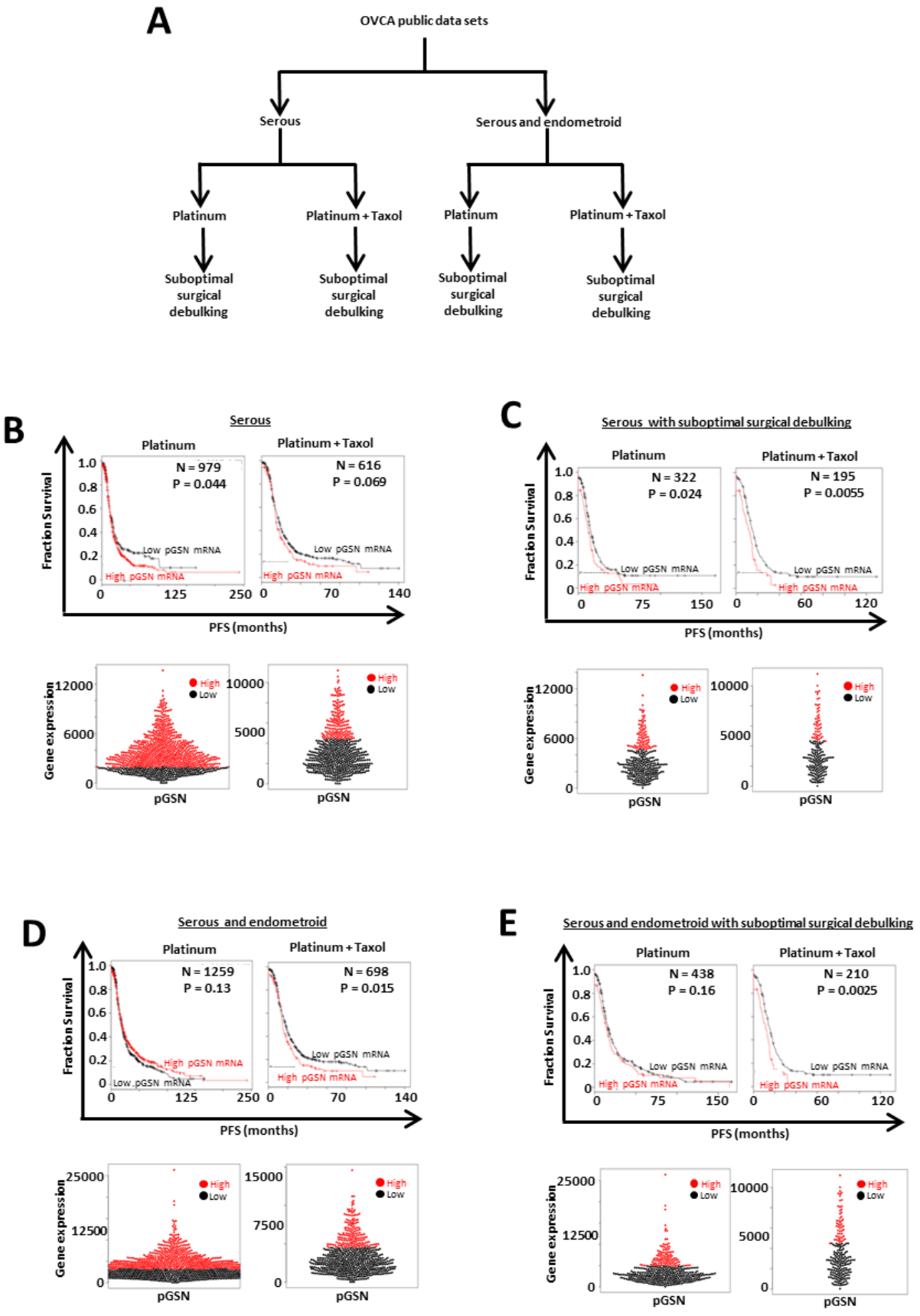
A
OVCA public data sets
Serous
Serous and endometroid
Platinum
Platinum + Taxol
Platinum
Platinum + Taxol
Suboptimal surgical debulking
Suboptimal surgical debulking
Suboptimal surgical debulking
Suboptimal surgical debulking
B
Serous
Platinum
Platinum + Taxol
N = 979
P = 0.044
N = 616
P = 0.069
Fraction Survival
Low pGSN mRNA
High pGSN mRNA
PFS (months)
Gene expression
High
Low
pGSN
C
Serous with suboptimal surgical debulking
Platinum
Platinum + Taxol
N = 322
P = 0.024
N = 195
P = 0.0055
D
Serous and endometroid
Platinum
Platinum + Taxol
N = 1259
P = 0.13
N = 698
P = 0.015
E
Serous and endometroid with suboptimal surgical debulking
Platinum
Platinum + Taxol
N = 438
P = 0.16
N = 210
P = 0.0025

Fig. 3.1 High pGSN expression is associated with tumour recurrence in patients with ovarian cancer. (A) Ovarian cancer public data sets were stratified using histological subtype (serous and endometrioid), chemotherapeutic agents and suboptimal surgical debulking. Kaplan–Meier survival analysis and beeswarm plots with optimal cutoff values of pGSN expression were performed on **(B)** only serous patients, **(C)** serous and endometrioid patients, **(D)** serous patients with suboptimal surgical debulking and **(E)** serous and endometroid patients with suboptimal surgical debulking with treatments containing either platinum or platinum + taxol. *P*-values were calculated by the log–rank test.

Supplementary Table 3.3 Information on OVCA cell lines

Cell line	Tumour origin	TP53 status	Other	Chemosensitivity
A2780s	Ovarian endometroid adenocarcinoma	Wild type	PTEN/ARID1A	Sensitive
A2780cp	Ovarian endometroid adenocarcinoma	Mutant V127F, R260S	PTEN/ARID1A	Resistant
SKOV3	Ovarian endometroid adenocarcinoma	Null	PI3KCIA/ARID1A	Resistant
PA-1	Ovarian endometroid adenocarcinoma	Wild type	None Detected	Sensitive
Hey	Ovarian serous cyst adenocarcinoma	Wild type	KRAS	Resistant
OV2295	High grade serous ovarian cancer	Mutant IIe195Thr	Non Detected	Sensitive
OV4453	High grade serous ovarian cancer	Mutant Splice	None Detected	Sensitive
OV90	High grade serous ovarian cancer	Mutant Ser215Arg	None Detected	Resistant
OV866(2)	High grade serous ovarian cancer	Mutant Arg249Trp	None Detected	Resistant

Information on OVCA cell lines: The characterization of these cell lines has been verified in previous literature (Anglesio *et al*.,2013; Leroy *et al*., 2014; Provencher *et al*., 2000; Fleury *et al*., 2015; Letourneau *et al*., 2012).

Cellular and secreted pGSN in the resistant HGS cells (OV90, Hey, OV866 (2)) were not affected by CDDP treatment although their contents decreased in the chemosensitive HGS cell lines (OV2295, OV4453) (Fig. 2A, Fig. S1A). CDDP induced apoptosis in the chemosensitive HGS cells but not the resistant phenotypes (Fig. 2A, Fig. S1A). Likewise, pGSN content in OVCA cells of endometroid subtypes was expressed and secreted in larger amounts in the chemoresistant cells than their sensitive counterparts, irrespective of their p53 status (Fig. 2B, Fig. S1B-C, Fig. S2). CDDP decreased cellular and secreted pGSN contents in the CDDP-sensitive cells but not in the resistant cells (Fig. 2A-B, Fig. S1, Fig. S2). CDDP induced concentration-dependent apoptosis in chemosensitive cells but not in the resistant cells (***$p < 0.001$) (Fig. 2A-B, Fig. S1) suggesting a possible association between pGSN overexpression and OVCA chemoresistance.

pGSN is involved in the regulation of CDDP sensitivity in OVCA cells.

To further examine whether CDDP responsiveness of OVCA cells is regulated by pGSN, chemoresistant OVCA cells [OV866 (2) (Fig. 2C), Hey (Fig. S3A) and A2780cp (Fig. 2D, Fig. S3B) were transfected with either pGSN or scramble (control) small interfering RNAs (siRNA; 50 nM; 24 h) and treated with CDDP (0 and 10 µM; 24 h) to determine if pGSN knockdown would sensitize the chemoresistant OVCA cells to CDDP-induced apoptosis. pGSN knockdown resulted in the sensitization of the resistant cells to CDDP-induced apoptosis (10 µM; Fig. 2C-D, Fig. S3B; ***$p < 0.001$). Moreover, chemosensitive OV2295 and A2780s cells transfected with pGSN cDNA (empty vector as control; 1 µg; 24 h) and subsequently treated with CDDP (0 and10 µM; 24 h) exhibited significant attenuation in CDDP-induced apoptotic response (***$p < 0.001$; Fig. 2E-F). A2780cp cells treated with GSN siRNA (known to down-regulate both cGSN and pGSN) was reconstituted with rhpGSN and then treated with CDDP. pGSN content in

A2780cp cells was significantly decreased (both in the cells and conditioned media) by GSN siRNA and also sensitized the resistant cells to CDDP-induced apoptosis (10 μM; ***$p < 0.001$; Fig. 2G). rhpGSN reconstitution (10 μM; 24 h) attenuated CDDP-induced apoptosis in A2780cp cells in which GSN was knocked down (Fig. 2G), suggesting that the anti-apoptosis response of GSN was primarily that of the pGSN. Taken together, these findings suggest that pGSN plays a key role in OVCA responsiveness to CDDP and its down-regulation may present as an opportunity to sensitize chemoresistant OVCA cells to CDDP-induced apoptosis.

pGSN is transported by exosomes which auto-upregulate pGSN content through α5β1 integrin signaling.

To investigate the mode of secretion and extracellular transport of pGSN, chemosensitive (OV2295, OV4453, A2780s, PA-1) and chemoresistant (OV90, OV866(2), A2780cp, Hey) OVCA cells were cultured in the absence and presence of CDDP (10 μM; 24 h) and extracellular vesicles (exosomes and microparticles) in conditioned media were isolated and characterized by WB, NTA, and iEM. Although both the sensitive and resistant cells secreted both types of extracellular vesicles (Fig. 3A-C, Fig. S4A-B), the resistant cells secreted significantly more exosomes compared to their sensitive counterparts (Fig. 3D-E); regardless of the CDDP sensitivity of the cells.

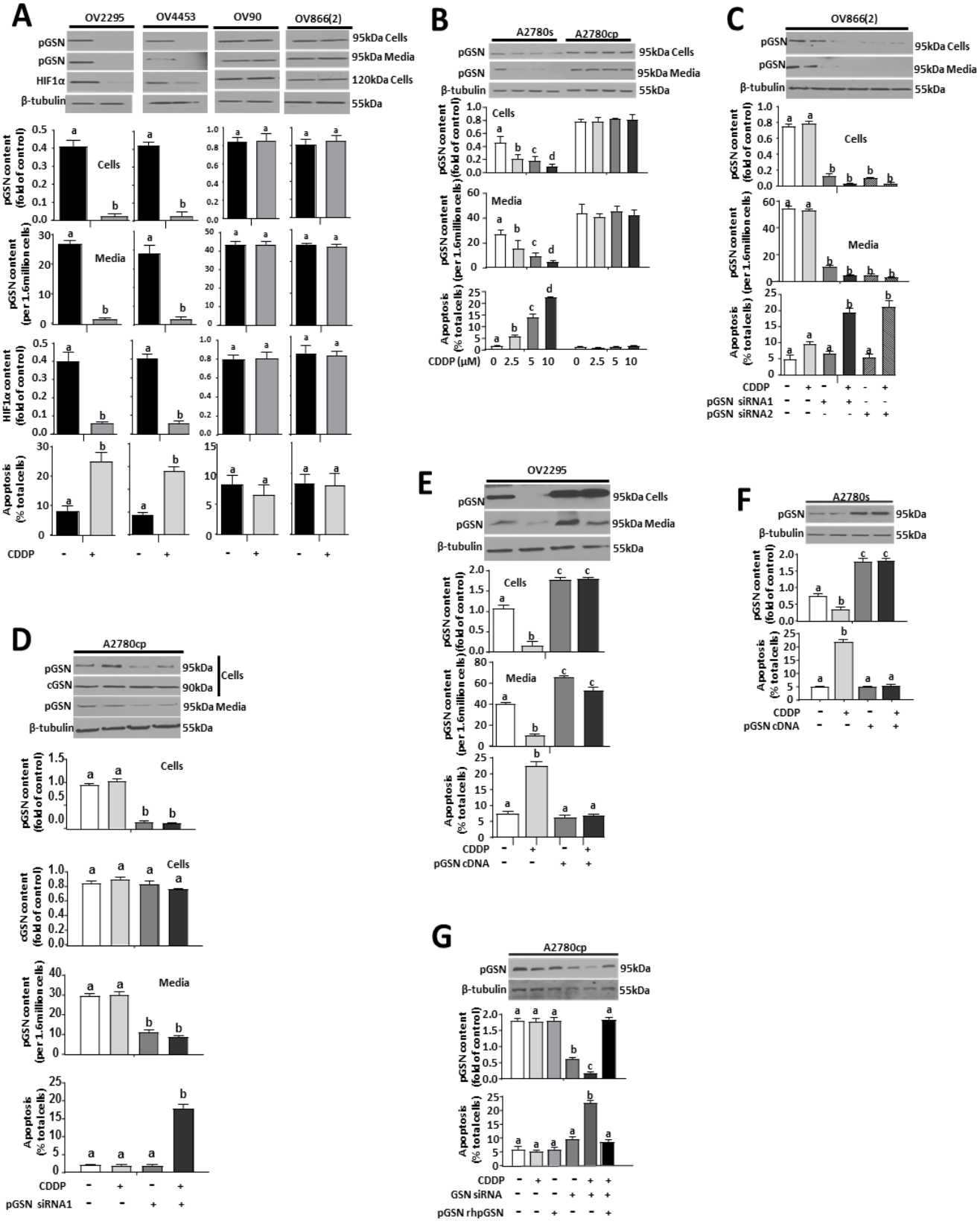
A
OV2295
OV4453
OV90
OV866(2)
pGSN
pGSN
HIF1α
β-tubulin
95kDa Cells
95kDa Media
120kDa Cells
55kDa
pGSN content (fold of control)
Cells
pGSN content (per 1.6million cells)
Media
HIF1α content (fold of control)
Apoptosis (% total cells)
CDDP
B
A2780s
A2780cp
pGSN
pGSN
β-tubulin
95kDa Cells
95kDa Media
55kDa
Cells
Media
Apoptosis (% total cells)
CDDP (μM) 0 2.5 5 10 0 2.5 5 10
C
OV866(2)
pGSN
pGSN
β-tubulin
95kDa Cells
95kDa Media
55kDa
Cells
Media
Apoptosis (% total cells)
CDDP
pGSN siRNA1
pGSN siRNA2
D
A2780cp
pGSN
cGSN
pGSN
β-tubulin
95kDa
90kDa
95kDa Media
55kDa
Cells
pGSN content (fold of control)
cGSN content (fold of control)
Cells
pGSN content (per 1.6million cells)
Media
Apoptosis (% total cells)
CDDP
pGSN siRNA1
E
OV2295
pGSN
pGSN
β-tubulin
95kDa Cells
95kDa Media
55kDa
Cells
pGSN content (fold of control)
Media
pGSN content (per 1.6million cells)
Apoptosis (% total cells)
CDDP
pGSN cDNA
F
A2780s
pGSN
β-tubulin
95kDa
55kDa
pGSN content (fold of control)
Apoptosis (% total cells)
CDDP
pGSN cDNA
G
A2780cp
pGSN
β-tubulin
95kDa
55kDa
pGSN content (fold of control)
Apoptosis (% total cells)
CDDP
GSN siRNA
pGSN rhpGSN

Fig. 3.2 pGSN regulates CDDP-induced apoptosis in OVCA cells. (A and B) CDDP decreased pGSN content and induced apoptosis in chemosensitive (OV2295, OV443, A2780s) but not chemoresistant (OV90, OV866(2), A2780cp) OVCA cells. OVCA cells were cultured with or without CDDP (10 μM; 24 h). **(C, D)** Silencing pGSN in OV866(2) and A2780cp cells sensitized them to CDDP-induced apoptosis. OV86692) and A2780cp cells were transfected with pGSN siRNA (50 nM, 24 h; which specifically knocked down pGSN but not cGSN) and then treated with or without CDDP (10 μM; 24 h). **(E, F)** Over-expression of pGSN cDNA attenuated CDDP-induced apoptosis in OV2295 and A2780s cells. OV2295 and A2780s cells were transfected with pGSN cDNA (2 μg; 24 h) and cultured with or without CDDP (10 μM; 24 h). **(G)** A2780cp (with total GSN knocked down) were cultured with rhpGSN (10 μM; 24 h) before treatment with CDDP (0 and 10 μM; 24 h). pGSN, cGSN and β-tubulin (loading control) contents were assessed by Western blotting (WB) and apoptosis determined morphologically by Hoechst 33258 DNA staining. *[**A**, (a; ***p<0.001 vs b, c and d); **B**, (a; ***p<0.001 vs b); **C**, (a; ***p<0.001 vs b and c); **D**, (a; ***p<0.001 vs b); **E**, (a; ***p<0.001 vs b and c); **F**, (a; ***p<0.001 vs b and c); **G**, (a; ***p<0.001 vs b and c);]*. N = 3.

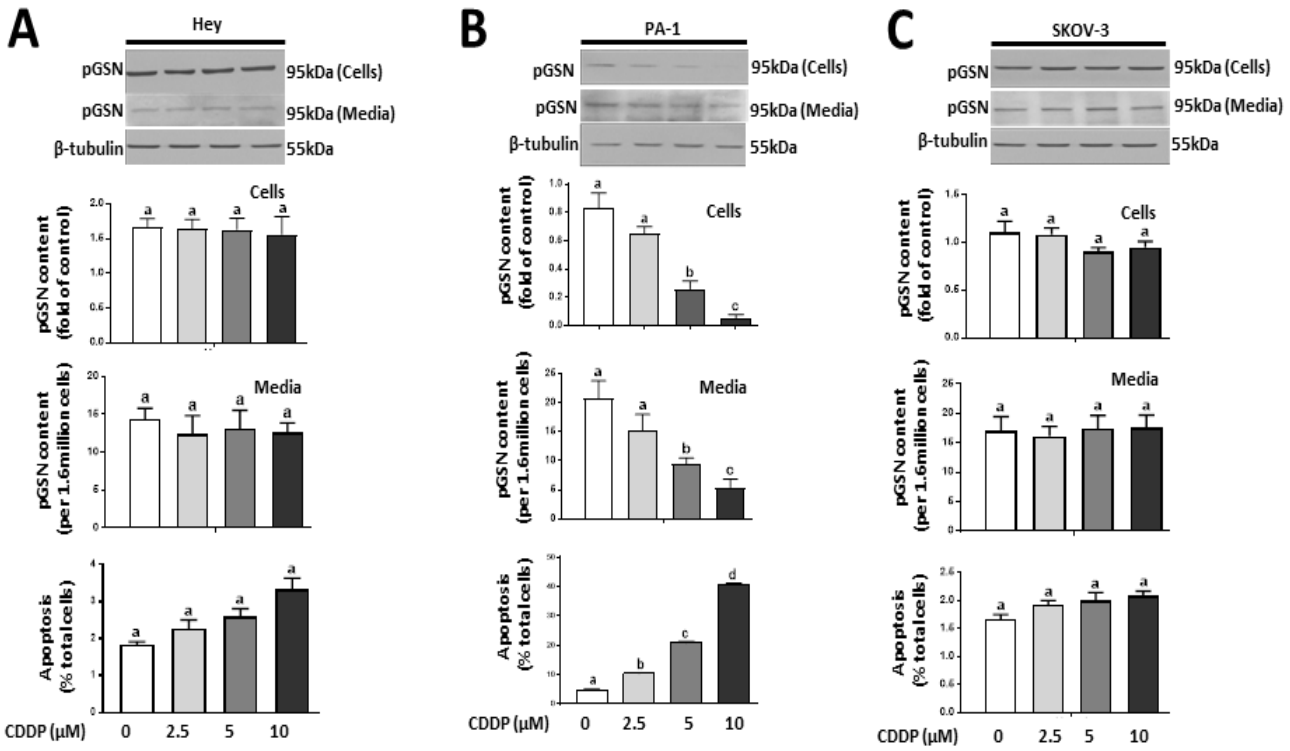

Fig. 3.S1 CDDP decreases pGSN content in the chemosensitive cells but not their resistant counterparts. (A – C) Hey, PA-1 and SKOV-3 cells were cultured with or without CDDP (10 μM; 24 h). pGSN contents in conditioned media and cell lysates were assessed by WB. β-tubulin was used as a loading control. CDDP-induced apoptosis was analysed morphologically using Hoechst DNA staining. ***[B,** (a; ***p<0.001 vs b, c and d)]*. N = 3

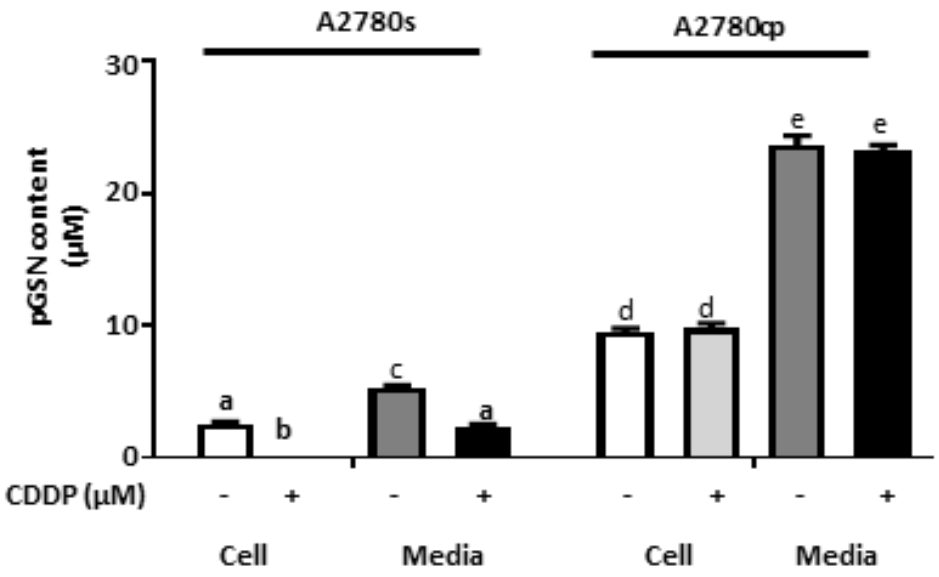

Fig. 3.S2 Higher levels of pGSN are secreted than retained in OVCA cells *in vitro*. A2780s and A2780cp cells were cultured with or without CDDP (10 μM; 24 h). Conditioned media and cell lysates were processed for pGSN detection by sandwich ELISA. *[(a; ***p<0.001 vs b, c, d and e)]*. N = 3

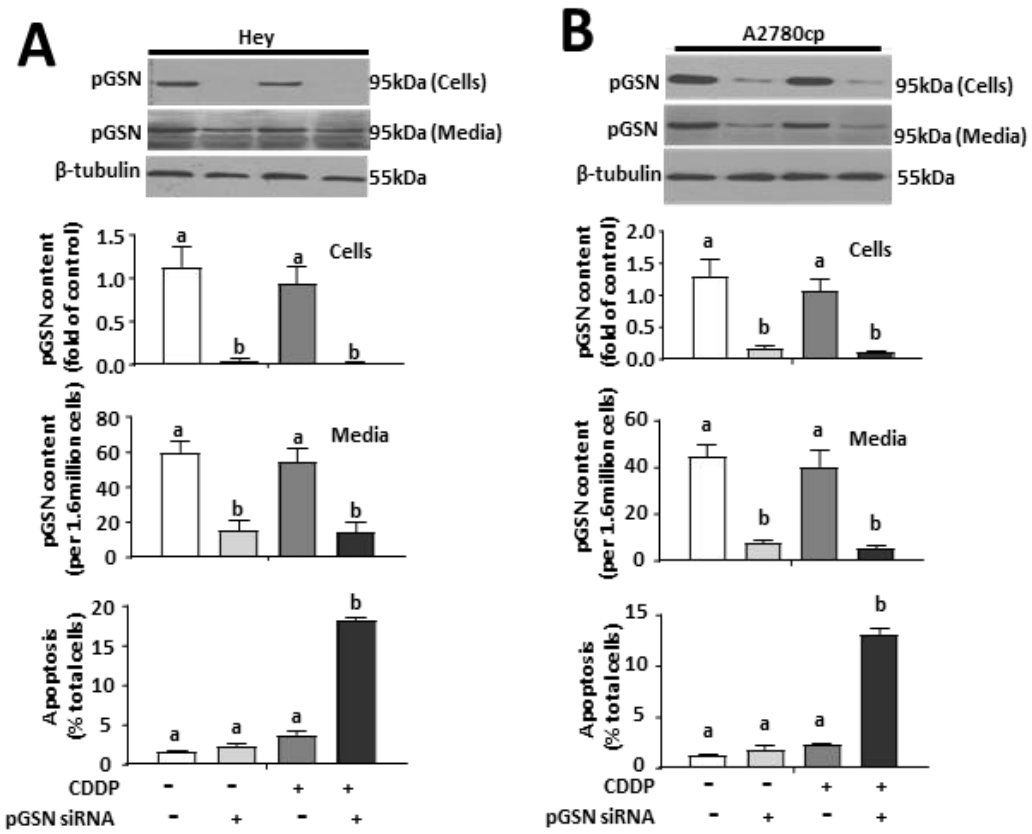

Fig. 3.S3 GSN knock-down sensitizes chemoresistant cells to CDDP-induced apoptosis. Hey **(A)** and A2780cp **(B)** cells were transfected with total pGSN siRNA (50 nM; 24 h) and then cultured with or without CDDP (10 µM; 24 h). Cell lysates and conditioned media were collected and pGSN and β-tubulin (loading control) contents assessed by WB. CDDP-induced apoptosis was analysed morphologically using Hoechst DNA staining. *[**A**, (a; ***p<0.001 vs b); **B**, (a; ***p<0.001 vs b)]*. N = 3

Exosome secretion was not affected by CDDP (Fig. 3C-E). Microparticles blebbed from the cell membrane with an average size of 500 nm whereas exosomes were formed in multivesicular bodies with an average size of 100 nm. pGSN was detected in both exosomes and microparticles using 18-nm colloidal gold particles (Fig. 3G). Chemoresistant cells-derived exosomes contained increased levels of pGSN compared with microparticles (Fig. 3F). Exosomal pGSN was secreted in greater amounts in the resistant cells compared to their sensitive counterparts (Fig. 3F).

Despite the observation that pGSN interacts with α5β1 integrin receptor [15], whether and how this interaction regulates chemosensitivity in OVCA remains to be demonstrated. To investigate this possibility, A2780s cells were treated with the α5β1 integrin inhibitor ATN 161 (0 and 40 μM; 3 h) or FAK siRNA (0 and 20 pmol; 24 h) before treatment with exosome containing pGSN (Ex-pGSN; 40 μg; 24 h) or exogenous human recombinant pGSN (rhpGSN; 10 μM; 24 h) (Fig. 4A-C). Ex-pGSN and exogenous pGSN significantly increased the contents of endogenous pGSN and HIF1α; however, these responses were attenuated by the presence of the α5β1 integrin receptor antagonist and FAK down-regulation (Fig. 4A-C). The downregulation of endogenous pGSN also resulted in decreased levels of secreted pGSN (Fig. 4A-C). This is suggestive that the α5β1 integrin signaling pathway is involved in the autocrine-mediated up-regulation of endogenous pGSN content.

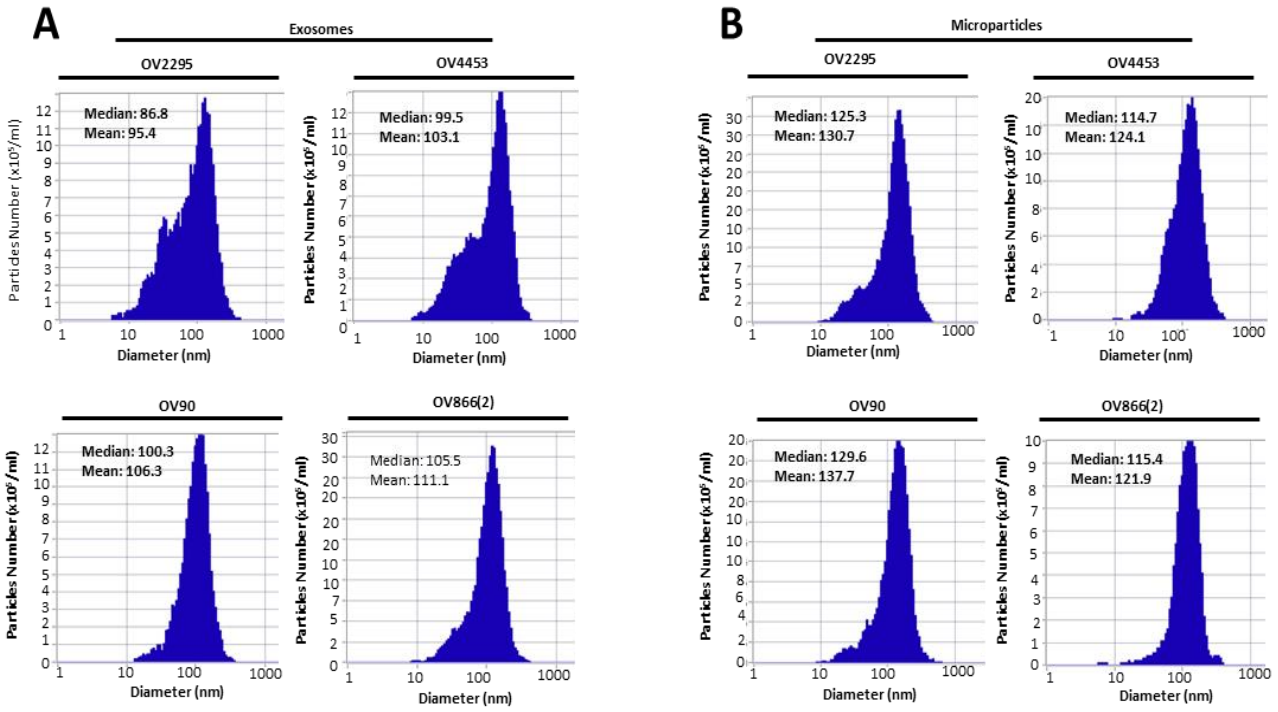
A
Exosomes
OV2295
Median: 86.8
Mean: 95.4
OV4453
Median: 99.5
Mean: 103.1
OV90
Median: 100.3
Mean: 106.3
OV866(2)
Median: 105.5
Mean: 111.1
Particles Number (x10⁶/ml)
Diameter (nm)
B
Microparticles
OV2295
Median: 125.3
Mean: 130.7
OV4453
Median: 114.7
Mean: 124.1
OV90
Median: 129.6
Mean: 137.7
OV866(2)
Median: 115.4
Mean: 121.9

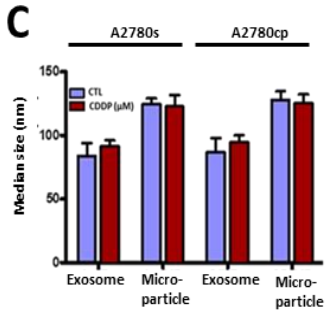
C
A2780s
A2780cp
CTL
CDDP (μM)
Median size (nm)
Exosome
Micro-particle
Exosome
Micro-particle

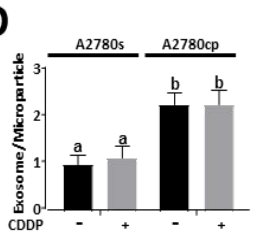
D
A2780s
A2780cp
Exosome/Microparticle
CDDP

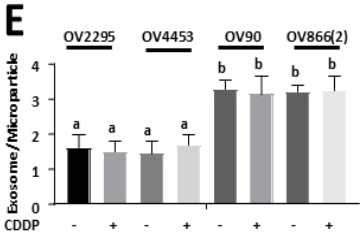
E
OV2295
OV4453
OV90
OV866(2)
Exosome/Microparticle
CDDP

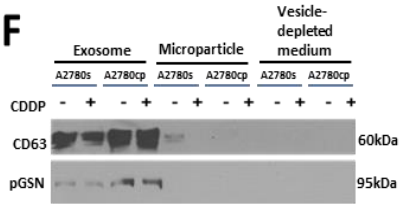
F
Exosome
Microparticle
Vesicle-depleted medium
A2780s
A2780cp
CDDP
CD63
60kDa
pGSN
95kDa

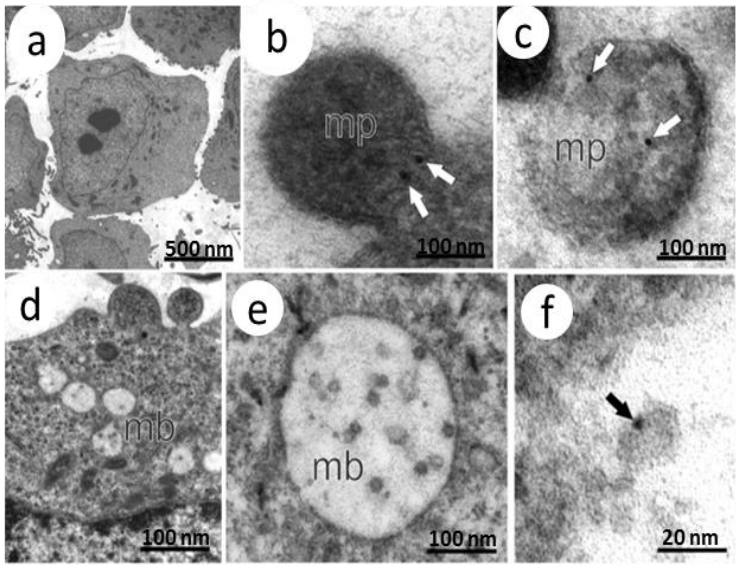
G
a
500 nm
b
mp
100 nm
c
mp
100 nm
d
mb
100 nm
e
mb
100 nm
f
20 nm

Fig. 3.3 Extracellular vesicle characterization and CDDP effect on vesicle size distribution. HGS chemosensitive and resistant cells secrete exosomes **(A)** and microparticles **(B)** as confirmed by nanoparticle tracking. **(C)** A2780s and A2780cp cells secrete both exosomes and microparticles. OVCA cells were cultured with or without CDDP (10 μM; 24 h). Exosomes and microparticles were isolated from their conditioned media by ultracentrifugation and characterized by Nanoparticle Tracking Analyser. **(D and E)** The exosome-to-microparticle ratio is higher in chemoresistant cells compared to chemosensitive cells; their concentrations were not affected by CDDP treatment. **(F)** pGSN is predominantly identified in the exosomes compared to microparticles of A2780s and A2780cp; however, pGSN content is higher in the A2780cp cells compared to A2780s cells. Exosomes and microparticles were isolated as described above and pGSN and CD63 (exosome marker) contents assessed by WB. **(G)** Electron micrograph showing pGSN in microparticles (mp) and multivesicular bodies/exosomes (mb); white and black arrows showing pGSN in mp and mb respectively. pGSN in fixed A2780cp cells was immunostained with 18-nm colloidal gold particles, observed and photographed with a Jeol JEM 1230 transmission electron microscope. Scale bars, 500 nm (a), 100 nm (b, c, d, e) and 20 nm (f). *[**D**, (a; **p<0.01 vs b); **E**, (a; **P<0.01 vs b)]*. N = 3

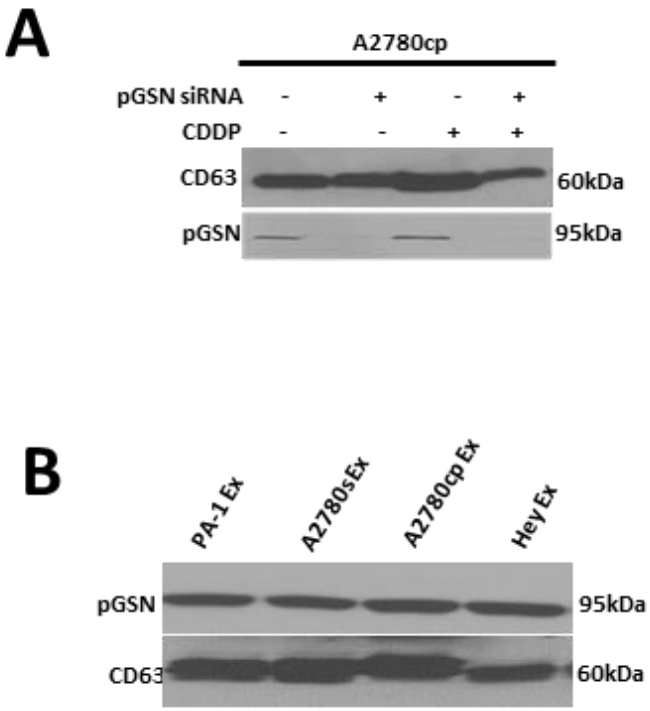

Fig. 3.S4. pGSN is detectable in both chemosensitive and chemoresistant OVCA cell lines and could be successfully knocked-down (KD) in exosomes from chemoresistant cells. (A) pGSN in A2780cp cells was transfected with siRNA (50 nM; 24 h) cultured with and without CDDP (10 µM; 24 h). pGSN knock down was confirmed using WB. **(B)** Exosomes from the conditioned media of PA-1, A2780s, A2780cp and Hey cell lines were isolated and characterized as previously described. Exosome marker (CD63) and pGSN contents were assessed by WB.

Akt and HIF1α up-regulation promotes the expression and anti-apoptotic action of pGSN on CDDP-induced apoptosis.

As observed with pGSN, HIF1α was also highly expressed in the resistant cells compared to their sensitive counterparts; CDDP decreased HIF1α content and induced apoptosis in the CDDP-sensitive but not resistant cells (Fig. 4D). HIF1α down-regulation by siRNA (200 pmol; 24 h) decreased pGSN content in A2780cp cells and sensitized them to CDDP-induced apoptosis ($P < 0.001$) (Fig. 4E). We further analyzed the possibility that the expression and anti-apoptotic action of pGSN may be mediated by Akt and HIF1α. Triple mutant dominant negative Akt (DN-Akt), A2780cp and A2780s cells constitutively expressing an activated Akt (A-Akt) and their respective control cells with empty vectors were cultured with and without CDDP (10 μM; 24 h) to examine the regulatory role of Akt in HIF1α and pGSN contents, as well as apoptotic response to CDDP. Up-regulating Akt function in the chemosensitive cells by forced expression of activated Akt significantly increased contents of HIF1α and pGSN and attenuated CDDP-induced apoptosis (Fig. 5A). In contrast, Akt down-regulation in the chemoresistant cells by DN-Akt expression resulted in decreased pGSN and HIF1α contents and facilitated CDDP-induced apoptosis (Fig. 5B).

CDDP-induced proteasomal degradation of HIFlα regulates the pGSN content.

To demonstrate if changes in HIF1α stability may influence the regulation of pGSN content, we treated A2780s cells with the proteasomal degradation inhibitor epoxomycin (10 nM; 3 h prior to CDDP treatment) or ΔHIF1α cDNA [with the degradation domain mutated (1 μg; 24 h)] and then treated with or without CDDP (10 μM; 24 h). Inhibition of HIF1α degradation by Epoxomycin (Fig. 5C) or forced expression of non-degradable mutant HIF1α (Fig. 5D) in the chemosensitive cells resulted in increased pGSN content and attenuated CDDP-

induced apoptosis. When HIF1α was down-regulated in the resistant cells (A2780cp) in the presence of 1-methyl PA (10 μM; 3 h), a pharmacological inducer of HIF1α degradation, pGSN content was reduced and the resistant cells were sensitized to CDDP-induced apoptosis (Fig. 5E). These findings suggest that CDDP regulates the pGSN content and the responsiveness of OVCA cells by modulating proteasomal HIF1α degradation.

Chemoresistant cells-derived exosomes induce CDDP resistance to chemosensitive OVCA cells by upregulating pGSN contents.

We have examined the possibility that pGSN in chemoresistant cells-derived exosomes induces CDDP resistance in chemosensitive OVCA cells. A2780s, OV2295 and OV4453 (target cells) were co-cultured with chemosensitive and chemoresistant OVCA cells (CDDP; 10 μM; Fig. 6A), conditioned media (Fig. 6B; 3 ml, 24 h) or exosomes (Fig. 6C-G; 40 μg/400,000 cells, 24 h). Chemoresistant-derived conditioned media and exosomes induced upregulation of pGSN content and CDDP resistance in chemosensitive OVCA cells. Immunofluorescent studies with A2780s (target cells) tagged with PKH26 (red fluorophore) and exosomes tagged with GFP indicated that exosomes were taken up by the cells irrespective of the chemosensitivity of the OVCA cells from which the spent media or exosomes were derived, indicating that the observed phenomenon was not due to differential uptake of the exosomes (Fig. 6D-G).

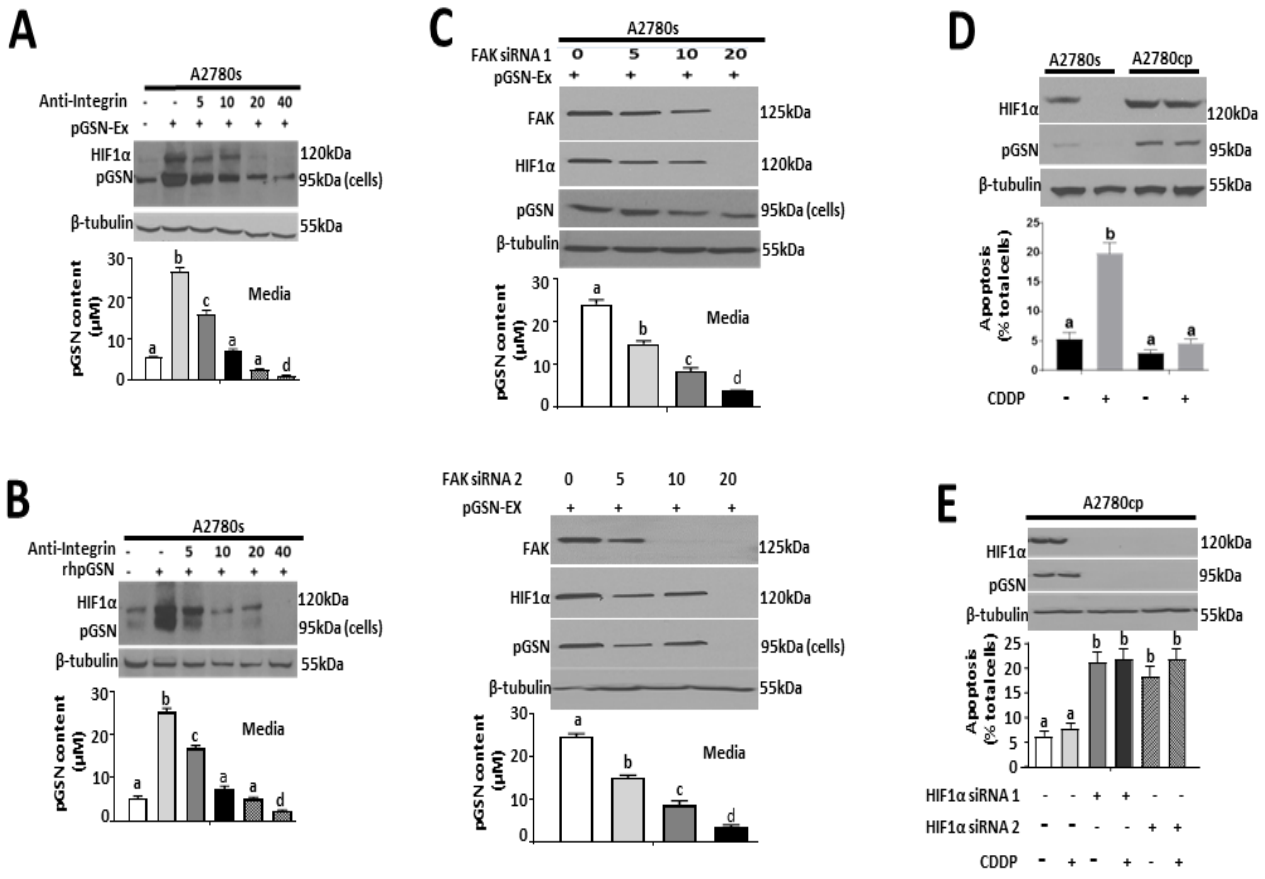

Fig. 3.4 The integrin signalling pathway is involved in the autocrine up-regulation of pGSN content by pGSN. (A & B) The α5β1 integrin receptor blocker ATN 161 attenuates the up-regulation of pGSN by Ex-pGSN **(A)** and rhpGSN **(B)**. A2780s cells were treated with anti-α5β1 integrin (40 μM; 3 h) followed by A2780cp-derived Ex-pGSN (40 μg/400,000 cells; 24 h) or rhpGSN (10 μM; 24 h). **(C)** Knock-down of FAK resulted in the downregulation of HIF1α and pGSN contents. A2780s cells were transfected with FAK siRNA1 and siRNA2 (0-20 pmol; 24 h) before culture with A2780cp-derived Ex-pGSN (40 μg/400,000 cells; 24 h). **(D)** pGSN and HIF1-α contents were higher in A2780cp cells compared to A2780s cells; CDDP reduced their content in A2780s but not in A2780cp cells. CDDP-induced apoptosis in A2780cp cells was higher than that in A2780s cells. A2780s and A2780cp cells were cultured with or without

CDDP (10 µM; 24 h). **(E)** HIF1-α silencing reduced the content of pGSN and sensitized A2780cp cells to CDDP-induced apoptosis. A2780cp cells were transfected with HIF1α siRNA1 and siRNA2 (200 pmol; 24 h) before culture with or without CDDP (10 µM; 24 h). pGSN, FAK, HIF1α and β-tubulin (loading control) contents were assessed by WB and apoptosis determined morphologically by Hoechst 33258 DNA staining. pGSN levels in the conditioned media were assessed by sandwich ELISA. *[**A**, (a; ***P<0.001 vs b, c, d); **B**, (a; ***P<0.001 vs b, c, d); **C**, (a; ***P<0.001 vs b, c, d); **D**, (a; ***p<0.001 vs b); **E**, (a; ***p<0.001 vs b)]*. N = 3

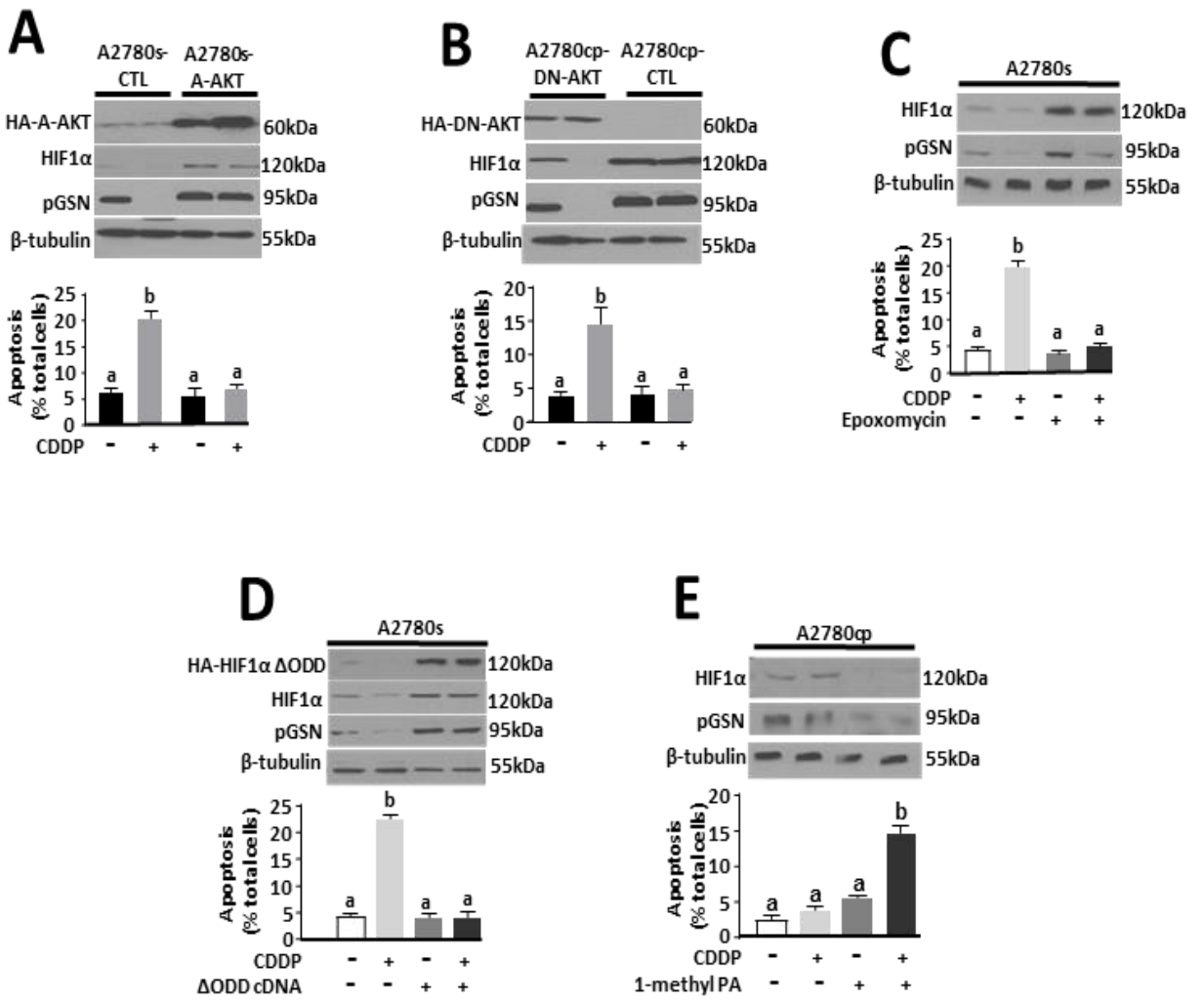

Fig. 3.5 pGSN-mediated OVCA chemoresistance involves HIF1α modulation by Akt. (A) Activation of Akt in chemosensitive cells increases the contents of pGSN and HIF1α and renders them resistant to CDDP-induced apoptosis. A2780s cells constitutively expressing an activated Akt (A2780s-A-AKT) and its scrambled control cells (A2780s-CTL) were cultured with or without CDDP (10 μM; 24 h). **(B)** pGSN and HIF1α contents are decreased and CDDP-induced apoptosis enhanced in chemoresistant cells when Akt function is down-regulated. A2780cp cells constitutively expressing triple-mutant dominant Akt (A2780cp-DN-AKT) or scrambled control (A2780cp-CTL) cultured with or without CDDP (10 μM; 24 h). **(C)** Inhibition of proteasomal

degradation of HIF1α in chemosensitive cells increases the content of pGSN and attenuates CDDP-induced apoptosis. A2780s cells were pre-treated with epoxomycin (10 nM; 3 h) and cultured with or without CDDP (10 μM; 24 h) in the presence of the inhibitor. **(D)** Forced expression of a proteasomal non-degradable mutant of HIF1α increases pGSN content and inhibits CDDP-induced apoptosis in chemosensitive cells. A2780s cells were transfected with ΔHIF1α cDNA (1 μg; 24 h) and treated with or without CDDP (10 μM; 24 h). **(E)** Induction of proteasomal HIF1α degradation in chemoresistant cells decreases pGSN content and renders them sensitive to CDDP-induced apoptosis. A2780cp cells were pre-treated with the proteasome activator 1-methyl PA (10 μM; 3 h) and then cultured with or without CDDP (10 μM; 24 h) in the presence of the activator. pGSN, HIF1α and β-tubulin (loading control) contents were assessed by WB and apoptosis determined morphologically by Hoechst 33258 DNA staining. *[**A**, (a; ***p<0.001 vs b); **B**, (a; ***p<0.001 vs b); **C**, (a; ***p<0.001 vs b); **D**, (a; ***p <0.001vs b); **E**, (a; ***p<0.001 vs b)]*. N = 3.

These findings suggest that chemoresistant cells-derived EXs are capable of inducing CDDP resistance in chemosensitive OVCA cells. The exosome-mediated induction of resistance in chemosensitive cells was markedly suppressed when the pGSN in the exosomes isolated from chemoresistant cells was knocked down (siRNA; 50 nM, 24 h). This suggests that the attenuation of CDDP-induced apoptosis in the chemosensitive cells was a result of pGSN in the exosomes from chemoresistant OVCA cells (Fig. 6G). In reciprocal studies (as control experiments), exosomes from chemosensitive cells failed to alter the responsiveness of chemoresistant cells (A2780cp) to CDDP (Fig. S5A). In addition, to validate the above pGSN-effect, we knocked-down pGSN (siRNA) in A2780cp cells (target cells) and co-cultured with Ex-pGSN from A2780s and A2780cp cells before CDDP treatment (10 μM; 24 h). pGSN content in pGSN-depleted-A2780cp cells was restored after co-culture with exosomes derived from chemoresistant but not chemosensitive cells; the former response was associated with significant attenuation of CDDP-induced apoptosis (Fig. S5B).

In order to investigate whether HIF1α mediates the auto-induction of pGSN, we examined by ChIP assay the potential transcriptional regulatory role of HIF1α in pGSN expression in A2780s and A2780cp cells treated with or without CDDP (10 μM, 12 h; Fig 6H) and Ex-pGSN (Fig 6I). HIF1α binding to the pGSN DNA promoter was higher in the chemoresistant OVCA cells compared to their sensitive counterparts (Fig. 6H). Although CDDP treatment failed to significantly decrease HIF1α occupancy in the sensitive cells (Fig. 6H), a significant apoptosis was observed (Fig. 6H). CDDP slightly increased HIF1α occupancy in the chemoresistant cells although that was not significant (Fig. 6H); a response that was associated with attenuation of CDDP-induced apoptosis. Chemoresistant cells-derived exosomes enhanced HIF1α binding to the pGSN promoter in the chemosensitive cells; CDDP treatment failed to

induce apoptosis in these cells (***$p < 0.001$) (Fig. 6I). Taking together, our findings suggest significant evidence to support a direct regulatory role of HIF1α on pGSN auto-induction.

DISCUSSION

Although pGSN has been implicated in various inflammatory disorders, injuries and bacterial infections[23], whether and how it is involved in the regulation of chemosensitivity in OVCA is not known. Our present study has demonstrated that pGSN levels are higher in chemoresistant than chemosensitive OVCA cells and are reduced in the presence of CDDP in the sensitive but not the resistant cells *in vitro*. Gain- and lost-of function studies support the notion that pGSN confers CDDP resistance in OVCA cells. Secreted by exosome, pGSN up-regulates its own expression via the α5β1 integrin-FAK-Akt-HIF1α signaling pathway and inhibits CDDP-induced apoptosis. pGSN in chemoresistant cells-derived exosomes induces resistance in chemosensitive cells through exosomal uptake and the upregulation of pGSN. In addition, increased expression of pGSN in ovarian cancer patients significantly correlates with shortened progression-free survival.

To our knowledge, the present communication is the first report on pGSN gene expression in human cancer patients and their application for predicting clinical outcomes. Suboptimal surgical debulking is a key determinant of tumour recurrence and chemoresistance[24] hence, we examined its association with pGSN expression.

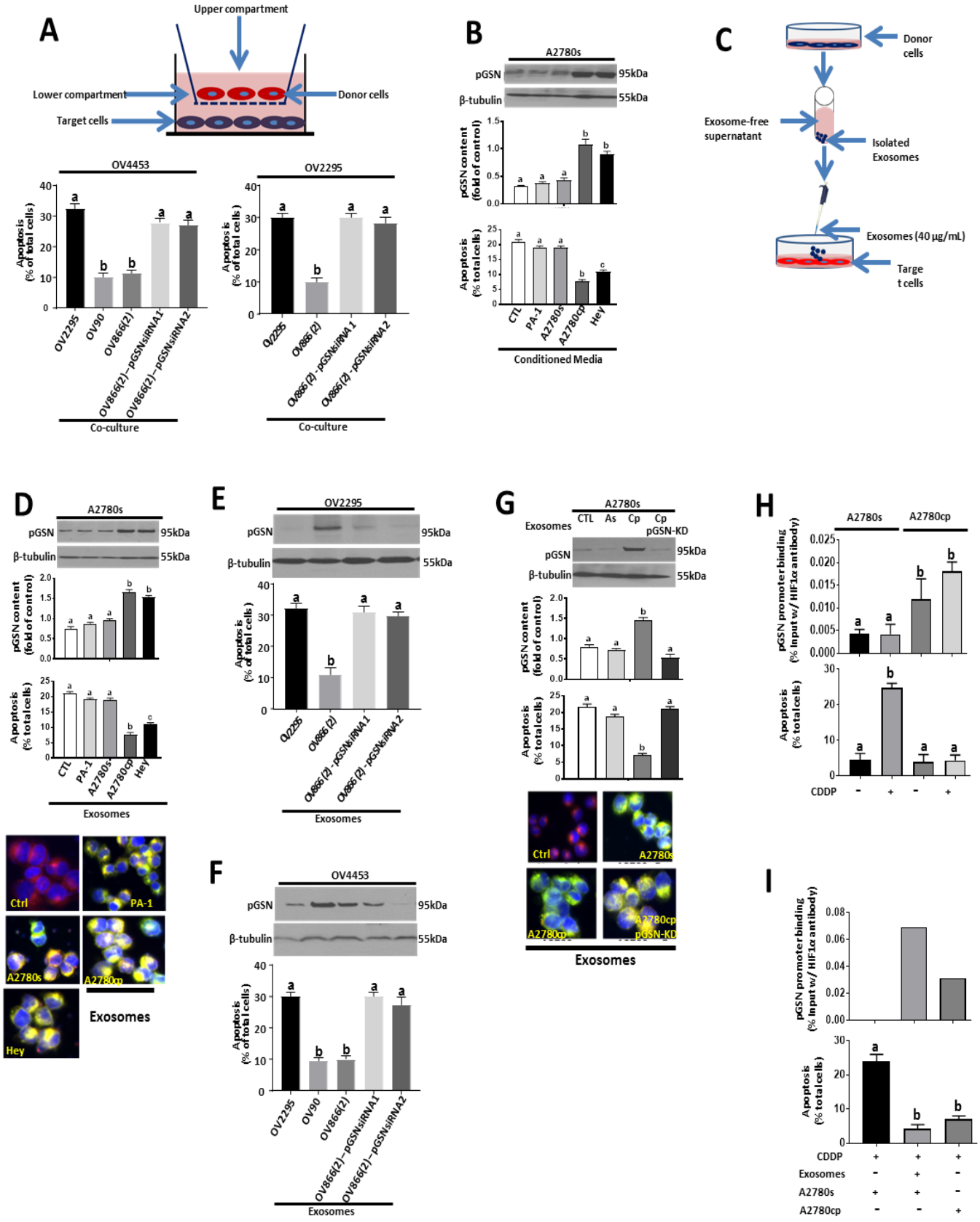
A
Upper compartment
Lower compartment
Donor cells
Target cells
OV4453
OV2295
Apoptosis (% of total cells)
OV2295
OV90
OV866(2)
OV866(2)−pGSNsiRNA1
OV866(2)−pGSNsiRNA2
Co-culture
B
A2780s
pGSN
β-tubulin
95kDa
55kDa
pGSN content (fold of control)
Apoptosis (% total cells)
CTL
PA-1
A2780s
A2780cp
Hey
Conditioned Media
C
Donor cells
Exosome-free supernatant
Isolated Exosomes
Exosomes (40 μg/mL)
Targe t cells
D
A2780s
Ctrl
PA-1
A2780s
A2780cp
Hey
Exosomes
E
OV2295
OV866(2)
OV866(2)-pGSNsiRNA1
OV866(2)-pGSNsiRNA2
F
OV4453
OV2295
OV90
OV866(2)
OV866(2)−pGSNsiRNA1
OV866(2)−pGSNsiRNA2
G
A2780s
Exosomes
CTL
As
Cp
Cp pGSN-KD
Ctrl
A2780s
A2780cp
A2780cp pGSN-KD
H
A2780s
A2780cp
pGSN promoter binding (% Input w/ HIF1α antibody)
CDDP
I
pGSN promoter binding (% Input w/ HIF1α antibody)
CDDP
Exosomes
A2780s
A2780cp

Fig. 3.6 Chemoresistant cells-derived exosomes enhance HIF1α binding to pGSN promoter region and induces CDDP resistance in chemosensitive OVCA cells. (A) Chemosensitive OVCA cells (target cells; OV4453, OV2295) were co-cultured with chemoresistant OVCA cells (OV90, OV866 (2)), chemosensitive OVCA cells (OV2295) and pGSN-knocked down OV866 (2) cells followed by CDDP treatment (10 μm; 24 h). Chemoresistant (OV90 and OV866(2)) but not the chemosensitive OVCA cells conferred CDDP resistance to chemosensitive OVCA cells. OV866 (2) cells whose pGSN was knocked down failed to protect OV4453 and OV2295 against CDDP-induced apoptosis. **(B, C)** Conditioned media and exosomes from chemoresistant OVCA cells but not the chemosensitive cells increased pGSN content and conferred CDDP resistance to chemosensitive cells. A2780s cells were treated with conditioned media (**B**, 3 ml; 24 h) or exosomes (**C-G**, 40 μg/400,000 cells; 24 h) derived from cultures of A2780s, PA-1, Hey, OV2295, OV866 (2), OV90 and A2780cp cells and then cultured with or without CDDP (10 μM; 24 h). Exosomes were tagged with pCT-CD63-GFP (1 μg; 24 h) and their uptake by recipient cells (A2780s, labeled with PKH26 red fluorescent dyes) was assessed by IF. **(E and F)** Exosomes from chemoresistant cells depleted of pGSN failed to upregulate pGSN content and facilitated CDDP-induced apoptosis compared with exosomes with pGSN. Exosomal pGSN from chemoresistant OVCA cells confer resistance in OV2295 and OV4453 cells. **(G)** A2780s cells were cultured with exosomes (40 μg/400,000 cells; 24 h) derived from A2780s, A2780cp and A2780cp following pGSN knock-down (A2780cp-pGSN-KD) afterwhich they were treated with or without CDDP (10 μM; 24 h). pGSN and β-tubulin contents (loading control) were examined by WB. **(H)** HIF1α-pGSN promoter binding is higher in A2780cp than A2780s cells. A2780s and A2780cp cells were cultured with or without CDDP (10 μM; 24 h) and HIF1α-pGSN promoter binding was assessed by CHIP assay. **(I)** Chemoresistant cells-derived exosomes

increase HIF1α-pGSN promoter binding and attenuate CDDP-induced apoptosis in chemosensitive cells. A2780s cells were cultured with A2780cp cells-derived exosomes (40 μg/400,000 cells; 24 h) and then cultured with or without CDDP (10 μM; 24 h). HIF1α-pGSN promoter binding was assessed by ChIP. *[**A**, (a; ***p < 0.001 vs b); **B**, (a; ***p<0.001 vs b and c); **D**, (a; ***p<0.001 vs b and c); **E**, (a; ***p<0.001 vs b); **F**, (a; ***p<0.001 vs b); **G**, (a; ***P<0.001 vs b); **H**, (a; **P<0.01 vs b); **I**, (a; **P<0.01 vs b)]*. N = 3.

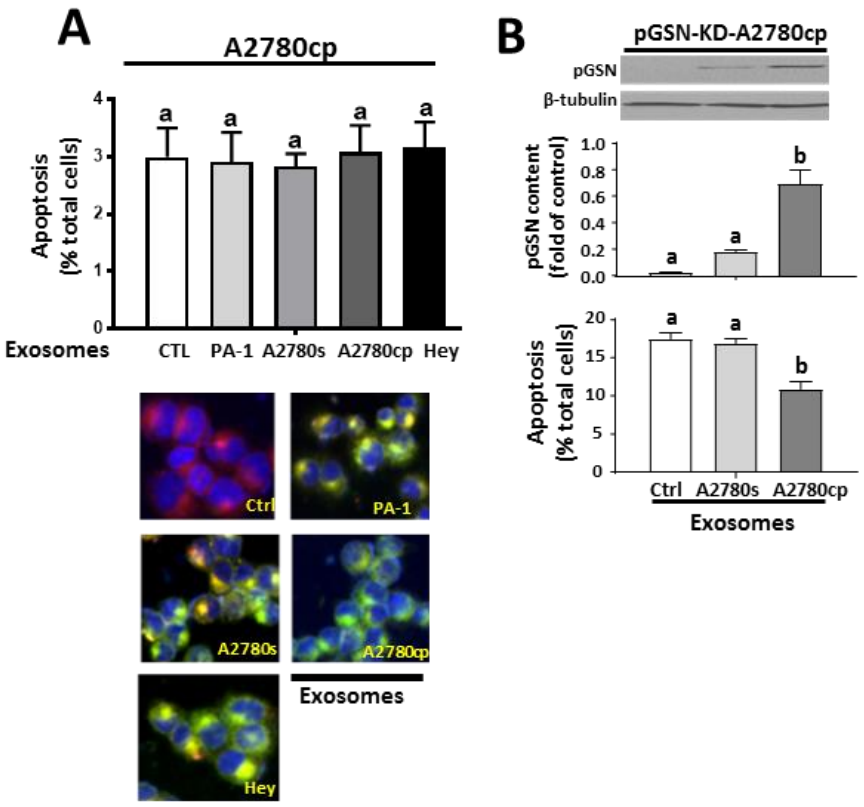

Fig. 3.S5. Chemoresistant cells-derived exosomes induce CDDP resistance to pGSN-KD-chemosensitive OVCA cells. (A) Chemosensitive cells (A2780s)-derived exosomes did not alter CDDP responsiveness in A2780cp cells. Exosome uptake was assessed by IF and apoptosis analysed morphologically using Hoechst DNA staining. **(B)** pGSN content in A2780cp previously treated with siRNA (A2780cp-KD-pGSN) was upregulated after being treated with A2780cp-derived exosomes, a response associated with attenuation of CDDP-induced apoptosis. A2780-KD-pGSN cells were treated with exosomes (40µg/400,000 cells; 24 h) derived from A2780s and A2780cp cells before CDDP treatment (0 and10 µM; 24 h). Exosome uptake, pGSN content, β-tubulin (loading control) as well as CDDP-induced apoptosis were assessed as previously described. *[**A**, (a; ***p<0.001 vs b)]*. N = 3

Our observation indicates that elevated expression of pGSN significantly correlate with poorer PFS in serous OVCA patients as well as those with suboptimal surgical debulking irrespective of chemotherapeutic composition. PFS is suggestive of the time frame for tumour recurrence[25,26] and directly reflects the biology of the tumour hence, plays a key role in chemoresistance. With the median survival observed in both cohorts, it's likely the patients under study are largely clinically platinum sensitive (PFS of at least more than 6 months). Lots of effective palliative treatments exist to manage this patient group thus, not surprising that no significant OS differences post-recurrence was observed. This could in part explain why the levels of pGSN associate with a relatively minor impact on PFS. The value of the marker could help to stratify different levels of platinum sensitivities to further refine treatment recommendations and used as a prognostic marker for counselling and follow up of these patients. In patient cohorts with more resistant tumours, pGSN is likely to have a major impact on PFS and thus could therefore serve as a potential therapeutic candidate for further mechanistic studies which could provide information to enhance patient survival. When serous patients were combined with endometroid patients, clinical significance was only observed in those treated with taxol and platinum derivatives. This observation is consistent with the heterogenous nature of OVCA cells and combinational treatments are more beneficial to OVCA patients than platinum alone. Although this observation is the first for pGSN, it is in support of the notion of a prognostic significance of total GSN expression in pancreatic cancers[27], gynecological cancers[9], colorectal cancers[13] and head-and-neck cancers[28]. The findings in these clinical datasets are consistent with the obervation that chemoresistant OVCA cells express higher levels of pGSN compared to their sensitive counterparts. The expression of pGSN at diagnosis could therefore be

used as a possible predictive marker for patient outcomes as well as a potential target for personalized therapeutics for chemoresistant OVCA.

Exosomal transport have emerged as key mechanism of cell-cell communications[17,18] and with its secretion of Annexin A3, miR-200b and miR-200c significantly associated with FIGO stage[29], lymph metastasis[29] and platinum resistance[30]. Cancer associated adipocytes and fibroblasts secrete exosomal miR-21 which attenuates CDDP-induced apoptosis and promotes CDDP resistance in ovarian cancer cells by targeting APAF1[20]**.** NAV3 is also a target for exosomal miR-21-3p in promoting CDDP resistance[31]**,** suggesting an important role of exosomes in cell-cell communication in the development of drug resistance in a plethora of cancers, including ovarian cancer. Regardless, targeting these genes has yielded no improvement in patient survival. There is therefore the urgent need to investigate other exosome-mediated mechanisms that could play an etiologic role in CDDP resistance. Here, we demonstrate a novel mechanism through which exosomal pGSN induces CDDP resistance in ovarian cancer cells by upregulating pGSN content in chemosensitive OVCA cells. The secretion of pGSN-containing exosomes by chemoresistant OVCA cells may represent an interesting opportunity to attenuate CDDP resistance in OVCA by inhibiting the transfer of exosomal pGSN. Unlike other proteins and nucleic acids[20,31-33], pGSN promotes its own expression through exosomal transport, thus making it a unique and reliable candidate for therapeutic target. This novel phenomenon could be exploited to reverse the sensitivity of chemoresistanct cells.

Aside the exosomal-mediated paracrine role of pGSN in CDDP resistance, exosomal pGSN can act in an autocrine manner to induce its own expression via α5β1 integrin signaling. In previous reports, increased α5β1 integrin expression is significantly associated with increased OVCA progression, residual disease, surgical stage and drug resistance[34,35]**.** Increased secreted

phosphoprotein 1 (SPP1) also activated integrin β1/FAK/Akt pathway, leading to cell proliferation, migration and invasion[36]**.** Although pGSN interaction with α5β1 integrin through fibronectin has been shown in *in vivo* assay[15], how this receptor signals in pGSN-induced chemoresistance in OVCA cells is yet to be demonstrated. Results from the current study support the hypothesis that high levels of exosomal pGSN auto-induce endogenous pGSN contents and promote CDDP resistance in OVCA cells by activating α5β1 integrin signaling. For the first time, we have shown that exosomal pGSN and rhpGSN activate with α5β1 integrin signaling cascade, induce endogenous pGSN contents and inhibit CDDP-induced apoptosis in chemosensitive cells. This autocrine signaling cascade serves as a positive feedback mechanism to increase pGSN production, thus resulting in the resistance of the cells to CDDP. This phenomenon is consistent with the observation that OVCA patients with increased α5β1 integrin expression respond poorly to treatment[35,36] and support the notion that increased α5β1 integrin expression together with abundant supply of pGSN could fuel the proposed positive feedback mechanism of pGSN and protects cells from CDDP-induced cell death. Antagonising the α5β1 integrin could also provide therapeutic benefits to patients since its binding to potential ligands such as pGSN, osteopontin and SPP1 will be abrogated. Concurrently, blocking the release of exosomal pGSN and other ligands that stimuate this signaling cascade in a similar manner could provide additional therapeutic advantages.

Since α5β1 integrin is known to be mediated through a host of signaling pathways, including FAK/ERK/MAPK, RAC/NFkB, Wnt/β-catenin and FAK/Crk/Jnk[34-37], it is possible that these pathways might be affected and thus the fate of the cells when α5β1 integrin activation is suppressed. These possibilities need to be investigated. Moreover, the possibility that the target cells for pGSN could take up exosomal pGSN via receptor-dependent and -independent

endocytosis to modulate their cellular fate could not be excluded and is a subject for future investigation (Fig. 7).

The activation of α5β1 integrin cascade by exosomal pGSN also resulted in increased levels of HIF1α content. Although it well established that HIF1α over-expression is associated with OVCA tumour aggresiveness, progression and metastasis[38-40], inhibiting HIF1α as a therapeutic option has yielded no success[41]. Previous study detected by co-precipitation suggests that HIF1α binds to gelsolin complex although a functinal link between the two proteins has not been established[38]**.** We have demonstrated that HIF1α knock-down decreases the content of pGSN and sensitizes chemoresistant cells to CDDP-induced death. Taking together, we hypothesized that auto-induction of pGSN is mediated via HIF1α. We investigated the binding of HIF1α to pGSN DNA promoter region in OVCA cells and for the first time HIF1α binds to the pGSN promoter and is involved in pGSN-induced pGSN expression/secretion. HIF1α occupancy was higher in the chemoresistant cells compared to their sensitive counterparts at basal levels. Although HIF1α occupancy was not significantly decreased by CDDP treatment in the sensitive cells, it was enough to induce apoptosis in these cells. Chemoresistant-derived exosomal pGSN however, increased HIF1α binding in chemosensitive cells which rendered them resistant to CDDP-induced death. HIF1α-pGSN binding motifs are currently being investigated to develop inhibitors that will distrupt their interaction and reduce pGSN production and increase responsiveness to CDDP-induced death.

In the present study we further investigated the role of Akt in pGSN-mediated OVCA chemoresistance. We and others have previously demonstrated the the important role of Akt in cell survival[5,42,43], protein synthesis[44,45] and cell cycle progression and proliferation[46,47]**,** although whether Akt activation regulates pGSN production is not known. Up-regulating Akt function in

the chemosensitive cells significantly increased pGSN and HIF1α contents and attenuated CDDP-induced apoptosis, responses not observed in the resistant cells when Akt function was down-regulated. In contrast, Akt activation in chemosensitive cells promotes HIF1α-mediated auto-induction of pGSN and CDDP resistance. These findings are consistent with the observation that cancer patients with increased Akt activation respond poorly to chemotherapeutic agents and have worst survival outcomes[5,48]. Clinical trials with Akt inhibitors are currently in progress to determine its therapeutic efficiency in patients with chemoresistant OVCA[49,50] although the role of pGSN remains uncertain. There is currently no evidence to indicate HIF1α is a substrate of Akt and sequence analysis of HIF1α indicates the absence of Akt consensus sites[51]. We therefore envisage that Akt activates HIF1α indirectly via other kinases such as CKI-Ser247[51], GSK3β-Ser551[51], CKII-Thr796[51], Erk1-Ser641[51] and PKA-Ser643[51], possibilities worthy of future investigation.

In conclusion, we have shown for the first time the dual functions of pGSN and that pGSN tranported via exosomes is a determinant of chemoresistance in OVCA cells. We have demonstrated that the autocrine action of exosomal pGSN in OVCA cells is via α5β1 integrin - HIF1α-mediated auto-induction of pGSN, a response promoted by Akt activation and resulted in CDDP resistance (Fig. 7). In addition, chemoresistant cells-derived exosomes confer CDDP resistance in a paracrine manner to otherwise chemosensitive OVCA cells by increasing endogenous pGSN content. These findings support our hypothesis that exosomal pGSN promotes cancer cell survival through both autocrine and paracrine mechanisms which induces resistant phenotype in the chemosensitive cells (Fig. 7A). To our knowledge, this is the first study to demonstrate that pGSN is involved in α5β1 integrin/FAK/Akt/HIF1α/pGSN signaling cascade (Fig. 7A). Further studies are however, needed to examine other mechanisms that could

be potentially implicated in pGSN-mediated chemoresistance (Fig. 7B). It is also possible that pGSN bound to α5β1 integrin could be internalized and exosomal-pGSN released and secreted via transcytosis (Fig. 7B). pGSN could also be released from the exosomes in the cytosol and trigger signaling cascade resulting in pGSN-mediated chemoresistance (Fig. 7B). Cancer cells may also uptake exosomal-pGSN in a receptor-independent manner, release pGSN into the cytosol to activate chemoresistant signaling pathways (Fig. 7B). Although increased expression of pGSN in the ovarian tumour microenvironment correlates with poorer survival, whether it has a suppressive effect on anti-tumour cells is currently under investigation. Exosomal pGSN could be a clinically useful prognostic marker in the tumour microenvironment as well as offer novel insights into developing individualized treatments for chemoresistant OVCA patients.

MATERIALS AND METHODS

Ovarian Cancer Survival Analysis. pGSN gene expression analysis was performed on primary ovarian cancer datasets using the 200696_s_at probe specific for pGSN (Supplementary Table 1) available publicly on www.kmplot.com[22]. Patients were stratified using the following clinical parameters: histological subtypes (serous; serous and endometroid), treatments containing either platinum agents or platinum and taxol derivatives and suboptimal surgical debulking. Kaplan-Meier survival analysis was used to correlate pGSN gene expression with progression free survival (PFS) and overall survival (data not shown) using optimal cut-offs in each case. Statistical parameters were calculated by log-rank. Beeswarm plots were used to visualize gene expression in each stratified parameter.

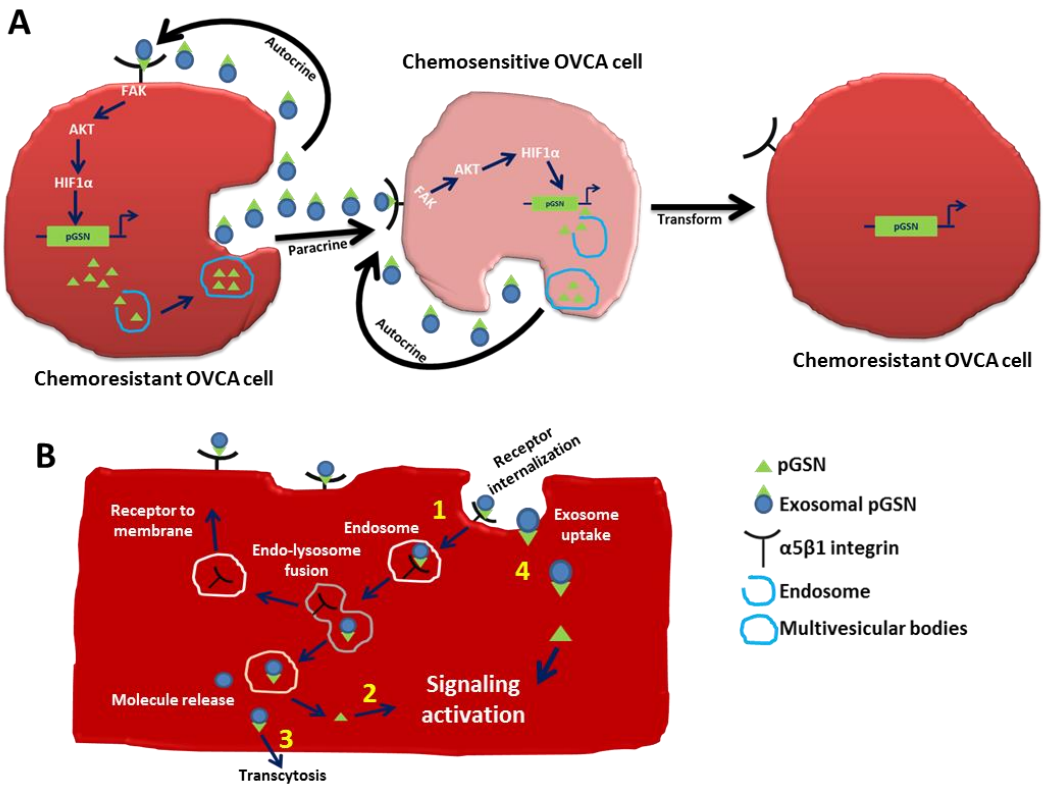

Fig. 3.7 Hypothetical models illustrating the autocrine and paracrine mechanisms of Ex-pGSN in OVCA chemoresistance. (A) Chemoresistant cells (CR)-derived Ex-pGSN autoregulates its own gene expression and induces CDDP resistance in chemosensitive OVCA cells (CS) in a paracrine manner by activating the α5β1/FAK/Akt/HIF1α/pGSN signaling pathway. **(B)** Aside the direct activation of the α5β1/FAK/Akt/HIF1α/pGSN signaling pathway, it is also possible that exosomal pGSN-α5β1 integrin could be internalized (1) leading to the release of pGSN which further activates (2) signaling cascades resulting in chemoresistance. Upon internalization, exosomal-pGSN could be released from the endosomes and secreted via transcytosis (3); a phenomenon that could propel the autocrine and paracrine mechanisms described in fig. 7A. There is also the possibility that exosomal-pGSN could be uptaken and pGSN released to activate (4) signaling cascades resulting in chemoresistance.

Kmplotter Analysis. We interrogated all data sets available on kmplotter using only the 200696_s_at probe regardless of tumour stage, grade or p53 statuses. This probe specifically targets 11 sequences on the transcript variant 1 (mRNA) of GSN isoform a (pGSN; Supplementary Table 1) but not any other isoform (Supplementary Table 2). Using the optimal cut off point, the patients were dichotomized into low pGSN and high pGSN groups with no specific follow-up threshold selected. The analyses were restricted to either serous or all (serous + endometroid) histological subtypes available. All databases were included in the analyses with biased array excluded. The analyses were limited to patients treated with either platinum or platinum + taxol. Unless otherwise stated (suboptimal debulking), all patients who underwent debulking surgery were included in the analyses regardless of the residual disease. Patients surviving over the specific thresholds were censored instead of being excluded.

Reagents. Cis-diaminedichloroplatinum (CDDP), phenylmethylsulfonyl fluoride (PMSF), aprotinin, dimethyl sulfoxide (DMSO), sodium orthovanadate (Na_3VO_4) and Hoechst 33258 were supplied by Sigma (St. Louis, MO). GSN siRNA and scrambled sequence siRNA (control) were purchased from Ambion (Burlington, Canada) and Dharmacon (Colorado, USA) respectively. ΔHIF1α cDNA was purchased from Addgene (Cambridge, USA0. 1 methyl-PA, PKH67 and PKH26 Fluorescent Cell Linker Kits and epoxomycin were purchased from MilliporeSigma (Canada). siRNAs for HIF1α and FAK, and their scrambled sequence siRNA (control) were supplied from Santa Cruz (Mississauga, Canada). Recombinant human plasma gelsolin (rhpGSN) was purchased from Cytoskeleton, Inc, USA. pGSN cDNA and 3.1A vector plasmids were produced in the lab of Dr. Dar-Bin Shieh, National Cheng Kung University Hospital, Taiwan. pCT-CD63-GFP was purchased from System Biosciences, LLC. ATN 161 was from R & D Systems (Minnesota, USA). Sandwich pGSN ELISA kits were from Aviscera

Bioscience, Inc. CA. See Supplementary Tables 4 and 5 for details on antibodies and pGSN-specific siRNA sequences, respectively. The Dominant negative Akt (DN-Akt) and constitutively active Akt (A-Akt) adenoviruses were generous gifts from Dr. Kenneth Walsh (Boston University School of Medicine, Boston, MA) and have been routinely used in our laboratory[42,43]. The DN-Akt is a triple mutant with a dead-kinase [with an alanine at the Thr308 and Ser473 (required in phosphorylation for Akt activation[52,53] and at Lys179 (within the kinase domain and required for phosphate transfer[54]]. The active Akt is a meristoylated Akt2. The availability HA-tagged DN-Akt and HA-tagged A-Akt virus allows for easy confirmation of their expression by western blot.

Cell Lines and Cell Culture. Chemosensitive and chemoresistant OVCA cell lines of high grade serous (HGS) and endometroid histologic subtypes and with various p53 status were tested in the present studies: HGS [OV2295 (p53-mutant; sensitive), OV4453 (p53-mutant, sensitive), OV90 (p53-mutant, resistant), OV866(2) (p53-mutant, resistant), Hey (p53-wt, resistant)] and Endometroid [A2780s (p53-wt, sensitive), PA-1 (p53-wt; sensitive), A2780cp (p53-mutant, resistant), SKOV-3 (p53-null, resistant)]. The OVCA cell lines were cultured in Dulbecco's modified Eagle medium (DMEM)/F12 and RPMI 1640 as previously reported[8,43]. All experiments were carried out in serum-free media. See supplementary Table 3 for details on cells.

RNA Interference. Cells were transfected (50-200 nM, 24 h) with siRNAs for total GSN [(Ambion and Dharmacon; HIF1α and FAK (Santa Cruz)] or their scrambled control, using lipofectamine 2000, and were subsequently treated with CDDP (10 μM; 24 h) and harvested for analysis, as previously described[8,43,55]. siRNA against total GSN targets the C terminal region which is shared by both cGSN and pGSN. However, siRNA against pGSN specifically targets

and degrades pGSN mRNA without affecting that of cGSN. Two different siRNAs (Supplementary Table 5) were used for each target to exclude off-target effects. Successful knock-down was confirmed by Western blotting[9]. (See Supplementary Table 4 for details on antibodies).

Transient Transfection. Cells were transfected with pGSN and ΔHIF1α pcDNA3.1-derived vectors (empty vector as controls), using lipofectamine 2000, and were then cultured with CDDP (10 μM; 24 h) and harvested for further analysis[8,43,55]. Successful overexpression was confirmed by Western blotting (See Supplementary Table 4 on antibodies).

ChIP Assay. Chromatin immunoprecipitation (ChIP) assays were performed on human ovarian cancer cells, as previously described[56]**.** The antibodies and primers used for verifying the occupancy of HIF1α on the pGSN promoter are shown in the Supplementary Tables 4 and 6, respectively**.** Sequence -3000 base pairs upstream of TSS was analyzed for potential promoter and based on the score of the promoter strength, primers were designed to determine HIF1a binding (Supplementary Table 6).

Extracellular Vesicle Isolation and Characterization. Serum-free conditioned media from cultured cells were used for extracellular vesicle isolation and characterization, as described[57]**.** Total EV concentration was determined by BCA Protein Assay Kit (Thermo Fisher Scientific). When fresh exosomes (40 μg/400,000cells) were not required, they were suspended in PBS and stored at -80^{o}C for subsequent analysis.

Nanoparticle Tracking Analysis (NTA). EVs in PBS were analyzed, using the ZetaView PMX110 Multiple Parameter Particle Tracking Analyzer (Particle Metrix, Meerbusch, Germany)

in size mode using ZetaView software version 8.02.28, as previously described[57,58]. EVs were captured at 11 camera positions at 21^{o}C and pellet size and concentration evaluated.

Transmission Electron Microscopy (TEM). OVCA cell were pelleted (4000 g; 20 min) and processed, as previously described[59]**.** Resin sections were stained with uranyl acetate and lead citrate solutions and examined with a Jeol JEM 1230 transmission electron microscope (Japan).

Immunoelectron Microscopy (iEM). Cell pellets (4000 g; 20 min) were processed as previously described[59]**.** The grids were washed three times in PBST, immunostained with anti-pGSN antibody (Supplementary Table 4), rinsed in distilled water, stained with uranyl acetate and lead citrate, and photographed with a Jeol JEM 1230 transmission electron microscope (Japan).

Exosome Labeling, Uptake and Fluorescent Microscopy. Donor cells were transfected with pCT-CD63-GFP to label the exosomes (1 µg; 24 h) while recipient cells were labeled with PKH26 red fluorescent dyes (Sigma-Aldrich, MO), as previously described[57,58]. Nuclei were counterstained with DAPI, cells were mounted onto coverslips and exosome uptake examined, as previously described[57,58].

Protein Extraction and Western blot Analysis. Western blotting (WB) was carried out as previously described[8,9,43]. Membranes containing transferred proteins were incubated with primary antibodies (1:1000) in 5% (wt/vol) Blotto and subsequently with the appropriate horseradish peroxidase (HRP)-conjugated secondary antibody (1:2000) in 5% (wt/vol) Blotto (Supplementary Table 4 for details on antibodies). Peroxidase activity was visualized on a film with the Enhanced Chemiluminescent Kit (Amersham Biosciences) and signal intensity densitometrically determined (Image J software).

ELISA. pGSN contents in cell-free conditioned media and lysates from OVCA cells were assayed by sandwich ELISA (Aviscera Bioscience, Inc. CA), according to manufacturer's instructions.

Assessment of Apoptosis. CDDP-induced apoptosis was assessed morphologically[8,55], using Hoechst 33258 nuclear stain. Using a random selection of fields, a minimum of 400 cells with typical apoptotic nuclear morphology (nuclear condensation, shrinkage and fragmentation) were counted in each group and expressed as the percentage of total cells. "Blinded" counting approach was used to prevent experimental bias.

Statistical Analyses. Results are expressed as the mean ± SD of at least 3 independent experiments. Statistical analysis was carried out by one- or two-way ANOVA and differences between multiple experimental groups was determined by Bonferroni *post-hoc* test, using the PRISM software (Version 7.0; GraphPad, San Diego, CA). Statistical significance was inferred at $p < 0.05$. Statistical parameters for Kaplan-Meier survival analysis were calculated by log-rank.

Supplementary Table 3.4: Antibodies used in the present studies

Primary Antibodies						Secondary Antibodies					
Application	**Target**	**Antibody**	**Company**	**Catalog #**	**Dilution**	**Antibody**	**Conjugate**	**Company**	**Catalog #**	**Dilution**	**Note**
WB	pGSN	Anti-pGSN Goat polyclonal	Antibodies online(Atlanta, USA)	ABIN1019662	1:1000	Dnk polyclonal to Goat IgG	HRP	Abcam (Toronto, Canada)	Ab97110	1:2000	
WB	cGSN	Anti-GSN mouse monoclonal	MilliporeSigma (Oakville, Canada)	G4896	1:1000	Goat Anti-mouse IgG (H+L)	HRP	Bio-Rad (Mississauga, Canada)	170-6516	1:2000	
WB	HIF1α	Anti- HIF1α mouse monoclonal	MilliporeSigma (Oakville, Canada)	H6536	1:1000	Goat Anti-mouse IgG (H+L)	HRP	Bio-Rad (Mississauga, Canada)	170-6516	1:2000	
WB	CD63	Anti-CD63 mouse monoclonal	Abcam (Toronto, Canada)	Ab193349	1:1000	Goat Anti-mouse IgG (H+L)	HRP	Bio-Rad (Mississauga, Canada)	170-6516	1:2000	
WB	FAK	Anti-FAK mouse monoclonal	MilliporeSigma (Oakville, Canada)	396500	1:1000	Goat Anti-mouse IgG (H+L)	HRP	Bio-Rad (Mississauga, Canada)	170-6516	1:2000	
WB	HA	Anti-HA mouse monoclonal	Santa-Cruz (Mississauga, Canada)	Sc-805	1:1000	Goat Anti-mouse IgG (H+L)	HRP	Bio-Rad (Mississauga, Canada)	170-6516	1:2000	
WB	β-tubulin	Anti- β-tubulin mouse monoclonal	MilliporeSigma (Oakville, Canada)	SAB4200715	1:1000	Goat Anti-mouse IgG (H+L)	HRP	Bio-Rad (Mississauga, Canada)	170-6516	1:2000	
ChIP	HIF1α	Anti- HIF1α mouse monoclonal	MilliporeSigma (Oakville, Canada)	H6536	5 µg	N/A					Used in Fig. 6H.
ChIP	HIF1α	Anti- HIF1α mouse monoclonal	Novus Biologicals (Oakville, Canada)	NB100-105	5 µg	N/A					Used in Fig. 6I.
iEM	pGSN	Anti-pGSN mouse monoclonal	ABGENT (San Diego, US)	AM1936a	1:100	Goat-anti-mouse-IgG	Colloidal gold	Jackson (PA, USA)	115-215-068	1:50	

Supplementary Table 3.5: Customized siRNA oligonucleotide duplexes

Product	Target	Species	Company	Catalog #	Target sequence	Anti-sense sequence	Position on mRNA
siRNA 1	pGSN	Human	IDT (Iowa, USA)	N/A	GCGACCCGAGGCCGCGGCU	AGCCGCGGCCUCGGGUCGC	12
siRNA 2	pGSN	Human	IDT (Iowa, USA)	N/A	UGCCCGAGGCGCGGCCCAA	UUGGGCCGCGCCUCGGGCA	192

Supplementary Table 3.6: primer sequences for amplifying the gelsolin promoter.

HIF1a_pGSN FP: GGCCCATGTATATGTCCTGA
HIF1a_pGSN RP: AGTTTGGGCTTCAGCAACAG

Acknowledgement: This work was supported by the Canadian Institutes of Health Research (MOP-15691), the Dragon Gate Program (MOST 105-2911-I-006-529), and research grants (MOST 104-2314-B-006-063-MY3, 106-2627-M-006-001, 107-2321-B-006-019, and 107-2314-B-006-029) from the Taiwan Ministry of Science and Technology, the Center of Applied Nanomedicine, National Cheng Kung University, The Featured Areas Research Center Program within the framework of the Higher Education Sprout Project, the Taiwan Ministry of Education.

CHAPTER 4 – CANCER RESEARCH, 10.1158/0008-5472.CAN-20-0788 (2020)

(Formatted as per Cancer Research requirements)

Plasma gelsolin inhibits CD8+ T cell function and regulates glutathione production in conferring chemoresistance in ovarian cancer

Meshach Asare-Werehene[1,2,3], Laudine Communal[4], Euridice Carmona[4], Youngjin Han[5,6], Yong Sang Song[5,6], Dylan Burger[2,3], Anne-Marie Mes-Masson[4], and *Benjamin K Tsang[1,2,3]

[1]Department of Obstetrics & Gynecology, University of Ottawa, Ottawa, Ontario, Canada K1H 8L6;

[2]Chronic Disease Program, Ottawa Hospital Research Institute, Ottawa, Ontario, Canada K1H 8L6

[3]Department of Cellular & Molecular Medicine and Centre for Infection, Immunity and Inflammation, University of Ottawa, Ottawa, Ontario, Canada K1H 8L6;

[4]Centre de Recherche du CHUM et Institut du Cancer de Montréal, Département de Médecine, Université de Montréal, Montréal, Québec, Canada H2X 0A9

[5]Cancer Research Institute, Seoul National University College of Medicine, Seoul 110-799, Korea

[6]Department of Obstetrics and Gynecology, Seoul National University College of Medicine, Seoul 110-744, Korea

Running Title: pGSN hinders the anti-tumor effects of CD8+ T cells.

*Correspondence: Dr. Benjamin K Tsang, Chronic Disease Program, Ottawa Hospital Research Institute, The Ottawa Hospital (General Campus), Ottawa, Canada K1H 8L6; Tel: 1-613-798-5555 ext 72926; Email: btsang@ohri.ca

Competing Interests:

The authors declare no competing interests.

ABSTRACT

Although initial treatment of ovarian cancer (OVCA) is successful, tumors typically relapse and become resistant to treatment. Due to poor infiltration of effector T cells, patients are mostly unresponsive to immunotherapy. Plasma gelsolin (pGSN) is transported by exosomes (sEV) and plays a key role in OVCA chemoresistance, yet little is known about its role in immunosurveillance. Here we report the immunomodulatory roles of sEV-pGSN in OVCA chemoresistance. In chemosensitive conditions, secretion of sEV-pGSN was low, allowing for optimal CD8+ T cell function. This resulted in increased T cell secretion of IFNγ, which reduced intracellular glutathione (GSH) production and sensitized chemosensitive cells to cisplatin (CDDP)-induced apoptosis. In chemoresistant conditions, increased secretion of sEV-pGSN by OVCA cells induced apoptosis in CD8+ T cells. IFNγ secretion was therefore reduced, resulting in high GSH production and resistance to CDDP-induced death in OVCA cells. These findings support our hypothesis that sEV-pGSN attenuates immunosurveillance and regulates GSH biosynthesis, a phenomenon that contributes to chemoresistance in OVCA.

SIGNIFICANCE

Findings provide new insight into pGSN-mediated immune cell dysfunction in OVCA chemoresistance and demonstrate how this dysfunction can be exploited to enhance immunotherapy.

KEY WORDS: Plasma gelsolin, ovarian cancer, cisplatin (CDDP), chemoresistance, CD8+ T cells

INTRODUCTION

Ovarian cancer (OVCA) is the fifth most commonly diagnosed but most fatal gynecological cancer worldwide. In the US, one out of 95 women will die as a result of OVCA. Ovarian cancer originating from the epithelial cells comprises of 90% of all reported cases and approximately 70% of these are high grade serous subtype (HGS) (1). The standard treatment for OVCA is a combination of cytoreductive surgery and chemotherapeutic treatment with platinum and taxane derivatives (1). Although treatment is initially efficient, the tumor relapses and become resistant to treatment. The mechanisms involved in OVCA chemoresistance are multi-factorial with mutation of tumor suppressor genes, activation of oncogenes, dysregulation of apoptotic signaling and immune-suppression playing key roles (2). OVCA is considered a cold tumor hence has poor immune cell infiltration. Thus, immunotherapy is relatively ineffective to date (3-5). There is still more to learn about the molecular contributors to chemoresistance in OVCA to afford new diagnosis and treatment.

The tumor microenvironment (TME) is a strong contributing factor for chemoresistance (2). Both cytolytic (CD8+, CD4+, granzyme b, and IFN-γ) and suppressive (PD-1+ TIL, CD25+ FoxP3+ T-regs, PDL1+ and CTLA-4) subsets are co-localized in OVCA, resulting in an immunological stalemate and net positive association with survival (3-5). Thus, multipronged approaches for immunotherapy are needed for effectiveness and should be tailored to the baseline features of the TME. Although colon, melanoma and lung cancer patients respond well to immunotherapy, OVCA patients are unresponsive due in part to the coldness of OVCA (3, 4, 6). There is thus an urgent need to explore and target novel pathways responsible for the coldness of OVCA in order to make them more receptive to the immune system to enhance the efficacy of alternative immunotherapies.

Plasma gelsolin (pGSN) is the secreted isoform of the gelsolin (GSN) gene and a multifunctional actin binding protein (7, 8). Total GSN forms a complex with Fas-associated death domain-like interleukin-1β–converting enzyme (FLICE)-like inhibitory protein (FLIP) and Itch which regulates caspase-3 activation and chemoresistance in gynecological cancer cells (9, 10). Small EVs (sEVs; mostly called exosomes) are vesicles of approximately 30-100 nm in size and formed within endosomes by membrane invaginations, whereas large EVs (lEVs; mostly called microvesicles) range from 0.1 to 1.0 μm and are produced by membrane blebbing by cells under stress (11, 12). We have previously demonstrated that pGSN is highly expressed and secreted in chemoresistant OVCA cells compared to its chemosensitive counterparts (13). pGSN is transported via exosomes (sEVs) and up-regulates HIF1α–mediated pGSN expression in chemoresistant OVCA cells in an autocrine manner, and confers cisplatin resistance in otherwise chemosensitive OVCA cells (13). We have also shown that elevated circulating pGSN is associated with higher levels of residual disease after surgery and allows for detection of early stage ovarian cancer (14). However, little is known about its interaction with immune cells in the tumor microenvironment (TME). Whether pGSN contributes to immuno-surveillance escape in the tumor microenvironment remain to be examined.

Glutathione (GSH) and the nuclear factor erythroid 2-related factor (NRF2)-dependent genes help to maintain homeostasis in normal cells but can also provide a huge advantage to cancer cells to become CDDP resistant and escape immune-surveillance (15-17). NRF2 activation results in elevated levels of intracellular GSH which inactivates and efflux toxic therapeutic agents from cancer cells as well as increase DNA repair (15-17). However, it has not been demonstrated if and how pGSN induce GSH production in OVCA cell lines. Also, as to whether NRF2, an antioxidant transcription factor, is involved is yet to be investigated in the

context of pGSN-mediated OVCA chemoresistance (18). NRF2-dependent genes such as cystine/glutamate transporter (xCT) and glutamate-cysteine ligase regulatory subunit (GCLM) are associated with drug resistance in cancer (18-20). xCT is a membrane amino-acid transporter that regulates the influx of cysteine and the efflux of glutamate. GCLM regulates the first step of GSH synthesis from L-cysteine and L-glutamate. Although suppressing GSH biosynthesis has a potential of enhancing tumor killing, no significant clinical advantage has been achieved (15-17). Exogenous pGSN treatment increases GSH levels in the blood which mitigates radiation induced injury in mice (21) although the exact mechanism has not been investigated. As to whether pGSN regulates GSH biosynthesis, is not known. The purpose of this study is to investigate the immuno-inhibitory and GSH regulatory role of pGSN in OVCA chemoresistance.

We hypothesized that increased pGSN will suppress CD8+ T cell function as well as promote GSH production, an outcome that contributes to OVCA chemoresistance. For the first time, we report in this study that in chemosensitive condition, OVCA secrete low levels of sEV-pGSN which is unable to suppress the functions of CD8+ T cells. Thus, optimal secretion of IFNγ inhibits the production of GSH in OVCA cells. In chemoresistant conditions, increased pGSN promotes NRF2-dependent production of GSH in OVCA cells as well as caspase-3-dependent apoptosis in CD8+ T cells.

MATERIALS AND METHODS

Ethics Statement and Tissue Sampling

A written informed consent was obtained from all subjects. The study was conducted in accordance with the appropriate guidelines approved by the Centre hospitalier de l'Universite de Montreal (CHUM) Ethics Committee (IRB approval number; BD 04-002) and the Ottawa Health

Science Network Research Ethics Board (IRB approval number; OHSN-REB 1999540-01H). Normal and tumor tissues were collected from OVCA patients receiving treatment from 1992 to 2012 at the CHUM, Montreal. 208 formalin-fixed paraffin-embedded HGS and unverified OVCA tissues as well as 14 normal fallopian tube samples in duplicates were used to build a tissue microarray (TMA), as previously described (22). Details of patient population are outlined in **Supplementary Table S1**. Patients were diagnosed, tissues examined and clinical data gathered as previously described (22).

Interrogation of OVCA public datasets

Two (2) ovarian serous cystadenocarcinoma datasets publicly available on cbioportal (https://www.cbioportal.org/) were interrogated: TCGA, Nature 2011 (n=489) and TCGA, Firehouse legacy (n=530). The mRNA expression patterns of pGSN (GSN), NRF2 (NFE2L2), xCT (SLC7A11), GCLM, IFNγ (IFNG), granzyme b (GZMB) and perforin (PRF1) were evaluated in each patient and presented as heat maps. Pearson' and Spearman's correlation tests were performed to assess the association between pGSN and the other genes. Significant correlations were inferred as $P \leq 0.05$.

Supplementary Table 4.1. Epithelial expressions of markers in OVCA patients

Variable	Number of Patients	Median survival (months)
Age (Range; 36 – 89 years)		
≤ 62	109	
> 62	99	
Stage (FIGO)		
1	13	
2	20	
3	153	
4	22	
Histological Subtypes		
Not verified	33	
HGSC	174	
Endometrioid	1	
Residual disease (RD)		
≤ 1 cm	86	
> 1 cm	109	
Progression-free survival (PFS)		18
Non-recurrence	36	
Recurrence	172	
Overall Survival (OS)		49
Alive	37	
Deceased	162	

HGSC, high grade serous carcinoma; FIGO, International Federation of Gynecology and Obstetrics

Immunofluorescence (IF)

Tissue sections (TMAs) were immunostained using the BenchMark XT automated stainer (Ventana Medical System Inc. Tucson, AZ), as previously described (22). After deparaffinisation and antigen retrieval, the tissues were stained with their respective antibodies. Details of staining are described in the **Supplementary methods**.

Immunohistochemistry (IHC).

OVCA cell pellets (TMA) were immunostained using BenchMark XT automated stainer (Ventana Medical System Inc. Tucson, AZ). After deparaffinisation and antigen retrieval, the tissues were stained with anti-pGSN and then incubated in a secondary antibody. Details on tissue staining and antibodies used are described in the **Supplementary methods** and **Supplementary Table S2** respectively.

Reagents.

Cis-diaminedichloroplatinum (CDDP), phenylmethylsulfonyl fluoride (PMSF), aprotinin, dimethyl sulfoxide (DMSO), sodium orthovanadate (Na_3VO_4), CCK-8 and Hoechst 33258 were supplied by Millipore Sigma (St. Louis, MO). Two preparations of pGSN siRNA (siRNA1 and 2) and scrambled sequence siRNA (control) were purchased from Integrated DNA Technology (Iowa, USA) and Dharmacon (Colorado, USA), respectively. Human CRISPR/Cas9 KO and CRISPR activation (OX) plasmid for FLIP (short and long), and their scrambled sequence siRNA (control) were purchased from Santa Cruz (Mississauga, Canada). Recombinant human plasma gelsolin (rhpGSN) and IFNγ (rhIFNγ) were purchased from Cytoskeleton, Inc, USA and Life Technologies, Canada, respectively. pGSN cDNA and 3.1A vector plasmids were

generously provided by Dr. Dar-Bin Shieh, National Cheng Kung University Hospital, Taiwan. pCT-CD63-GFP was purchased from System Biosciences, LLC. See **Supplementary Table S2** for details on antibodies and other reagents.

Cell Lines and Primary Cells.

Human peripheral CD8+ and CD4+ T cells were purchased from Stemcell Technologies, Canada. T cells were expanded with ImmunoCult XF T cell expansion media and activated using ImmunoCult Human CD3/CD28/CD2 T cell activator. Both expansion and activating media were purchased from Stemcell Technologies, Canada. Chemosensitive and chemoresistant OVCA cell lines (1.6×10^6 cells) of HGS and endometrioid histologic subtypes were used for all *in vitro* studies. The endometrioid cell lines were generously donated by Dr. Barbara Vanderhyden (Ottawa Hospital Research Institute, Ottawa, Canada) whereas the HGS cell lines were kindly provided by Dr. Anne-Marie Mes-Masson [Centre de recherche du Centre hospitalier de l'Université de Montréal (CRCHUM), Canada]. Cell lines used were tested for *Mycoplasma* contamination using PlasmoTest™ Mycoplasma Detection kit (Invivogen; catalog number: rep-pt1), authenticated and continuously monitored for morphological changes as well as growth rate for any batch-to-batch change. Cell lines were maintained between passages 10 and 21 during the study after thawing. Details on the histologic subtypes and mutations of the cell lines used are described in **Supplementary Table S3**. The HGS cell lines were cultured and maintained in OSE medium (Wisent Inc., St-Bruno, QC, Canada) whereas the endometrioid cell lines were cultured and maintained in Dulbecco's Modified Eagle Medium (Gibco DMEM/F12; Life Technologies, NY, USA; catalog numbers 10565-018/10313-021) and/or Gibco RPMI 1640 (Life Technologies, NY, USA; catalog number: 31800-022), as previously reported (23-26).

Media were supplemented with 10% FBS (Millipore Sigma; St. Louis, MO), 50 U/mL penicillin, 50 U/mL streptomycin, and 2 mmol/L l-glutamine (Gibco Life Technologies, NY, USA). All experiments were carried out in serum-free media.

Gene Interference and Transient Transfection.

Cells were transfected (50 nM, 24 h) with CRISPR/Cas9 KO plasmids (2 μg; 24 h) and siRNAs (empty vector as controls) using lipofectamine 2000. Cells were transfected (2 μg; 24 h) with pGSN cDNA and FLIP activation plasmid (empty vector as controls). Cells were then treated with CDDP (10 μM; 24 h) or sEV-pGSN (40 μg/400,000 cells; 24 h) and harvested for analysis, as previously described (23, 24, 27). Two different siRNAs were used for each target to exclude off-target effects. Successful knock-down/knock-out and overexpression were confirmed by Western blotting (9). See **Supplementary Table S2** for details on antibodies.

Extracellular Vesicle (EVs) Isolation, Characterization and Nanoparticle Tracking Analysis (NTA).

Serum-free conditioned media from cultured cells were used for extracellular vesicle isolation and characterization, as described (28)**.** sEVs were isolated by differential ultracentrifugation: 300 g for 10 min at room temperature (RT) to remove cells; 20,000 g for 20 min, RT to remove large EVs (microparticles) and then 100,000 × g for 90 min at 4°C for sEVs (exosomes). Details on EV characterization and NTA are provided in the **Supplementary methods**.

sEV-GFP tagging and uptake.

Chemosensitive and chemoresistant OVCA cell lines (1.6 x 10^6 cells) were transfected with exosome cyto-tracer, pCT-CD63-GFP (SBI System Biosciences; CYTO120-PA-1; 1 µg) for 24 h in serum-free RPM1-1640. Conditioned media were collected and sEVs isolated. Activated human peripheral CD8+ T cells were treated with sEVs (40 µg/400,000 cells; 24 h). Cells were collected and WB used to assess pGSN and GFP contents. Details on antibodies are described in **Supplementary Table S2**.

Protein Extraction and Western blot Analysis.

Western blotting (WB) procedure for proteins were carried out as described previously (9, 23, 24). After protein transfer, membranes were incubated with primary antibodies (1:1000) in 5% (wt/vol) blotto and subsequently with the appropriate horseradish peroxidase (HRP)-conjugated secondary antibody (1:2000) in 5% (wt/vol) blotto. See **Supplementary Table S2** for details of antibodies used. Chemiluminescent Kit (Amersham Biosciences) was used to visualize the peroxidase activity. Signal intensities generated on the film were measured densitometrically using Image J.

ELISA

Concentrations of IL-2, TGF-β, TNF-α, IL-12, IL-4 and IFNγ in cell-free conditioned media from human peripheral CD8+ and CD4+ T cells treated with sEVs and rhpGSN were measured by Multi-Analyte ELISArray Kit (Qiagen, USA) and pGSN (patient plasma) by sandwich ELISA (Aviscera Bioscience, Inc. CA), as previously determined (14). Details of the assay are provided in the **Supplementary methods**.

Intracellular GSH detection

Intracellular GSH in cell lysates (100 µl) were colorimetrically determined at 450 nm, using a GSH detection assay kit (ab239727) and a microtiter plate reader, as per manufacturer's instructions. 1.6 x 10^6 cells [cultured in Dulbecco's Modified Eagle Medium (DMEM)] were used in each experiment in triplicates. Concentrations were reported as µM/mg protein.

Assessment of Cell Proliferation and Apoptosis.

Apoptosis and cell proliferation were assessed morphologically with Hoechst 33258 nuclear stain and colorimetrically with the CCK-8 assay, respectively. "Blinded" counting approach was used to prevent experimental bias with the Hoechst 33258 nuclear staining.

Statistical Analyses.

Statistical analyses were performed using the SPSS software version 25 (SPSS Inc., Chicago, IL, USA), PRISM software version 8.3 (Graphpad, San Diego, CA), student *t*-test, one- or two-way ANOVA and Bonferroni *post-hoc* tests (to determine the differences between multiple experimental groups). Two-sided $P \leq 0.05$ was inferred as statistically significant. The relationship of variables to other clinicopathologic correlates was examined using Fisher exact test, T test and Kruskal Wallis Test, as appropriate. Survival curves (PFS and OS) were plotted with Kaplan-Meier and P-values calculated using the log-rank test. Univariate and multivariate Cox proportional hazard models were used to assess the hazard ratio (HR) for age, residual disease, stage (FIGO), pGSN and CD8+ T cells as well as corresponding 95% confidence intervals (CIs).

Supplementary Table 4.2 Information on antibodies and reagents

Primary Antibodies						Secondary Antibodies					
Application	**Target**	**Antibody/reagent**	**Company**	**Catalog #**	**Dilution**	**Antibody**	**Conjugate**	**Company**	**Catalog #**	**Dilution**	**Note**
WB	pGSN	Anti-pGSN Goat polyclonal	Antibodies online(Atlanta, USA)	ABIN1019662	1:1000	Dnk polyclonal to Goat IgG	HRP	Abcam (Toronto, Canada)	Ab97110	1:2000	
WB	β-tubulin	Anti-tubulin rabbit monoclonal	Abcam (Toronto, Canada)	ab179511	1:1000	Goat Anti-rabbit IgG (H+L)	HRP	Bio-Rad (Mississauga, Canada)	170-6515	1:2000	
WB	β-actin	Anti-actin mouse monoclonal	Abcam (Toronto, Canada)	ab8226	1:1000	Goat Anti-mouse IgG (H+L)	HRP	Bio-Rad (Mississauga, Canada)	170-6516	1:2000	Fig. S2A
IHC	pGSN	Anti-pGSN mouse polyclonal	Antibodies online(Atlanta, USA)	ABIN659182	1:500						Fig. S1A
IF	CD8a	Anti-CD8 mouse monoclonal	Leica Biosystems, UK	NCL-L-CD8-4B11	1:50						
IF	pGSN	Anti-pGSN mouse polyclonal	Antibodies online(Atlanta, USA)	ABIN659182	1:500						
IF	Activated caspase-3	Anti-casp3 rabbit monoclonal	Cell signaling Technology, MA, USA	9661S	1:200						
IF	Cytokeratin 8/18	Anti-KRT mouse antibody	Dako	EP17/EP30	1:200						
WB	FADD	Anti-FADD rabbit monoclonal	Cell signaling Technology, MA, USA	2782S	1:1000	Goat Anti-rabbit IgG (H+L)	HRP	Bio-Rad (Mississauga, Canada)	170-6515	1:2000	
WB	FLIP	Anti-FLIP mouse monoclonal	Santa Cruz Biotechnology, USA	sc-5276	1:1000	Goat Anti-mouse IgG (H+L)	HRP	Bio-Rad (Mississauga, Canada)	170-6516	1:2000	
WB	Caspase-8	Anti-caspase-8 mouse monoclonal	Cell signaling Technology, MA, USA	9746	1:1000	Goat Anti-mouse IgG (H+L)	HRP	Bio-Rad (Mississauga, Canada)	170-6516	1:2000	
WB	Caspase-3	Anti-caspase-3 rabbit monoclonal	Cell signaling Technology, MA, USA	14220	1:1000	Goat Anti-rabbit IgG (H+L)	HRP	Bio-Rad (Mississauga, Canada)	170-6515	1:2000	
WB	Activated caspase-3	Anti-cleaved caspase-3 rabbit polyclonal	Cell signaling Technology, MA, USA	9661	1:1000	Goat Anti-rabbit IgG (H+L)	HRP	Bio-Rad (Mississauga, Canada)	170-6515	1:2000	
WB	NRF2	Anti-NRF2 mouse monoclonal	Abcam (Toronto, Canada)	ab89443	1:1000	Goat Anti-mouse IgG (H+L)	HRP	Bio-Rad (Mississauga, Canada)	170-6516	1:2000	
WB	p-NRF2	Anti-NRF2-pS40 rabbit monoclonal	Abcam (Toronto, Canada)	ab76026	1:1000	Goat Anti-rabbit IgG (H+L)	HRP	Bio-Rad (Mississauga, Canada)	170-6515	1:2000	
WB	γH2AX	Anti- γH2AX rabbit polyclonal	Abcam (Toronto, Canada)	ab11174	1:1000	Goat Anti-rabbit IgG (H+L)	HRP	Bio-Rad (Mississauga, Canada)	170-6515	1:2000	
WB	Stat1	Anti-Stat1 rabbit polyclonal	Abcam (Toronto, Canada)	ab99415	1:1000	Goat Anti-rabbit IgG (H+L)	HRP	Bio-Rad (Mississauga, Canada)	170-6515	1:2000	
WB	Stat1-p	Anti-Stat1-pY701 mouse monoclonal	Abcam (Toronto, Canada)	ab29045	1:1000	Goat Anti-mouse IgG (H+L)	HRP	Bio-Rad (Mississauga, Canada)	170-6516	1:2000	
WB	GFP	Anti-GFP chicken polyclonal	Abcam (Toronto, Canada)	ab13970	1:1000	Goat Anti-Chicken IgY (H+L)	HRP	Abcam (Toronto, Canada)	ab6877	1:2000	Fig. S2A
		Rh-IFNγ	Life technologies	PHC4033							
		Rh-pGSN	Cytoskeleton Inc.	HPG6							
		JAK inhibitor 1	Cell signaling Technology, MA, USA	14703							
	IFNGR1 Blocking antibody	Anti-IFNGR1	R&D Systems, USA	MAB6732							
T cell		ImmunoCult XF	Stemcell	10981							

expansion	T cell expansion media	technologies, Canada	
T cell activation	Immunocult Human CD3/CD28/CD2 T cell activator	Stemcell technologies, Canada	10970
	NAC	Millipore Sigma, Canada	A7250-10G
	BSO	Millipore Sigma, Canada	B2515-500MG

Supplementary Table 4.3 Information on OVCA cell lines

Cell line	Tumor origin	TP53 status	Other	Chemosensitivity
A2780s	Ovarian endometrioid adenocarcinoma	Wild-type	PTEN/ARID1A	Sensitive
A2780cp	Ovarian endometrioid adenocarcinoma	Mutant V127F, R260S	PTEN/ARID1A	Resistant
OV2295	High grade serous ovarian cancer	Mutant Ile195Thr	Not investigated	Sensitive
OV4453	High grade serous ovarian cancer	Mutant Splice	Not investigated	Sensitive
OV90	High grade serous ovarian cancer	Mutant Ser215Arg	Not investigated	Resistant
OV866(2)	High grade serous ovarian cancer	Mutant Arg249Trp	Not investigated	Resistant
TOV3133G	Serous-papillary adenocarcinoma	Nonsense	Not investigated	Sensitive
TOV2223G	Serous-papillary adenocarcinoma	Nonsense	Not investigated	Resistant
TOV3041G	Serous adenocarcinoma	Wild-type	Not investigated	Sensitive
OV1946	Serous-papillary adenocarcinoma	Missense	Not investigated	Resistant
TOV1946	Serous-papillary adenocarcinoma	Missense	Not investigated	Resistant
TOV1369	Serous-papillary adenocarcinoma	Missense	Not investigated	Resistant
OV3133	Serous-papillary adenocarcinoma	Nonsense	Not investigated	Sensitive

RESULTS

Patients' Characteristics.

Tumor staging and pathology were performed by a certified Gynecologic Oncology team. The characteristics of OVCA patients (N=208) are described in **Supplementary Table S1**. The median age of patients was 62 years (range; 36-89 years) and classified as FIGO stages 1 (N=13), 2 (N=20), 3 (N=153) and 4 (N=22). Patients in this study received no neoadjuvant chemotherapy or radiotherapy prior to sample collection at surgery. Eighty-six patients received complete/optimal cytoreduction. The median progression-free survival (PFS) and overall survival (OS) were 18 and 49 months respectively.

pGSN expression and CD8+ T cell infiltration in normal fallopian tube and HGS OVCA tissues.

Although increased pGSN expression renders HGS cancer cell lines resistant to CDDP treatment (13), the role of pGSN in the tumor microenvironment is not known. To investigate this, we first examined pGSN expression and CD8+ T cell infiltration using immunofluorescence (IF) on a TMA constructed with 208 OVCA specimens (174 HGS, 33 unverified and 1 endometrioid) and 14 normal fallopian tube tissues **(Fig. 1A, Supplementary Table S1)**. Prior to the study, staining of pGSN expression was optimized in 9 HGS OVCA cell pellets (WB and IHC; TMA) as well as a test TMA comprising of 15 HGS OVCA tissues and 7 normal fallopian tube tissues (IF; **Fig. S1A & B**). We then determined by digital image analysis and measure of mean fluorescence intensity (MFI), the relative levels of pGSN expression in the epithelial and stromal areas of the tissues as well as their prognostic impact on the survival of the patients.

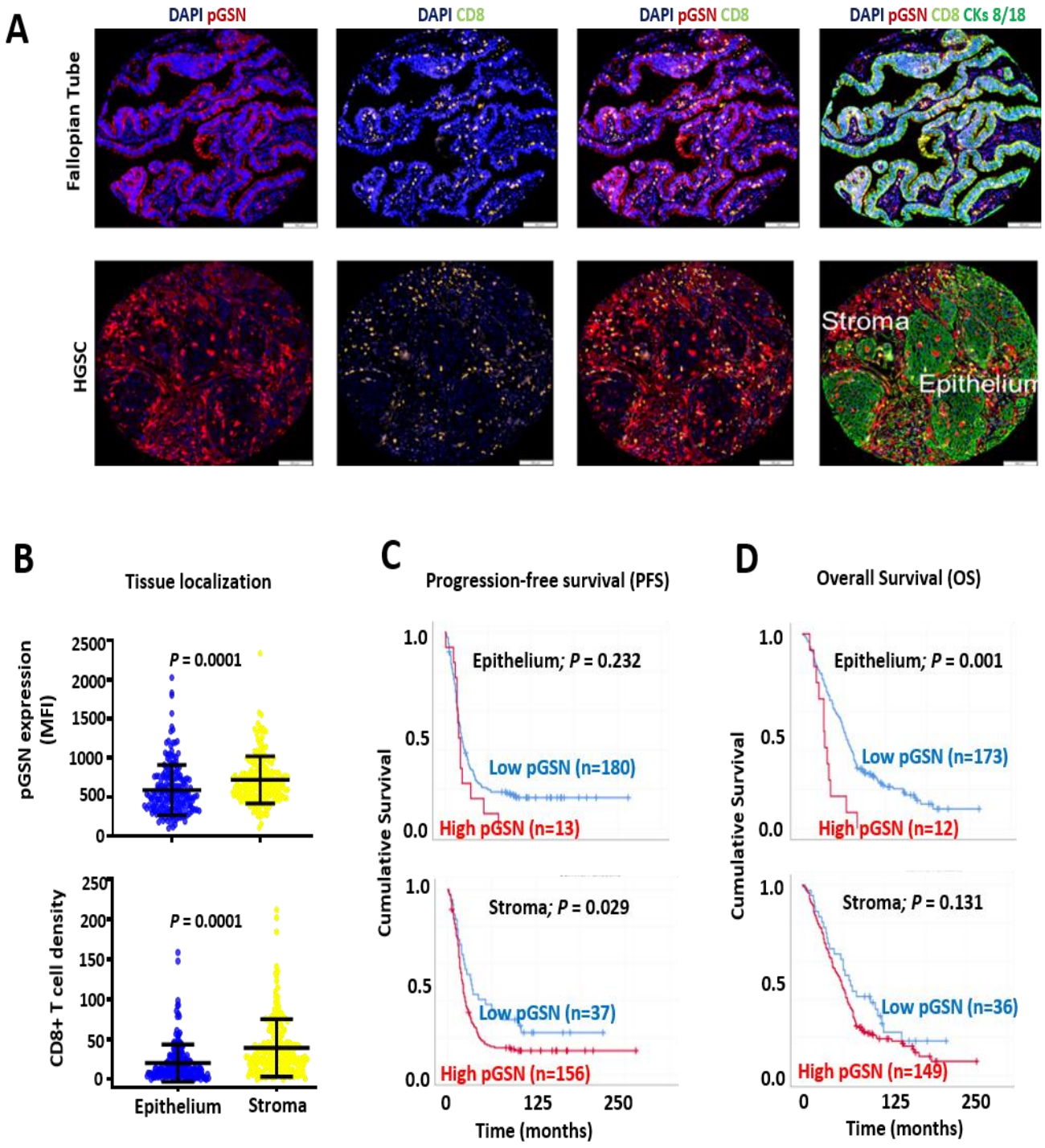
A
DAPI pGSN
DAPI CD8
DAPI pGSN CD8
DAPI pGSN CD8 CKs 8/18
Fallopian Tube
HGSC
Stroma
Epithelium
B
Tissue localization
pGSN expression (MFI)
P = 0.0001
CD8+ T cell density
P = 0.0001
Epithelium
Stroma
C
Progression-free survival (PFS)
Cumulative Survival
Epithelium; P = 0.232
Low pGSN (n=180)
High pGSN (n=13)
Stroma; P = 0.029
Low pGSN (n=37)
High pGSN (n=156)
Time (months)
D
Overall Survival (OS)
Epithelium; P = 0.001
Low pGSN (n=173)
High pGSN (n=12)
Stroma; P = 0.131
Low pGSN (n=36)
High pGSN (n=149)

Figure 4.1 pGSN expression and CD8+ T cell infiltration in normal fallopian tube and HGS OVCA tissues. (A) 208 high grade serous ovarian cancer tissues and normal fallopian tubes were immuno-stained with anti-pGSN (red), anti-CD8 (yellow), anti-cytokeratin (green) and dapi (blue). **(B)** pGSN expression (N=198) and infiltrated CD8+ T cells (N=198) were quantified and compared in the epithelial and stromal components using scatter plots (mean ± SD). **(C)** pGSN expression in both the epithelial and stroma were correlated with progression free survival (PFS) time of the patients. Kaplan-Meier survival curves with dichotomized pGSN expression (low and high group, epithelial MFI cut-off = 1141; stromal MFI cut-off = 475.4) and log rank test were used to compare the survival distributions between the groups. **(D)** pGSN expressions in epithelium and stroma were correlated with OS. Kaplan Meier survival curves with dichotomized pGSN expression (low and high group, epithelial MFI cut-off = 1141; stromal MFI cut-off = 475.4) and log rank test were used to compare the survival distributions between the groups. *P*-values were calculated by independent sample *t*-test. N = number of patients in each group.

A

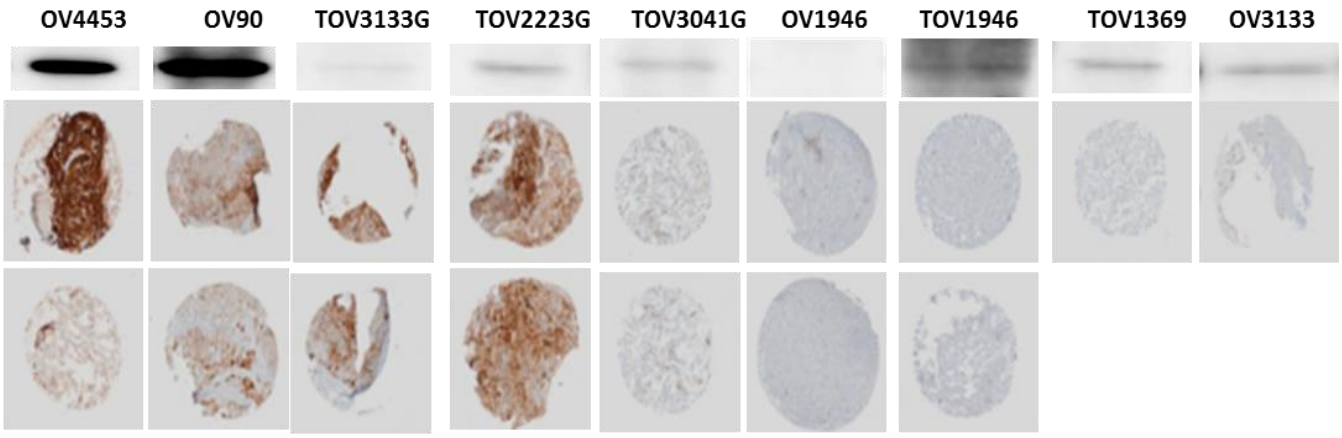

B

HGSC		Fallopian tube	
651	3465	3350	3351
768	2647	3415	3514
1118	2332	3531	3538
1159	1793		3568
1317	1792		
1334	1791		
1396	1710		
1464			

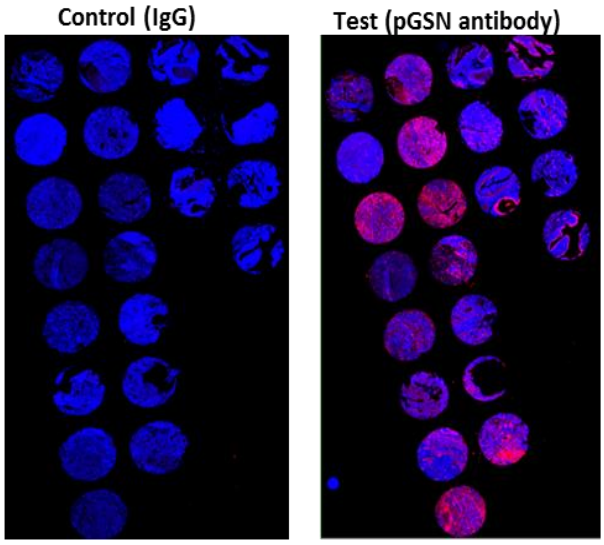

C

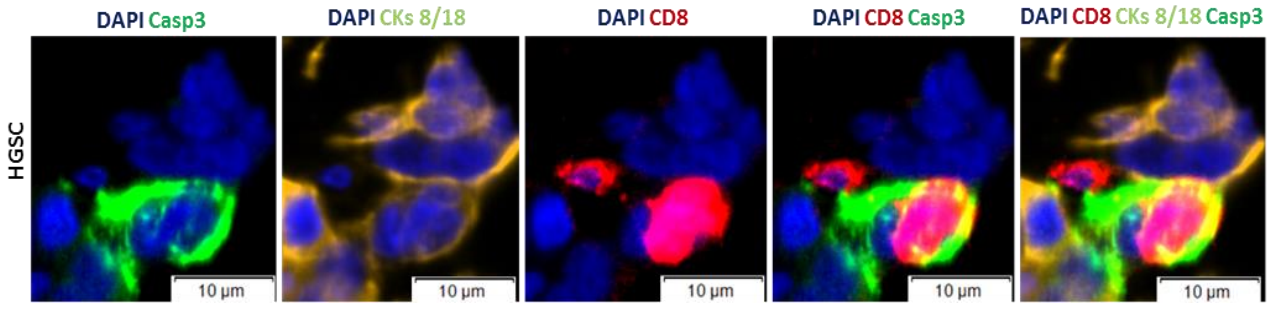

Fig. 4.S1. pGSN expression was validated in HGS OVCA cell pellets, tissues and normal fallopian tube tissues. (A). 9 HGS OVCA cell pellets were immunostained with anti-pGSN antibody using Western blot and IHC. **(B)**15 HGS OVCA tissues and 7 normal fallopian tube tissues were immunostained with anti-pGSN (red) and dapi (blue). **(C)** 208 high grade serous ovarian cancer tissues were immunostained with anti-caspase-3 (green), anti-CD8 (red), anti-cytokeratin (yellow) and dapi (blue).

Supplementary Table 4.4 Epithelial expressions of markers in OVCA patients

Tissue Marker Expression (MFI)	Number of Patients
Epithelial pGSN (Cut-off = 659)	
Low	135
High	63
Epithelial pGSN (Cut-off = 1141)	
Low	185
High	13
Stromal pGSN (Cut-off = 475.4)	
Low	38
High	160
Epithelial CD8+ T cells (Cut-off = 40.64)	
Low	173
High	25
Stromal CD8+ T cells (Cut-off = 33.84)	
Low	113
High	85
Epithelial CD8+ T cells (Cut-off = 40.64)/ Epithelial pGSN (Cut-off = 659)	15
Low pGSN/High CD8+ T cells	10
High pGSN/High CD8+ T cells	120
Low pGSN/Low CD8+ T cells	53
High pGSN/Low CD8+ T cells	
Circulatory pGSN (Cut-off = 79.61)	
Low	68
High	24

IRS, immunoreactive score; pGSN, plasma gelsolin

pGSN was rarely expressed in epithelial and stromal areas of the fallopian tube tissue although CD8+ T cell infiltration was detectable **(Fig. 1A; Supplementary Table S4)**. In contrast, pGSN expression was clearly detectable in HGS OVCA tissues, with the stromal levels [mean ± SD (717.4 ± 303.4)] being higher (P = 0.0001) than the epithelial levels [mean ± SD (586.9 ± 323.2)]. HGS OVCA tissues were positive for CD8+ T cells with stromal localisation [mean ± SD (39.3 ± 35.9 vs. 20.3 ± 23.2)] being higher **(**P = 0.0001**; Fig. 1B)**. Increased expression of pGSN was significantly associated with progression-free survival (PFS) in the stroma region (P = 0.029) but not in the epithelial region (P = 0.232) **(Fig 1C)**. Patients with increased epithelial pGSN expression had significantly poorer overall survival (OS) compared with patients with lower pGSN expression **(**P = 0.001**; Fig. 1D)**. However, no significant difference was observed in OS between patients with lower and higher stromal pGSN expression (P = 0.131; **Fig. 1D**).

Increased pGSN expression is associated with reduced survival impact of tumor infiltrated CD8+ T cells on patient survival.

After demonstrating in HGS OVCA tissues that patients with increased levels of pGSN are highly associated with poor chemoresponsiveness and survival, we hypothesized that pGSN expression may influence the prognostic impact of infiltrated CD8+ T cells. Thus, we analysed the MFI of pGSN expression and CD8+ T cell density in the epithelial and stromal regions of the HGS OVCA TMAs and determined the prognostic impact of pGSN and CD8+ T cell co-localisation in HGS OVCA patients **(Fig. 2; Supplementary Table S4)**. pGSN expression and CD8+ T cell infiltration were clearly detectable in the epithelial and stromal regions of 95% of the HGS OVCA TMA investigated **(Fig. 2A).** Chemosensitive patients [progression-free interval

(PFI) > 12 months; N = 135] had increased CD8+ T cell infiltration regardless of the tissue location [mean ± SD; epithelium: 21.8 ± 25.6 (chemosensitive) vs. 18.0 ± 17.1 (chemoresistance); stroma: 43.5 ± 40.0 (chemosensitive) vs. 30.9 ± 23.1 (chemoresistance)] compared with chemoresistant patients (PFI ≤ 12 months; N = 58), although the difference was only significant in the stromal compartment (epithelium: P = 0.23; stroma: *P* = 0.03) **(Fig. 2B).** Patients with increased epithelial CD8+ T cell infiltration had improved PFS (*P* = 0.005) and OS (*P* = 0.042) compared with patients with lower CD8+ T cell infiltration **(Fig. 2C)**. Patients with lower pGSN expression but higher CD8+ T cell infiltration had improved PFS and OS compared with higher pGSN but lower CD8+ T cell infiltration. Interestingly, increased pGSN expression appeared to be associated with lower protective effect of elevated levels of CD8+ T cell infiltration as observed in the OS (*P* = 0.05) and DFS (*P* = 0.019) of patients with high pGSN and high CD8+ T cells **(Fig. 2C)**. To determine why most infiltrated CD8+ T cells stained positive for pGSN and their survival impact on patients hindered by increased pGSN expression, we immunostained the HGS OVCA tissues for activated caspase-3, a marker for apoptotic cell death **(Fig. S1C).** Caspase-3 activation was observed in both CD8 T cells and epithelial cells and was difficult attributing the caspase activation to only CD8+ T cells **(Fig. S1C)**. T cells barely express pGSN at both mRNA and protein levels **(Fig. S2A & B)**, hence it was surprising that CD8+ T cells stained positive for pGSN in both the epithelial [N = 195; mean ± SD (739.4 ± 352.7) and stromal regions [N = 196; mean ± SD (798.9 ± 336.4)] although there was no significant difference between the locations **(***P* = 0.09**; Fig. 2D)**. We further analysed the correlation between circulatory pGSN and infiltrated CD8+ T cells in the epithelium and stroma **(Fig. 2E)**. Circulatory pGSN of patients were analysed and dichotomized into low and high groups. The epithelial and stromal CD8+ T cell infiltration were quantitated and compared.

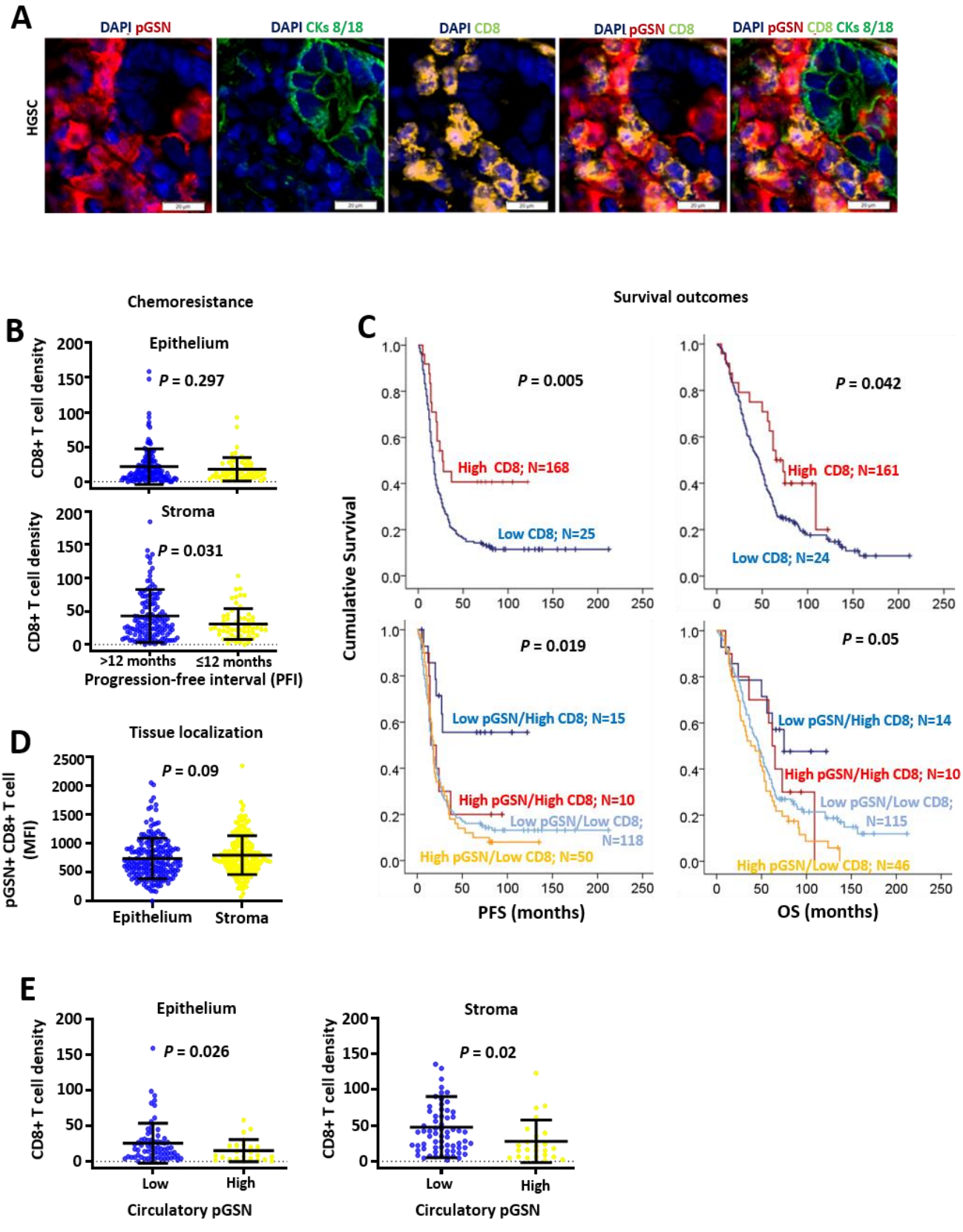
A
DAPI pGSN
DAPI CKs 8/18
DAPI CD8
DAPI pGSN CD8
DAPI pGSN CD8 CKs 8/18
HGSC
B
Chemoresistance
Epithelium
P = 0.297
CD8+ T cell density
Stroma
P = 0.031
>12 months
≤12 months
Progression-free interval (PFI)
C
Survival outcomes
P = 0.005
High CD8; N=168
Low CD8; N=25
P = 0.042
High CD8; N=161
Low CD8; N=24
P = 0.019
Low pGSN/High CD8; N=15
High pGSN/High CD8; N=10
Low pGSN/Low CD8; N=118
High pGSN/Low CD8; N=50
P = 0.05
Low pGSN/High CD8; N=14
High pGSN/High CD8; N=10
Low pGSN/Low CD8; N=115
High pGSN/Low CD8; N=46
Cumulative Survival
PFS (months)
OS (months)
D
Tissue localization
P = 0.09
pGSN+ CD8+ T cell (MFI)
Epithelium
Stroma
E
Epithelium
P = 0.026
CD8+ T cell density
Low
High
Circulatory pGSN
Stroma
P = 0.02
CD8+ T cell density
Low
High
Circulatory pGSN

Figure 4.2 Increased pGSN expression is associated with reduced survival impact of tumor infiltrated CD8+ T cells. A) 208 high grade serous ovarian cancer tissues were immunostained with anti-pGSN (red), anti-CD8 (yellow), anti-cytokeratin (green) and dapi (blue). **(B)** CD8+ T cell infiltration in both the epithelial and stroma compartments were correlated with chemoresponsiveness [chemosensitivity (PFI > 12 months), N = 135; chemoresistance (PFI ≤ 12 months), N = 58]. The difference between the two groups was compared using scatter plots (mean ± SD). **(C)** pGSN expression and infiltrated CD8+ T cells in epithelium were correlated with PFS and OS. Kaplan Meier survival curves of categorized pGSN expression (low and high group, MFI cut-off = 659.4) and CD8 density (low and high group, density cut-off = 40.64) and log rank test were used to compare the survival distributions between the groups. **(D)** CD8+ T cells which stained positive for pGSN were quantified and compared in the epithelial (N=195) and stromal (N=196) components. The difference between the two groups was compared using scatter plots (mean ± SD). **(E)** Using a cut-off of 79.61, patients were stratified into two groups (low; N = 68 and high; N = 24) according to their circulatory pGSN levels. Infiltrated CD8+ T cells in the epithelium and stroma of the groups were compared and represented as scatter plots (mean ± SD). *P*-values were calculated by independent sample *t*-test. N = number of patients in each group.

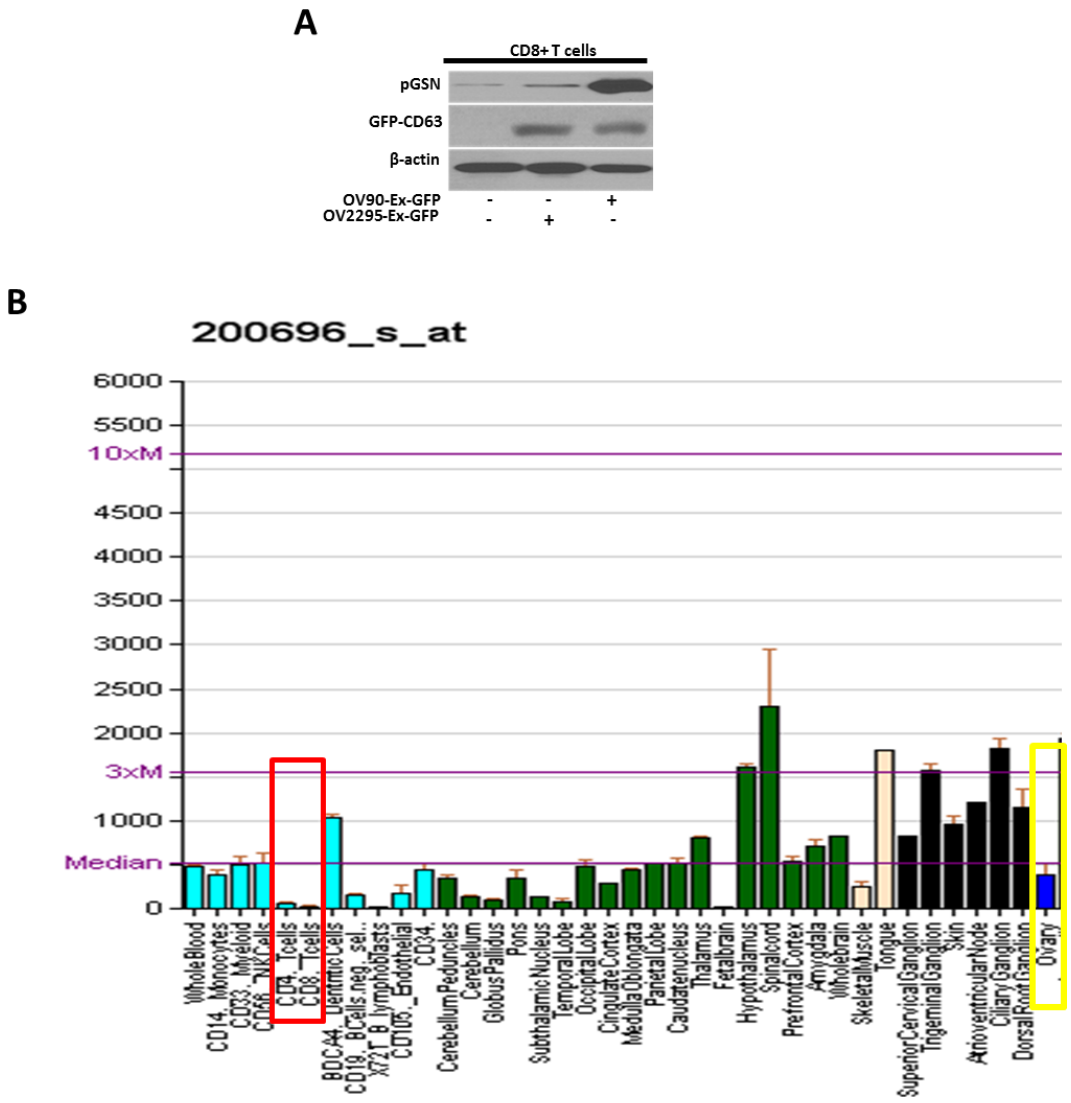

Fig. 4.S2 pGSN mRNA is barely expressed in CD8+ T cells. (A) Activated human peripheral CD8+ T cells were treated with sEVs (40 µg/400,000 cells; 24 h) tagged with CD63-GFP (1 ug; 24h). Western blot was used to examine the contents of pGSN, GFP-CD63 and β-actin. **(B)** pGSN mRNA expression in 79 human tissues were assayed on a genome scale. pGSN mRNA expression in T cells (Red box) is barely detectable compared with the ovary (yellow box). Diagram created by Andrew GNF based on data from Su AI, Wiltshire T, Batalov S, et al (2004). "A gene atlas of the mouse and human protein-encoding transcriptomes".

Interestingly, patients with low levels of circulatory pGSN had increased infiltration of CD8+ T cells compared with patients with higher circulatory pGSN levels in both the epithelial [P = 0.026; N = 92; (mean ± SD; 25.7 ± 28.0 vs 15.1 ± 15.6)] and stroma [P = 0.02; N = 92; (mean ± SD; 47.0 ± 42.7 vs 28.0 ± 29.7)] compartments **(Fig. 2E)**. This supports the hypothesis that secreted pGSN regulates immune cell infiltration and function.

Prognostic impact of epithelial pGSN and relationship with other clinicopathologic parameters

The prognostic impact of epithelial pGSN and CD8+ T cell density together with other clinicopathological parameters (age, residual disease and stage) were evaluated using uni- and multivariate Cox regression analyses, as demonstrated in **Supplementary Tables S5 and S6**, respectively. The optimal (using Fisher's exact test) cut-offs for the markers were used to predict PFS and OS. From the univariate Cox regression analysis, only stage (FIGO), residual disease and CD8+ T cell density demonstrated a significant association with PFS (**Supplementary Table S5**). Unlike PFS, all parameters analysed showed a significant association with OS. In the multivariate Cox regression analysis (**Supplementary Table S6**), only residual disease (HR, 0.552; CI, 0.359-0.850; P = 0.007) significantly predicted PFS. In predicting increased risk of death, only pGSN (HR, 0.185; CI, 0.089-0.373; $P < 0.001$) was significantly associated with OS (**Supplementary Table S6**).

Supplementary Table 4.S5 Univariate Cox regression analysis for progression-free and overall survival

	Univariate Analysis					
Variable	**PFS**			**OS**		
	HR*	**95% CI^**	***P*-value**	**HR***	**95% CI^**	***P*-value**
Age (years) **≤62 vs >62**	0.887	0.657 – 1.197	0.433	0.706	0.518 – 0.961	**0.027**
Stage (FIGO) **≤2 vs >2**	0.342	0.208 – 0.556	**<0.001**	0.418	0.249 – 0.702	**0.001**
RD (cm) **≤1 vs >1**	0.392	0.283 – 0.542	**<0.001**	0.525	0.376 – 0.731	**<0.001**
pGSN^{epi} **Low vs high**	0.713	0.404 – 1.260	0.244	0.376	0.206 – 0.687	**0.001**
CD8+ T cell^{epi} **Low vs high**	2.129	1.229 – 3.686	**0.007**	1.726	1.010 – 2.949	**0.046**

HR, hazard ratio; PFS, progression-free survival; OS, overall survival; CI, confidence interval; RD, residual disease; pGSN, plasma gelsolin; FIGO, International Federation of Gynecology and Obstetrics; vs, versus; epi, epithelial

*Estimated from Cox proportional hazard regression model.

^Confidence interval of the estimated HR.

Supplementary Table 4.S6 Multivariate Cox regression analysis for progression-free and overall survival

Multivariate Analysis						
Variable	**PFS**			**OS**		
	HR*	**95% CI^**	***P*-value**	**HR***	**95% CI^**	***P*-value**
Age (years) **≤62 vs >62**	0.909	0.634 – 1.303	0.604	0.717	0.492 – 1.044	0.083
Stage (FIGO) **≤2 vs >2**	0.625	0.330 – 1.184	0.150	0.744	0.372 – 1.487	0.402
RD (cm) **≤1 vs >1**	0.552	0.359 – 0.850	**0.007**	0.675	0.432 – 1.055	0.085
pGSN^{epi} **Low vs high**	0.656	0.351 – 1.229	0.188	0.185	0.089 – 0.373	**<0.001**
CD8+ T cell^{epi} **Low vs high**	1.452	0.748 – 2.817	0.270	1.272	0.655 – 2.470	0.477

HR, hazard ratio; PFS, progression-free survival; OS, overall survival; CI, confidence interval; RD, residual disease; pGSN, plasma gelsolin; FIGO, International Federation of Gynecology and Obstetrics; vs, versus; epi, epithelial

*Estimated from Cox proportional hazard regression model.

^Confidence interval of the estimated HR.

sEV-pGSN induces CD8+ T cell death via FLIP down-regulation and caspase-3 activation.

We had earlier detected that elevated pGSN expression in HGS OVCA tissues was associated with shortened survival of patients with tumors highly infiltrated by CD8+ T cells **(Fig. 2)**. Although activated caspase-3 was detected in the tissues, it was difficult attributing it to infiltrated CD8+ T cells or the epithelial cells **(Fig. S1C)**. We therefore hypothesized that sEV-pGSN induced apoptosis in CD8+ T cells via caspase-3 activation. Using standard *in vitro* techniques, we validated the pro-apoptotic role of pGSN in CD8+ T cells as well as the mechanism involved. Conditioned media from chemoresistant and chemosensitive OVCA cells were collected and sEVs isolated. sEVs were characterized as previously determined (13); pGSN knock-down and over-expression in sEVs was confirmed in chemoresistant and chemosensitive OVCA cells respectively (**Fig. S3A & B**).

Human peripheral CD4+ and CD8+ T cells were activated (using ImmunoCult Human CD3/CD28/CD2 T cell activator) and expanded (using ImmunoCult XF T cell expansion media purchased from Stemcell Technologies). Activated CD8+ T cells were treated with exogenous pGSN and sEV-pGSN derived from chemosensitive (OV2295), chemoresistant (OV90) and pGSN-knockdown (siRNA) chemoresistant (OV90-pGSN-KD) OVCA cancer cell lines. The influence of pGSN on apoptotic cell death and cell proliferation of T cells were assessed morphologically (Hoechst nuclear staining) and colorimetrically (CCK-8), respectively. Only exogenous pGSN and chemoresistant cell-derived sEV-pGSN induced apoptosis and decreased proliferation in CD8+ T cells **(Fig. 3A),** responses that were concentration-dependent **(Fig. S4A)**. In contrast, CD4+ T cell survival was not affected by sEV-pGSN treatment irrespective of the resistance status of donor cells **(Fig. S4B)**; however, were polarized into type 2 helper CD4+ T cells, as evident by increased IL4/IFNγ ratio **(Fig. S4C & D)**.

To further investigate the mechanism involved, activated CD8+ T cells were treated with exogenous pGSN, and CD8+ T cell death and caspase 3-dependent signaling proteins were assessed upon sEV uptake **(Fig. S2A)**. The apoptotic response of CD8+ T to treatment with chemoresistant cell-derived sEV was associated with decreased FLIP content and activation of caspase-8 and caspase-3 **(Fig. 3B)**. To demonstrate the role of FLIP in the action of pGSN, this cell survival protein was force-expressed or knocked-out in activated CD8+ T cells and then treated with chemoresistant cell-derived sEVs **(Fig. 3C & D)**. Forced-expression of FLIP attenuated pGSN-induced apoptosis whereas FLIP KO further sensitized CD8+ T cells to pGSN-induced apoptosis **(Fig. 3C & D)**. Co-culturing activated CD8+ T cells with pGSN-KD-chemoresistant cells (OV90 and A2780cp) failed to induce caspase-3 activation and apoptosis **(Fig. 3E)**. pGSN-cDNA-chemosensitive cells (OV2295 and A2780s) induced caspase-3 activation and apoptosis in activated CD8+ T cells after co-culturing for 24 h **(Fig. 3F)** suggesting the pro-apoptotic role of pGSN in activated CD8+ T cells.

Increased pGSN expression promotes NRF2-dependent GSH production.

NRF2 is a transcription factor that controls the body's homeostatic balance by regulating the production of antioxidant proteins such as GSH and xCT (18). Elevated GSH production is associated with CDDP resistance in ovarian and other cancer types (15-17); however, the role of pGSN in regulating NRF2-dependent GSH biosynthesis is yet to be demonstrated. To investigate the expression and possible role of GSH in the regulation of chemoresponsiveness in OVCA, we assessed the intracellular GSH production of chemoresistant and sensitive OVCA cells after treatment with CDDP (10 μM; 24 h).

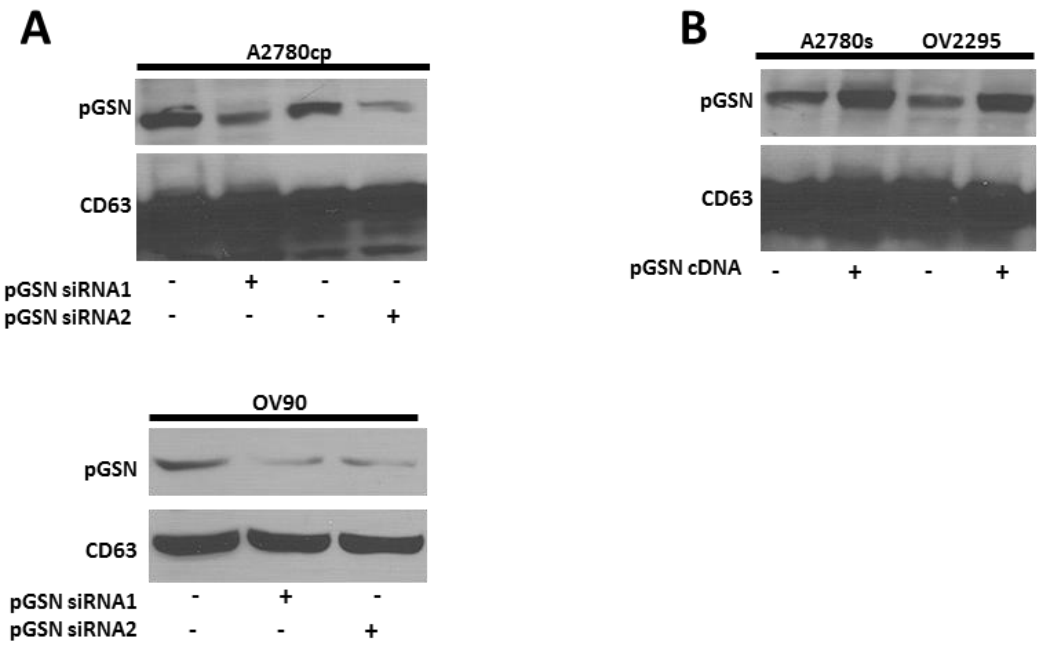

Fig. 4.S3 pGSN knock-down and over-expression in sEVs. (A) Chemoresistant OVCA cells (A2780cp and OV90) were treated with pGSN siRNA1 and 2 (50 nM; 24 h). (B) Chemosensitive OVCA cells (A2780s and OV2295) were treated with pGSN cDNA (2 µg; 24 h). Conditioned media from treated cells were collected and sEVs isolated. pGSN and exosome marker (CD63) contents were assessed by Western blot.

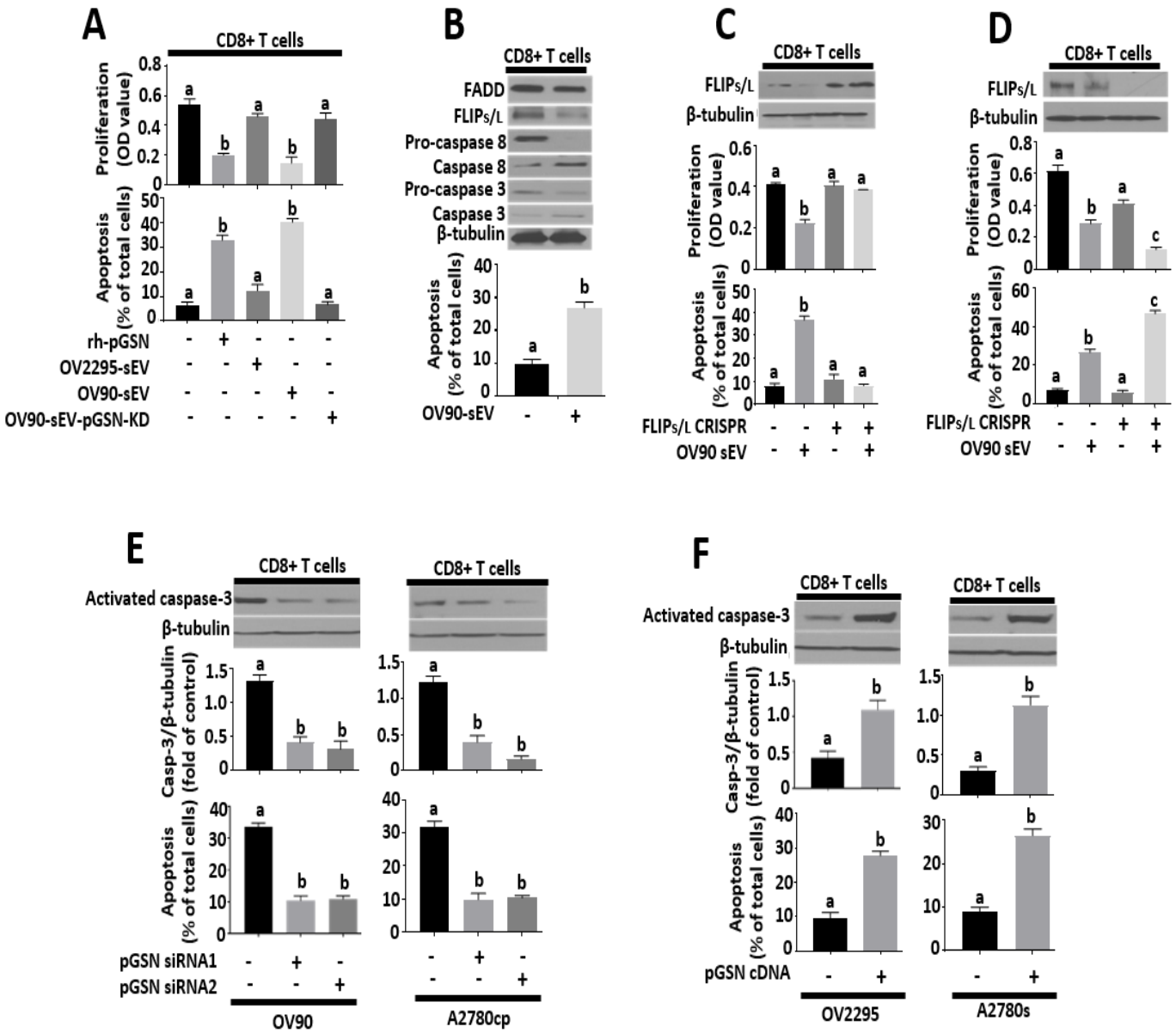

Figure 4.3 sEV-pGSN induces CD8+ T cell death via FLIP down-regulation and caspase-3 activation. (A) Activated human peripheral CD8 T cells were treated with human recombinant (rh) pGSN (10 µM; 24 h), sEVs (40 µg/400,000 cells; 24 h) derived from chemosensitive (OV2295) and chemoresistant HGS OVCA cell lines (OV90) and sEVs (40 µg/400,000 cells; 24 h) derived from pGSN knocked down (KD) chemoresistant cell lines (OV90). **(B)** Activated human peripheral CD8+ T cells were treated with OV90-derived sEVs (40 µg/400,000 cells; 24

h). sEV-depleted conditioned media was used as control. **(C)** FLIPs/l was forced expressed (CRISPR/OX, 2 µg; 24h) or **(D)** knock out (CRISPR KO, 50 nM; 24h) in activated CD8+ T cells and then treated with sEVs (40 µg/400,000 cells; 24 h). **(E)** Activated human peripheral CD8+ T cells were treated with sEVs (40 µg/400,000 cells; 24 h) derived from chemoresistant OVCA cell lines (OV90 and A2780cp) with or without pre-treatment with two different siRNAs for pGSN knocked down (siRNA1 or siRNA2; 50 nM, 24 h). **(F)** Activated human peripheral CD8+ T cells were treated with sEVs (40 µg/400,000 cells; 24 h) derived from chemosensitive OVCA cell lines (OV2295 and A2780s) with or without pGSN forced expression (cDNA, 2 µg; 24 h). Cell proliferation and apoptosis were assessed by CCK-8 assay and Hoechst staining respectively. Western blotting was used to examine protein contents (FADD, FLIP, Caspase 8, Caspase 3 and β-tubulin). Results are expressed as means ± SD from three independent replicate experiments. *[**A**, (a; ***P<0.001 vs b); **B**, (a; ***P<0.001 vs b); **C**, (a; ***P<0.001 vs b); **D**, (a; ***P<0.001 vs b and c); **E**, (a; ***P<0.001 vs b); **F**, (a; ***P<0.001 vs b)]*.

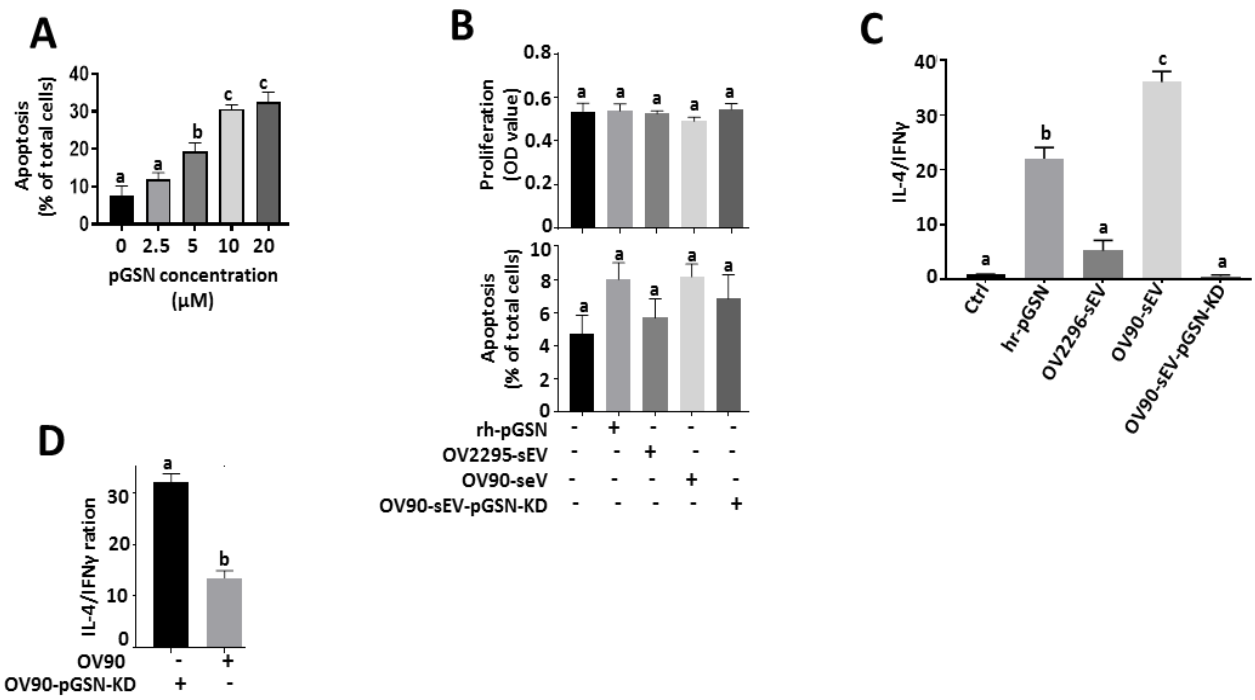

Fig. 4.S4 pGSN induces CD8+ T cell death whereas sEV-pGSN polarizes naïve CD4+ T cells towards type 2 helper cells. (A) CD8+ T cells were treated with increasing dose of recombinant human pGSN (0 – 20 μM; 24 h). Apoptosis was analyzed by morphologically by Hoechst staining. **(B and C)** Activated human primary naïve CD4+ T cells were treated with human recombinant (rh) pGSN (10 μM; 24 h), exosomes (40 μg/400,000 cells; 24 h) derived from chemosensitive (OV2295) and chemoresistant HGSC cell lines (OV90) and pGSN knocked down (KD) exosomes (40 μg/400,000 cells; 24 h) derived from chemoresistant cell lines (OV90). **(D)** CD8+ T cells (400,000 cells) were co-cultured with chemoresistant (OV90) cells and OV90-pGSN-KD cells (24 h). IL-4 and IFNγ levels were measured by ELISA. Cell proliferation and apoptosis were assessed by CCK-8 assay and Hoechst staining respectively. IL-4 and IFNγ levels were measured using sandwich ELISA. Results are expressed as means ± SD from three or more independent replicate experiments. *[**A**, (a; *P<0.05 vs b), (a; **P<0.01 vs c); **B**, (a; ***P<0.001 vs b and c); **C**, (a; ***P<0.001 vs b)]*.

Chemoresistant OVCA cell lines (OV90 and A2780cp) produced higher levels of intracellular GSH compared with their sensitive counterparts (OV2295 and A2780s) **(Fig. 4A & B)**. This phenomenon was associated with increased pGSN, total NRF2 and phospho-NRF2 **(Fig. 4A & B)**. Increased γH2AX (an indicator of DNA damage as a result of CDDP accumulation) and CDDP-induced apoptosis were detected in the chemosensitive cells but not in their resistant counterparts **(Fig. 4A & B)**. To investigate the role of pGSN in GSH production, pGSN was knocked down in chemoresistant cell (OV90) using siRNA (50 nM; 24 h) and then treated with CDDP (10 μM; 24 h). pGSN down-regulation resulted in a decrease in total NRF2, phospho-NRF2 and intracellular GSH as well as sensitized the resistant cells to CDDP-induced γH2AX content and apoptosis **(Fig. 4C)**. Forced expression of pGSN (2 μg cDNA; 24 h) in chemosensitive OVCA cells (OV2295) increased total NRF2, phospho-NRF2 and intracellular GSH; responses that were not affected by CDDP treatment. pGSN forced expression also attenuated CDDP-induced γH2AX and apoptosis in the sensitive OVCA cells **(Fig. 4D)**. Our interrogation of cbioportal public datasets (TCGA firehouse legacy) revealed a positive and significant correlation between pGSN and NFE2L2 (NRF2) and SLC7A11 (xCT) involved in GSH production (**Fig. 4E & F).** Our interrogation of TCGA nature 2011 datasets also revealed a weak but significant association between pGSN mRNA expression and NFE2L2 (NRF2) and SLC7A11 (xCT) **(Fig. S5A – C),** providing supporting evidence that pGSN mediates GSH production via activation of the NRF2 pathway.

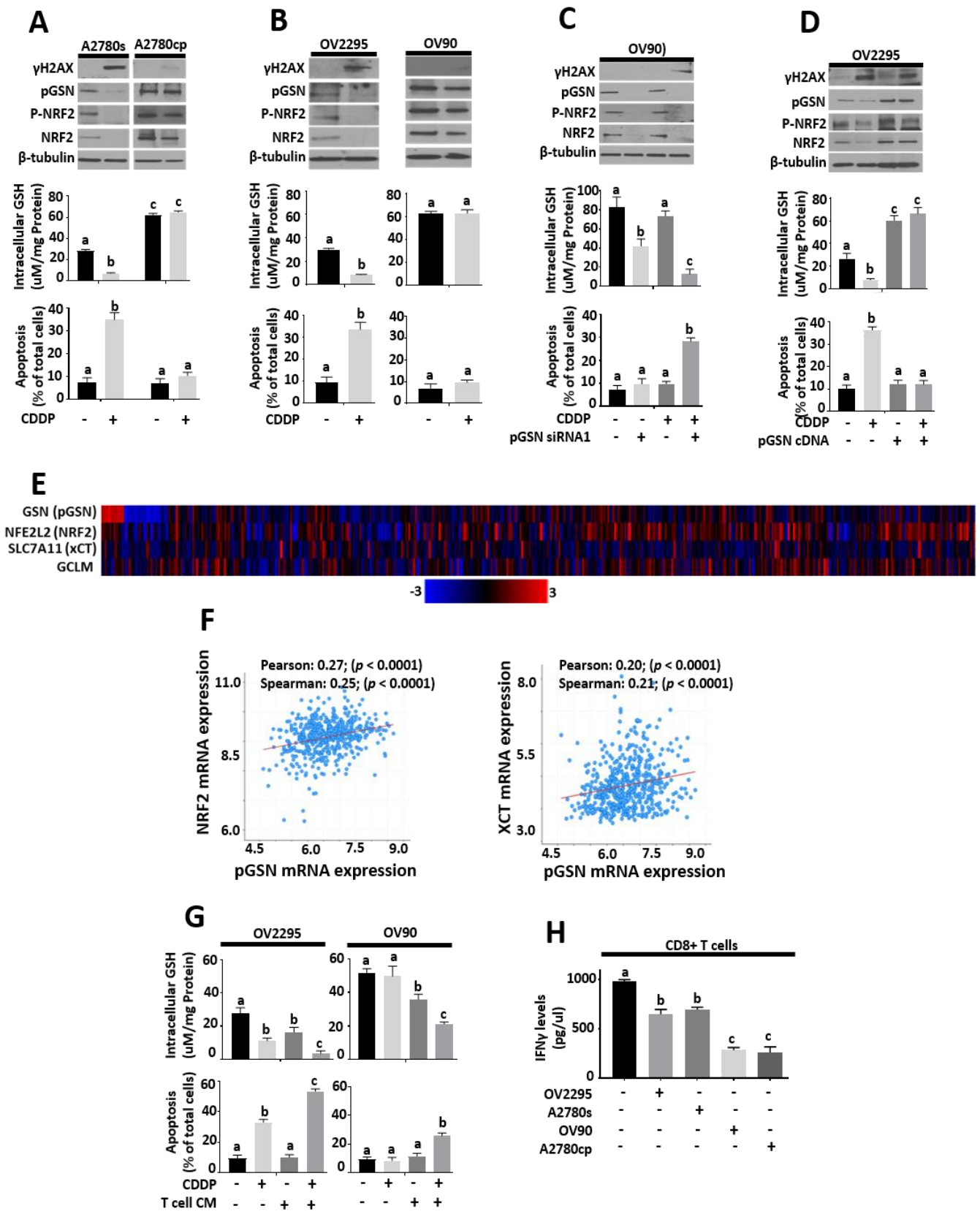
A
A2780s
A2780cp
γH2AX
pGSN
P-NRF2
NRF2
β-tubulin
Intracellular GSH (uM/mg Protein)
Apoptosis (% of total cells)
CDDP
B
OV2295
OV90
C
OV90)
pGSN siRNA1
D
OV2295
pGSN cDNA
E
GSN (pGSN)
NFE2L2 (NRF2)
SLC7A11 (xCT)
GCLM
-3
3
F
Pearson: 0.27; (p < 0.0001)
Spearman: 0.25; (p < 0.0001)
NRF2 mRNA expression
pGSN mRNA expression
Pearson: 0.20; (p < 0.0001)
Spearman: 0.21; (p < 0.0001)
XCT mRNA expression
G
T cell CM
H
CD8+ T cells
IFNγ levels (pg/ul)

Figure 4.4 Increased pGSN expression promotes NRF2-dependent GSH production. (A) Chemosensitive (A2780s) and resistant (A2780cp) paired cell lines were treated with or without CDDP (10 μM; 24 h). **(B)** Chemosensitive (OV2295) and chemoresistant (OV90) HGSC cell lines were treated with or without CDDP (10 μM; 24 h). **(C)** pGSN expression in chemoresistant HGSC cell line (OV90) was silenced (siRNA1, 50 nM; 24 h) and treated with or without CDDP (10 μM; 24 h). **(D)** pGSN was force expressed in chemosensitive HGSC cell line (OV2295) (cDNA, 2 μg; 24 h) and treated with or without CDDP (10 μM; 24 h). **(E)** Heat map and **(F)** Pearson's/Spearman's analysis of the association between NFR2-dependent mRNAs (NRF2 and xCT) and pGSN mRNA expression. **(G)** Chemosensitive (OV2295) and resistant (OV90) cell lines were primed with CM (3 ml; 24 h) from activated CD8+ T cells and then treated with or without CDDP (10 μM; 24 h). **(H)** Activated human peripheral CD8+ T cells were co-cultured with chemosensitive (OV2295 and A2780s) and chemoresistant (OV90 and A2780cp) cell lines (24 h). mRNA analysis was interrogated using TCGA datasets on cbioportal. Intracellular GSH was measured by colorimetric assays and Western blotting used to examine protein contents (γH2AX, pGSN, pNRF2, NRF2 and β-tubulin). Apoptosis were measured morphologically by Hoechst staining and IFNγ levels assayed using sandwich ELISA. Results are expressed as means ± SD from three independent replicate experiments. *[**A**, (a; ***P<0.001 vs b and c); **B**, (a; ***P<0.001 vs b); **C**, (a; **P<0.01 vs b, a; ***P<0.001 vs c); **D**, (a; ***P<0.001 vs b and c); **G**, (a; **P<0.01 vs b, a; ***P<0.001 vs c); **H**, (a; **P<0.01 vs b, a; ***P<0.001 vs c)].*

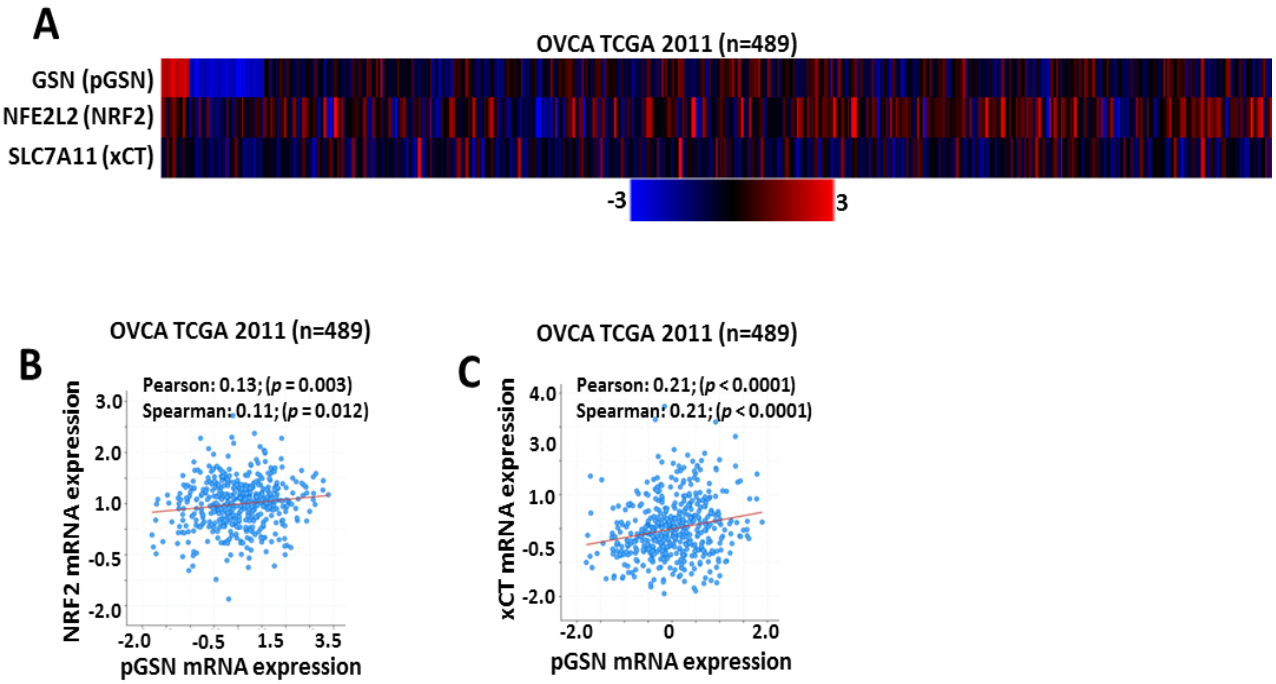

Fig. 4.S5 pGSN positively correlate with NRF2-dependent genes. (A) Heat map and **(B and C)** Pearson's/Spearman's analysis of the association between NRF2-dependent genes and pGSN mRNA expression. Data was interrogated from TCGA 2011 and Firehouse legacy datasets publicly available on cbioportal.

IFNγ secreted by activated CD8+ T cells reduces GSH production and sensitizes chemoresistant OVCA to CDDP-induced death.

The functionality of intra-tumoral CD8+ T cells is central to the efficiency of cancer treatment (3, 4, 29). Although increased pGSN induces apoptosis in CD8+ T cells as well as increases GSH production in OVCA cells **(Fig. 4 & 5)**, whether and how decreased viability of CD8+ T cells affects intracellular GSH production and OVCA chemoresistance is not known. To examine if intracellular GSH production in OVCA cells could be altered by CD8+ T cells, chemoresistant (OV90) and sensitive (OV2295) OVCA cells were cultured with conditioned media (CM) from activated CD8+ T cells (24 h) and then treated with or without CDDP (10 μM; 24 h) **(Fig. 4G)**. Although treating sensitive OVCA cells with CM from activated CD8+ T cells decreased intracellular GSH production, cell death was not observed **(Fig. 4G)**. However, a significantly greater decrease in intracellular GSH production and a further increase in apoptosis were noted in the chemosensitive OVCA cells treated with CDDP following pre-treatment with CD8+ T cell CM **(Fig. 4G)**. Intracellular GSH remained elevated in the resistant cells regardless of treatment with CD8+ T cell CM, a response associated with CDDP-resistance **(Fig. 4G)**. CDDP treatment of resistant cells following pre-treatment with CD8+ T cell CM was associated with a significant decrease in intracellular GSH and increased CDDP-induced apoptosis **(Fig. 4G)**.

To further investigate the factor involved in reducing intracellular GSH and sensitizing resistant cells to CDDP-induced apoptosis, the cytokine profile in the CM from activated CD8+ T cells was assessed. IFNγ levels were elevated to the greatest extent compared with IL-2, TGF-β, TNF-α and IL-12 **(Fig. S6A)**. The functionality of activated CD8+ T cells by way of IFNγ secretion was tested by co-culturing with chemosensitive (OV2295 and A2780s) and resistant

(OV90 and A2780cp) OVCA cells **(Fig. 4H)**. The presence of chemoresistant OVCA cells markedly reduced IFNγ production compared with chemosensitive cells **(Fig. 4H),** suggesting a potential immuno-suppressive function of pGSN. This phenomenon was validated in OVCA public datasets (TCGA firehouse legacy and 2011) where negative significant although weak correlation was observed between pGSN and IFNγ mRNA expressions (**Figs. S6B - D**). Using heat map presentations, patients with low pGSN mRNA was observed to also express low levels of key anti-tumor soluble factors (granzyme b and perforin) derived from activated CD8+ T cells (**Figs. S6B - D**).

IFNγ-mediated suppression of GSH production is via STAT1 phosphorylation.

Janus kinase/signal transducers and activators of transcription (JAK/STAT) signaling pathway mediates cellular responses upon IFNγ stimulation (30). Thus, we investigated if JAK/STAT1 pathway is involved in IFNγ-mediated suppression of GSH production, using recombinant human (rh) IFNγ instead of CD8+ T cell CM **(Fig. 5A)**. Chemoresistant (OV90) and sensitive (OV2295) OVCA cells were stimulated with IFNγ (10 pg/ml; 24 h) and then treated with or without CDDP (10 μM; 24 h). In the chemosensitive condition, CDDP and IFNγ alone reduced intracellular GSH; however, apoptosis was only observed with treatment with CDDP but not with IFNγ **(Fig. 5A)**. In the chemoresistant condition, IFNγ treatment reduced intracellular GSH production but not apoptosis **(Fig. 5A)**. CDDP and IFNγ together significantly decreased intracellular GSH content and increased apoptosis **(Fig. 5A)**. In both chemosensitive and resistant conditions, STAT1 phosphorylation was only associated with either rh-IFNγ stimulation alone or in combination with CDDP treatment.

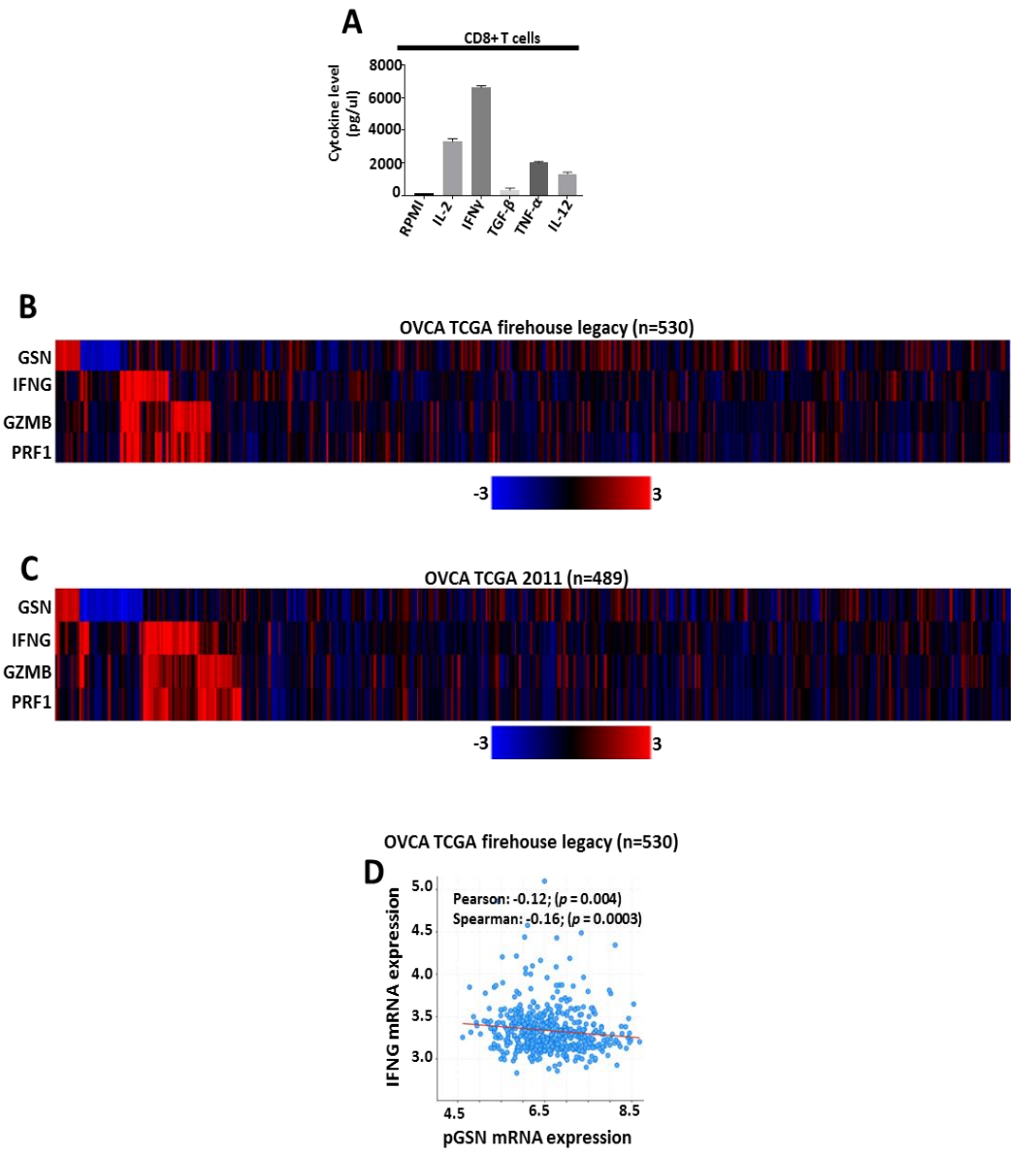

Fig. 4.S6 pGSN expression negatively correlates with CD8+ T cell anti-tumor factors. (A) Human peripheral CD8+ T cells were activated with anti-CD3/CD28/CD2 antibody (25 µl; 48 h). Cytokine levels were measured by ELISA. **(B and C)** Heat map representations of pGSN, IFNG, GZMB and PRF1 mRNA expressions. **(D)** Pearson's/Spearman's analysis of the association between IFNG and pGSN mRNA expressions. Data was interrogated from TCGA 2011 and firehouse legacy datasets publicly available on cbioportal. Results are expressed as means ± SD from three or more independent replicate experiments.

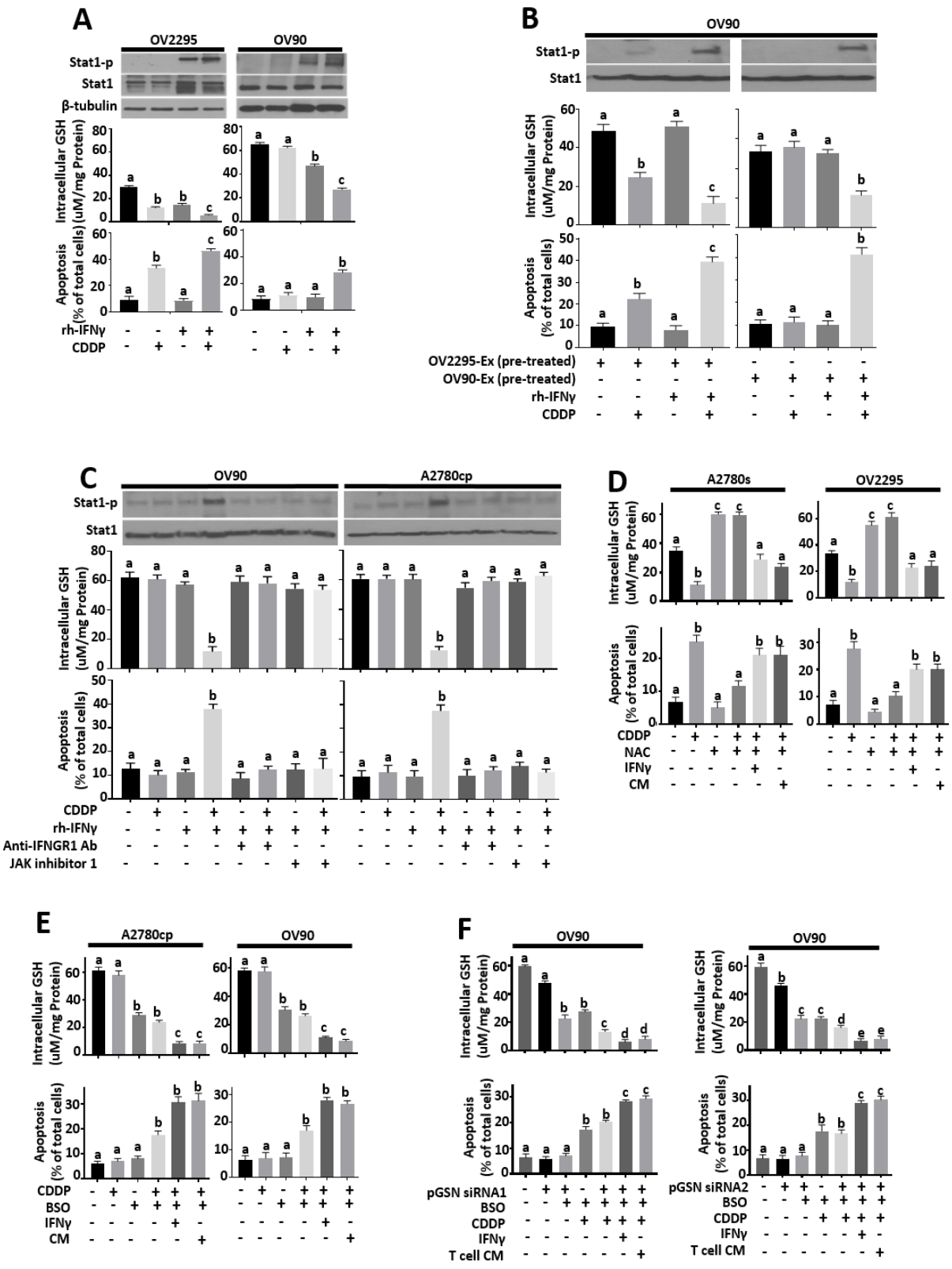
A
OV2295
OV90
Stat1-p
Stat1
β-tubulin
Intracellular GSH (uM/mg Protein)
Apoptosis (% of total cells)
rh-IFNγ
CDDP
B
OV90
Stat1-p
Stat1
Intracellular GSH (uM/mg Protein)
Apoptosis (% of total cells)
OV2295-Ex (pre-treated)
OV90-Ex (pre-treated)
rh-IFNγ
CDDP
C
OV90
A2780cp
Stat1-p
Stat1
Intracellular GSH (uM/mg Protein)
Apoptosis (% of total cells)
CDDP
rh-IFNγ
Anti-IFNGR1 Ab
JAK inhibitor 1
D
A2780s
OV2295
Intracellular GSH (uM/mg Protein)
Apoptosis (% of total cells)
CDDP
NAC
IFNγ
CM
E
A2780cp
OV90
Intracellular GSH (uM/mg Protein)
Apoptosis (% of total cells)
CDDP
BSO
IFNγ
CM
F
OV90
OV90
Intracellular GSH (uM/mg Protein)
Apoptosis (% of total cells)
pGSN siRNA1
BSO
CDDP
IFNγ
T cell CM
Intracellular GSH (uM/mg Protein)
Apoptosis (% of total cells)
pGSN siRNA2
BSO
CDDP
IFNγ
T cell CM

Figure 4.5 IFNγ-mediated suppression of GSH production is via STAT1 phosphorylation. **(A)** Chemosensitive (OV2295) and chemoresistant (OV90) HGS OVCA cell lines were treated with rhIFNγ (10 pg/ml; 24 h) and/or CDDP (10 μM; 24 h). **(B)** Activated human peripheral CD8+ T cells were pre-treated with sEVs (400 μg/400,000 cells) derived from chemosensitive (OV2295) or chemoresistant (OV90) HGS OVCA cell lines (24 h). Chemoresistant (OV90) HGS OVCA cell lines were treated with CM (3 ml; 24 h; collected from pre-treated activated CD8+ T cells), rhIFNγ (10 pg/ml; 24 h) and/or CDDP (10 μM; 24 h). **(C)** Chemoresistant (OV90 and A2780cp) cell lines were treated with rhIFNγ (10 pg/ml; 24 h), CDDP (10 μM; 24 h), JAK1 inhibitor (5 μM) and/or anti-IFNGR1 blocking antibody (2 μg/mL; 24h). **(D)** Chemosensitive cells (A2780s and OV90) were pre-treated with NAC (200 μM; 12 h) and then treated with or without IFNγ (10 pg/ml; 24 h), CDDP (10 μM; 24 h) and T cell CM (3 ml; 24 h). **(E)** Chemoresistant cells (A2780cp and OV90) were pre-treated with BSO (6μM; 12 h) and then treated with or without IFNγ (10 pg/ml; 24 h), CDDP (10 μM; 24 h) and T cell CM (3 ml; 24 h). **(F)** pGSN was silenced with two (2) siRNAs (50 nM; 24 h) in OV90 cells and treated with or without BSO (6 μM; 12 h), IFNγ (10 pg/ml; 24 h), CDDP (10 μM; 24 h) and T cell CM (3 ml; 24 h). Intracellular GSH was measured by colorimetric assays and Western blotting used to examine protein contents (pSTAT1, STAT1 and β-tubulin). Apoptosis were measured morphologically by Hoechst staining. Results are expressed as means ± SD from three independent replicate experiments. *[**A**, (a; **P<0.01 vs b, a; ***P<0.001 vs c); **B**, (a; ***P<0.001 vs b and c); **C**, (a; ***P<0.001 vs b); **D**, (a; ***P<0.001 vs b and c); **E**, (a; ***P<0.001 vs b and c); **F**, (a; ***P<0.001 vs b, c, d and e)]*.

We were also interested to know whether pGSN-induced chemoresistance could be mediated through suppression of IFNγ secretion in CD8+ T cells. To investigate this possibility, we primed activated CD8+ T cells with sEVs (40 µg/400,000 cells; 24 h) derived from either chemosensitive (OV2295) or chemoresistant OVCA cells (OV90) **(Fig. 5B)**. CM from the primed CD8+ T cells were collected and added to OV90 OVCA cultures with/without IFNγ (10 pg/ml; 24 h) and/or CDDP (10 µM; 24 h). CM from CD8+ T cells primed with sEVs from OV2295 cells failed to decrease intracellular GSH and attenuated apoptosis **(Fig. 5B)**. CDDP treatment alone decreased intracellular GSH which was associated with increased apoptosis **(Fig. 5B)**. Combined IFNγ and CDDP treatment drastically reduced intracellular GSH and significantly increased apoptosis, responses that were associated with increased STAT1 phosphorylation **(Fig. 5B)**. Following pre-treatment with sEVs derived from chemoresistant cells, IFNγ and CDDP alone failed to decrease intracellular GSH; CDDP-induced apoptosis was also attenuated **(Fig. 5B)**. However, combined treatment with CDDP and IFNγ resulted in marked decrease in intracellular GSH, increased STAT1 phosphorylation and increased apoptosis **(Fig. 5B)**.

To further investigate the role of IFNGR/JAK/STAT1 pathway in IFNγ-induced GSH production, chemoresistant OVCA cells lines (OV90 and A2780cp) pre-treated with anti-IFNGR1 blocking antibody (2 µg/mL; 24 h) and/or JAK inhibitor 1 (5 µmol/L; 24 h) were treated with either IFNγ (10 pg/ml; 24 h) or/and CDDP (10 µM; 24 h) **(Fig. 5C)**. In both OV90 and A2780cp cell lines, only combined treatment with IFNγ and CDDP increased the phosphorylation of STAT1, reduced intracellular GSH and increased apoptosis **(Fig. 5C)**. These effects were attenuated in the presence of IFNγ receptor blocking antibody as well as JAK1

inhibitor **(Fig. 5C),** suggesting the possible role of IFNGR1 and JAK1 in IFNγ-induced GSH production.

We extended our study to examine how intracellular GSH regulates the response of OVCA cells' to CDDP and IFNγ treatments and how pGSN could play a role in the mechanism. The GSH precursor N-acetyl cysteine (NAC) was used to promote GSH production in chemosensitive cells whereas buthionine sulfoximine (BSO), an inhibitor of the first rate-limiting enzyme (glutamate-cysteine ligase) of GSH synthesis, was used to deplete GSH production in chemoresistance OVCA cells. Chemosensitive cells (A2780s and OV2295) were pre-treated with NAC (200 μM; 12 h) and then treated with or without IFNγ (10 pg/ml; 24 h), CDDP (10 μM; 24 h) or CM from activated CD8+ T cells (3 ml; 24 h) **(Fig. 5D)**. NAC alone significantly induced intracellular GSH production without increasing apoptosis. CDDP failed to decrease NAC-induced GSH production, a response associated with reduced apoptosis **(Fig. 5D).** Combining IFNγ or CM with CDDP and NAC significantly reduced GSH production and increased apoptosis **(Fig. 5D).** GSH production in chemoresistant OVCA cells (A2780cp and OV90) were decreased with BSO (6 μM; 12 h) and then treated with or without IFNγ (10 pg/ml; 24 h), CDDP (10 μM; 24 h) or CM from activated CD8+ T cells (3 ml; 24 h) (**Fig. 5E).** Although GSH production was significantly reduced, apoptosis was unaffected by BSO alone (**Fig. 5E)**. CDDP however, increased apoptosis in cells pre-treated with BSO **(Fig. 5E).** The addition of IFNγ or CM with BSO and CDDP significantly and further reduced GSH production in the chemoresistant cells, a response associated with marked apoptosis **(Fig. 5E).**

To investigate the role of pGSN in the above phenomena, pGSN was knocked down using two siRNAs (50 nM; 24 h) in OV90 cells and treated with or without BSO (6 μM; 12 h), IFNγ (10 pg/ml; 24 h), CDDP (10μm; 24 h) or CM from activated CD8+ T cells (3 ml; 24 h)

(Fig. 5F). Silencing pGSN expression decreased GSH level with no effect on apoptosis **(Fig. 5F).** BSO treatment further reduced GSH levels in pGSN-KD OV90 cells without affecting apoptosis. CDDP treatment following pGSN KD and BSO treatment further reduced GSH production and increased apoptosis, phenomena markedly enhanced by the addition of IFNγ or CM from activated CD8+ T cells **(Fig. 5F)**.

DISCUSSION

In the current study, we have demonstrated that the functionality but not the mere presence of infiltrated CD8+ T cells plays a significant role in prolonging the survival of OVCA patients. pGSN expression was significantly associated with poor chemo-responsiveness and shortened OS in HGS OVCA patients, making pGSN a poor prognostic marker. This is consistent with our previous study (13) as well as supports other studies where total GSN was shown as a poor prognostic marker in gynecological, colon, pancreatic, breast and head-and-neck cancers (9, 10, 31, 32). Reliable prognostic factors are crucial to achieving therapeutic success and improving patient survival. In our Cox regression analysis, RD was observed to be an independent predictor of OVCA recurrence whereas epithelial pGSN presented as independent predictor for OVCA death. This is consistent with our earlier findings where circulatory pGSN and RD significantly predicted patient survival (14). Combining RD and pGSN in both blood and tissues could provide a reliable prognostic index to enhance OVCA patient survival and optimal management.

Tumor infiltration by CD8+ T cells provide survival benefits to cancer patients (3, 4) and our findings that increased infiltrated CD8+ T cells is associated with reduced tumor recurrence are consistent with this notion. Interestingly, the prognostic benefits of infiltrated CD8+ T cells

on patients' survival were inversely associated with increased pGSN levels. pGSN is highly secreted in OVCA patients compared with normal subjects (14) and transported via sEVs (13). Patients with higher levels of circulatory pGSN had decreased infiltration of CD8+ T cells compared with the cohorts with lower levels. This suggests that circulatory pGSN levels could predict the immunological status of OVCA patients that could inform physicians on the possible therapeutic options.

We have previously shown that caspase-3, a mediator of apoptotic cell death, could be regulated by GSN (9). We thus examined caspase-3 activation in the same clinical samples and observed immunoreactivity. As to whether the caspase-3 activation was CD8+ T cell specific or not, was difficult to interpret since IF does not provide a time lapse to examine such mechanism. sEVs derived from chemoresistant but not chemosensitive OVCA cells induced apoptosis in CD8+ T cells via FLIP downregulation and caspase-8/3 activations, responses that were aborted when pGSN was silenced in the sEVs. This is consistent with our previous study where the interaction of GSN with FLIP and Itch had a direct effect on caspase-3 activation (9). To date, this is the first study to provide mechanistic detail on how sEV-pGSN induces apoptosis in CD8+ T cells via activation of the FLIP/caspase-8 axis. This is consistent with the findings of Wieckowski *et al*, who have shown that tumor-derived vesicles promote apoptosis of activated CD8+ T cells (33) as well as other studies where GSN-induced death in natural killer/T cells (34). Interestingly, sEV pGSN had no apoptotic effect on CD4+ T cells, which were however polarized towards type 2 helper cells as evident by increased secretion of IL-4. Our findings are consistent with the findings by Chen *et al.* showing secreted gelsolin in prostate cancer desensitizes and induces apoptosis in infiltrated effector T cells but not CD4 T cells (31) and provide new insights into how pGSN transported by sEVs induce apoptosis of CD8+ T cells in

OVCA, a phenomenon with significant impact on chemo-responsiveness. The decrease in IFNγ secretion as observed in the CD8+ T cells co-cultured with resistant cells and granzyme b and perforin in public datasets might be as a result of the decreased number of T cells left after pGSN-induced death. Detailed investigations are however needed to demonstrate if pGSN directly affects their gene expression independent of pGSN-induced CD8+ T cell death. This could explain in part why most immunotherapy trials in OVCA patients have not achieved significant success (35-37). Silencing pGSN expression and secretion could hold the key to maximizing immunotherapy efficiency in OVCA patients and other solid tumors. Whether this indeed is true requires further investigation.

Intracellular GSH at a basal level provides antioxidant functions to cells by detoxifying and removing carcinogens (15-17). However, elevated levels of intracellular GSH chelate chemotherapeutic agents which are subsequently effluxed from the cell, thus reducing their cellular accumulation needed for tumor cell death (15-17)**.** This conference of resistance to chemotherapeutic agents provides protection to OVCA cells and in many cancers (15-17)**.** It is yet to be shown if pGSN plays a role in regulating intracellular GSH production in OVCA cells. We observed that increased pGSN activates the NRF2-antioxidant pathway leading to increased production of intracellular GSH. GSH therefore chelates, detoxifies and effluxes CDDP, reducing γH2AX levels (an indicator of CDDP accumulation and DNA double-strand break) in tumor cells and protecting them from CDDP-induced apoptosis. It has been demonstrated that GSH secreted by fibroblasts are taken up by cancer cells which protects them from CDDP-induced apoptosis (30) and marked increased GSH synthesis in OVCA cells is a contributing factor to CDDP resistance (16, 17). Moreover, depleting GSH in human neuroblastoma MNS cells inhibits gelsolin expression although this response was not sustained (38). As to whether

GSN has a positive feedback effect on GSH production is yet to be investigated. pGSN treatment provides an antioxidant advantage by way of elevating circulating GSH levels to mitigate radiation injury (21). Our current data is consistent with these findings and also advances an intrinsic regulatory mechanism by which GSH is involved in pGSN-mediated OVCA chemoresistance.

Infiltration of the tumor crest by effector T cells is significantly associated with prolonged survival in OVCA patients treated with CDDP and other treatment modalities (4, 35, 36). Thus, we investigated the potential involvement of CD8+ T cells in sEV-pGSN-mediated regulation of intracellular GSH production. We observed that CD8+ T cells-derived IFNγ activated the IFNGR1/JAK/STAT1 pathway in OVCA cells, leading to reduced intracellular GSH level. As a result, OVCA cells became sensitized to CDDP-induced apoptosis. This is consistent with a report that CD8+ T cells-derived IFNγ regulates GSH and cysteine metabolism in fibroblasts via the JAK/STAT1 pathway (30). GSH antagonists, such as buthionine sulphoximine, phytochemical B-phenylethyl isothiocyanate, gossypol, 3-bromopyruvate and acetaminophen, have shown therapeutic promises (17) although no significant clinical advantage has been achieved to date due partly to their adverse side effects. In a phase III clinical trial (NCT00350948), the GSH analogue Telcyta (TLK286) together with doxorubicin recorded poorer outcomes compared with the standard treatment regimen (39, 40). The role of sEV-pGSN in regulating both intracellular GSH biosynthesis and immune-surveillance could hold the key to maximizing treatment efficiency in OVCA patients.

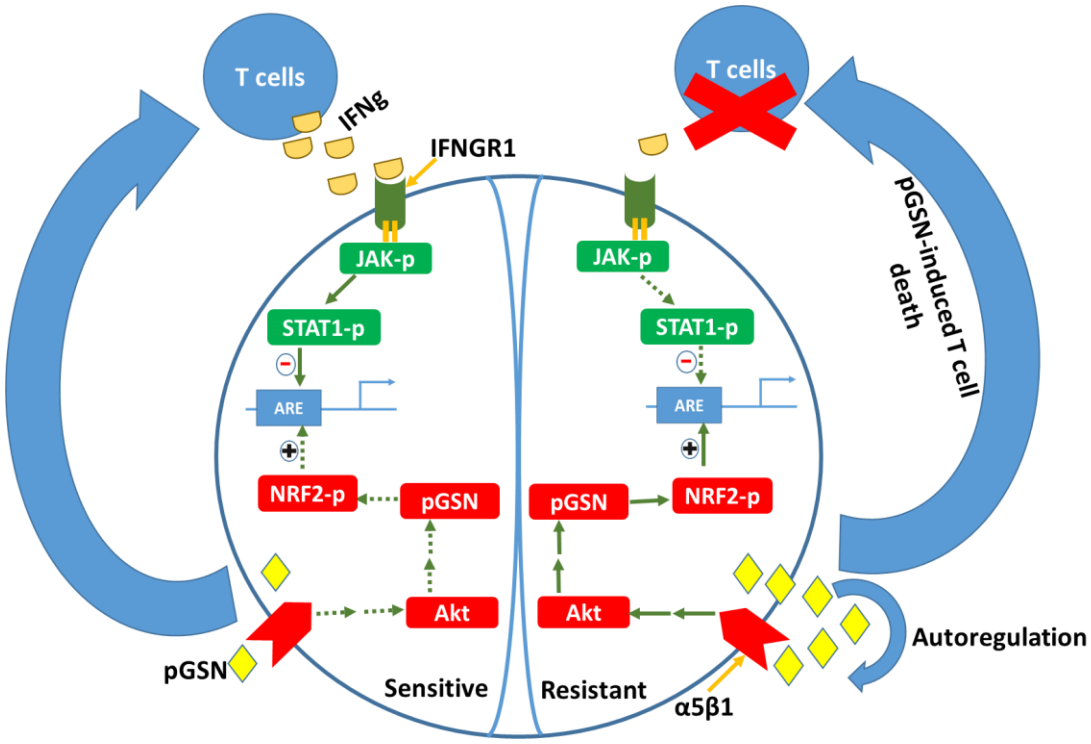

Figure 4.6 A Hypothetical model illustrating the expression and role of pGSN in the regulation of chemoresistance in OVCA. In chemosensitive condition, sEV-pGSN secretion in OVCA cells is low, hence T cell function is minimally affected. Functional CD8+ T cells can therefore secret higher levels of IFNγ which reduces GSH production in OVCA cells and sensitizes chemosensitive cells to CDDP-induced death. In the chemoresistant condition, high sEV-pGSN secretion by OVCA induces cell death in CD8+ T cells. This results in decreased levels of IFNγ, high NRF2-dependent GSH production and increased resistance to CDDP-induced death in OVCA cells.

In summary, we have demonstrated for the first time, the immuno-modulatory role of sEV-pGSN in OVCA chemoresistance. To facilitate future investigations, we offer the following hypothetical model for OVCA cell-CD8+ T cell interaction in the tumour microenvironment in the regulation of chemosensitivity in human ovarian cancer **(Fig. 6)**. In chemosensitive condition, sEV-pGSN secretion is relatively low in OVCA cells, hence CD8+ T cell function is minimally affected. Functional CD8+ T cells can therefore secrete higher levels of IFNγ which reduces NRF2-dependent GSH production in OVCA cells and sensitizes chemosensitive cells to CDDP-induced apoptosis. In the chemoresistant condition, marked sEV-pGSN secretion from OVCA cells induces cell death in CD8+ T cells. With a small population of CD8+ T cells left, IFNγ secretion is reduced, hence NRF2-dependent GSH production in OVCA cells remains high, resulting in resistance to CDDP-induced death. The above findings provide useful mechanistic and clinical information to maximize immunotherapy efficiency in chemoresistant OVCA as well as establish a reliable prognostic index for OVCA patients.

Acknowledgement: This work was supported by the Canadian Institutes of Health Research (PJT-168949) to B.K. Tsang and the Ovarian Cancer Canada (OCC) to M. Asare-Werehene. Tumor banking was supported by the Banque de tissus et de données of the Réseau de recherche sur le cancer du Fonds de recherche du Québec – Santé (FRQS), associated with the Canadian Tissue Repository Network (CTRNet). A.M. Mes-Masson is a researcher of the CRHUM who receives support from the FRQS. The funding agencies were not involved in the design, conduct, analysis or interpretation of the study.

SUPPLEMENTARY METHODS

Immunofluorescence (IF)

For the keratins in slides with CD8 + pGSN: a ready to use antibody cocktail against rabbit anti-KRT8/18 (FLEX, clone EP17/EP30; Dako) was used and coupled with AF488 anti-rabbit secondary Ab (Invitrogen; ref A11008); In slides with CD8 + Casp3: a cocktail of mouse antibodies against KRT7 (MS-1352-P; Neomarkers), KRT18 (sc-6259; Santa Cruz Biotechnology) and KRT19 (MS-198-P; Thermo Scientific) was used and coupled with AF546 anti-mouse secondary antibody (Invitrogen; ref. A10036). For CD8 staining in slides with CD8 + pGSN: anti-CD8 mouse monoclonal (Leica Biosystems; NCL-L-CD8-4B11) coupled with anti-mouse AF546 secondary antibodies (Invitrogen; ref. A10036) were used. In slides with CD8 + Casp 3, anti-CD8 mouse monoclonal (Leica Biosystems; ref. NCL-L-CD8-4B11) coupled with anti-mouse Cy5 (Invitrogen, ref. A10524) were used. For cleaved caspase 3 staining, anti-casp3 rabbit monoclonal (Cell signaling, ref. 9661S) antibody coupled with anti-rabbit AF488 (Invitrogen, ref. A11008) secondary antibody were used. For pGSN staining, anti-pGSN mouse polyclonal (Antibodies online, ref. ABIN659182) coupled with anti-mouse Cy5 (Invitrogen, ref. A10524) secondary antibodies were used in both panels. The nuclei of cells in the tissues were stained with DAPI and slides scanned with 20 x 0.7NA objective with a resolution of 0.3225um (VS110, Olympus, Center Valley, PA). VisiomorphTM (Visiopharm, Denmark) was used to identify the regions of interest (ROIs) - epithelium (keratin positive cells) and stroma (region negative for cytokeratin staining) - and to quantify the mean fluorescence intensity (MFI) of each marker into the ROIs. CD8 positive cells were counted into each tumor tissue ROI and a $CD8^+$ T cells density score corresponding to the number of CD8 per 100.000 pixels of ROI was

established. OVCA cell lines and their representative TMAs (lysates and pellets) were used to validate the specificity of antibodies using Western blot, IHC and IF.

Immunohistochemistry (IHC)

The TMA slide was reacted with 3,3′-diaminobenzidine solution and counterstained with Mayor's hematoxylin nuclei stain. Tissue slides were scanned with 20 x 0.7NA objective with a resolution of 0.3225um (VS110, Olympus, Center Valley, PA).

Extracellular Vesicle (EVs) Isolation, Characterization and Nanoparticle Tracking Analysis (NTA)

Total EVs concentration was determined by BCA Protein Assay Kit (Thermo Fisher Scientific). When fresh sEVs (40 µg/400,000 cells) were not required, they were suspended in PBS and stored at -80^{o}C for subsequent analysis. EVs diluted in PBS were analyzed, using the ZetaView PMX110 Multiple Parameter Particle Tracking Analyzer (Particle Metrix, Meerbusch, Germany) in size mode, and ZetaView software version 8.02.28. With 11 camera positions, EVs were captured at 21^{o}C. The sizes and concentrations of EVs were evaluated per samples in triplicates.

ELISA

pGSN levels were assayed in the plasma of OVCA patients (n = 92) by sandwich ELISA (Aviscera Bioscience, Inc. CA). The detection antibody was raised against human plasma (soluble) gelsolin. All ELISA measurements were carried out according to manufacturer's instructions. Optical densities (OD) were determined at 450 nm, using a microtiter plate reader and compared with the standard curve. The blank was subtracted from the triplicate readings for each standard and test samples.

CHAPTER 5 – Manuscript To Be Submitted

Plasma gelsolin modulates ovarian inflammation and confers chemoresistance in ovarian cancer by resetting the relative abundance and function of macrophage subtypes

Meshach Asare-Werehene[1,2,3], Hideaki Tsuyoshi[4], Huilin Zhang[1,2,3,4], Reza Salehi[1,2,3,7], Euridice Carmona[7], Clifford L. Librach[8,9], Anne-Marie Mes-Masson[7], Chia-Ching Chang[6], Dylan Burger[2,3], *Yoshio Yoshida[4], *Benjamin K. Tsang[1,2,3]

[1]Department of Obstetrics & Gynecology, University of Ottawa, Ottawa, Ontario, Canada, K1H 8L1

[2]Department of Cellular and Molecular Medicine, University of Ottawa, Ottawa, Ontario, Canada K1H 8M5

[3]Chronic Disease Program, Ottawa Hospital Research Institute, Ottawa, Ontario, Canada K1H 8L 6

[4]Department of Obstetrics and Gynecology, University of Fukui, Fukui, Japan

[5]Department of Obstetrics and Gynecology, Women's Hospital of Nanjing Medical University, Na njing Maternity and Child Health Care Hospital, Nanjing, 210004, People's Republic of China 210004

[6] Department of Biological Science and Technology, Department of Electrophysics and Center for Intelligent Drug Systems and Smart Bio-devices (IDS2B), National Chiao Tung University, Hsinchu; Institute of Physics, Academia Sinica, Taipei, Taiwan 30010

[7]Centre de recherche du CHUM et Institut du cancer de Montréal, Département of Médecine, Université de Montréal, Montreal, Quebec, Canada H2X 0A9

[8]CReATe Fertility Centre, 790 Bay Street, Suite 1100, Toronto, Ontario, M5G 1N8, Canada;

[9]Departments of Obstetrics & Gynecology and Physiology, and Institute of Medical Sciences, University of Toronto, Canada;

Running Title: pGSN overexpression suppresses M1 macrophage functions.

*Correspondence:

Yoshio Yoshida, MD, Department of Obstetrics and Gynecology, University of Fukui, Fukui, Japan; Email: yyoshida@u-fukui.ac.jp

Benjamin K Tsang, PhD, Chronic Disease Program, Ottawa Hospital Research Institute, The Ottawa Hospital (General Campus), Ottawa, Canada K1H 8L6; Email: btsang@ohri.ca

Author Contributions: M.A.W., E.C, A-M.M-M, D.B and B.K.T. conceived and designed the study. M.A.W. performed all experiments unless otherwise stated. H.T and Y.Y provided ovarian cancer tissues for IHC. M.A.W, B.K.T, H.T and Y.Y designed, performed and analysed IHC data. C.C.C. synthesized the human recombinant pGSN used in the present studies. E.C and A-M.M-M provided HGS cell lines. M.A.W and H.Z performed all *in-vitro* studies. R.S and C.L.L performed the flow cytometry for macrophage differentiation. Extracellular vesicles isolation and characterization were done by M.A.W and D.B. M.A.W. analysed the data with scientific input from B.K.T., H.T., D.B, E.C, A-M.M-M and Y.Y. M.A.W. wrote the paper with input and feedback from all authors.

Competing Interests: The authors declared no conflicts of interest.

ABSTRACT

Ovarian cancer (OVCA) is the most lethal gynaecological cancer with a 5-year survival rate less than 50%. Despite new therapeutic strategies, such as targeted therapies and immune checkpoint blockers (ICBs), tumor recurrence and drug resistance remain key obstacles in achieving long term therapeutic success. Therefore, there is an urgent need to understand the cellular mechanisms of immune dysregulation in chemoresistant ovarian cancer in order to harness the host's immune system to improve cancer survival. Over-expression of plasma gelsolin (pGSN; an actin binding protein) mRNA is associated with a poorer prognosis in OVCA patients; however, its immuno-modulatory role has not been elucidated. In this study, we report for the first time, pGSN as an inhibitor of M1 macrophage anti-tumor functions in OVCA chemoresistance. Increased epithelial pGSN expression was associated with loss of chemoresponsiveness and poor survival. While patients with increased M1 macrophage infiltration exhibited better survival, cohorts with poor survival had higher infiltration of M2 macrophages. Interestingly, increased epithelial pGSN expression was significantly associated with reducing the survival benefits of infiltrated M1 macrophages, through apoptosis via increased caspase-3 activation and reduced TNFα secretion. Additionally, epithelial pGSN expression was an independent prognostic marker in predicting progression-free survival (PFS). These findings support our hypothesis that pGSN is a modulator of inflammation and confers chemoresistance in OVCA, in part by resetting the relative abundance and function of macrophage subtypes in the ovarian tumour microenvironment. Our findings raise the possibility that pGSN may be a potential therapeutic target for immune-mediated chemoresistance in ovarian cancer.

SIGNIFICANCE

This study demonstrates the novel inhibitory role of pGSN on tumor infiltrated M1 macrophages and also offers new insights in maximizing the effectiveness of immunotherapy for ovarian cancer patients.

Key words:

Tumor-associated macrophages (TAMs), plasma gelsolin (pGSN), ovarian cancer (OVCA), Small extracellular vesicles (sEV), chemoresistance

INTRODUCTION

Ovarian cancer (OVCA) is ranked the fifth most commonly diagnosed female cancer; however, it is the most fatal amongst all gynecologic cancers (1-3). This is due primarily to late diagnosis, recurrence and chemoresistance, resulting in no significant improvement in the 5-year survival rate in the last decade (1-3) regardless of the ethnic backgrounds of the patients. Although cancer immunotherapy has improved the survival of patients with melanoma, colorectal cancer and blood cancers, it has not achieved great therapeutic success in OVCA patients (4-7). There is therefore an urgent need to better understand the molecular and cellular basis of these poor outcomes in patients with diverse ethnic backgrounds, and to investigate novel therapeutic targets to maximize survival in OVCA patients.

Tumor-associated macrophages (TAMs) possess immuno-modulatory functions and, depending on their phenotypic state, may either promote tumor progression or regression (8, 9). TAMs are conventionally classified as M1 or M2 depending on the cytokine components of their environment. M1 macrophages are pro-inflammatory and have the ability to phagocytose; functions associated with an anti-tumor effect, enhanced treatment response and overall improvement in patient survival (10, 11). Higher tumor infiltration of M1 macrophages is associated with improved patient survival and this correlation has been shown in a plethora of neoplastic diseases such as ovarian, colorectal, breast, gastric, lung and head-and-neck cancers (8, 9, 12-14). TAMs exhibiting M2 phenotypes are classically anti-inflammatory and are involved in wound repair and pro-tumorigenesis effects. The immuno-suppressive functions of M2 macrophages have been implicated in breast, ovarian, prostate, lung and brain cancers. The ratio of M1-to-M2 provides prognostic significance in OVCA patients and has been shown to correlate with tumor recurrence and chemoresistance (10, 11, 15). However, the mechanism

involved in regulating TAMs infiltration and anti-tumor functions have not been well studied in the context of chemoresistance.

Plasma gelsolin (pGSN), a multi-functional actin binding protein, is the secreted isoform of the gelsolin (GSN) gene (16, 17). Just like total GSN, pGSN has been implicated in many of disease conditions such as bacterial infection, sepsis, arthritis and cancer (16, 18). In our previous studies, we have shown that pGSN is transported by small extracellular vesicles (sEVs) – often referred to as exosomes - which can auto-regulate their own gene expression and, in a paracrine manner, transform chemosensitive cells to acquire a chemoresistant phenotype (19). Thus, sEV-pGSN is a determinant of OVCA chemoresistance. sEVs measure approximately 30-150 nm in size. This is different from large extracellular vesicles (microvesicles) which measure approximately 0.1 to 1.0 μm in size and are produced by membrane blebbing by cells under stress (19, 20).

OVCA patients whose tumor tissues show lower expression of pGSN mRNA have prolonged progression-free survival compared with those with higher pGSN mRNA expressions (19). In addition to OVCA, pGSN has been implicated in other types of cancer such as breast, prostate and colon (12, 19, 21-25). Recently, we have also demonstrated that aside the tumor expression of pGSN, circulating pGSN is a novel candidate for the early detection of OVCA, as well as predicting residual disease (26). To date, the involvement of pGSN in the regulation of the immune system is still not well understood. As to whether pGSN overexpression suppresses immune cell function and contributes to chemoresistance is yet to be examined. After the emergence of checkpoint blockers that activate T cells, one could have expected that OVCA patients would respond well to these new therapeutics. Unfortunately, immunotherapy with check point blockers has shown relatively low success in ovarian cancer (5, 7). It has therefore

become important to investigate other immune cells such as macrophages, to determine if they hold the key to maximizing the effectiveness of immunotherapy.

In this study, we investigated the immuno-suppressive role of pGSN in the tumor microenvironment (TME) of Asian OVCA patients. Specifically, increased tumor pGSN expression attracts M1 macrophages and suppresses their viability and function without affecting M2 macrophages; an action that regulates the inflammatory environment by decreasing the M1/M2 ratio. These results support the notion that these events contribute to chemoresistance and shortened patient survival.

MATERIALS AND METHODS

Ethics Statement

All patients provided a written informed consent. The study was performed in accordance with the appropriate guidelines approved by the institutional review board of the University of Fukui Hospital (IRB approval number; 20180140) and the Ottawa Health Science Network Research Ethics Board (IRB approval number; OHSN-REB 1999540-01H).

Tissue Samples

The study included tumor tissues with various histologic subtypes collected from 94 OVCA patients receiving treatment from 2007 to 2018 at the University of Fukui Hospital, Fukui, Japan. Patients were diagnosed, clinicopathological parameters and follow-up data gathered as previously described. Details of patient population and demographics are outlined in **Supplementary Table S1**.

Supplementary Table 5.S1 Patients Demographics

Variable	Number of Patients
Age (Range; 29 – 87 years)	
≤56	51
>56	43
Stage (FIGO)	
1	55
2	9
3	23
4	7
Stage (FIGO)	
≤2	64
>2	30
Histological Subtypes	
Clear cell	26
HGS	33
Mucinous	14
Endometrioid	14
LGS	4
Carcinosarcoma	3
Residual disease (RD)	
≤1 cm	79
>1 cm	15
Progression-free survival (PFS)	
Recurrent	26
Non-recurrent	68
Median PFS	33.5 months
Overall Survival (OS)	
Deceased	14
Alive	80
Median OS	56.2 months

HGSC, high grade serous carcinoma; RD, residual disease; FIGO, International Federation of Gynecology and Obstetrics

Supplementary Table 5.S2 Information on antibodies and Reagents

Application	Target	Primary Antibody	Company	Catalog #	Dilution	Secondary Antibody	Conjugate	Company	Catalog #	Dilution
WB	pGSN	Anti-pGSN Goat polyclonal	Antibodies online(Atlanta, USA)	ABIN1019662	1:1000	Dnk polyclonal to Goat IgG	HRP	Abcam (Toronto, Canada)	Ab97110	1:2000
WB	CD63	Anti-CD63 mouse monoclonal	Abcam (Toronto, Canada)	Ab193349	1:1000	Goat Anti-mouse IgG (H+L)	HRP	Bio-Rad (Mississauga, Canada)	170-6516	1:2000
WB	β-actin	Anti-actin mouse monoclonal	Abcam (Toronto, Canada)	ab8226	1:1000	Goat Anti-mouse IgG (H+L)	HRP	Bio-Rad (Mississauga, Canada)	170-6516	1:2000
IHC	pGSN	Anti-pGSN mouse polyclonal	Antibodies online(Atlanta, USA)	ABIN659182	1:1000	MAX-PO (MULTI)				
IHC	HLA-DR	Anti-HLA-DR mouse monoclonal	Abcam (Canada)	Ab20181	1:1000	MAX-PO (MULTI)				
IHC	CD68	Anti-CD68 rabbit polyclonal	Abcam (Canada)	Ab125212	1:50	MAX-PO (MULTI)				
IHC	CD163	Anti-CD163 rabbit polyclonal	Abcam (Canada)	Ab87099	1:400	MAX-PO (MULTI)				
WB	CD14	Anti-CD14 rabbit monoclonal	Abcam (Canada)	Ab183322	1:1000	Goat Anti-mouse IgG (H+L)	HRP	Bio-Rad (Mississauga, Canada)	170-6516	1:2000
WB	HLA-DR	Anti-HLA-DR mouse monoclonal	Abcam (Canada)	Ab20181	1:1000	Goat Anti-mouse IgG (H+L)	HRP	Bio-Rad (Mississauga, Canada)	170-6516	1:2000
WB	CD68	Anti-CD68 rabbit polyclonal	Abcam (Canada)	Ab125212	1:1000	Goat Anti-rabbit IgG (H+L)	HRP	Bio-Rad (Mississauga, Canada)	170-6515	1:2000
WB	CD163	Anti-CD163 rabbit polyclonal	Abcam (Canada)	Ab87099	1:1000	Goat Anti-rabbit IgG (H+L)	HRP	Bio-Rad (Mississauga, Canada)	170-6515	1:2000
WB	Activated caspase-3	Anti-cleaved caspase-3 rabbit polyclonal	Cell signaling Technology, MA, USA	9661	1:1000	Goat Anti-rabbit IgG (H+L)	HRP	Bio-Rad (Mississauga, Canada)	170-6515	1:2000
iNOS detection	iNOS		Abcam (Canada)	Ab211085						
TNF alpha ELISA kit	TNF alpha		Abcam (Canada)	Ab46087						
Caspase-3 activation detection	Caspase-3		Thermofisher Scientific (Canada)	C10723						
Annexin V-FITC	Annexin V		Fisher Scientific (Canada)	50-930-1						
		PMA	Sigma (Canada)	P8139-1MG						
		LPS	Sigma (Canada)	L2630-10MG						
		hrIFN gamma	Stemcell Technologies (Canada)	78020						
		Cisplatin	Sigma (Canada)	P4394-100MG						
		Etoposide	Sigma (Canada)	E1383-25MG						

Supplementary Table 5.S3 Information on OVCA cell lines

Cell line	Tumor origin	TP53 status	Other	Chemosensitivity
A2780s	Ovarian endometrioid adenocarcinoma	Wild type	PTEN/ARID1A	Sensitive
A2780cp	Ovarian endometrioid adenocarcinoma	Mutant V127F, R260S	PTEN/ARID1A	Resistant
OV2295	High grade serous ovarian cancer	Mutant IIe195Thr	Not investigated	Sensitive
OV90	High grade serous ovarian cancer	Mutant Ser215Arg	Not investigated	Resistant

Information on OVCA cell lines: The characterization of these cell lines has been verified in previous literature (Anglesio et al., 2013; Leroy et al., 2014; Provencher et al., 2000; Letourneau et al., 2012).

Immunohistochemistry (IHC)

Cryostat sections (2.5 um) were obtained from 94 formalin fixed, paraffin-embedded ovarian cancer tissues and immunohistochemically stained. Tissue samples were immuno-stained (overnight) with primary antibodies to pGSN (x1000), CD68 (total macrophage M0 marker; x50), HLA-DR (M1 marker; x1000) and CD163 (M2 marker; x400). After primary incubation, sections were washed 3x in PBS for 5 min and then incubated (30 min, RT) with secondary antibody [MAX-PO (MULTI)]. Immunoreaction was monitored and developed. Tissues were then counterstained (nuclei staining) with Mayer's Hematoxylin solution and mounted. Staining intensity and distribution was evaluated by two blinded independent observers using a semi-quantitative method (IRS-score), as described previously (27). Tissue sections treated with no primary antibodies were used as negative controls. Tissue sections were observed using Olympus Bx50F-3 (Olympus Optical Co., Nagano, Japan) and scanned with FlexScan S2000. Details of antibodies are outlined in **Supplementary Table S2**. The IHC was quantified by a semi-quantitative method [immunoreactive (IRS)-score]. IRS-score was calculated as follows: IRS = SI x PP, where SI is the optical stain intensity graded as 0 = no staining, 1 = weakly stained, 2 = moderately stained and 3 = strongly stained. PP is the degree of positively stained cells defined as 0 = no staining, 1 = <10%, 2 = 11–50%, 3 = 51–80%, and 4 = >81%).

Reagents.

Cis-diaminedichloroplatinum (CDDP), phenylmethylsulfonyl fluoride (PMSF), aprotinin, dimethyl sulfoxide (DMSO), sodium orthovanadate (Na_3VO_4), and Hoechst 33258 were supplied by Millipore Sigma (St. Louis, MO). pGSN siRNA1 and 2 and scrambled sequence siRNA (control) were purchased from Integrated DNA Technology (Iowa, USA) and Dharmacon

(Colorado, USA) respectively. Recombinant human plasma gelsolin (rh-pGSN) was purchased from Cytoskeleton, Inc, USA and donated by Dr. Chia-Ching Chang. pGSN cDNA and 3.1A vector plasmids were produced in the lab of Dr. Dar-Bin Shieh, National Cheng Kung University Hospital, Taiwan. See **Supplementary Tables S2** for details on antibodies and reagents.

Cell Lines and Primary Cells.

THP-1 monocytes were purchased from ATCC (VA, USA). HGS cell lines (28, 29) (OV2295, chemosensitive and OV90, chemoresistant) were kindly provided by Dr. Anne-Marie Mes-Masson [Centre de recherche du Centre hospitalier de l'Université de Montréal (CRCHUM), Canada] and were culture in OSE medium (Wisent Inc., St-Bruno, QC, Canada). Endometrioid cell lines (A2780, chemosensitive and A2870cp, chemoresistant) were generously donated by Dr. Barbara Vanderhyden (Ottawa Hospital Research Institute, Ottawa, Canada) and were cultured in Gibco RPMI 1640 (Life Technologies, NY, USA; catalog number: 31800-022). Cell lines were authenticated, frequently tested for *Mycoplasma* contamination using PlasmoTest^{TM} Mycoplasma Detection kit (Invivogen; catalog number: rep-pt1) and continuously checked for morphological changes as well as growth rate for any batch-to-batch change. Media were supplemented with 10% FBS (Millipore Sigma; St. Louis, MO), 50 U/mL penicillin, 50 U/mL streptomycin, and 2 mmol/L l-glutamine (Gibco Life Technologies, NY, USA). Details on histologic subtypes and genetic alterations of cell lines used are described in **Supplementary Table S3**. All experiments were carried out in serum-free media.

Gene Interference.

Cells were transfected (50 nM, 24 h) with siRNAs (scrambled sequence as controls) using lipofectamine 2000 and harvested for analysis**.** Two different siRNAs were used for each target to exclude off-target effects. Successful knock-down was confirmed by Western blotting, as previously described (19). (See **Supplementary Table S2** for details on antibodies).

Transient Transfection.

Chemosensitive OVCA cells were transfected with pGSN cDNA (2 µg, 24 h) plasmid (empty vector as controls) using lipofectamine 2000 and harvested for further analysis. Successful over-expression was confirmed by Western blotting, as previously described (19, 30-32).

Extracellular Vesicle Isolation and Characterization.

Serum-free conditioned media from cultured cells were used for extracellular vesicle isolation and characterization, as described previously (19)**.** Total EV concentration was determined by BCA Protein Assay Kit (Thermo Fisher Scientific, Whitby, Canada). When fresh sEVs (40 µg/400,000cells) were not required, they were suspended in PBS and stored at -80^{o}C for subsequent analysis.

Nanoparticle Tracking Analysis (NTA).

EVs in PBS were analyzed, using the ZetaView PMX110 Multiple Parameter Particle Tracking Analyzer (Particle Metrix, Meerbusch, Germany) in size mode using ZetaView

software version 8.02.28, as previously described (19). EVs were captured at 11 camera positions at 21^{o}C and particle size and concentration evaluated.

Protein Extraction and Western blot Analysis.

Western blotting (WB) procedure for proteins were carried out as described previously (19, 30-33). After protein transfer, membranes were incubated with primary antibodies (1:1000) in 5% (wt/vol) blotto and subsequently treated with the appropriate horseradish peroxidase (HRP)-conjugated secondary antibody (1:2000) in 5% (wt/vol) blotto. Details on antibodies used are described in **Supplementary Table S2**. Peroxidase activity was visualized using Chemiluminescent Kit (Amersham Biosciences, Little Chalfont, UK). Image J was used to densitometrically measure the signal intensity generated on the film.

ELISA

Concentrations of TNFα were measured by ELISA in 100 µl of cell-free conditioned media from M1 macrophage after being treated with sEV, CM or co-cultured with OVCA cancer cells. All ELISA measurements were carried out according to manufacturer's instructions. Optical densities (OD) were determined using a microtiter plate reader at 450 nm and compared to a standard curve. The blank was subtracted from the triplicate readings for each standard and test sample.

THP-1 Monocyte Differentiation and Macrophage Polarization

THP-1 monocytes were treated with PMA (150 nM; 24 h) with RPMI. Treatment was removed and cells were left to grow in PMA-free RPMI for another 24 h. M0 macrophages were polarized to M1 macrophages with IFNγ (20 ng/ml) + LPS (10 pg/ml) treatment for 24 h.

Macrophage differentiation and flow cytometry

CD14 (VioBlue, 1:50; Miltenyi Biotec, Cambridge, USA) and CD68 (PE, 1:50; Miltenyi Biotec, Cambridge, USA) were assessed by using flow cytometry in THP1 and PMA-treated THP1. Inside Stain Kit (Miltenyi Biotec, Cambridge, USA; Cat# 130-090-477) was used for the fixation and permeabilization of cells for CD68 staining.

Assessment of Cell Proliferation and Apoptosis.

Apoptosis was assessed morphologically using Hoechst 33258 nuclear stain, as previously described (19, 24, 31). "Blinded" counting approach was used to prevent experimental bias with the Hoechst 33258 nuclear staining.

Annexin V flow cytometry

Treated cells were washed in cold 1X PBS before suspending in binding buffer at a concentration of $1x10^6$ cells/ml. Cells were stained with annexin V-FITC solution (1µl of annexin V stain in 100 µl of binding solution) and incubated for 15 mins. Cells were washed in 1X binding buffer and analyzed immediately by flow cytometry. Details of the annexin V-FITC are described in **Supplementary Table S2**.

Caspase-3 detection assay

Caspase-3 activation was detected in treated cells by washing the cells in PBS and staining with 100 µl of working solution as recommended by the manufacturer (Fisher Scientific, Whitby, Canada; Cat.#: C10723). Cells were then fixed with 3.7% formaldehyde (15 min) and counterstained with Dapi (3 min). Cells on the slides were mounted and examined microscopically. Percentage of caspase-3 positive M1 macrophages of the total cells per field was determined.

iNOS detection assay

Treated cells were washed with assay buffer and stained with the working solution (1 h, 37^{o}C) (1:200), as recommended by the manufacturer (Abcam, Toronto, Canada; Cat.#: ab211085). Cells were then analysed in a microplate reader (Ex/Em = 485nm/530nm).

Statistical Analyses.

Statistical analyses were performed using the SPSS software version 25 (SPSS Inc., Chicago, IL, USA) and PRISM software version 8.0 (Graphpad, San Diego, CA). The statistical analyses were performed as independent sample *t*-test, one- or two-way ANOVA and Bonferroni *post-hoc* tests to determine the differences between multiple experimental groups. Two-sided $p \leq 0.05$ was inferred as statistically significant. The relationship of variables to other clinicopathologic correlates was examined using Fisher exact test, T test and Kruskal Wallis Test, as appropriate. Survival curves (PFS and OS) were plotted with Kaplan Meier and P-values calculated using the log-rank test. Univariate and multivariate Cox proportional hazard models

were used to assess the hazard ratio (HR) for pGSN, M0, M1 and M2 macrophages, stage, RD and age as well as corresponding 95% confidence intervals (CIs).

RESULTS

Patients' Characteristics

Detailed histologic subtype (high grade serous, HGS; low grade serous, LGS; endometrioid; mucinous; clear cell and carcinosarcoma) description of OVCA patients (N=94) are described in **Supplementary Table S1**. A certified Gynecologic-Oncology team performed tumor staging and pathology. Patients recruited in the study did not receive neoadjuvant chemotherapy prior to sample collection at surgery. The age range of patients was 29 – 87 years (median age; 56 years) with FIGO stages classified as 1 (N=55), 2 (N=9), 3 (N=23) and 4 (N=7) (**Supplementary Table S1)**. Seventy-nine (79) patients received complete/optimal cytoreduction compared with 15 patients who had suboptimal cytoreduction. The median progression-free survival (PFS) and overall survival (OS) were 33.5 and 56.2 months respectively (**Supplementary Table S1)**.

pGSN expression and infiltrated TAMs in OVCA tissues

Chemoresistant OVCA cells express and secrete higher levels of pGSN, compared with their sensitive counterparts (19). Thus, we examined the clinical relevance of pGSN as well as infiltrated tumor associated macrophages (TAMs) in OVCA tissues. Ovarian tissue sections (2.5 um) were collected from 94 OVCA patients and immunohistochemically stained with anti-pGSN, anti-CD68 (M0 macrophage marker), anti-HLA-DR (M1 macrophage marker) and anti-CD163 (M2 macrophage marker). Primary antibodies were omitted in tissues used as controls.

Supplementary Fig. S1A shows negative and positive pGSN expressions as well as infiltration of TAMs [M0 (CD68), M1 (HLA-DR) and M2 (CD163)] in the epithelial (cancer islet) and stromal regions. pGSN expression (cut-off=6) and TAMs infiltration (cut-off=6) in OVCA tissue compartments with respective to patients' number is described in **Supplementary Table S4**. pGSN expression was not significantly different between epithelial and stromal regions (**Supplementary Fig. S1B**). Total macrophage (M0) infiltration in the stroma was higher compared with that of the epithelial region (**Supplementary Fig. S1B**). However, there was no significant difference in M1 macrophage infiltration between epithelial and stromal regions although M2 infiltration was higher in the epithelial region (**Supplementary Fig. S1B**). The M1/M2 ratio (cut-off=1) was significantly higher in the stroma compared with the epithelial compartment (Supplementary Fig. S1B). This could result in a suppressed inflammatory environment in the tumor islet, an action that promotes tumor progression and chemoresistance.

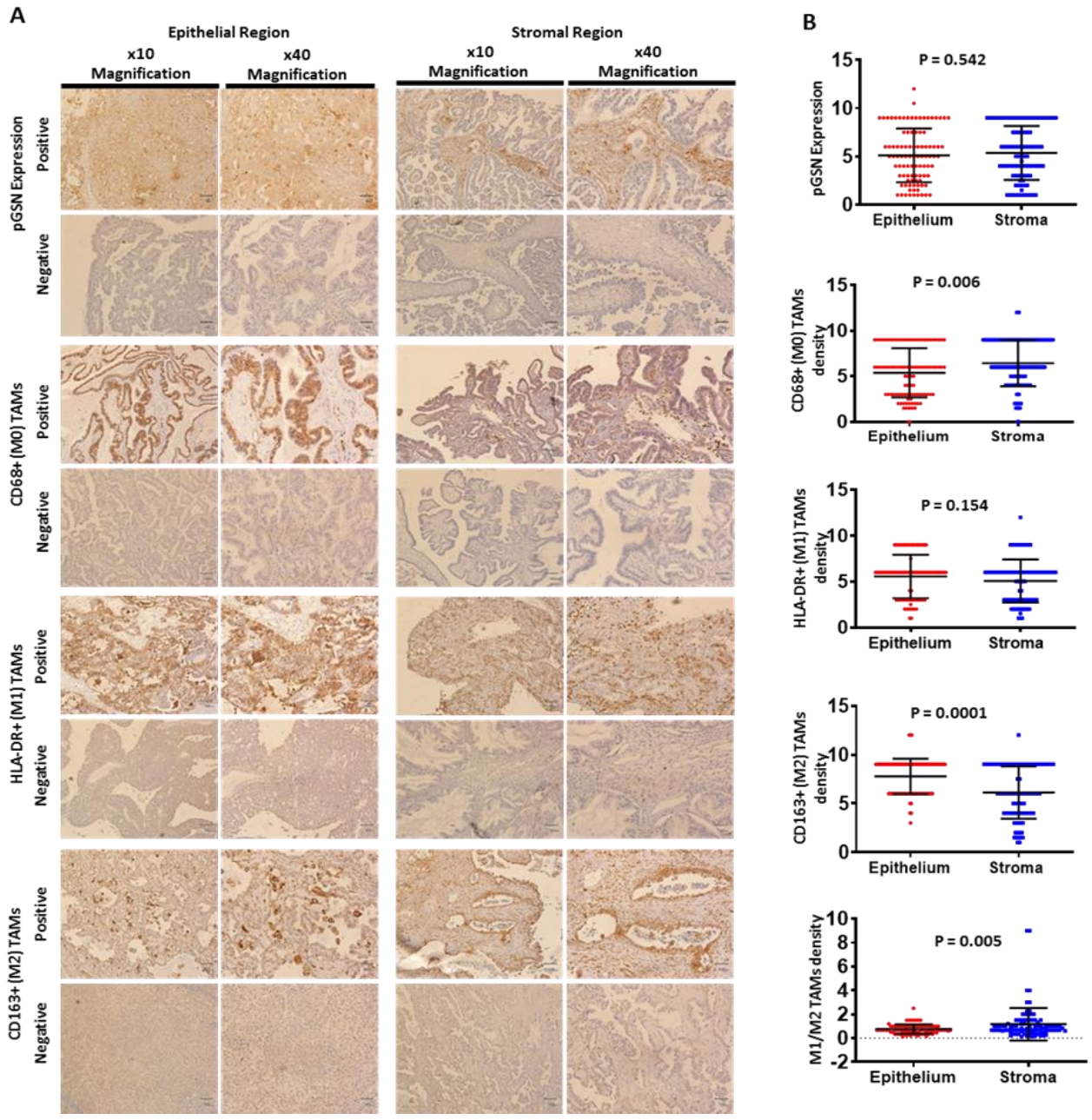

Sup. Fig. 5.S1 pGSN expression and infiltrated TAMs in OVCA tissues. (A) 94 OVCA tissues were immunostained with anti-pGSN, anti-CD68 (M0 macrophage), anti-HLA-DR (M1 macrophage marker) and anti-CD163 (M2 macrophage marker) antibodies in the epithelial and stromal compartments. **(B)** pGSN expression and tissue infiltrated macrophages were quantified, compared between epithelial (n=94) and stromal (n=94) regions and presented as scatter plots (mean ± SD). P-values were calculated by independent sample t-test. Scale bar is 50 μm.

Supplementary Table 5.S4 pGSN expression and TAMs infiltration in OVCA tissue compartments

Tissue Marker Expression (IRS)	Number of Patients
Epithelial pGSN	
≤6 (Low)	68
>6 (High)	26
Stromal pGSN	
≤6 (Low)	62
>6 (High)	32
Tumor pGSN	
≤6 (Low)	50
>6 (High)	44
Epithelial CD68 (M0)	
≤6 (Low)	68
>6 (High)	26
Stromal CD68 (M0)	
≤6 (Low)	57
>6 (High)	37
Tumor CD68 (M0)	
≤6 (Low)	56
>6 (High)	38
Epithelial HLA-DR (M1)	
≤6 (Low)	73
>6 (High)	21
Stromal HLA-DR (M1)	
≤6 (Low)	81
>6 (High)	13
Tumor HLA-DR (M1)	
≤6 (Low)	68
>6 (High)	26
Epithelial CD163 (M2)	
≤6 (Low)	38
>6 (High)	56
Stromal CD163 (M2)	
≤6 (Low)	57
>6 (High)	37
Tumor CD163 (M2)	
≤6 (Low)	14
>6 (High)	80
Epithelial M1/M2 Density	
≤1 (Low)	65
>1 (High)	29
Stromal M1/M2 Density	
≤6 (Low)	53
>6 (High)	41
Tumor M1/M2 Density	
≤6 (Low)	81
>6 (High)	13

IRS, immunoreactive score; pGSN, plasma gelsolin

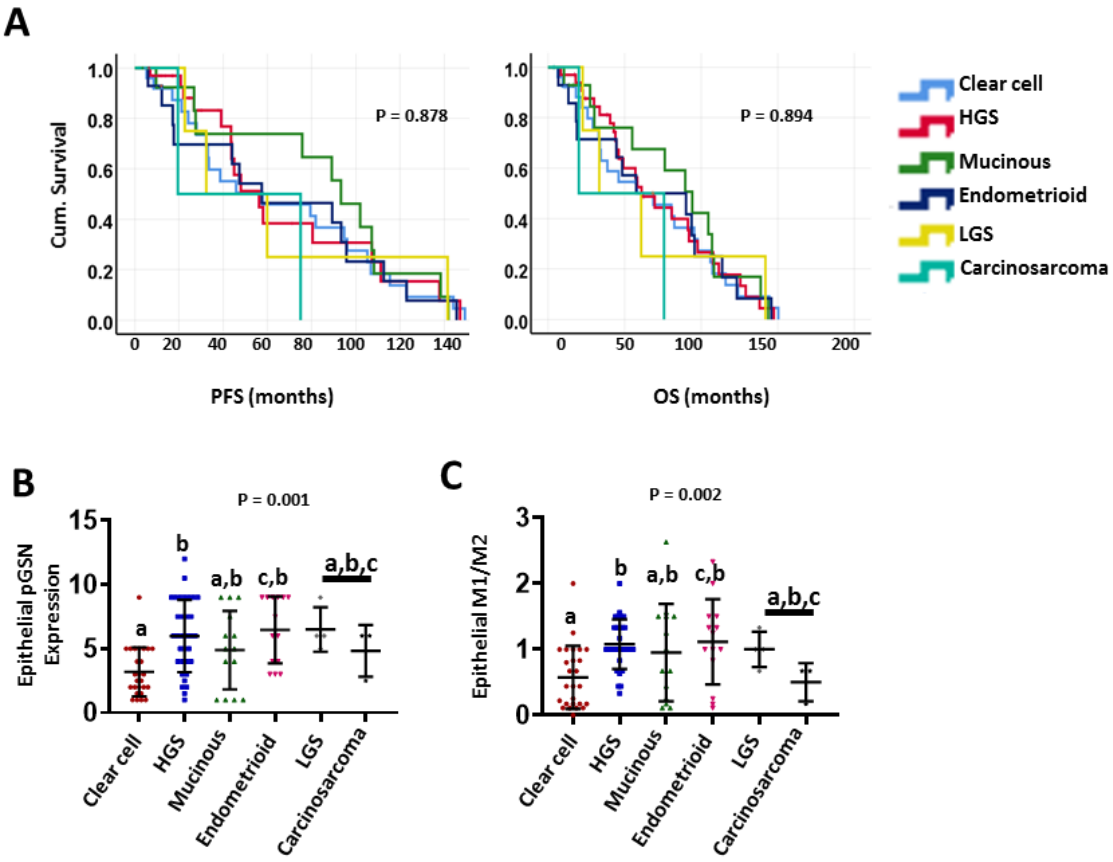

Sup. Fig. 5.S2 Epithelial pGSN expression, M1/M2 density and survival in OVCA histologic subtypes. (A) Patients were stratified using their histologic subtypes (Clear cell; n=26, HGS; n=33, Mucinous; n=14, Endometrioid; n=14, LGS; n=4, Carcinosarcoma; n=3) and correlated with PFS and OS. Kaplan Meier survival curves and log rank test were used to compare the survival distributions between the groups. **(B)** Epithelial pGSN expression was compared between patients with Clear cell; n=26, HGS; n=33, Mucinous; n=14, Endometrioid; n=14, LGS; n=4 and Carcinosarcoma; n=3. **(C)** Epithelial M1/M2 was calculated and compared between patients with Clear cell; n=26, HGS; n=33, Mucinous; n=14, Endometrioid; n=14, LGS; n=4 and Carcinosarcoma; n=3. n = number of patients in each group. P values were calculated using Kruskal-Wallis test (with Dunn's multiple comparison test). *[**B**, (a; **P<0.01 vs b), (a; **P<0.01 vs c); **C**, (a; **P<0.01 vs b), (a; *P<0.05 vs c)]*

The patients were stratified according to their histologic subtypes and their survival impact determined. No significant difference was observed with both PFS (P=0.894) and OS (P=0.878) (**Supplementary Fig. S2A**). The epithelial pGSN expression and M1/M2 ratio in patients grouped into histologic subtypes were quantitated and compared. Epithelial pGSN was highly (cut-off=6) expressed in patients with HGS [mean ± SD (6.0 ± 2.8)], endometrioid [mean ± SD (6.5 ± 2.6)] and LGS [mean ± SD (6.5 ± 1.7)] compared with clear cell [mean ± SD (3.2 ± 1.9)], mucinous [mean ± SD (4.9 ± 3.1)] and carcinosarcoma [mean ± SD (4.8 ± 2.0)] (**Supplementary Fig. S2B**). M1/M2 ratio (cut-off=1) in the epithelium was higher in patients with HGS [mean ± SD (1.0 ± 0.4)], mucinous [mean ± SD (1.0 ± 0.7)], endometrioid [mean ± SD (1.1 ± 0.6)] and LGS [mean ± SD (1.0 ± 0.3)] compared with patients with clear cell [mean ± SD (0.6 ± 0.5)] and carcinosarcoma [mean ± SD (0.5 ± 0.3)] (**Supplementary Fig. S2C**).

Increased epithelial pGSN expression is associated with suppressed survival benefits of infiltrated M1 macrophages in OVCA patients

Patients were grouped into sub-categories based on their level of pGSN expression and TAM infiltration (low or high), and their survival benefits were determined. A significant (*P*=0.008) difference was observed between the groups and PFS but not OS (*P*=0.12) (**Fig. 1A).** Patients with low pGSN-low M1 macrophages, low pGSN-high M1 macrophages, high pGSN-low M1 macrophages and high pGSN-high M1 macrophages had mean PFSs of 55.5, 85.5, 35.9 and 28.2 months, respectively (**Fig. 1A**). A significant difference (*P*=0.01) was also observed with PFS but not OS when stratified by M2 macrophage infiltration (**Fig. 1B**). Patients with low pGSN-low M2 macrophages, low pGSN-high M2 macrophages, high pGSN-low M2 macrophages and high pGSN-high M2 macrophages had mean PFSs of 68.1, 54.3, 32.9, 33.0

months respectively (**Fig. 1B**). When stratified by M1/M2 macrophage ratio, a significant association was observed with PFS (*P*=0.01) but not with OS (*P*=0.62). Patients with low pGSN-low M1/M2, low pGSN-high M1/M2, high pGSN-low M1/M2 and high pGSN-high M1/M2 had mean PFSs of 57.9, 67.5, 25.7 and 41.3 months, respectively (**Fig. 1C**). This suggests that a pro-inflammatory environment with reduced pGSN expression is key to prolonging tumor recurrence.

Chemoresistance is associated with increased epithelial pGSN expression and M2 infiltration

Before determining the relationship between epithelial pGSN and chemoresistance, we assessed TAMs density between patients with high and low epithelial expression of pGSN. We observed that patients with high epithelial pGSN expression had significantly higher epithelial infiltration of total macrophages (M0; *P*=0.03), M1 macrophages (*P*=0.001) and M1/M2 ratio (*P*=0.003) but not M2 macrophages (*P*=0.602) (**Fig. 2A-D**). Interestingly, no significant difference was seen in the stromal compartments regardless of the TAMs phenotype (**Fig. 2A-D**). To demonstrate the association between chemoresistance and epithelial pGSN expression and TAMs, patients were stratified by their progression-free interval (PFI). Patients were stratified as chemoresistant if the PFI was ≤ 12 months and chemosensitive if the PFI was > 12 months. Patients with a PFI ≤ 12 were significantly associated with increased levels of pGSN expression in the epithelial (*P*=0.005), but not stromal region (*P*=0.689) (**Fig. 2E**). Chemoresistant and sensitive patients showed no difference in M1 macrophage infiltration regardless of the tissue compartment (epithelium; *P*=0.451, stroma; *P*=0.989) (**Fig. 2F**). However, chemoresistant patients had significantly higher infiltration of M2 macrophages in the

epithelial region (*P*=0.007), but not the stroma (*P*=0.563) (**Fig. 2G**). M1/M2 macrophage ratio showed no significant difference between chemosensitive and resistant patients as stratified (epithelium; *P*=0.682, stroma; *P*=0.787) (**Fig. 2H**). No significant difference was also observed between total TAMs (M0; CD68+) and chemoresponsiveness, regardless of the tissue compartment (epithelium; *P*=0.278, stroma; *P*=0.268) (**Fig. 2I**). The expression of pGSN and the relative abundance of M1 and M2 macrophages in the cancer islet are therefore important factors in determining patients' sensitivity to treatment.

Increased pGSN expression is associated with poor patient survival, whereas increased epithelial M1/M2 macrophage density is associated with improved patient survival

The clinical relevance of pGSN expression and macrophage infiltration to patient survival was first assessed. Patients with decreased levels of pGSN had prolonged PFS (epithelium; *P*=0.002, stroma; *P*=0.055) and OS (epithelial; *P*=0.081, stroma; *P*=0.02) regardless of the tissue compartment (**Fig. 2J & K**). We further examined the survival benefits of the various subtypes of infiltrated TAMs. Lower infiltration of total macrophages (M0) in both epithelial (PFS; *P*=0.036, OS; *P*=0.03) and stromal (PFS; *P*=0.009, OS; *P*=0.002) compartments was associated with survival benefits to patients (**Fig. 2J & K**). OVCA patients with higher infiltration of M1 macrophages had significantly prolonged PFS (epithelium; *P*=0.038, stroma; *P*=0.065) and OS (epithelium; *P*=0.032, stroma; *P*=0.042) compared with patients with lower M1 infiltration (**Supplementary Fig. S3A**). Unlike M1 macrophages, no significant survival difference in PFS and OS was observed with M2 macrophages infiltration, regardless of the tissue compartment (**Supplementary Fig. S3B**). Although increased M1/M2 macrophage density was associated with improved PFS (*P*=0.018) and OS (*P*=0.007) in the epithelial region,

no significant survival difference was observed in the stroma (PFS; *P*=0.722, OS; *P*=0.595) (**Supplementary Fig. S3C**). This suggests that the survival of OVCA patients could be impacted by the level of pGSN expression and the ratio of M1/M2 macrophages present in the cancer nest.

We then investigated the association between pGSN and TAMs infiltration in the tumor microenvironment. A significant positive correlation between epithelial pGSN expression and total (M0) macrophage infiltration was observed in the epithelial region (r=0.31; *P*=0.002) but not the stroma (r=0.16; *P*=0.13) (**Supplementary Fig. S4A**) although these correlations were weak. There was a weak but positive significant association between epithelial pGSN expression and M1 macrophage infiltration in the epithelial (r=0.41; *P*=0.0001) and stromal regions (r=0.25; *P*=0.005) (**Supplementary Fig. S4B**). Unlike M1 macrophages, no significant correlation was observed with M2 macrophage infiltration and pGSN, regardless of the tissue compartment (epithelium; r=0.12; *P*=0.25, stroma; r=0.11; *P*=0.30) (**Supplementary Fig. S4C**). When the relationship between M1/M2 macrophage ratio and epithelial pGSN expression was assessed, we observed a weak but positive and significant correlation between epithelial pGSN expression and the M1/M2 macrophage ratio, regardless of tissue compartment (epithelial; r=0.33; *P*=0.001, stroma; r=0.28; *P*=0.005) (**Supplementary Fig. S4D**), suggesting that a pro-inflammatory ovarian tumour microenvironment may be an important determinant of the pGSN-mediated reduction in OVCA patient survival.

A

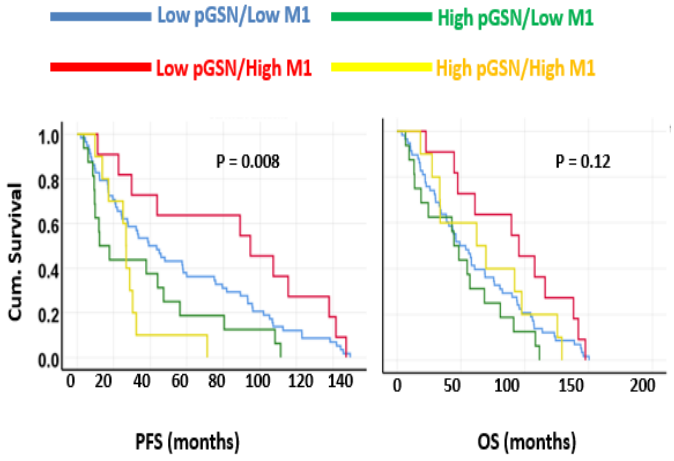

Mean survival	PFS (months)	OS (months)
Low pGSN low M1	55.5	61.3
Low pGSN High M1	**85.5**	**92.1**
High pGSN Low M1	35.9	49.8
High pGSN High M1	**28.2**	**69.0**

B

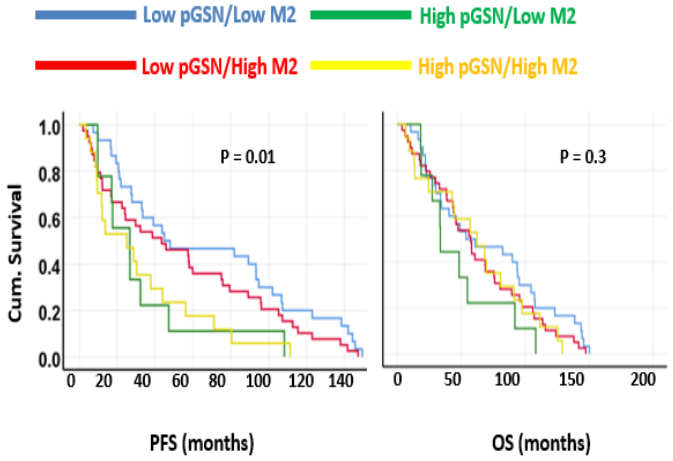

Mean survival	PFS (months)	OS (months)
Low pGSN Low M2	**68.1**	**71.2**
Low pGSN High M2	54.3	62.4
High pGSN Low M2	**32.9**	**48.5**
High pGSN High M2	**33.0**	**61.8**

C

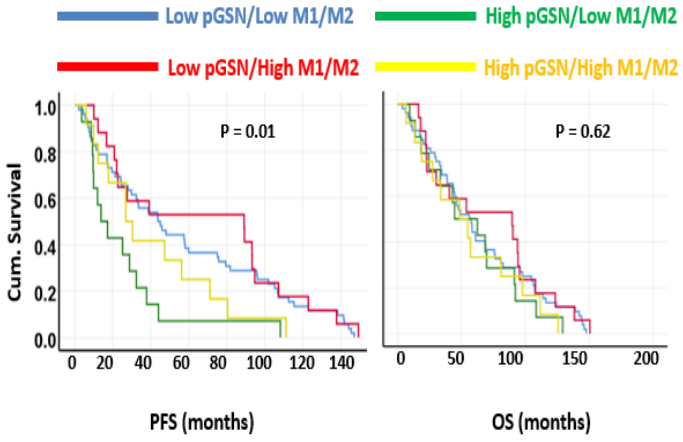

Mean survival	PFS (months)	OS (months)
Low pGSN low M1/M2	57.9	64.6
Low pGSN High M1/M2	**67.5**	**71.2**
High pGSN Low M1/M2	25.7	57.8
High pGSN High M1/M2	**41.3**	**56.4**

Figure 5.1 Increased epithelial pGSN expression is associated with suppressed survival benefits of infiltrated M1 macrophages in OVCA patients. 94 OVCA tissues were immunostained with anti-pGSN, anti-CD68 (M0 macrophage marker), anti-HLA-DR (M1 macrophage marker) and anti-CD163 (M2 macrophage marker) antibodies. pGSN expression (cut-off = 6) was assessed together with infiltrated (**A**) M1 (cut-off = 6), (**B**) M2 (cut-off = 6) and (**C**) M1/M2 macrophages (cut-off = 1) in the epithelial region and then correlated with PFS and OS. Kaplan Meier survival curves with cut-off values and log rank test were used to compare the survival distributions between the groups.

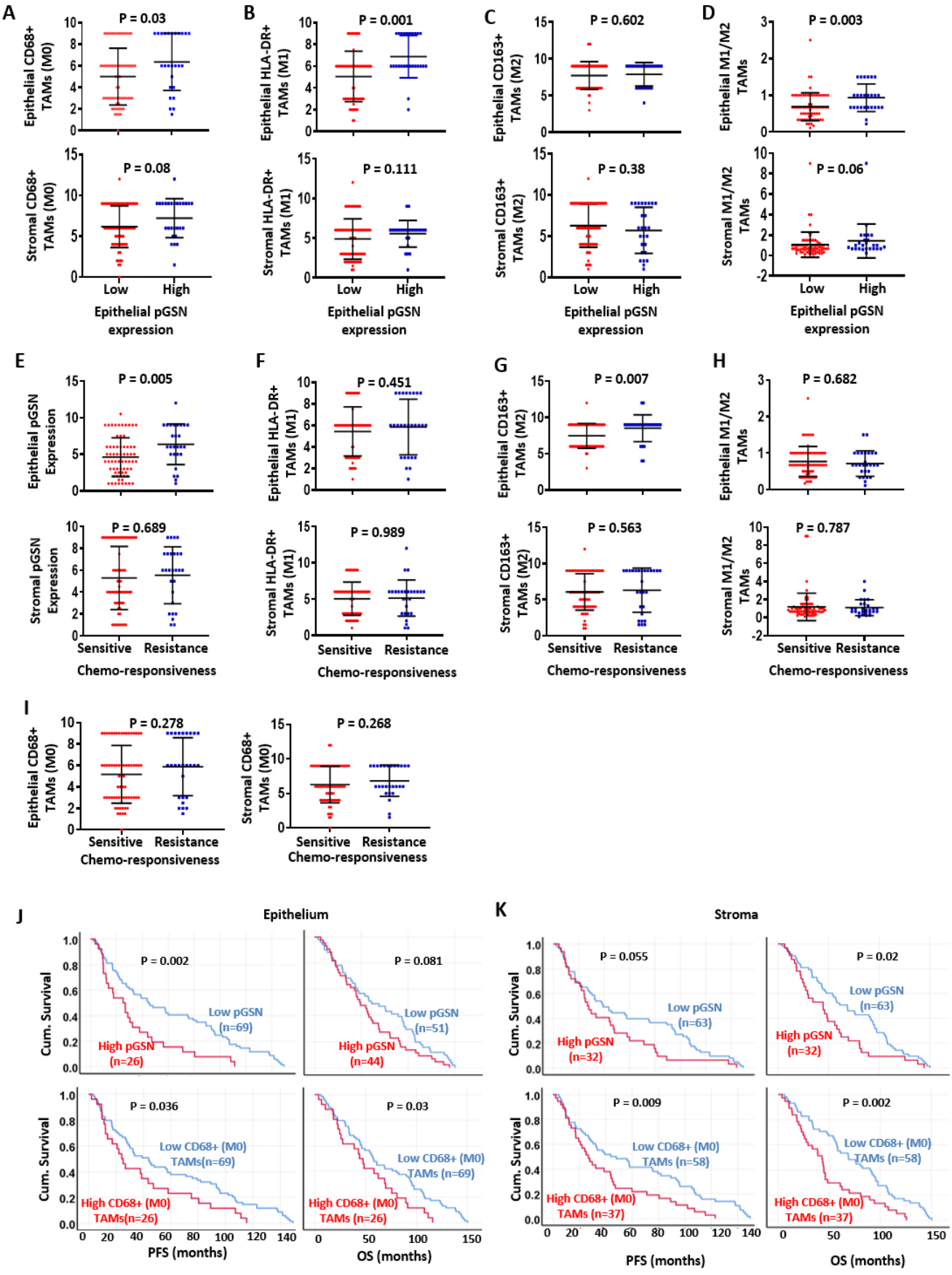
A
Epithelial CD68+ TAMs (M0)
P = 0.03
Stromal CD68+ TAMs (M0)
P = 0.08
Low
High
Epithelial pGSN expression
B
Epithelial HLA-DR+ TAMs (M1)
P = 0.001
Stromal HLA-DR+ TAMs (M1)
P = 0.111
Low
High
Epithelial pGSN expression
C
Epithelial CD163+ TAMs (M2)
P = 0.602
Stromal CD163+ TAMs (M2)
P = 0.38
Low
High
Epithelial pGSN expression
D
Epithelial M1/M2 TAMs
P = 0.003
Stromal M1/M2 TAMs
P = 0.06
Low
High
Epithelial pGSN expression
E
Epithelial pGSN Expression
P = 0.005
Stromal pGSN Expression
P = 0.689
Sensitive
Resistance
Chemo-responsiveness
F
Epithelial HLA-DR+ TAMs (M1)
P = 0.451
Stromal HLA-DR+ TAMs (M1)
P = 0.989
Sensitive
Resistance
Chemo-responsiveness
G
Epithelial CD163+ TAMs (M2)
P = 0.007
Stromal CD163+ TAMs (M2)
P = 0.563
Sensitive
Resistance
Chemo-responsiveness
H
Epithelial M1/M2 TAMs
P = 0.682
Stromal M1/M2 TAMs
P = 0.787
Sensitive
Resistance
Chemo-responsiveness
I
Epithelial CD68+ TAMs (M0)
P = 0.278
Stromal CD68+ TAMs (M0)
P = 0.268
Sensitive
Resistance
Chemo-responsiveness
J
Epithelium
Cum. Survival
P = 0.002
Low pGSN (n=69)
High pGSN (n=26)
P = 0.081
Low pGSN (n=51)
High pGSN (n=44)
P = 0.036
Low CD68+ (M0) TAMs(n=69)
High CD68+ (M0) TAMs(n=26)
PFS (months)
P = 0.03
Low CD68+ (M0) TAMs (n=69)
High CD68+ (M0) TAMs (n=26)
OS (months)
K
Stroma
Cum. Survival
P = 0.055
Low pGSN (n=63)
High pGSN (n=32)
P = 0.02
Low pGSN (n=63)
High pGSN (n=32)
P = 0.009
Low CD68+ (M0) TAMs (n=58)
High CD68+ (M0) TAMs (n=37)
PFS (months)
P = 0.002
Low CD68+ (M0) TAMs (n=58)
High CD68+ (M0) TAMs (n=37)
OS (months)

Figure 5.2 Chemoresistance is associated with increased epithelial pGSN expression and M2 infiltration. 94 OVCA patients were stratified into two groups depending on their level of pGSN expression (low; n=69 vs high; n=25). (**A**) M0, (**B**) M1, (**C**) M2 and (**D**) M1/M2 densities in the epithelium and stroma were compared and represented as scatter plots (mean ± SD). P-values were calculated by independent sample t-test. Patients were also grouped into chemoresistant (PFI ≤ 12 months; n=67) and chemosensitive (PFI > 12 months; n=27) groups. Epithelial and stromal expressions of (**E**) pGSN, (**F**) M1, (**G**) M2, (**H**) M1/M2 and (**I**) M0 were quantitated, compared and represented as scatter plots (mean ± SD). P-values were calculated by two sided non-parametric Mann-Whitney test. **(J)** Epithelial and (**K)** stromal pGSN expression (cut-off=6) and infiltrated M0 (CD68+) macrophages (cut-off=6) were correlated with PFS and OS. Kaplan Meier survival curves of categorized pGSN expression (low and high group, cut-off=6) and M0 density (low and high group, cut-off=6) and log rank test were used to compare the survival distributions between the groups. n = number of patients in each group.

Prognostic impact of epithelial pGSN, TAMs and other clinicopathologic parameters.

We assessed the prognostic impact of epithelial pGSN, TAMs and other clinicopathological parameters using uni- and multivariate Cox regression analyses as shown in **Tables 1 and 2**, respectively. Median cut-offs were used to predict PFS and OS. In the univariate Cox regression analysis (**Table 1**), age, stage (FIGO), residual disease (RD) and M2 macrophage (CD163) showed a significant association with PFS and OS. Epithelial pGSN only showed a significant association with PFS (HR, 1.233; CI, 1.07-1.420; P=0.004) but not OS (HR, 1.054; CI, 0.870-1.276; P=0.591). In the multivariate Cox regression analysis (**Table 2**), only epithelial pGSN (HR, 1.181; CI, 1.010-1.381; P=0.038), histologic subtype (HR, 0.547; CI, 0.312-0.954; P=0.035) and RD (HR, 0.138; CI, 0.049-0.391; P<0.001) were found to be significant predictors of PFS. With regards to OS, only RD was significantly associated with an increased risk of death. Taken together, these findings suggest that increased tumor pGSN expression plays a key role in ovarian tumor progression and could serve as a marker for suboptimal residual disease and tumor recurrence.

Chemoresistant cells-derived sEV attenuates M1 macrophage's anti-tumor function by increased caspase-3-dependent apoptosis and decreased secretion of iNOS and TNFα

In the OVCA tissues, we observed that although increased expression of pGSN is associated with increased M1 macrophage density, patient survival is reduced. We therefore hypothesized that increased pGSN expression attracts M1 macrophages into the cancer nest and suppress their viability, thus leading to a change in the pro-inflammatory environment (M1/M2 ratio) and decreased patient survival. Thus, we further examined utilizing *in vitro* techniques, how this phenomenon occurs. Chemoresistant OVCA secrete increased levels of exosomal

pGSN that confers cisplatin resistance on otherwise sensitive cells and regulates immune cells. We therefore hypothesized that exosomal pGSN derived from chemoresistant OVCA cells will induce apoptosis in M1 macrophages, as well as reduce the secretion of iNOS and TNFα. Human THP-1 monocytes were differentiated and polarized into M1 macrophages (**Supplementary Fig. S5A**). M1 macrophage polarization was confirmed by microscopy (**Supplementary Fig. S5B**), flow cytometry (**Supplementary Fig. S5C**) and Western blotting (**Supplementary Fig. S5D**).

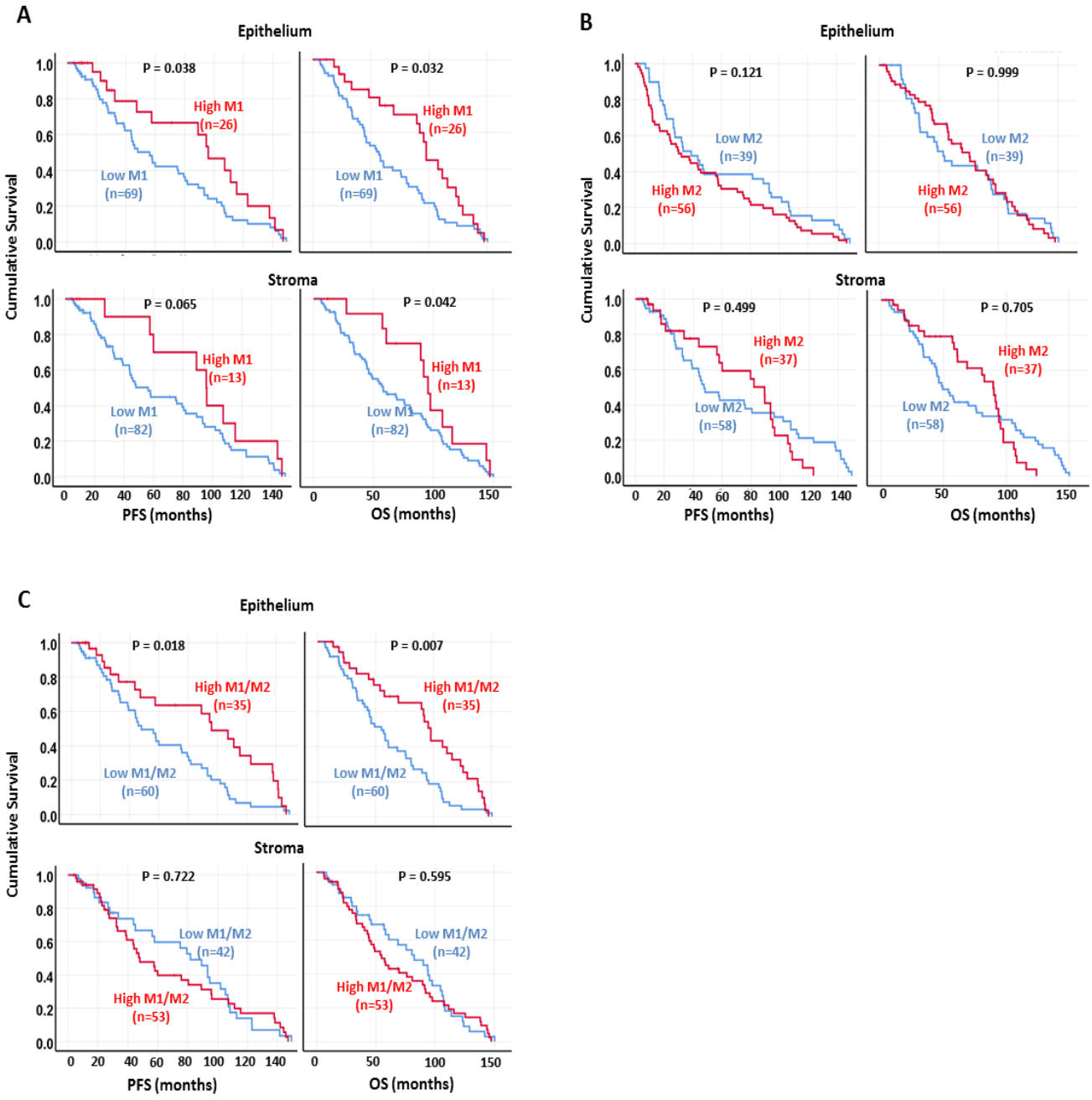

Sup. Fig. 5.S3 Higher infiltration of M1 but not M2 macrophages is associated with improved survival. (A) M1 (cut-off = 6), **(B)** M2 (cut-off = 6) and **(C)** M1/M2 infiltrated macrophages (cut-off = 1) in the epithelial and stromal regions were correlated with PFS and OS. Kaplan Meier survival curves with cut-off values and log rank test were used to compare the survival distributions between the groups. n = number of patients in each group.

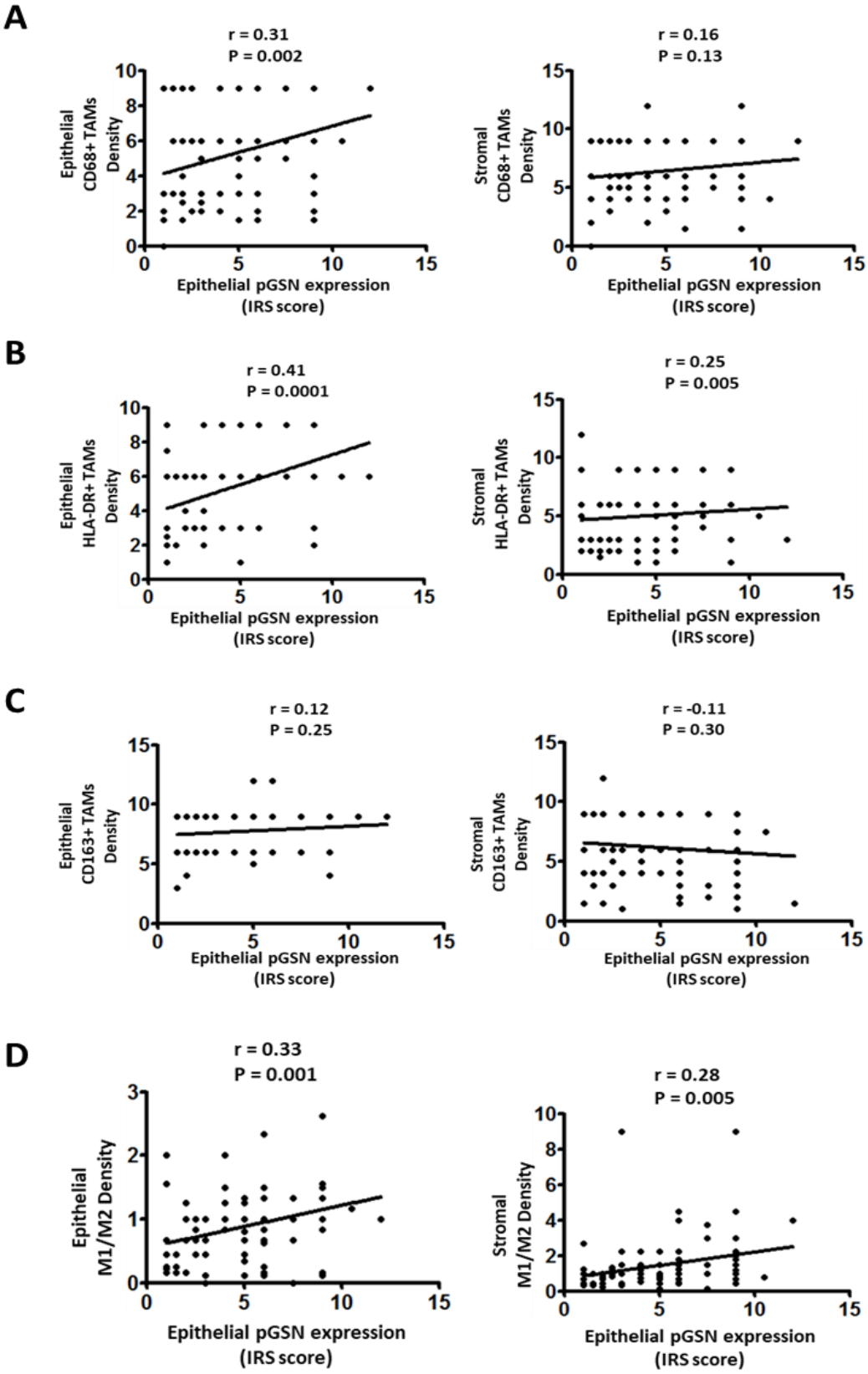
A
r = 0.31
P = 0.002
Epithelial CD68+ TAMs Density
Epithelial pGSN expression (IRS score)
r = 0.16
P = 0.13
Stromal CD68+ TAMs Density
Epithelial pGSN expression (IRS score)
B
r = 0.41
P = 0.0001
Epithelial HLA-DR+ TAMs Density
Epithelial pGSN expression (IRS score)
r = 0.25
P = 0.005
Stromal HLA-DR+ TAMs Density
Epithelial pGSN expression (IRS score)
C
r = 0.12
P = 0.25
Epithelial CD163+ TAMs Density
Epithelial pGSN expression (IRS score)
r = -0.11
P = 0.30
Stromal CD163+ TAMs Density
Epithelial pGSN expression (IRS score)
D
r = 0.33
P = 0.001
Epithelial M1/M2 Density
Epithelial pGSN expression (IRS score)
r = 0.28
P = 0.005
Stromal M1/M2 Density
Epithelial pGSN expression (IRS score)

Sup. Fig. 5.S4 Epithelial pGSN expression is significantly correlated with M1/M2 macrophage ratio. Epithelial pGSN expression was correlated with epithelial and stromal densities of **(A)** M0, **(B)** M1, **(C)** M2 macrophages and **(D)** M1/M2 macrophage ratio. Pearson's analysis was used to examine the correlation between epithelial pGSN and TAMs.

Table 5.1 Univariate Cox regression analysis for PFS and OS

	Univariate					
Variable	**PFS**			**OS**		
	HR*	**95% CI^**	***P*-value**	**HR***	**95% CI^**	***P*-value**
Age (years) **≤56 vs >56**	1.046	1.012 – 1.082	**0.008**	1.049	1.002 – 1.098	**0.041**
Stage (FIGO) **≤2 vs >2**	4.803	2.153 – 10.717	**<0.001**	3.682	1.232 – 11.005	**0.020**
RD (cm) **≤1 vs >1**	0.114	0.052 – 0.251	**<0.001**	.117	0.039 – 0.350	**<0.01**
pGSN^{epi} **Low vs high**	1.233	1.07 – 1.421	**0.004**	1.054	0.870 – 1.276	0.591
CD68^{epi} **Low vs high**	1.092	0.946 – 1.26	0.23	1.011	0.832 – 1.228	0.915
HLA-DR (M1)^{epi} **Low vs high**	1.035	0.881 – 1.215	0.676	0.826	0.661 – 1.033	0.093
CD163 (M2)^{epi} **Low vs high**	1.328	1.065 – 1.658	**0.012**	1.436	1.047 – 1.971	**0.025**
M1/M2^{epi} **Low vs high**	0.787	0.391 – 1.584	0.503	0.397	0.138 – 1.137	0.085
Histologic subtype	0.787	0.549 – 1.129	0.194	0.806	0.488 – 1.333	0.401

HR, hazard ratio; PFS, disease free survival; OS, overall survival; CI, confidence interval; RD, residual disease; pGSN, plasma gelsolin; FIGO, International Federation of Gynecology and Obstetrics; vs, versus; epi, epithelial

*Estimated from Cox proportional hazard regression model.

^Confidence interval of the estimated HR.

Table 5.2 Multivariate Cox regression analysis for PFS and OS

	Multivariate Analysis					
Variable	**PFS**			**OS**		
	HR*	**95% CI^**	***P*-value**	**HR***	**95% CI^**	***P*-value**
Age (years) **≤56 vs >56**	1.126	0.387 – 3.279	0.828	1.352	0.331 – 5.530	0.675
Stage (FIGO) **≤2 vs >2**	1.090	0.358 – 3.320	0.880	0.945	0.183 – 4.874	0.946
RD (cm) **≤1 vs >1**	0.103	0.033 – 0.322	**<0.001**	0.139	0.032 – 0.605	**0.009**
pGSN^{epi} **Low vs high**	1.300	1.096 – 1.541	**0.003**	1.019	0.793 – 1.309	0.884
CD68^{epi} **Low vs high**	0.939	0.764 – 1.154	0.549	0.943	0.706 – 1.261	0.694
HLA-DR (M1)^{epi} **Low vs high**	1.030	0.809 – 1.312	0.808	0.828	0.552 – 1.242	0.362
CD163 (M2)^{epi} **Low vs high**	1.274	0.969 – 1.674	0.082	1.481	0.910 – 2.413	0.114
M1/M2^{epi} **Low vs high**	0.603	0.198 – 1.836	0.373	1.173	0.174 – 7.912	0.870
Histologic subtype	0.547	0.312 – 0.954	**0.035**	0.730	0.354 – 1.503	0.393

HR, hazard ratio; PFS, disease free survival; OS, overall survival; CI, confidence interval; RD, residual disease; pGSN, plasma gelsolin; FIGO, International Federation of Gynecology and Obstetrics; vs, versus; epi, epithelial

*Estimated from Cox proportional hazard regression model.

^Confidence interval of the estimated HR.

M1 macrophages were treated with serum-free RPMI 1640 media (negative control), 0.5μM etoposide (positive control), sEVs (40 μg/400,000 cells) and co-cultured with chemosensitive (HGS, OV2295 and endometrioid, A2780s) and chemoresistant OVCA cells (HGS, OV90; endometrioid, A2780cp) for 48 h (**Fig. 3A**). Apoptosis of M1 macrophages was assessed using annexin V flow cytometry (**Fig. 3B)** and caspase-3 fluorescence microscopic detection (**Fig. 3C)** as well as Western blotting and Hoechst staining (**Fig. 3D & E**). Chemoresistant cell-derived sEVs and chemoresistant OVCA cells significantly induced M1 macrophage apoptosis (assayed morphologically by Hoechst nuclear staining; **Fig. 3D & E**), compared with chemosensitive cells, which was evidenced by increased annexin v+ cells (**Fig. 3B**) and increased caspase-3 activation (**Fig. 3C - E**). Tumor infiltrated M1 macrophages secrete anti-tumor factors such as iNOS and TNFα, which induce apoptosis in cancer cells thereby contributing to improved patient survival (34, 35)**.** Thus, we examined iNOS and TNFα production by M1 macrophages after their co-culture with OVCA cancer cells. iNOS and TNFα secretions by M1 macrophages were significantly decreased when treated with chemoresistant cells-derived sEVs or co-cultured with chemoresistant OVCA cells compared with chemosensitive cells, regardless of the histologic subtype (**Fig. 3D - E**). This suggests that sEVs derived from chemoresistant OVCA cells, regardless of histologic subtype are capable of suppressing the viability and anti-tumor functions of M1 macrophages.

pGSN is directly involved with M1 macrophages apoptosis and anti-tumor suppression

To further demonstrate that pGSN is indeed involved in the induction of M1 macrophage apoptosis as observed above, we performed loss- and gain-of-function studies in which pGSN in chemoresistant OVCA cells (OV90 and A2780cp) was knocked down (KD) with two (2)

different siRNAs (50 nM; 24 h), as well as over-expressed (OX) in chemosensitive cells, which otherwise express low pGSN (OV2295 and A2780s) using cDNA (2 µg; 24 h) (**Fig. 4A & B**). Scrambled plasmids were used as controls. pGSN KD and OX were confirmed by Western blotting **(Supplementary Fig. S6A & B).** M1 macrophages were then co-cultured with chemoresistant cells-pGSN-KD and chemosensitive cells-pGSN-OX and their respective control cells for 48 h. Knocking down pGSN from chemoresistant OVCA cells significantly reduced caspase-3 activation and apoptosis in M1 macrophages; a response that was associated with increased secretion of iNOS and TNFα (**Fig. 4B**). Overexpressing pGSN in chemosensitive OVCA cells resulted in significantly increased caspase-3 activation and apoptosis, which was associated with decreased iNOS and TNFα secretion (compared with control cells; **Fig. 4B**). This suggests that pGSN is an inhibitor of M1 macrophage function.

To further investigate the role of pGSN in M1 macrophage suppression, M1 macrophages were treated with chemoresistant cells-derived conditioned media (CM)+IgG, sEV-depleted CM from chemoresistant cells+IgG (control), chemoresistant cells-derived CM+pGSN blocking antibody (bAb), as well as chemoresistant derived CM+pGSN-bAb+sEVs (**Fig. 4C & D**). Increased caspase-3 activation and apoptosis were observed in M1 macrophages when treated with CM+IgG; a response that was attenuated by the presence of pGSN-bAb (**Fig. 4D**). Moreover, this blocking effect of the pGSN antibody could be overcome by sEVs (CM+pGSN-bAb+sEVs), a phenomenon that was associated with decreased iNOS and TNFα secretion (**Fig. 4D**). M1 macrophage apoptosis was further validated using recombinant human pGSN (10 µM; 24 h) **(Supplementary Fig. S6C)**. M1 macrophage apoptosis was increased after rhpGSN treatment, which was marked by increased annexin V+ M1 macrophages **(Supplementary Fig. S6C)**. Together, these findings demonstrate that pGSN is the key molecule in the

chemoresistant-derived sEVs responsible for suppressing the viability and anti-tumor functions of M1 macrophages.

DISCUSSION

In this present study, we have demonstrated for the first time the role of exosomal pGSN as a modulator of inflammation, leading to chemoresistance in OVCA in part by resetting the relative abundance and function of macrophage subtypes in the ovarian tumour microenvironment. Unlike our previous studies which involved patients from Western countries, the cohort used in the current study involves Asian patients which have an unusual patient distribution in histology (high number of non-serous), age (< average age at diagnosis), tumor stage (~60% stage 1), surgical outcomes (> average complete/optimal residual disease) and treatment regimen (increased treatment response). This diversity could impart patient survival and could explain why this cohort of patients has relatively higher PFS compared with patients from Western countries. These strengthen the point that ethnic differences may play a huge role in ovarian cancer pathology, management and patient survival.

Using this Asian cohort, we have shown that increased epithelial expression of pGSN is associated with poor survival and chemoresistance. Although there was no significant difference between pGSN expression in the epithelial and stromal regions, the epithelial pGSN expression provided the most clinical relevance. These findings are consistent with our previous studies where increased pGSN mRNA levels were associated with poor prognosis regardless of treatment regimen or the OVCA histological subtype (19). This also supports the findings from other studies in which pGSN levels were implicated in head-and-neck, ovarian and prostate cancers (19, 21, 22, 24, 25).

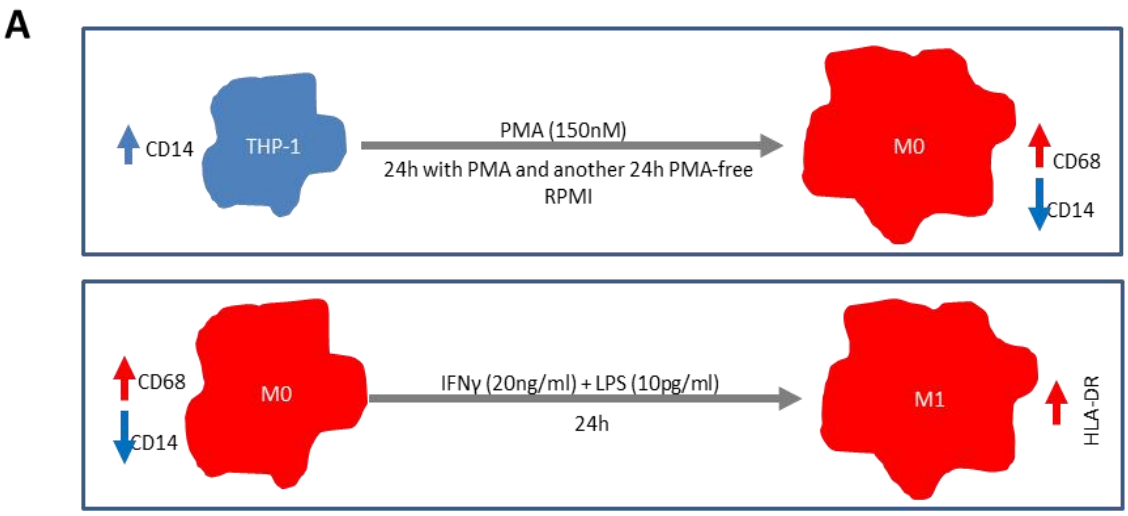
A
CD14
THP-1
PMA (150nM)
24h with PMA and another 24h PMA-free RPMI
M0
CD68
CD14
CD68
M0
CD14
IFNγ (20ng/ml) + LPS (10pg/ml)
24h
M1
HLA-DR

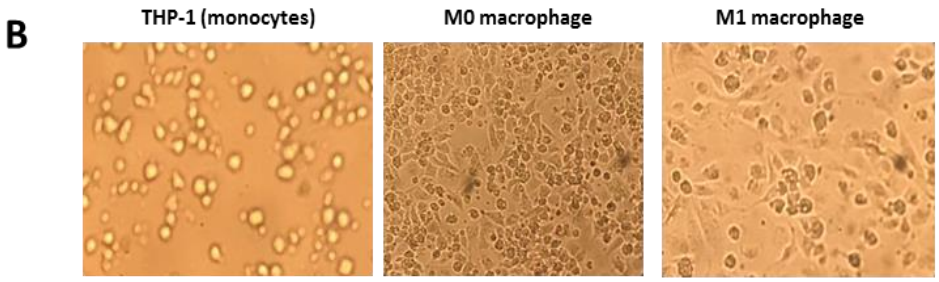
B
THP-1 (monocytes)
M0 macrophage
M1 macrophage

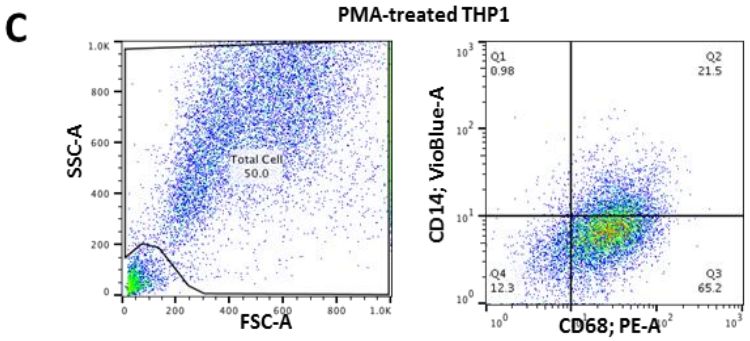
C
PMA-treated THP1
SSC-A
FSC-A
Total Cell
50.0
CD14; VioBlue-A
CD68; PE-A
Q1
0.98
Q2
21.5
Q4
12.3
Q3
65.2

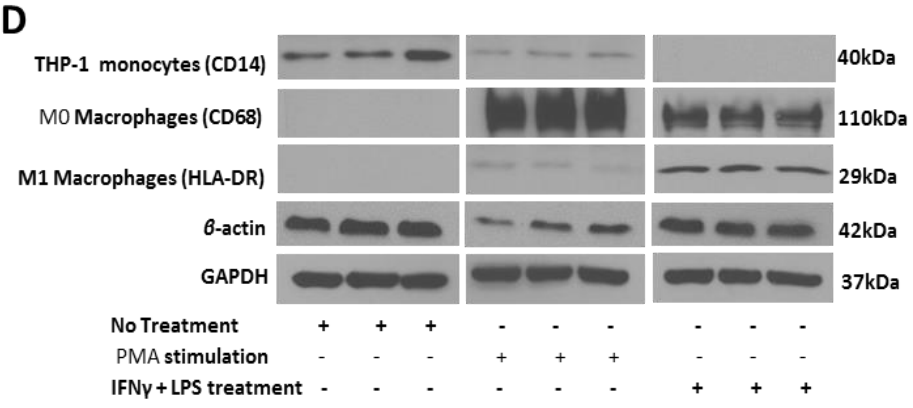
D
THP-1 monocytes (CD14)
M0 Macrophages (CD68)
M1 Macrophages (HLA-DR)
β-actin
GAPDH
40kDa
110kDa
29kDa
42kDa
37kDa
No Treatment
PMA stimulation
IFNγ + LPS treatment

Sup. Fig. 5.S5 M1 macrophage differentiation and polarization. (A) THP-1 monocytes were differentiated into M0 macrophages by PMA treatment (150 nM; 24 h). M0 macrophages were polarized to M1 macrophages with IFNγ (20ng/ml) + LPS (10pg/ml) for 24 h. Differentiation and polarization were confirmed by **(B**) microscopy, **(C**) flow cytometry and **(D)** Western blot (CD14, CD68, HLA-DR, beta actin and GAPDH).

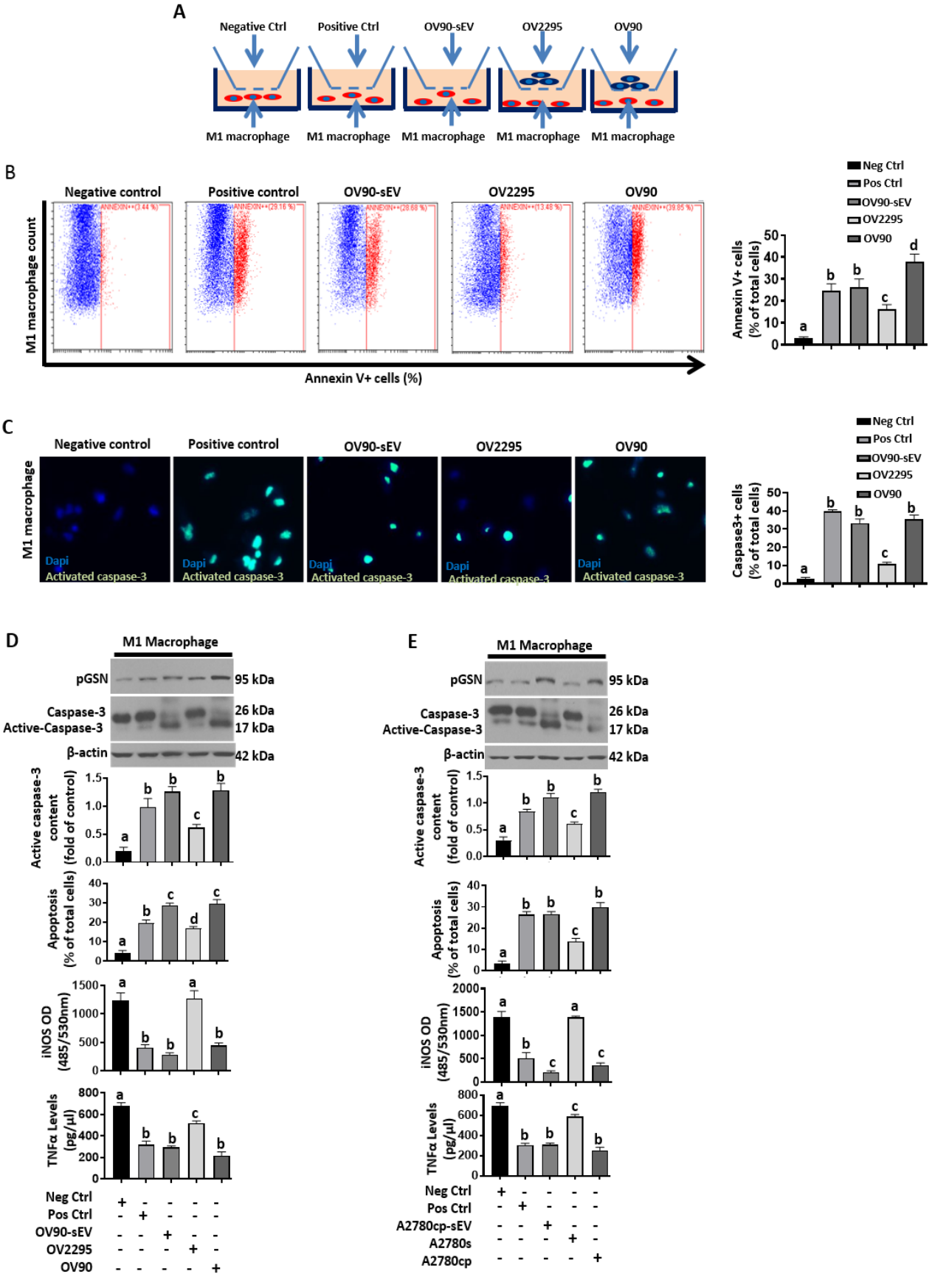
A
Negative Ctrl
Positive Ctrl
OV90-sEV
OV2295
OV90
M1 macrophage
B
Negative control
Positive control
OV90-sEV
OV2295
OV90
M1 macrophage count
Annexin V+ cells (%)
Neg Ctrl
Pos Ctrl
OV90-sEV
OV2295
OV90
Annexin V+ cells (% of total cells)
C
Negative control
Positive control
OV90-sEV
OV2295
OV90
M1 macrophage
Dapi
Activated caspase-3
Caspase3+ cells (% of total cells)
D
M1 Macrophage
pGSN
95 kDa
Caspase-3
Active-Caspase-3
26 kDa
17 kDa
β-actin
42 kDa
Active caspase-3 content (fold of control)
Apoptosis (% of total cells)
iNOS OD (485/530nm)
TNFα Levels (pg/μl)
Neg Ctrl
Pos Ctrl
OV90-sEV
OV2295
OV90
E
M1 Macrophage
pGSN
95 kDa
Caspase-3
Active-Caspase-3
26 kDa
17 kDa
β-actin
42 kDa
Active caspase-3 content (fold of control)
Apoptosis (% of total cells)
iNOS OD (485/530nm)
TNFα Levels (pg/μl)
Neg Ctrl
Pos Ctrl
A2780cp-sEV
A2780s
A2780cp

Figure 5.3 Chemoresistant cells-derived sEV attenuates the anti-tumor function of M1 macrophages by increased caspase-3-dependent apoptosis and decreased secretion of iNOS and TNFα. (A – E) M1 macrophages were co-cultured with serum-free media (negative control; 48 h), etoposide (0.5 µM; 48 h), OV90- and A2780cp-derived sEV (40 µg/400,000 cells; 48 h), OV2295 and A2780s (48 h) and OV90 and A2780cp (48 h). M1 macrophage apoptosis was assessed by Annexin V-FITC flow cytometry, caspase-3 activation detection assay, morphologically by Hoechst 33258 DNA staining) and Western blot. iNOS (M1 macrophage) and TNFα secretions (M1 macrophage conditioned media0 were determined by fluorometric assay (Ex/Em=485/530nm) and ELISA respectively. Pro-caspase-3, activated caspase-3, pGSN and beta-actin contents were assessed by Western blot (M1 macrophage lysates). Results are expressed as means ± SD from three independent replicate experiments. *[**B**, (a; ***P<0.001 vs b, c and d); **C**, (a; ***P<0.001 vs b, a; *P<0.05 vs c); **D**, (a; **P<0.01 vs b and c); **E**, (a; **P<0.01 vs b and c)]*. Scale bar is 100 µm.

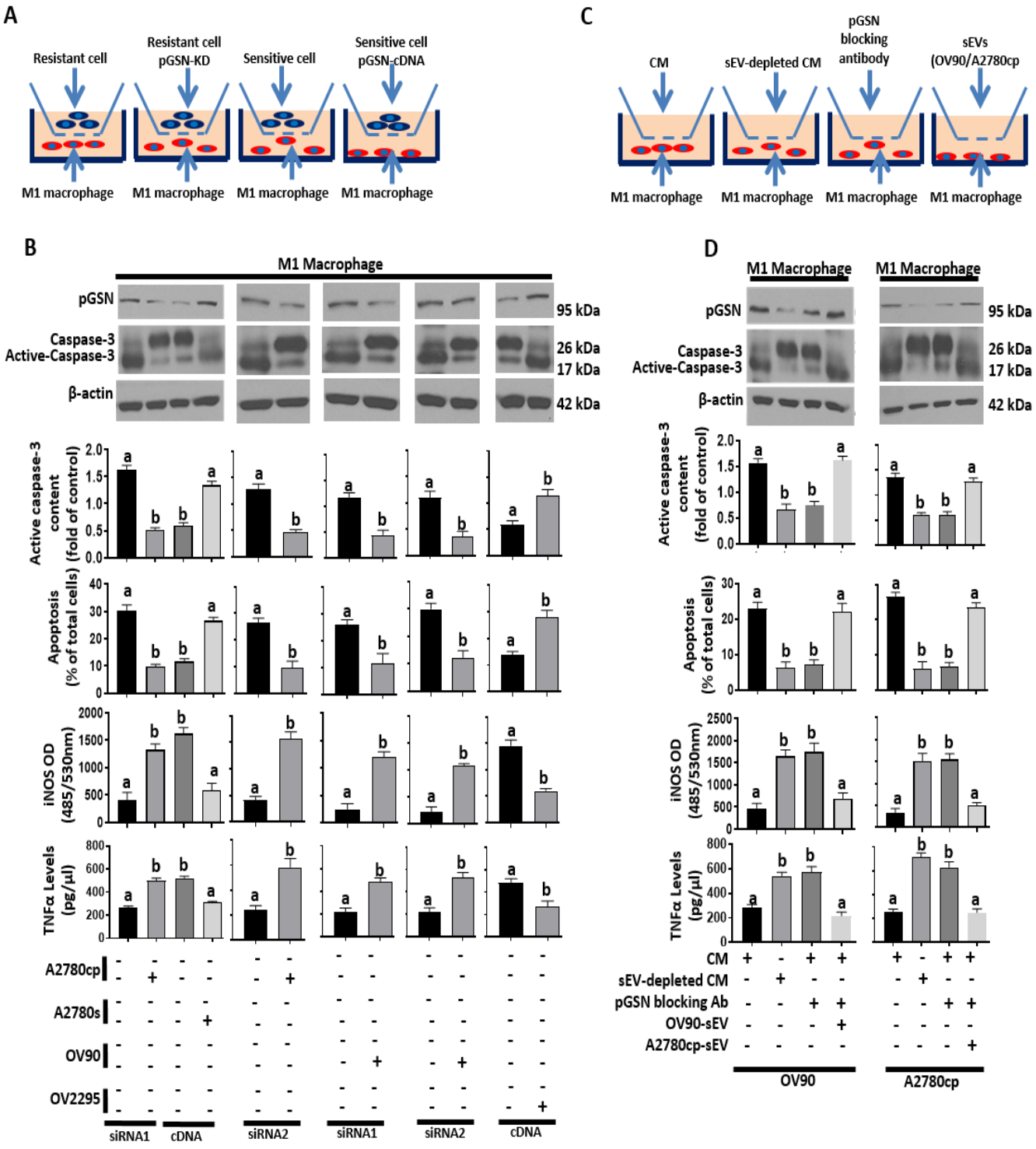
A
Resistant cell
Resistant cell pGSN-KD
Sensitive cell
Sensitive cell pGSN-cDNA
M1 macrophage
M1 macrophage
M1 macrophage
M1 macrophage
C
CM
sEV-depleted CM
pGSN blocking antibody
sEVs (OV90/A2780cp
M1 macrophage
M1 macrophage
M1 macrophage
M1 macrophage
B
M1 Macrophage
pGSN
Caspase-3
Active-Caspase-3
β-actin
95 kDa
26 kDa
17 kDa
42 kDa
Active caspase-3 content (fold of control)
Apoptosis (% of total cells)
iNOS OD (485/530nm)
TNFα Levels (pg/μl)
A2780cp
A2780s
OV90
OV2295
siRNA1
cDNA
siRNA2
siRNA1
siRNA2
cDNA
D
M1 Macrophage
M1 Macrophage
pGSN
Caspase-3
Active-Caspase-3
β-actin
95 kDa
26 kDa
17 kDa
42 kDa
Active caspase-3 content (fold of control)
Apoptosis (% of total cells)
iNOS OD (485/530nm)
TNFα Levels (pg/μl)
CM
sEV-depleted CM
pGSN blocking Ab
OV90-sEV
A2780cp-sEV
OV90
A2780cp

Figure 5.4 pGSN is directly involved with M1 macrophages apoptosis and anti-tumor suppression. (A) M1 macrophages (bottom chamber) were co-cultured with OVCA cells [upper chamber; chemoresistant, chemoresistant-pGSN-KD (siRNA 1 and 2; 50 nM; 24 h), chemosensitive and chemosensitive-pGSN-OX cells (cDNA; 2 µg; 24 h)] of different histologic subtypes (HGS and endometrioid OVCA cells; 48 h). **(B)** M1 macrophages were co-cultured with OV90/A2780cp (pGSN siRNA1 and 2; 50 nM; 24 h) and OV2295/A2780s (cDNA 2 µg; 24 h). Scramble RNAs and empty vectors were used as control for the knock down and overexpression respectively. **(C)** M1 macrophages were treated with the following: CM + IgG, sEV-depleted CM + IgG (control), CM + pGSN blocking antibody (bAb) and CM + pGSN-bAb + sEVs. CM was derived from chemoresistant cells (OV90 and A2780cp). **(D)** M1 macrophages were treated with CM + IgG, sEV-depleted CM + IgG (control), CM + pGSN-bAb and CM + pGSN-bAb + sEVs (3 ml; 48 h). Pro-caspase-3, activated caspase-3, pGSN and beta-actin contents were assessed by Western blotting assay (M1 macrophage lysates) and apoptosis determined morphologically by Hoechst 33258 DNA staining. iNOS (M1 macrophage) and TNFα secretions (M1 macrophages conditioned media) were determined by fluorometric assay (Ex/Em=485/530nm) and ELISA, respectively. Results are expressed as means ± SD from three independent replicate experiments. *[**B**, (a; ***P<0.001 vs b); **C**, (a; ***P<0.001 vs b]*

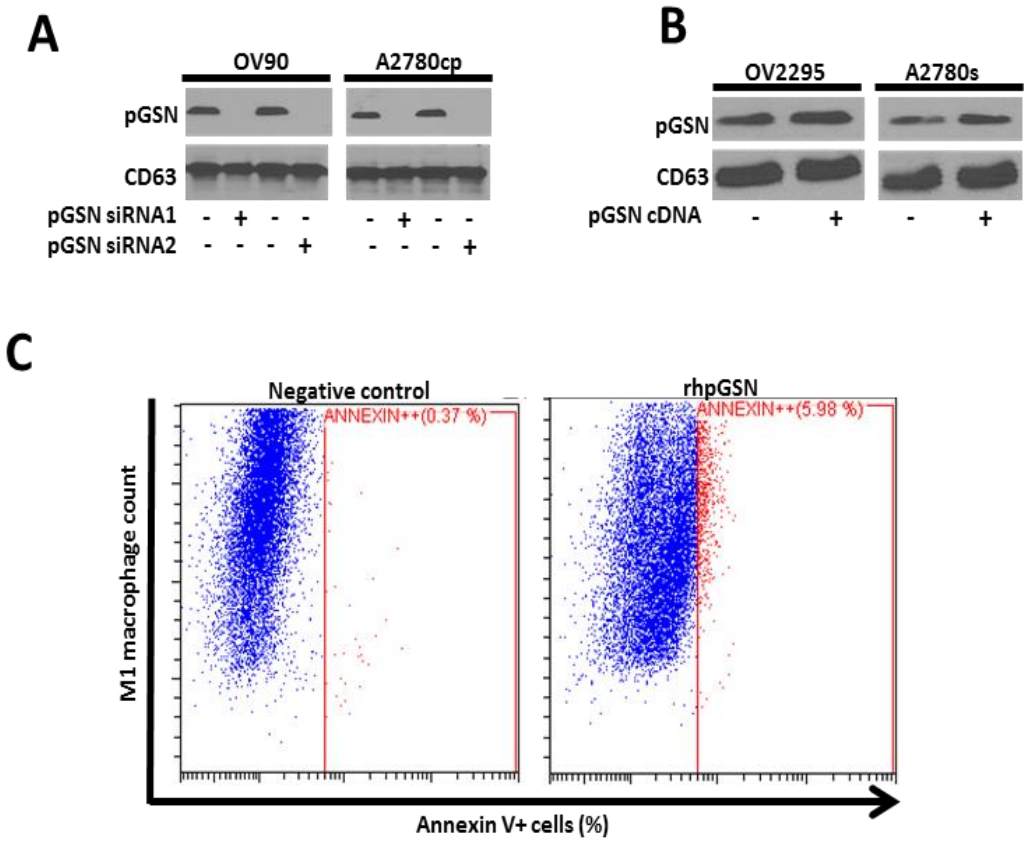

Sup. Fig. 5.S6 pGSN knockdown and overexpression confirmation in sEVs and rhpGSN-induced apoptosis in M1 macrophages. (A) Chemoresistant OVCA cells (OV90 and A2780cp) were treated with pGSN siRNA1 and 2 (50 nM; 24 h). **(B)** Chemosensitive OVCA cells (OV2295 and A2780s) were treated with pGSN cDNA (2 µg; 24 h). Conditioned media from treated cells were collected and sEVs isolated. pGSN and sEV marker (CD63) contents were assessed by Western blotting. **(C)** M1 macrophages were treated with rhpGSN (10 µM; 24 h). DMSO was used as control. Apoptosis was analysed by counting Annexin V+ M1 macrophages using flow cytometry.

Thus, targeting pGSN by way of monoclonal antibodies or small molecule inhibitors could provide therapeutic advantages to patients with OVCA regardless of their ethnic background. Since pGSN is highly detectable in all histologic subtypes, targeting it will not only provide therapeutic advantage to patients with HGS, but to all patients with other histologic subtypes.

Harnessing the anti-tumor functions of CD8+ T cells has shown much promise, however minimal therapeutic success has been achieved (5, 36, 37). This has motivated us to investigate other anti-tumor immune cells such as tumor-associated macrophages (TAMs) to determine if they could be re-programmed to kill OVCA cells in the tumor microenvironment. Although there was no significant difference with M1 macrophage infiltration in both compartments, a prolonged survival was observed in patients who had increased infiltration in the cancer islet (epithelial compartment). This is consistent with other findings in breast, colon, lung and head-and-neck cancers where M1 macrophage infiltration was associated with better survival and improved treatment responses (38-41). TAMs that exhibit M1 phenotypes are classically pro-inflammatory and have high phagocytic properties. These cells in their functional state also produce increased levels of TNFα and iNOS, which contribute to the killing of tumor cells. Thus, increasing the presence of M1 macrophages in the tumor environment while inhibiting the expression of tumor pGSN could provide survival benefits to patients. This might explain the correlation between increased M1 macrophage infiltration and prolonged survival.

Increased M2 macrophage infiltration in the epithelium, but not the stroma, was associated with chemoresistance, although no difference in infiltration was identified between patients with high and low pGSN levels. M2 macrophages possess pro-tumorigenic properties and secrete cytokines such as IL-4, IL-10 and IL-13 that inhibit other immune cells and promote

tumor growth (8, 9, 13). Thus, it is not surprising that increased infiltration of this population of cells reduced responsiveness to chemotherapy. These findings are consistent with other studies showing similar associations in breast, glioblastoma, lung, prostate, gastric, prostate and colorectal cancers (8, 9, 38, 39, 42). Re-engineering TAMs to express M1 macrophage phenotypic genes provides anti-tumor effects and has the potential of increasing patients' survival (40).

We further investigated the potential relationship between epithelial pGSN expression and TAM infiltration. We observed a significant positive correlation between pGSN expression and M1/M2 ratio in both the epithelial and stroma compartments. This ratio, indicative of the inflammatory status of the ovarian TME, provides the relative abundance of the two cell populations at a time and could be used as a diagnostic index. Interestingly, we observed that, although epithelial pGSN positively correlated with M1 macrophages, the survival impact of the M1 macrophages were hindered. Specifically, the mean PFS dropped significantly from 85.5 months to 28.2 months. Similar phenomena were seen when the M1/M2 macrophage ratio was used. This was only significant with PFS but not OS. PFS is suggestive of the tumor biology and is a key determining factor for tumor recurrence and chemoresistance. Although this cohort is a mix of different histologies and difficult to stratify the biologic effects for each subtype due to sample size, the observed findings are intriguing and worth investigating further.

Establishing reliable diagnostic and prognostic factors in cancer, especially OVCA, is key to improving the overall survival of patients. In both uni- and multivariate analysis, epithelial pGSN and residual disease (RD) emerged as independent predictors – amongst all prognostic factors investigated – associated with progression-free survival. Although there was no significant correlation between epithelial and stromal expression of pGSN, epithelial pGSN

expression increased with stage and residual disease **(Supplementary Fig. 7A-C)**. Therefore, it is not surprising that epithelial pGSN was found to be an independent prognostic marker, together with RD. This observation is consistent with our previous study where pre-operative circulating pGSN presented as a less-invasive marker for predicting residual disease and indicating stage 1 OVCA (26). Thus, we were further motivated to investigate the inhibitory role of pGSN in M1 macrophages *in vitro*.

Chemoresistant OVCA cells secrete increased levels of pGSN that are transported via sEVs (19). sEVs containing pGSN auto-regulates its gene and in a paracrine manner confers cisplatin resistance to otherwise chemosensitive cells (19). We therefore hypothesized that exosomal pGSN modulates the pro-inflammatory environment in the ovarian TME in part by down-regulating M1 macrophage viability and function, an effect that lowers the M1/M2 ratios associated with a shortening patient survival. Upon investigation, we demonstrated that chemoresistant cells-derived sEVs compared with their sensitive counterparts induced M1 macrophage death via caspase-3 activation, phenomena associated with a secondary suppression of iNOS and TNFα production. Silencing the pGSN gene in chemoresistant OVCA cells resulted in attenuation of M1 macrophage caspase-3 activation, apoptosis and the elevated productions of iNOS and TNFα. These responses were the opposite when pGSN was overexpressed in chemosensitive cells. These observations support our hypothesis and are also consistent with other studies where exosomal pGSN suppresses the anti-tumor functions of immune cells such as CD8+ T cells and natural killer T cells (22, 43). To the best of our knowledge, this is the first study to demonstrate the inhibitory role of pGSN on M1 macrophage viability and function in the ovarian TME. The possibility that pGSN may also alter the phenotype of TAMs is worth considering in future studies.

Although the precise cellular mechanism by which pGSN promote chemoresistance in OVCA remains unclear, that pGSN modulates the inflammatory microenvironment by reducing the viability of M1 macrophages in the cancer islet could provide part of the explanation. Although the functional relationship between pGSN-induced M1 tumour infiltration and apoptotic response is unclear, the possibility that pGSN induces migration of macrophages into the tumour nest to better facilitate its pro-apoptotic function, remains to be determined. Our findings are also consistent with other studies where recombinant human pGSN reduced inflammatory cytokines such as iNOS, TNFα and IL-6 in LPS-stimulated human keratinocytes (44), RAW264.7 (45), peritoneal macrophages (45) and THP-1 cells (45) as well as carrageenan-induced paw edema in mice (46). We would predict based on our results that combining pGSN inhibitors with other immune checkpoint blockers, such as anti-PD-1 and anti-PDL1 will significantly inhibit tumor growth and unleash the anti-tumor properties of CD8+ T cells, NK cells and M1 macrophages. This will provide a broad anti-tumor approach and could enhance patient survival.

In conclusion, we have demonstrated for the first time that increased pGSN modulates the pro-inflammatory environment in the ovarian TME, favouring chemoresistance and poor patient survival. In patients with low pGSN expression, the M1/M2 ratio was elevated, which predicts improved survival and chemoresponsiveness **(Fig. 5A)**. In patients with high pGSN expression, M1 macrophages are selectively attracted into the cancer islet and their viability reduced without affecting the viability of M2 macrophages. Thus, the M1/M2 ratio is significantly decreased and favors poor survival and chemoresistance **(Fig. 5B)**.

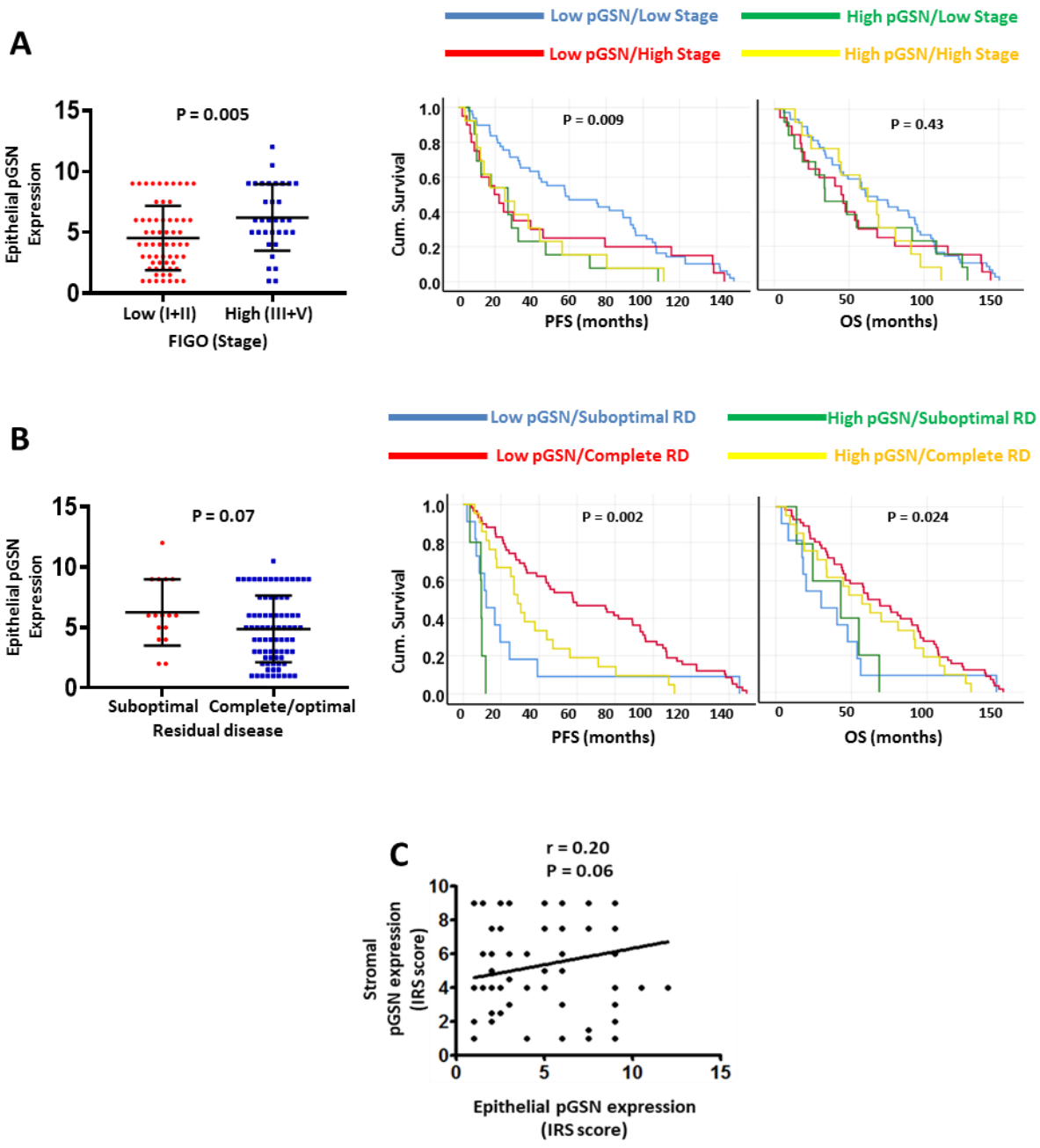
A
Low pGSN/Low Stage
High pGSN/Low Stage
Low pGSN/High Stage
High pGSN/High Stage
P = 0.005
Epithelial pGSN Expression
Low (I+II)
High (III+V)
FIGO (Stage)
P = 0.009
P = 0.43
Cum. Survival
PFS (months)
OS (months)
B
Low pGSN/Suboptimal RD
High pGSN/Suboptimal RD
Low pGSN/Complete RD
High pGSN/Complete RD
P = 0.07
Suboptimal
Complete/optimal
Residual disease
P = 0.002
P = 0.024
C
r = 0.20
P = 0.06
Stromal pGSN expression (IRS score)
Epithelial pGSN expression (IRS score)

Sup. Fig. 5.S7 Epithelial pGSN expression increases with increased tumor stage and suboptimal residual disease. (A) Epithelial pGSN expression was compared between patients with low (n=62) and high (n=32) stage. Patients were stratified using epithelial pGSN and tumor stage. **(B)** Epithelial pGSN expression was compared between patients with complete/optimal (n=79) and suboptimal (n=15) RD. P values was calculated using independent sample t test. Patients were stratified using epithelial pGSN and residual disease. pGSN (cut-off = 6) in combination with tumor stage and residual disease were correlated with PFS and OS. Kaplan Meier survival curves with cutoff values and log rank test were used to compare the survival distributions between the groups. **(C)** Epithelial pGSN was correlated with stromal pGSN expression using Pearson's analysis. n = number of patients in each group.

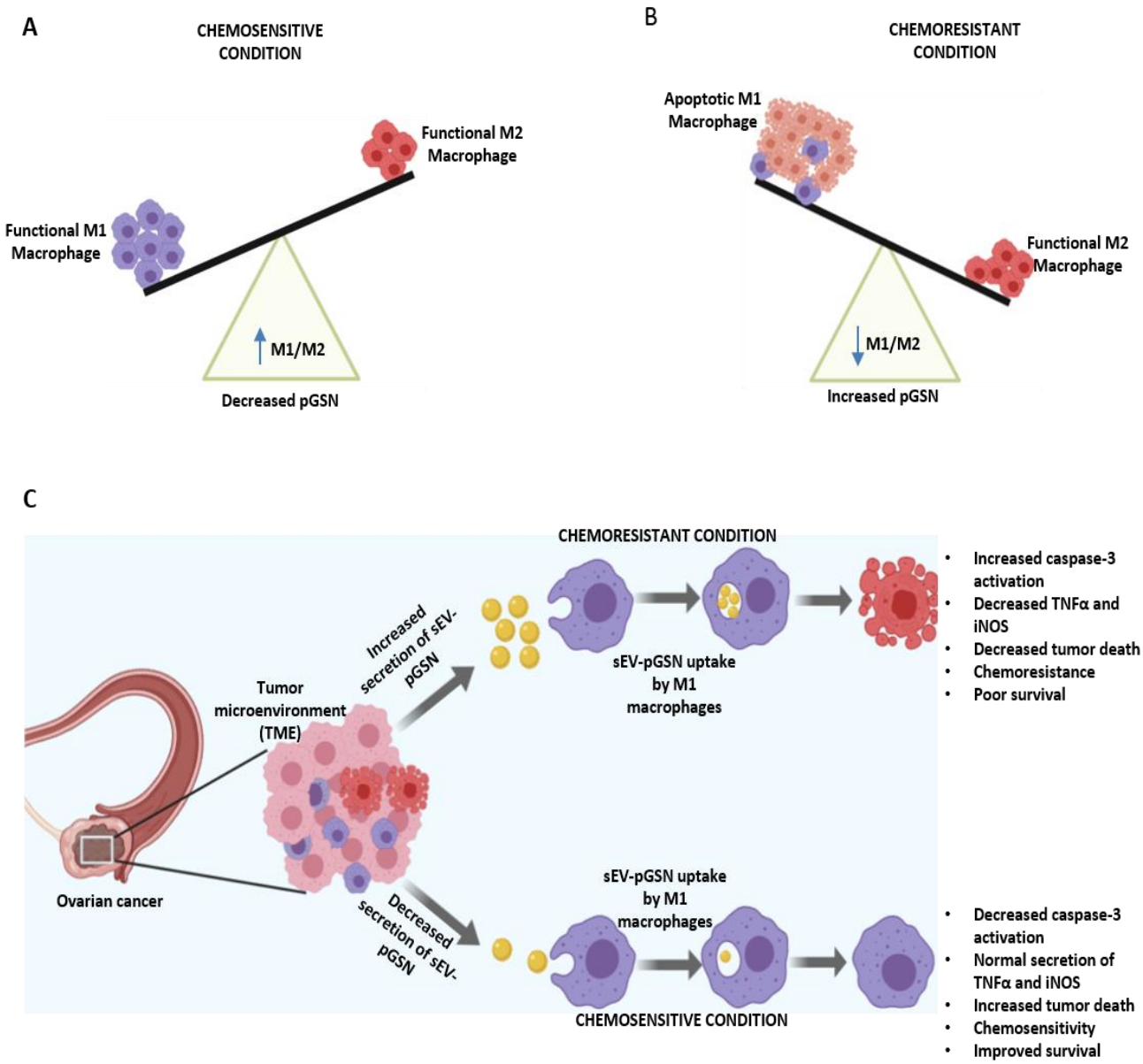
A
CHEMOSENSITIVE CONDITION
Functional M2 Macrophage
Functional M1 Macrophage
M1/M2
Decreased pGSN
B
CHEMORESISTANT CONDITION
Apoptotic M1 Macrophage
Functional M2 Macrophage
M1/M2
Increased pGSN
C
CHEMORESISTANT CONDITION
Increased secretion of sEV-pGSN
sEV-pGSN uptake by M1 macrophages
Tumor microenvironment (TME)
Ovarian cancer
Decreased secretion of sEV-pGSN
sEV-pGSN uptake by M1 macrophages
CHEMOSENSITIVE CONDITION
• Increased caspase-3 activation
• Decreased TNFα and iNOS
• Decreased tumor death
• Chemoresistance
• Poor survival
• Decreased caspase-3 activation
• Normal secretion of TNFα and iNOS
• Increased tumor death
• Chemosensitivity
• Improved survival

Figure 5.5 Hypothetical model illustrating the role of sEV-pGSN in modulating pro-inflammatory environment in OVCA chemoresistance. (A) In chemosensitive condition, there is an increase in M1/M2 ratio due to decreased pGSN expression. **(B)** In chemoresistant condition, M1 macrophages are selectively attracted into the cancer islet and executed without affecting the viability of M2 macrophages. Thus, the M1/M2 ratio is significantly decreased and favors poor survival. **(C)** In chemosensitive condition, OVCA cells secrete decreased levels of sEV containing pGSN which have minimal suppression on M1 macrophages. In chemoresistant condition, OVCA cells secrete higher levels of sEV containing pGSN which suppress the anti-tumor functions of M1 macrophages by i) inducing apoptosis and ii) decreasing TNFα and iNOS production. *Diagram designed using biorender*.

Specifically, in the chemosensitive condition, OVCA cells secrete decreased levels of sEV containing pGSN, rendering them incapable of inhibiting the anti-tumor functions of M1 macrophages (**Fig. 5C**). However, in the chemoresistant condition, OVCA cells secrete increased levels of sEV containing that are taken up by M1 macrophages (**Fig. 5C**). Upon uptake, pGSN is released and activates caspase-3, resulting in apoptosis. This is also associated with a secondary response where TNFα and iNOS productions are significantly reduced (**Fig. 5C**). These cumulative effects render infiltrated M1 macrophages non-functional and unable to kill tumor cells. While these findings are novel and are of clinical relevance, we also acknowledge the unusual patient distribution and small population of patients recruited making it difficult to analyse the biologic effects of each subtype. Thus, future studies that address the above-mentioned concerns will provide further validation of our observations and extend the applicability of the current study.

Acknowledgement:

The authors acknowledge Yuko Fujita (Department of Obstetrics and Gynecology, University of Fukui, Fukui, Japan) for her expert technical assistance on IHC. This work was supported by the Canadian Institutes of Health Research (PJT-168949), Mitacs Globalink Research Award, The Canada Foundation for Innovation (34468) and Grants-in-Aid for scientific research from the Japan Society for the Promotion of Science (18H02944). Tumor banking was supported by the Fukui Hospital, Japan. A.M.M.M is a researcher of the CRHUM who receives support from the FRQS. The funding agencies were not involved in the design, conduct, analysis or interpretation of the study.

CHAPTER 6 – SCIENTIFIC REPORTS 9, 13924 (2019)

(Formatted as per Scientific Reports requirements)

Pre-operative Circulating Plasma Gelsolin Predicts Residual Disease and Detects Early Stage Ovarian Cancer

Meshach Asare-Werehene[a,c], Laudine Communal[d], Euridice Carmona[d], Tien Le[e], Diane Provencher[d,f], Anne-Marie Mes-Masson[d,g], and *Benjamin K. Tsang[a,b,c]

[a]Departments of Obstetrics & Gynecology and Cellular & Molecular Medicine, University of Ottawa, Ottawa, Ontario, Canada, K1H 8L1;

[b]State Key Laboratory of Quality Research in Chinese Medicine, Macau Institute for Applied Research in Medicine and Health, Macau University of Science and Technology, Avenida Wai Long, Taipa, Macao, China;

[c]Chronic Disease Program, Ottawa Hospital Research Institute, Ottawa, Ontario, Canada K1H 8L6

[d]Centre de recherche du CHUM et Institut du cancer de Montréal, Montréal, Québec, Canada H2X 0A9

[e]Division of Gynecologic Oncology, Department of Obstetrics and Gynecology, University of Ottawa, Ottawa, Ontario Canada K1H 8L6

[f]Division of Gynecologic Oncology, Department of Obstetrics and Gynecology, Université de

Montréal, Montréal, Québec, Canada H3C 3J7

[g]Department of Medicine, Université de Montréal, Montréal, Québec, Canada H3C 3J7

***Correspondence:** Dr. Benjamin K Tsang, Chronic Disease Program, Ottawa Hospital Research Institute, The Ottawa Hospital (General Campus), Ottawa, Canada K1H 8L6;

Tel: 1-613-798-5555 ext 72926; Email: btsang@ohri.ca

Author Contributions: M.A.W. and B.K.T. conceived and designed the study. M.A.W. performed the ELISA assay. L.C., E.C. D.P. and A.M.M.M. collected the clinical data related to the samples, determined the sample selection criteria and matching scheme, and provided the clinical samples. M.A.W. analysed the data with scientific input from B.K.T., A.M.M.M., E.C. L.C. and T.L. M.A.W. wrote the paper with feedback from all authors.

Conflict of Interest Statement: The authors have declared no conflicts of interest.

ABSTRACT

Ovarian cancer (OVCA) patients with suboptimal residual disease and advanced stages have poor survival. pGSN is an actin binding protein which protects OVCA cells from cisplatin-induced death. There is an urgent need to discover reliable biomarkers to optimize individualized treatment recommendations. 99 plasma samples with pre-determined CA125 were collected from OVCA patients and pGSN assayed using sandwich-based ELISA. Associations between CA125, pGSN and clinicopathological parameters were examined using Fisher exact test, T test and Kruskal Wallis Test. Univariate and multivariate Cox proportional hazard models were used to statistically analyze clinical outcomes. At 64 µg/ml, pGSN had sensitivity and specificity of 60% and 60% respectively, for the prediction of residual disease where as that of CA125 at 576.5 U/mL was 43.5% and 56.5% respectively. Patients with stage 1 tumor had increased levels of pre-operative pGSN compared to those with tumor stage >1 and healthy subjects (P=0.005). At the value of 81 µg/mL, pGSN had a sensitivity and specificity of 75% and 78.4%, respectively for the detection of early stage OVCA. At the value of 0.133, the Indicator of Stage 1 OVCA (ISO1) provided a sensitivity of 100% at a specificity of 67% (AUC, 0.89; P<0.001). In the multivariate Cox regression analysis, pGSN (HR, 2.00; CI, 0.99 – 4.05; P=0.05) was an independent significant predictor of progression free survival (PFS) but not CA125 (HR, 0.68; CI, 0.41 – 1.13; P=0.13). Pre-operative circulating pGSN is a favorable and independent biomarker for early disease detection, residual disease prediction and patients' prognosis.

KEY WORDS: Plasma gelsolin, ovarian cancer, residual disease, early stage, CA125, biomarker

Introduction:

Ovarian cancer (OVCA) causes more death than any gynecological cancer as a result of late presentation, frequent recurrences and ultimately chemoresistance development[1]. It is estimated that around 70% of OVCA patients are diagnosed with late stage of the disease, resulting in 5-year survival rate of ~45% due predominantly to no specific signs and symptoms in the early disease phase[2-4]. This is even more challenging in high grade serous (HGS) OVCA patients who have the worst survival outcomes compared to other histologic subtypes[2-4]. Despite considerable efforts to screen for OVCA, minimal progress has been made to date[5,6]. Although CA-125 and other circulating markers (such as CA-153, LPA, prostasin, HE4, osteopontin, kallikreins, bikunin and VEGF) have been studied, little diagnostic success has been achieved [7]. In order to improve the pre-operative diagnosis of early OVCA and recurrence, multivariate index assays (ROMA[8], Overa[9] and Ova 1[10]) have been developed. These assays are modestly helpful, although their significance is mostly realised in OVCA surveillance and treatment monitoring. Plasma nucleic acids, including miR-21, miR-141, miR-214, let-7b, have shown promise; however, further validation studies are needed[11-13].

CA-125 is elevated in only ~40% of early-stage OVCA patients but more frequently elevated in advanced stages, thus making it an unsuitable candidate for early detection of the disease[5,6]. Regardless, CA125 and trans-vaginal ultrasound are widely used as screening tests for OVCA[11,14]. There are urgent needs for novel cost-effective diagnostic markers to better diagnose and manage OVCA patients. Another prognostic factor that reflects the survival of OVCA patients is the amount of residual disease after surgery[15-17]. Currently, there is no established marker to reliably predict residual disease pre-operatively[7]. Serum CA-125 remains a widely

used marker to screen for post-treatment tumor progression[18]. However, CA-125 is less sensitive and not specific in the detection of early stage disease[11,19-21].

pGSN is an actin binding protein and is present in the human plasma[22-25]. We have previously demonstrated that the over-expression of gelsolin protects ovarian cancer cells against cisplatin-induced death and could be a potential target for treatment[26]. pGSN has also been implicated in pathological disease conditions such as prostate cancer, breast cancer, sepsis, arthritis, microbial infections, hemodialysis and other inflammatory disorders[22,27-31]. Although pGSN is highly secreted in OVCA cells, its role in patients' plasma has not been investigated yet. Our previous observation of the possible involvement of pGSN in chemoresistance in OVCA has prompted us to investigate its importance in the plasma of OVCA patients. In this study, we determined if pre-operative circulating pGSN is a better indicator of early stage OVCA and predictor of residual disease compared to CA125.

Results:

Characteristics of patients

The validity of tumor stage was performed by certified Gynecologic-Oncology team. Clinicopathologic characteristics of the ovarian cancer patients are represented in Supplementary Table S1. Patients are classified as FIGO stages 1 (*N*=10), 2 (*N*=11), 3 (*N*=67) and 4 (*N*=11). No neoadjuvant chemotherapy or radiotherapy was used. The age of the patients ranged from 36 – 82 years and was dichotomized by their median into ≤61 (*N*=51) and >61 (*N*=48). Optimal cytoreduction was achieved in 50 patients in the cohort. CA125 and pGSN levels were measured and dichotomized by their medians (576.5 U/mL and 79 µg/mL) into low and high groups respectively.

An elevated level of pre-operative circulating pGSN is highly associated with increased residual disease.

Residual disease is a well validated predictor of patient prognosis and survival [15,16,32]; however, there is no test to reliably predict complete, optimal or suboptimal cytoreduction preoperatively[7]. Using a Kaplan Meier survival analysis, our patients with ≤1 cm residual disease had better DFS (**Fig. 1a**; *P*=0.0001; *N*=92; median DFS, 28 months) and OS (**Fig. 1b**; *P*=0.01; *N*=92; median OS, 58 months) compared with the >1 cm group (median DFS, 14 months; median OS, 42 months). Also, using box plots, we compared the means of CA125 and pGSN in both residual disease groups and statistical significance calculated by independent sample *t*-test. Although no significant difference was observed in the levels of CA125 between both groups (**Fig. 1c**; *P*=ns; *N*=92), patients with suboptimal surgical debulking had increased levels of preoperative pGSN compared with the optimal cytoreduction group (**Fig. 1d**; *P*=0.005; *N*=92). This phenomenon was also observed when heat maps were used to stratify the means of pGSN and CA125 levels against residual disease **(Fig. 1e and f)**. In **Supplementary Table S2**, levels of pGSN and CA125 were correlated with residual disease using the Pearson's correlation test. There was a significant positive correlation between pGSN and residual disease (R=0.29, *P*<0.01, *N*=92); however, no significant correlation was observed with CA125 (R=-0.01, *P*=0.91, *N*=92).

Supplementary Table 6.1 Characteristics of patients

Variable	Number of Patients
Age (Range; 36 – 82 years)	
≤61	51
>61	48
Stage (FIGO)	
1	10
2	11
3	67
4	11
Stage (FIGO)	
≤2	21
>2	78
Histological Subtypes	
Not verified	26
High Grade Serous (HGS)	69
Low Grade Serous (LGS)	4
Residual disease (RD)	
≤1 cm	50
>1 cm	42
CA-125 (U/ml)[a]	
Low (≤576.5)	49
High (>576.5)	50
pGSN (µg/ml)[a]	
Low (≤79)	70
High (>79)	29
pGSN (µg/ml)[a]	
Not verified	25
HGS	70
LGS	4
Healthy Subjects	32

[a]Median cut-off value. CA-125, cancer antigen 125; pGSN, plasma gelsolin; FIGO, International Federation of Gynecology and Obstetrics.

a

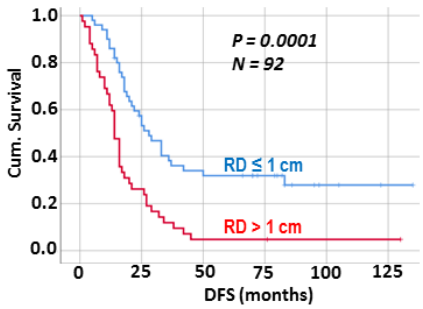

Residual Disease	Median DFS (months)
RD ≤ 1 cm	28
RD > 1 cm	14

b

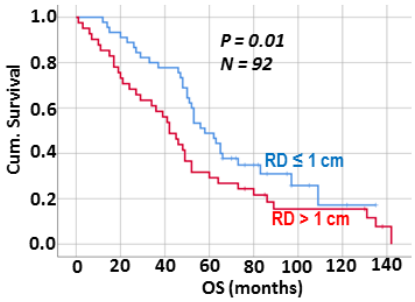

Residual Disease	Median OS (months)
RD ≤ 1 cm	58
RD > 1 cm	42

c

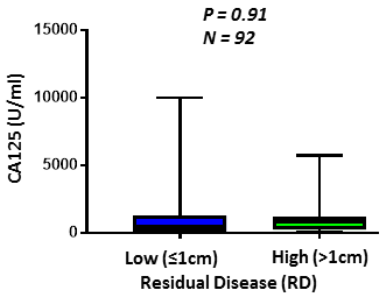

d

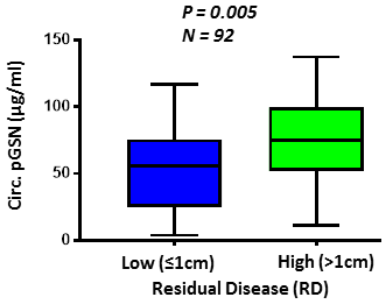

e

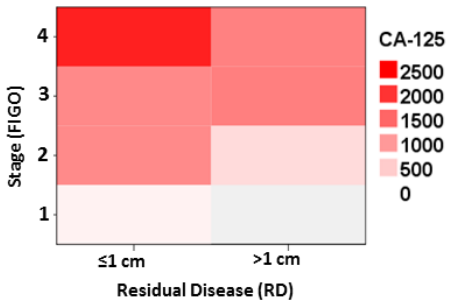

f

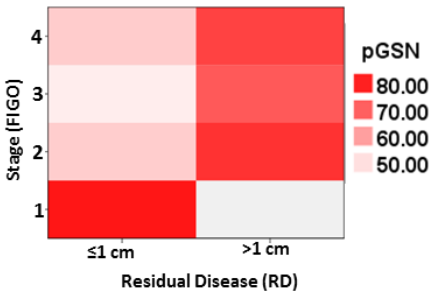

Fig. 6.1 Ovarian cancer patients with high residual disease (RD) have significantly high levels of circulating pGSN. (a and b) Kaplan Meier survival analysis stratified by RD (≤ 1 cm or > 1 cm). Patients with RD ≤ 1 cm have better DFS **(a)** and OS **(b)** compared with those with RD > 1 cm. P-values were calculated by the log-rank test. Distribution of CA-125 **(c)** and pGSN **(d)** in patients with low RD (≤ 1 cm) and high RD (> 1 cm) by bar charts. Although there was no significant difference with CA-125, high RD patients have significantly higher levels of pGSN compared with the low RD patients. Heat map was used to stratify the levels of CA-125 **(e)** and pGSN **(f)** against residual disease and stage. *P*-values were calculated by independent sample *t*-test.

Supplementary Table 6.2 Correlation between plasma pGSN and CA-125 levels and ovarian cancer residual disease and stage.

		CA-125 (U/ml)	pGSN (µg/ml)
Residual disease (RD)	R[a]	-0.01	0.29
	Sig. (2-tailed)	0.91	<0.01
	N[b]	92	92
Stage (FIGO)	R[a]	0.22	-0.20
	Sig. (2-tailed)	0.04	0.05
	N[b]	99	99

[a]Pearson's correlation, [b]Number of patients.

CA-125, cancer antigen 125; pGSN, plasma gelsolin; FIGO, International Federation of Gynecology and Obstetrics.

A pre-operative plasma level of pGSN is a better predictive marker for residual disease.

To assess the performance of pGSN as a predictor of residual disease in ovarian cancer patients as compared with CA125, we generated receiving operating characteristic (ROC) curves. The approximate area under the curve (AUC) derived from the ROC curve was used to assess the diagnostic performances of pGSN and CA125. The AUC of pGSN to predict suboptimal residual disease was 0.65 (*P*=0.03) where as that of CA125 was 0.54 (*P*=0.30) **(Fig. 2)**. At the value of 64 µg/ml (optimal cut-off using Fisher's exact test), pGSN has a sensitivity and specificity of 60% and 60% respectively, for the prediction of residual disease. CA125 value at 576.5 U/mL (optimal cut-off using Fisher's exact test) has a sensitivity and specificity of 43.5% and 56.5% respectively, in predicting suboptimal residual disease **(Supplementary Table S3)**.

A pre-operative plasma level of pGSN is a significantly sensitive diagnostic tool for early stage ovarian cancer.

Patients were classified into two groups based on their tumor stage (FIGO; ≤2 and >2) and their survival were assessed using Kaplan Meier survival analysis **(Fig. 3a and b)**. Patients with tumor stage ≤2 had better DFS (*P*=0.0001; *N*=96; median DFS, 83 months) and OS (*P*=0.009; *N*=96; median OS, 97 months) compared with their counterparts with >2 tumor stage (**Fig. 3a and b**; median DFS, 17 months; median OS, 49 months). Using box plots, we compared the means of CA-125 and pGSN from patients in all 4 tumor stages (FIGO; 1, 2, 3 and 4). While an increase in CA125 concentration was observed with increase in stage, this difference was not statistically significant (**Fig. 3c**; *P*=0.22; *N*=99). Patients who are more than 61 years old have decreased levels of CA125 compared with those below 61 years (**Fig. 3d**; *P*=0.042; *N*=99).

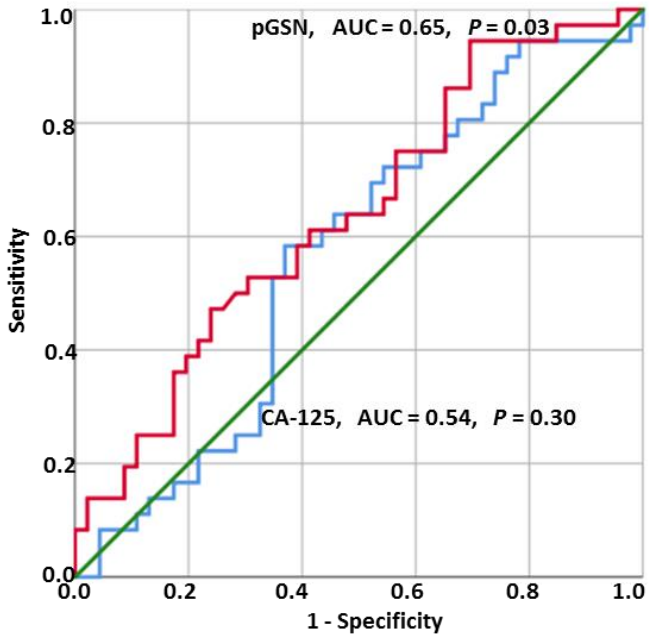

Fig. 6.2 Receiving operating characteristic (ROC) curves for pGSN and CA-125 in detection of residual disease (RD) in ovarian cancer patients. pGSN cutoff (64 µg/mL; sensitivity, 60%; specificity, 60%). CA125 cutoff (576.5 U/mL; sensitivity, 43.5%; specificity, 56.5%). CA-125 vs RD, *P*=0.30; pGSN vs RD, *P*=0.03.

Supplementary Table 6.3 The sensitivities and specificities of OVCA plasma biomarkers.

Biomarkers	Sensitivity (%)	Specificity (%)	AUC^
Stage 1 OVCA			
CA125	0	44.9	0.125
pGSN	75	78.4	0.724
ISO1* Index (pGSN/CA125)	100	67	0.89
Residual disease			
CA125	43.5	56.5	0.54
Pgsn	60	60	0.65
Late Stage (3 and 4)			
CA125	55.1	100	0.875
pGSN	21.6	0	0.276

OVCA, ovarian cancer; CA125, cancer antigen 125; pGSN, plasma gelsolin. *Indicator of Stage 1 OVCA. ^Area under the curve

pGSN levels were significantly higher in malignant patients (OVCA; *N*=99) compared with healthy subjects (*N*=32) without cancer (**Fig. 3e**; *P*=0.0001). Patients with stage 1 tumor had abundant levels of preoperative pGSN compared to patients with tumor stage >1 and the healthy subjects (**Fig. 3f**; *P*=0.005). Age had no significant effect on the levels of pGSN in OVCA patients (**Fig. 3g**; *P*=0.417; *N*=99). The means of pGSN and CA-125 levels were stratified against tumor stage using heat maps **(Fig. 1e and f)**.

We further tested how reliable pGSN could be used as an early diagnostic tool for ovarian cancer compared with CA-125. Using ROC curves, we derived AUC to assess the diagnostic performances of both markers. The AUC of pGSN to detect early stage ovarian cancer was 0.724 (*P*=0.04) where as that of CA-125 was 0.125 (*P*=0.001) **(Fig. 4a)**. At the value of 81 µg/mL (optimal cut-off using Fisher's exact test), pGSN had a sensitivity and specificity of 75% and 78.4%, respectively for the detection of early stage ovarian cancer **(Supplementary Table S3)**. Compared with pGSN (AUC, 0.276; *P*=0.04), CA-125 was a better marker for late stage ovarian cancer detection with an AUC of 0.875 (*P*=0.001) **(Fig. 4a)**. At the value of 576.5 U/mL (optimal cut-off using Fisher's exact test), CA-125 had a sensitivity and specificity of 55.1% and 100% respectively **(Supplementary Table S3)**, in detecting late stage ovarian cancer.

Combining pGSN and CA125 in a multivariate index assay provides 100% sensitivity detection for stage 1 OVCA.

To further increase the diagnostic accuracy of early stage OVCA, the pre-operative levels of pGSN and CA125 were combined in a multianalyte index assay. A formula, Indicator of Stage 1 OVCA (ISO1) index, was derived from the values of CA125 and pGSN after which the resulting values were used in a ROC curve analysis **(Fig. 4b)**. At the value of 0.133 (optimal cut-

off using Fisher's exact test), ISO1 provided a sensitivity of 100% at a specificity of 67% (AUC, 0.89; *P*<0.001) **(Fig 4b; Supplementary Table S3)**. The ISO1 index was derived as below:

ISO1 index = P / C,

Where P = pGSN (µg/mL), C = CA125 (U/mL) and ISO1 = Indicator of Stage 1 OVCA

Prognostic impact of pre-operative circulating pGSN and relationship with other clinicopathologic parameter.

We further evaluated the prognostic impact of pGSN, CA125 and other clinicopathological parameters using uni- and multivariate Cox regression analyses as shown in **Supplementary Tables S4 and S5**, respectively. Median cut-offs for pGSN and CA125 were used to predict DFS and OS. From the univariate analysis **(Supplementary Table S4)**, FIGO stage, residual disease, CA125 and pGSN showed a significant association with DFS and OS. In the multivariate Cox regression analysis **(Supplementary Table S5)**, pGSN (HR, 2.00; CI, 0.99 – 4.05; *P*=0.05) and optimal residual disease (HR, 0.39; CI, 0.23 – 0.68; *P*<0.01) were found to be significant predictors of DFS but not CA125 (HR, 0.68; CI, 0.41 – 1.13; *P*=0.13). Regarding overall survival, age (HR, 0.47; CI, 0.28 – 0.81; *P* = 0.01), residual disease (HR, 0.51; CI, 0.29 – 0.91; *P*=0.02) and CA125 (HR, 0.47; CI, 0.27 – 0.82; *P*=0.01) were found to be significantly associated with an increased risk for death.

a

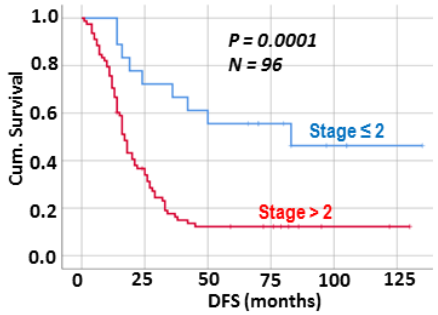

Stage (FIGO)	Median DFS (months)
Stage ≤ 2	83
Stage > 2	17

b

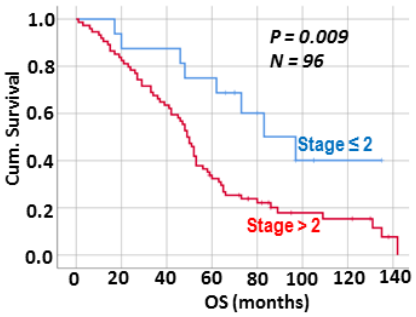

Stage (FIGO)	Median OS (months)
Stage ≤ 2	97
Stage > 2	49

c

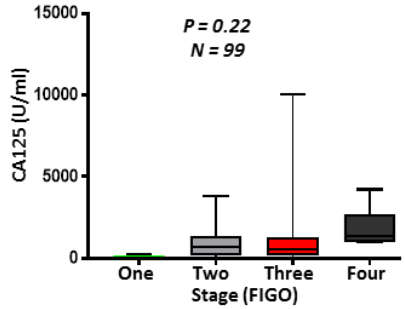

d

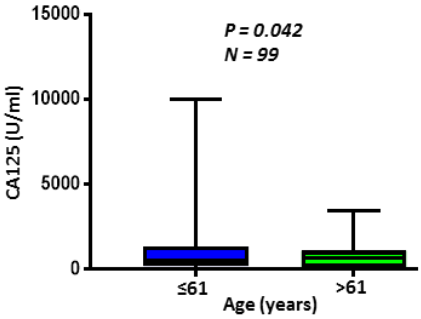

e

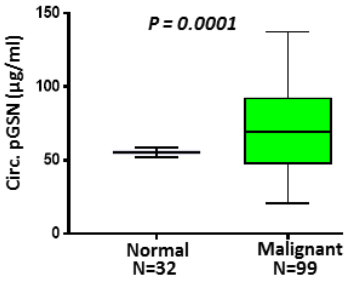

g

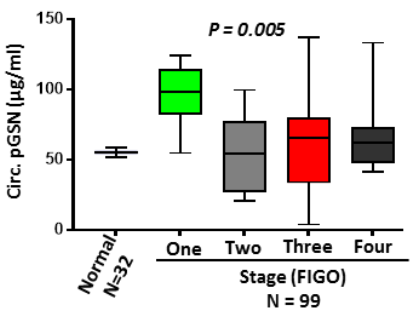

f

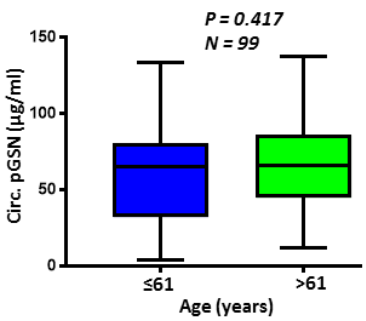

Fig. 6.3 Circulating pGSN is highly detected in ovarian cancer patients with stage 1 disease. **(a and b)** Kaplan Meier survival analysis stratified by Stage showed that patients with stage ≤ 2 have better DFS **(a)** and OS **(b)** compared with those with stage > 2. *P*-values were calculated by the log-rank test. Distribution of CA-125 **(c and d)** and pGSN **(e, f and g)** in patients stratified by stage and age using box plots. *P*-values were calculated by one-way ANOVA and independent sample *t*-test.

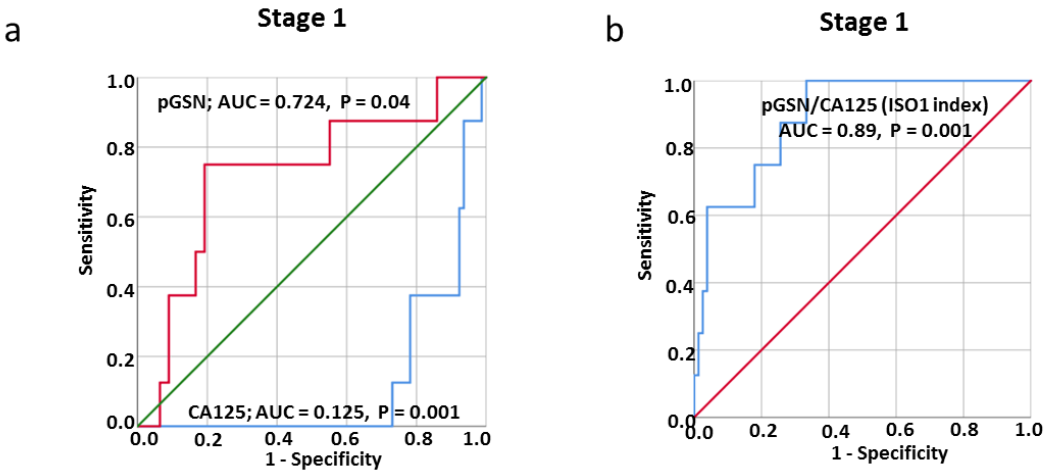

Fig. 6.4 Receiving operating characteristic (ROC) curves for pGSN, CA125 and ISO1 index in the detection of stage 1 disease in ovarian cancer patients. a) pGSN cutoff (81.09 µg/mL; sensitivity, 75%; specificity, 78.4%). **b)** ISO1 index cutoff (0.133; sensitivity, 100%; specificity, 67%). CA-125 vs stage 1, *P* = 0.001; pGSN vs stage 1, *P* = 0.04; ISO1 index vs stage 1, *P* < 0.001.

Supplementary Table 6.4 Univariate Cox regression analysis for disease-free and overall survival

	Univariate					
Variable	**DFS**			**OS**		
	HR*	**95% CI^**	***P*-value**	**HR***	**95% CI^**	***P*-value**
Age (years)						
≤61 vs >61	0.91	0.58 – 1.43	0.68	0.66	0.41 – 1.07	0.91
Stage (FIGO)						
≤2 vs >2	0.30	0.15 – 0.60	<0.01	0.39	0.19 – 0.82	0.01
Stage						
1 vs >1	0.15	0.04 – 0.60	<0.01	0.23	0.06 – 0.93	0.04
RD (cm)						
≤1 vs >1	0.31	0.19 – 0.53	<0.01	1.54	1.13 – 2.10	<0.01
CA-125						
Low vs high	0.59	0.36 – 0.97	0.04	0.48	0.28 – 0.80	0.01
pGSN						
Low vs high	1.81	1.05 – 3.12	0.03	1.94	1.08 – 3.48	0.03

HR, hazard ratio; DFS, disease free survival; OS, overall survival; CI, confidence interval; RD, residual disease; CA-125, cancer antigen 125; pGSN, plasma gelsolin; FIGO, International Federation of Gynecology and Obstetrics; vs, versus.

*Estimated from Cox proportional hazard regression model.

^Confidence interval of the estimated HR.

SupplementaryTable 6.5 Multivariate Cox regression analysis for disease-free and overall survival

	Multivariate Analysis					
Variable	**DFS**			**OS**		
	HR*	**95% CI^**	***P*-value**	**HR***	**95% CI^**	***P*-value**
Age (years) **≤61 vs >61**	0.76	0.47 – 1.25	0.29	0.50	0.29 – 0.86	0.01
Stage (FIGO) **≤2 vs >2**	0.63	0.27 – 1.47	0.29	0.63	0.25 – 1.57	0.32
Stage **1 vs >1**	0.40	0.08 – 2.00	0.27	0.78	0.15 – 4.04	0.76
RD (cm) **≤1 vs >1**	0.40	0.23 – 0.68	<0.01	0.51	0.28 – 0.91	0.02
CA-125 **Low vs high**	0.68	0.41 – 1.13	0.13	0.47	0.27 – 0.82	0.01
pGSN **Low vs high**	2.00	0.99 – 4.05	0.05	2.10	0.94 – 4.33	0.07

HR, hazard ratio; DFS, disease free survival; OS, overall survival; CI, confidence interval; RD, residual disease; CA-125, cancer antigen 125; pGSN, plasma gelsolin; FIGO, International Federation of Gynecology and Obstetrics; vs, versus.

*Estimated from Cox proportional hazard regression model.

^Confidence interval of the estimated HR.

Discussion

In this present study, we have demonstrated for the first time that pGSN is a better diagnostic tool for the detection of early stage ovarian cancer and prediction of suboptimal cytoreduction than the commonly used CA125. The overall sensitivity and specificity of pGSN were higher than those of CA125 in the detection of early stage OVCA. This was the same for predicting optimal residual disease status. The detection sensitivity for early stage OVCA was further enhanced by 35% when pGSN was combined with CA125 in a multianalyte assay analysis. CA125 however, showed a very high sensitivity and specificity for the detection of late stage ovarian cancer. These findings support our hypothesis that circulating pGSN is a novel marker for early stage OVCA detection and optimal residual disease prediction.

Although much efforts are made to early detect ovarian cancer, there is no reliable and validated circulating biomarker established[7]. Despite CA125 being used as a serum marker to detect early ovarian cancer and monitor the clinical course of these patients, its low sensitivity presents as the greatest obstacle for its use to improve patients prognosis[7,33]. In our current study, we have demonstrated that pre-operative circulating pGSN is a better diagnostic tool than CA125 to detect early stage ovarian cancers. Unlike CA125, circulating pGSN levels were not affected by age hence presents as a reliable marker for diagnosis. The overall early stage detection accuracy (sensitivity; 75% and specificity; 78.4%) of pGSN was higher than that of CA125. These findings are consistent with others who have similarly shown that CA125 has a lower sensitivity in detecting early stage ovarian cancer[34]. Although CA125 is frequently used in the clinical workup of a suspicious mass for OVCA, ~40% of all OVCA patients express little to no serum CA125 abnormalities in the early stages. This in addition to the absence of overt clinical significant symptoms leaves >70% of OVCA patients being diagnosed at the late stages of the

disease[19,35,36]. Unlike CA125, circulating pGSN was significantly elevated in early stage OVCA patients compared with the late stage disease. The positive and significant correlation between pGSN levels and stage 1 OVCA could be exploited to early diagnose patients and improve their overall survival. Given the heterogeneous nature of the OVCA tumor microenvironment and the relatively smaller HGS patients involved in this study, it is worth validating these findings in larger HGS OVCA cohorts as well as extend to other histologic subtypes such as endometrioid and clear cell carcinoma.

We also have shown the combination of pGSN and CA125 in a multivariate index assay to detect early stage OVCA provided a much higher sensitivity and specificity than individual markers. Using the IS1O formula, 100 % sensitivity was achieved in the detection of early stage OVCA. The IS1O formula derived from the pre-operative levels of pGSN and CA125 outperformed FDA approved OVCA multiplex assays such as ROMA (sensitivity; 89%)[33,36] and Overa (sensitivity; 91%)[9]**.** Ova1 is the most recent multivariate index assay to be approved by FDA and entails two upregulated markers (CA125II, β-microglobulin) and 3 downregulated markers (apolipoprotein A1, prealbumin, transferrin) incorporated on the same detection panel [10,33]. At a specificity of 54%, Ova1 has a sensitivity of 94%[10]; a diagnostic accuracy that is below the performance of the ISO1 index. We hypothesize that the usage of the ISO1 index in combination with trans-vaginal ultrasound will further provide additional diagnostic significance to early detect OVCA patients; an intervention that will improve patient survival.

Residual disease is considered one of the most important prognostic factors for survival in OVCA patients; however, there is no established reliable marker to predict suboptimal cytoreduction preoperatively[15,16,32]. Although CA125 and other circulating proteins have shown promise as predictors of residual disease, their overall accuracy and reliability is still

questionable. In this respect, there is an urgent need to identify novel predictive markers to predict residual disease; an effort that could improve clinical strategies and outcome in OVCA patients. In this study, we have observed for the first time that pre-operative circulating pGSN outperforms CA125 in predicting optimal residual disease. The sensitivity and specificity of pGSN were significantly higher compared to that of CA125; thus, presenting as a better predictor of residual disease. In addition to CA125, pre-operative pGSN has a higher accuracy rate to predict residual disease compared to other circulating markers[12,14,18-20]. This could provide significant information for counselling patients regarding surgical outcomes, influencing major decisions regarding primary cytoreduction versus neoadjuvant approach as well as explore other treatment options. In the future, it is worthwhile investigating if circulating pGSN will decline after post-cytoreduction. This could be used to determine perioperative changes in circulating pGSN in order to predict disease-specific survival of OVCA patients.

Establishing reliable prognostic factors in ovarian cancer is key to improving the overall management of OVCA patients. Early diagnosis, tumor grading, residual disease and poor performance status can affect to some extent patient survival[37]. In both uni- and multivariate analyses, pre-operative circulating pGSN also emerged in our study as an independent significant predictor – amongst all prognostic factors investigated – associated with disease free survival. This potentially provides a less invasive and inexpensive diagnostic test, which could be used together with other prognostic factors to enhance patient prognostication and optimal management. pGSN has also been evaluated in the serum of patients with disease conditions such as colon cancer, hemodialysis, arthritis, sepsis, burns and other inflammatory disorders[22]. We are the first however, to demonstrate the utility of circulating pGSN as a less-invasive

prognostic marker, and more also in ovarian cancer, when the majority patients are diagnosed at late stages at time of initial presentation.

We have recently shown in our *in-vitro* studies that pGSN is transported by exosomes secreted from ovarian cancer cell lines. This has directed our research attention into differentiating the pathological significance of exosomal pGSN from the normal physiological free-circulating pGSN. We consider this as a necessary step since pGSN is one of the most abundant proteins in human plasma and hence, investigating the clinical significance of its exosomal delivery into the plasma will offer a more accurate prognostification. In addition to pre-operative sample analysis, the levels of pGSN should be further monitored in post-operative and chemotherapy/radiationtherapy/immunotherapy/targeted therapy periods to define and optimize its performance.

Conclusion

For the first time, we have identified in the present study pre-operative circulating pGSN as a potential marker for the detection of early stage ovarian cancer, and predictor of optimal residual disease and as an independent prognostic factor in OVCA (Fig. 5); outperforming the established tumor marker, CA125. Pre-operative pGSN in the plasma could be used to discriminate early-stage OVCA patients. Pre-operative circulating pGSN is not only sensitive as an individual diagnostic marker; however, using it together with CA125 provides additional diagnostic sensitivity compared with currently FDA approved multianalyte assays. Detecting circulating pGSN by ELISA is less expensive, less labor-intensive, reproducible and commercially available, presenting as an advantage over other sophisticated techniques like whole-genome analysis, transcription profiling and proteomic analysis. While we are encouraged by the novelty and clinical importance of the present findings, we acknowledge the small

population of patients involved in this study and hence involvement of patients from multiple cohorts and stratification based on histological subtypes will help not only to validate the findings observed but extent the application of the current study.

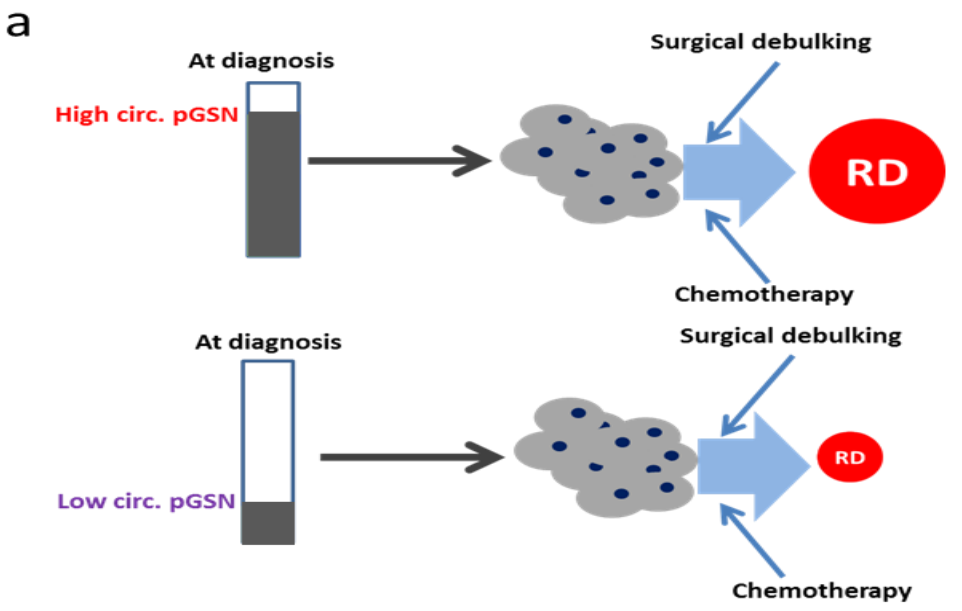
a
At diagnosis
High circ. pGSN
Surgical debulking
RD
Chemotherapy
At diagnosis
Low circ. pGSN
Surgical debulking
RD
Chemotherapy

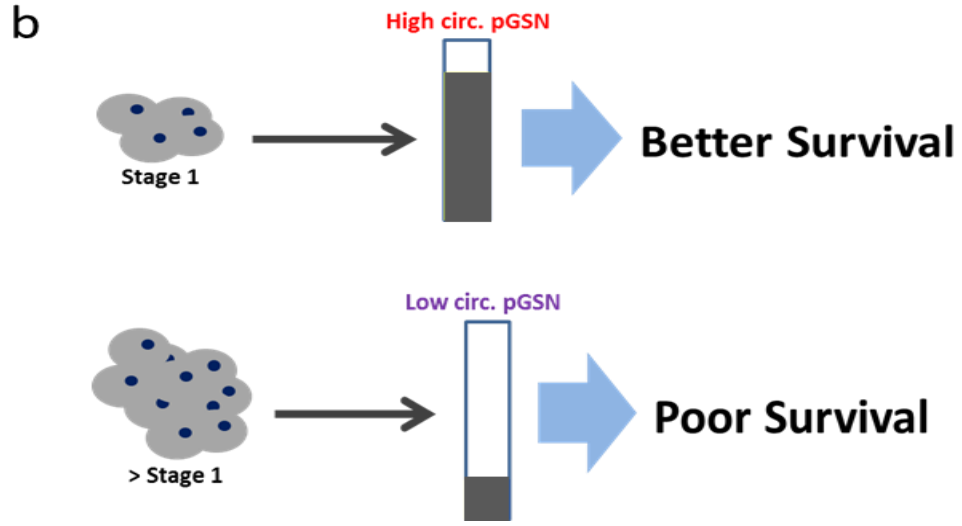
b
High circ. pGSN
Stage 1
Better Survival
Low circ. pGSN
> Stage 1
Poor Survival

Fig. 6.5 Hypothetical models illustrating how pre-treatment levels of pGSN could predict stage 1 ovarian cancer and residual disease (RD). (a) Increased pre-operative levels of pGSN at diagnosis could predict high residual disease in ovarian cancer patients before surgery/treatment while low levels of pGSN at diagnosis could indicate minimal residual disease after surgery. **(b)** During the onset of ovarian cancer (stage 1), increased levels of pGSN are detectable in the plasma of patients which could improve survival. However, in advanced stages of ovarian cancer pGSN levels in patients' plasma decrease, an indication of poor survival.

Patients and Methods:

Data reporting: A convenient sample size was chosen. During samples preparation and analyses, plasma samples were blinded.

Ethics Statement: This study was approved by the Centre hospitalier de l'Universite de Montreal (CHUM) ethics committee (IRB approval number; BD 04-002) and the Ottawa Health Science Network Research Ethics Board (IRB approval number; OHSN-REB 1999540-01H) and conducted in accordance with the appropriate guidelines. Written informed consent was obtained from all subjects.

Plasma Samples: 99 plasma samples with predetermined CA125 levels (HGS; 69, LGS; 4, not verified; 26) were collected from ovarian cancer patients at the CHUM from 1992 to 2012. Prior to plasma collection, patients did not receive any neoadjuvant chemotherapy or radiotherapy. pGSN was measured in these samples as well as plasma samples from 32 healthy non-cancerous subjects. Details of patient population and demographics are outlined in Supplementary Table S1. All samples were examined by one gynecologic-oncologic pathologist who assigned tumor grade and histopathological subtype according to the International Federation of Gynecology and Obstetrics (FIGO) criteria. All patients were managed with primary surgery. They include optimal residual disease categorized as being ≤1 cm and suboptimal residual disease defined as being >1 cm. Disease-free (DFS) and overall (OS) survival assessment was based on CA125 and CT imaging during follow-up. DFS was calculated from time of diagnosis to time of recurrence and OS from time of diagnosis to time of death.

ELISA: Pre-operative pGSN concentrations were assayed in OVCA patients (n=99) by sandwich ELISA (Aviscera Bioscience, Inc. CA), according to manufacturer's instructions. The detection antibody was raised against human plasma (soluble) gelsolin. Plasma samples were

diluted in a sample buffer (1/1500; Aviscera Bioscience, Inc. CA) and all analyses done in triplicate. Optical densities (OD) were determined using a microtiter plate reader at 450 nm. The blank was subtracted from the triplicate readings for each standard and sample and concentrations reported in µg/mL.

Biostatistical methods: The SPSS software version 25 (SPSS Inc., Chicago, IL, USA) and Graphpad Prism 7 (San Diego, CA, USA) were used to perform all statistical analyses and two-sided $P \leq 0.05$ considered to indicate statistical significance. Receiving operating characteristic (ROC) curves were used to assess the performances of pGSN and CA125 over their entire range of values. The area under the curve (AUC) was used as an index of global test performance. pGSN and CA125 concentrations were dichotomized by their medians cut-offs into low or high and correlated to residual disease and early stage using Pearson's correlation test (two-tailed). The means of pGSN and CA125 levels were plotted against age, stage and residual disease using bar chat and statistical analyses performed by using unpaired *t*-test and one-way ANOVA; Gaussian distribution was tested. The means of pGSN and CA125 levels were plotted against stage, age and residual disease using box plots. The box represents the interquartile (IQ) range, and the whiskers represent the highest and lowest values, which are no greater than 1.5 times the IQ range. Outliers are values greater than 1.5 times (circle) or 2 times (stars) the IQ range. The relationship of these dichotomous variables to other clinicopathologic correlates was examined using Fisher exact test, T test and Kruskal Wallis Test as appropriate. Survival curves (DFS and OS) were plotted with Kaplan Meier and *P*-values calculated using the log-rank test. Univariate and multivariate Cox proportional hazard models were used to assess the hazard ratio (HR) for CA125, pGSN, stage (FIGO), residual disease and age as well as corresponding 95% confidence intervals (CIs).

Acknowledgement:

This work was supported by the Canadian Institutes of Health Research (MOP-15691). Tumor and serum banking was supported by the Banque de tissus et de données of the Réseau de recherche sur le cancer du Fonds de recherche du Québec – Santé (FRQS), associated with the Canadian Tissue Repository Network (CTRNet). A.M.M. and D.P. are researchers of the CRHUM who receive support from the FRQS. The funding agencies were not involved in the design, conduct, analysis or interpretation of the study.

CHAPTER 7 - ADDITIONAL RESEARCH FINDINGS

7 Preview

During the course of my doctoral studies I have conducted experiments, the findings from which were not included in the manuscripts reported in Chapters 3, 4, 5 and 6. They were preliminary studies concerned with optimization of experimental conditions, validation of assay conditions and mechanism through which pGSN confers resistance in OVCA cells. While they are not central to the manuscripts mentioned, information gained will be an important reference and could form the foundation on which future investigations could be planned, and they are reported hereafter.

7.1 Specificity of antibody used for assessment of pGSN expression in OVCA cells

We first validated our antibody to see whether it specifically binds to pGSN and not cGSN (the cytoplasmic isoform) given the architectural difference is only 25 amino acids sequence present on the N-terminal of pGSN but absent in the cGSN. We successfully demonstrated that pGSN antibody specifically binds to pGSN but not cGSN **(Fig. 7.1)**.

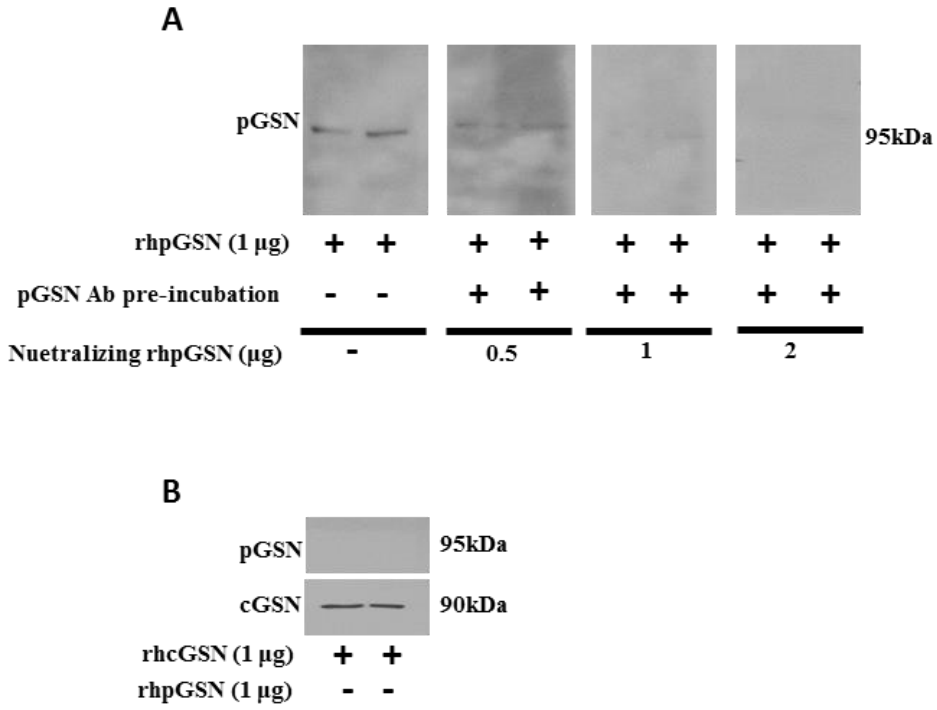

Fig. 7.1. **pGSN antibody (ABIN1019662) specifically targets the N-terminal region of pGSN but not cGSN. (A)** 1 µg of recombinant human (rh) pGSN was loaded for Western blotting. Primary pGSN antibody (ABIN1019662) was either pretreated with rhpGSN or not before incubating with the nitrocellulose membranes. **(B)** 1 µg of rhcGSN was loaded for Western blotting. Nitrocellulose membranes were then incubated with pGSN antibody (ABIN1019662) and cGSN antibody (G4896). Three independent replicate experiments were done, and representative blots shown here.

7.2 Specificity of siRNA for pGSN knockdown in OVCA cells

Given both gelsolin isoforms are transcribed from the same gene, we next validated our siRNAs to confirm that they target pGSN mRNA without affecting cGSN mRNA **(Fig. 7.2)**. When comparing three preparations of siRNA, we observed that whereas siRNA3 downregulated both cGSN and pGSN content in chemoresistant OVCA cells, siRNA1 and siRNA2 were specific for pGSN and were used in subsequent studies. Our findings are consistent with other studies where gelsolin was implicated in tumor progression and chemoresistance in OVCA, head-and-neck cancers and other cancer types although the specific isoform was not investigated in these studies[1-3].

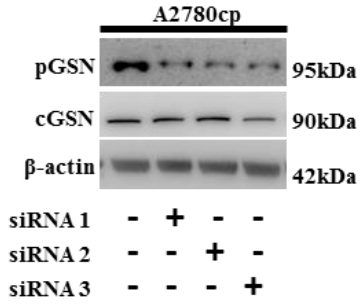

Fig. 7.2. pGSN siRNA 1 and 2 specifically targets pGSN without affecting cGSN. Chemoresistant OVCA cell line (A2780cp; 1.6 x 10^6) were treated with siRNAs (50 nM; 24 h). siRNA 1 and 2 target only pGSN whereas siRNA 3 targets both pGSN and cGSN. pGSN, cGSN and β-actin contents were assessed by Western blotting. Three independent replicate experiments were done, and representative blots shown here.

7.3 pGSN-mediated induction of stem-like features in OVCA cells.

α5β1 integrin overexpression is significantly associated with OVCA progression, suboptimal residual disease, migration and drug resistance[4-6]. Although pGSN has been shown to interact with α5β1 integrin through fibronectin[7], whether this interaction is involved in pGSN-mediated chemoresistance has been demonstrated in this thesis. We have demonstrated that exosomal pGSN as well as rhpGSN activated the α5β1 integrin signalling cascade and induced the endogenous pGSN expression in an autocrine manner, a response that inhibited CDDP-induced apoptosis in chemosensitive OVCA cells. Same responses explained how chemoresistant cells-derived pGSN in a paracrine manner conferred CDDP-resistance in otherwise chemosensitive OVCA cells. pGSN-mediated OVCA cell chemoresistance was associated with increased expression of the stem-like marker, Sall4 as well as increased colony formation, responses that may explain in part their resistance to CDDP treatment (**Fig. 7.3**).

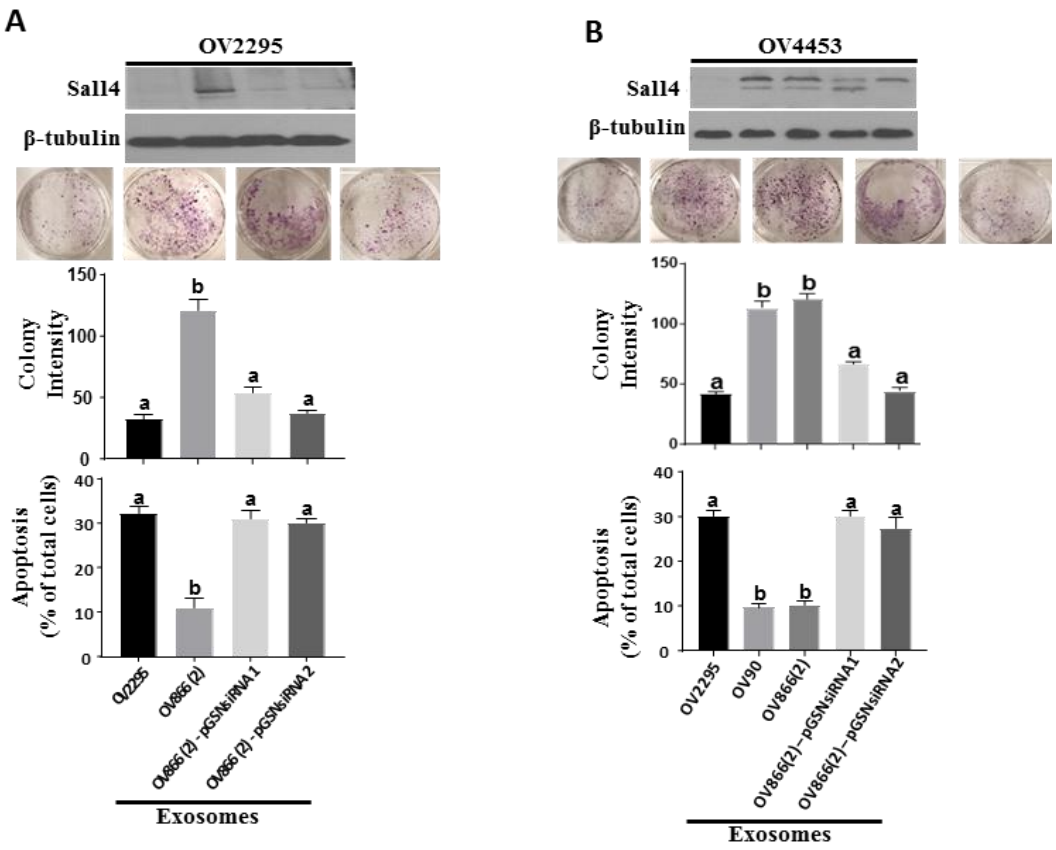

Fig. 7.3. pGSN-mediated OVCA chemoresistance induce stem-like features. Chemosensitive OVCA cells, **(A)** OV2295 and **(B)** OV4453 were treated with exosomes (40 ug/400,000 cells; 24 h) derived from OV2295 (chemosensitive), OV866(2) (chemoresistant), OV866(2)-pGSN-KD (siRNAs, 50 nM; 24 h), OV90 (chemoresistant) OVCA cells. OV2295 and OV4453 pretreated with exosomes were then treated with CDDP (10 μM; 24 h). Sall4 and β-tubulin contents were assessed by Western blotting. CDDP-induced apoptosis was measured by Hoechst staining morphologically. Colonies were stained by crystal violet and quantitated using image J. *(a; ***p<0.001 vs b).*

7.4 Exosomal pGSN is present in human plasma and urine

We have demonstrated that circulating pGSN presents as a reliable and less-invasive biomarker indicative of early stage OVCA and predicting residual disease compared with the conventional CA125. These findings are contrary to the observed increased pGSN expression with advanced tumor stage. Whether this is due to increased urinary secretion with tumor development is not known. This is conceivable since increased actin concentration facilitates the clearance of pGSN from the blood, a mechanism that could occur in OVCA progression[8]. These observations motivated us to examine the urine of healthy volunteers for the presence of pGSN as a proof-of-concept to warrant our future investigation of OVCA patients' urine, an approach that could provide a non-invasive platform to detect OVCA progression. Eight (8) healthy volunteers were thus, recruited and pGSN assessed in their urine using WB and sandwich ELISA (Aviscera Biosciences, Santa Clara, USA). We observed that pGSN and actin were present in the urine of all participants although at modest levels, suggesting that the levels could be elevated in OVCA progression due to increased clearance from the blood by actin[8] **(Fig. 7.4)**. Also, pGSN was detectable at 45 kDa, the molecular weight of actin, suggesting a possible truncation of pGSN and its interaction with actin. This could explain why circulatory pGSN levels decreased with increased tumor stage.

We have earlier shown that OVCA cells secrete pGSN of which a significant amount is carried via exosomes. Investigating exosomal pGSN in body fluids such as plasma and urine could therefore provide a more significant reflection of the tumor microenvironment. As a proof-of-concept, we investigated the presence of exosomal pGSN in the plasma of two (2) HGS OVCA patients. We demonstrated that exosomes containing pGSN were present in the plasma of both patients **(Fig. 7.5)**. The secretion of pGSN-containing exosomes by chemoresistant OVCA

cells could therefore present as a novel OVCA diagnostic opportunity as well as provide a more significant reflection of the tumor microenvironment. Future studies are therefore eminent to determine if circulating and urinary pGSN are predictive of OVCA stage, residual disease, chemoresponsiveness and survival in epithelial OVCA patients (as well as other histologic subtypes) by using **a)** whole pGSN and **b)** exosomal pGSN.

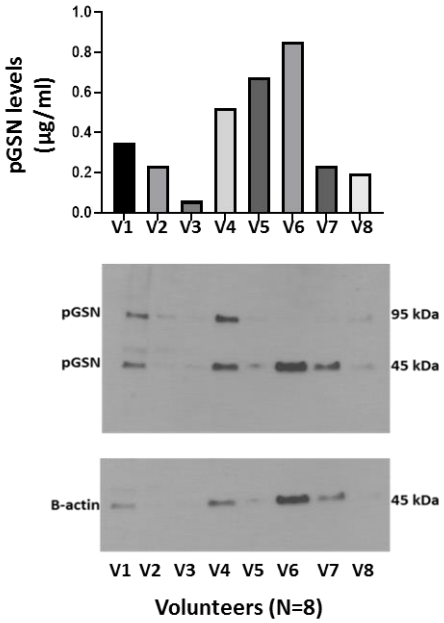

Fig. 7.4. pGSN and β-actin levels are detectable in the urine. 8 healthy volunteers were recruited, and urine samples collected. 100 µl of each sample was used in the pGSN assay using sandwich ELISA. The concentration of urine pGSN for each volunteer is plotted. 15 mL urine was concentrated and 30 µl of each sample used in the WB analysis and probed with pGSN and β-actin antibodies. N=number of volunteers.

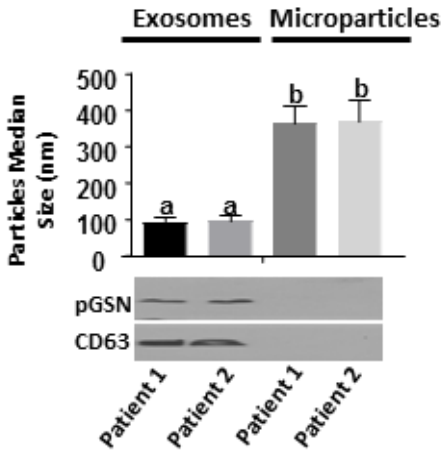

Fig. 7.5. Exosomal pGSN is detectable in the plasma of HGS ovarian cancer patients. Plasma samples were collected from two (2) HGS ovarian cancer patients from CHUM, Montreal, and exosomes were isolated using total exosome isolation kit (Fisher Scientific). The particles were characterized by nanoparticle tracking analysis (size distribution) and WB (CD63 marker). Vesicle concentration was analyzed in triplicated. pGSN content in exosomes and microparticles were detected using WB. *(a; ***$p<0.001$ vs b)*.

CHAPTER 8 - DISCUSSION

8 Overview and significance

Ovarian cancer is the most lethal gynaecological cancer with a 5-year survival rate <50%[1-3]. This is primarily due to late diagnosis, tumour recurrence and chemoresistance[2,4]. Although CA125 combined with trans-vaginal ultrasound is the conventional strategy to diagnose ovarian cancer, the non-specificity of CA125 makes this strategy unreliable[5,6]. Thus, most cases of ovarian cancer are diagnosed at late stages which compromise effective treatments and the survival of these patients. There is therefore the need for the discovery of novel, efficient and reliable biomarkers for the detection of ovarian cancer at an early stage. Chemoresistance is also a key obstacle to improved patient survival. The mechanisms involved with ovarian chemoresistance are multifactorial involving dysregulation of apoptotic genes, increased activation of oncogenes, increased metabolic activities and immune-suppression[7-12]. Although immunotherapy is effective in melanomas, breast cancers and other cancer types, little therapeutic success has been achieved in ovarian cancer[13-15]. Thus, there is an urgent need to investigate the ovarian tumour microenvironment to delineate the reason for the poor therapeutic success. pGSN is an actin-binding protein that has been implicated in inflammatory disorders, colon cancer metastasis and prostate cancer progression[16-20]. Although the cellular actions of gelsolin have been studied in the progression and treatment resistance of gastric[21], prostate[20], head-and-neck[10] and ovarian cancer[11], its role in the tumour microenvironment is yet to be established. Whether pGSN-mediated immune-suppression contributes to ovarian cancer chemoresistance remains to be investigated.

The goal of the thesis is to determine the role of pGSN in epithelial OVCA chemoresistance. The overall objective of the proposed study was to determine if and how

OVCA cell-immune cell interactions regulate chemosensitivity and how deregulation of these interactions modulate TME immunity as well as tumour chemosensitivity. We thus, investigated the autocrine and paracrine actions of pGSN in the ovarian tumour microenvironment as well as their prognostic significance using standard *in vitro* techniques and human clinical samples, respectively.

Exosomal pGSN induced HIF1α-mediated chemoresistance in an autocrine manner as well as conferred resistance to otherwise chemosensitive OVCA cell lines in a paracrine manner. pGSN-induced chemoresistance was also associated with increased endogenous production of pGSN, increased expression of stem-like marker, Sall4 and increased production of intracellular GSH. These responses could explain why CDDP accumulation (decreased phosphorylation of H2AX) was significantly decreased in pGSN-induced chemoresistant OVCA cells upon treating with CDDP. Although pGSN-mediated induction of stemness is intriguing, these findings are preliminary and therefore require further investigation.

Increased pGSN expression in OVCA tissues was significantly associated with poor prognoses regardless of the ethnic background of the patients and the histologic subtype of their tumour. Although increased infiltration of M1 macrophages and CD8+ T cells in the ovarian cancer islet was significantly associated with improved patient survival, increased expression of pGSN appeared to have blunted these survival benefits, an effect that drastically reduced patient survival. Further investigation revealed that pGSN induced caspase-3-dependent apoptosis in both CD8+ T cells and M1 macrophages, leading to decreased secretion of IFNγ and iNOS and TNFα respectively in these cells. Unlike CD8+ T cells and M1 macrophages, pGSN had no effects on CD4+ T cell viability but however, polarized them to type II helper T cells. These suggest that the mere presence of infiltrated immune cells in the ovarian tumour

microenvironment does not automatically imply patients will benefit from immunotherapy. This could explain why OVCA patients only benefit modestly from immunotherapies. Stratifying patients using tissue pGSN levels into immunotherapy responsive and non-responsive groups will therefore help maximize the therapeutic effects of these treatments.

We examined blood samples from OVCA patients if circulating pGSN could be used as an early diagnostic marker. Compared with CA125 (the conventional marker for OVCA diagnosis), pGSN had a higher test accuracy for the detection of stage 1 OVCA and residual disease. Combining pGSN and CA125 in a multi-analyte assay index exhibited significantly higher test accuracy for the detection of stage 1 diseases compared with either marker alone. Taking together, circulatory pGSN is a potential early detection marker as well as a reliable predictor of surgical outcomes. Although circulatory pGSN provides an improved test accuracy for early stage OVCA, we acknowledge that combining it with other biomarkers in a multi-analyte index assay could further enhance its diagnostic accuracy. Thus, further developmental studies are needed to explore this possibility.

These studies for the first time demonstrate the oncogenic and immuno-suppressive roles of pGSN in epithelial OVCA chemoresistance **(Fig. 1)**. Findings from these studies will provide insight to enhance the sensitivity of OVCA early detection, surgical interventions and maximize the efficacies of immunotherapy as well as other combinatory therapies to improve the 5-year survival rate of OVCA patients.

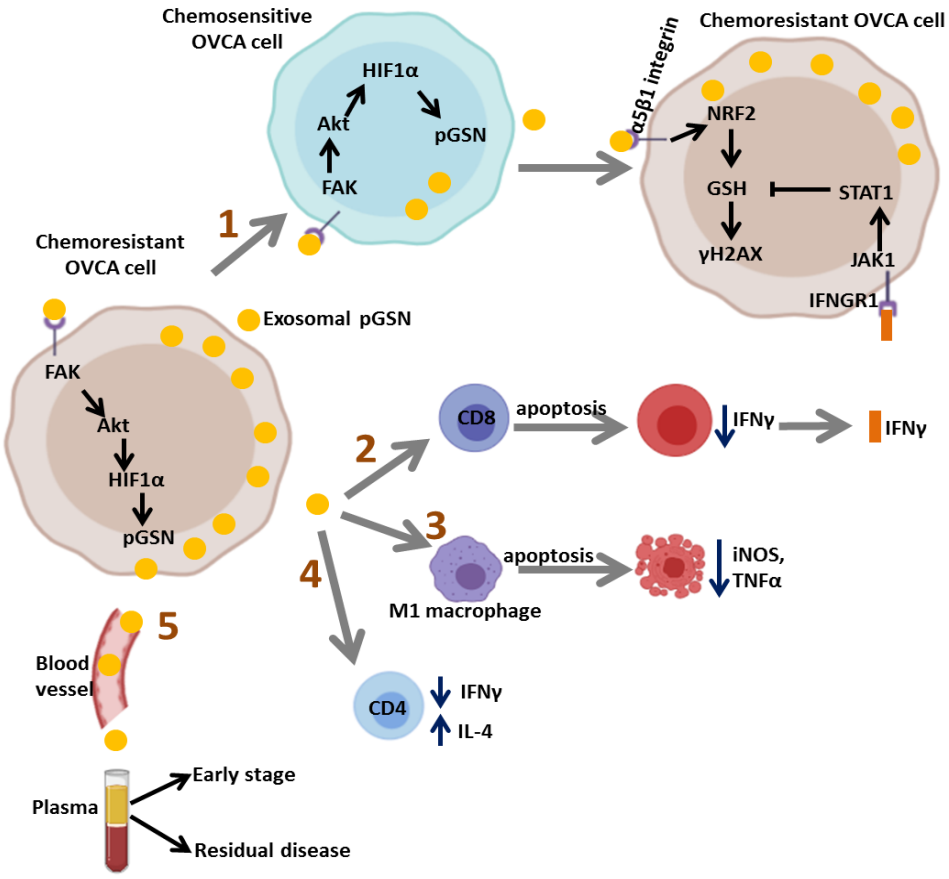

Fig. 8.1. Schematic diagram of the role of pGSN in epithelial OVCA chemoresistance. 1) pGSN is highly expressed and secreted (via exosomes) by chemoresistant OVCA cells compared with their sensitive counterparts. pGSN induce HIF1α-mediated chemoresistance in an autocrine manner as well as confers resistance to chemosensitive OVCA cells in a paracrine manner. Increased pGSN induce intracellular GSH production by activating NRF2. **2)** pGSN-induced CD8+ T cell apoptosis is associated with decreased IFNγ secretion, an outcome that leads to decreased JAK1/STAT1 activation and increased GSH production. **3)** pGSN induce M1 macrophage apoptosis via caspase-3-dependent apoptosis resulting in reduced secretion of iNOS and TNFα. **4)** Unlike CD8+ T cells, naïve CD4 T cells are polarized to type II helper T cells by pGSN which is marked by increased IL-4/IFNγ ratio. **5)** Increased pGSN is significantly associated early stage OVCA disease and predicts suboptimal residual disease.

8.1 Experimental significance for using isogenic paired cancer cell lines

In addressing the objectives and hypotheses of my thesis, chemosensitive parental (A2780s) and its isogenic chemoresistant phenotype (A2780cp) OVCA cell lines were utilized. These matched paired cell lines were generously donated by Dr. Barbara Vanderhyden, The Ottawa Hospital Research Institute, Ottawa, Canada. The A2780s cell lines were obtained from serous cystadenocarcinoma OVCA whereas the A2780cp cell lines were derived from their parental (A2780s) cell lines by continuous exposure to increasing concentrations of CDDP *in vitro* (14 – 21 days). The availability of these matched paired cell lines has enabled us to investigate the cellular and molecular basis of OVCA chemoresistance by comparing differences (molecular pathogenesis, treatment responses, protein contents and outcomes of loss- and gain-of functions) between chemosensitive and chemoresistant phenotypes. Since both cell lines have the same genetic background, using them provides critical information to better delineate the molecular mechanisms of chemoresistance in OVCA cells.

Despite the relevance of isogenic cancer cell lines in investigating chemoresistance, there are a few draw backs for using these cells. Aside not being a true representation of the *in vivo* tumour model, they could also lose their original phenotype after passages beyond 25. These changes could impact the behaviour of the cell as well as responses to treatment. Although passage numbers were maintained below 25 during these studies, using human primary OVCA cells in future studies will further provide clinical information that is closer to *in vivo* tumour model.

8.2 Experimental significance of the use of clinical samples

Clinical samples (OVCA tissues and blood samples) from chemo-naïve patients of Western and Asian backgrounds were used in the current studies. These samples had accompanied by the clinical records of patients as well as their clinicopathological parameters (age, histologic subtypes, stage, residual disease, overall survival, progression-free survival and CA125 levels) and enabled us to analyse differential expressions of markers of interest. These markers were quantified and correlated with clinicopathological parameters such as PFS, PFI, OS, stage, residual disease and histologic subtypes. Thus, we were able to analyse the co-localisation and association of pGSN and immune cells and provided the rationale to investigate the possible interaction of pGSN expression and immune cells in the OVCA cells. The outcome from these studies enabled us to better understand OVCA progression and response to chemotherapeutic agents, patient immunological statuses, surgical outcomes, early diagnosis and the possible interaction between pGSN and immune cells.

8.3 Antioxidant regulation in ovarian cancer chemoresistance

Glutathione (GSH) and the nuclear factor erythroid 2-related factor (NRF2)-dependent genes (xCT and GCLM) provide an advantage to cancer cells to become CDDP resistant[9,22]. Exogenous pGSN treatment increases GSH levels in the blood which mitigates radiation-induced injury in mice, although the exact mechanism has not been investigated[23]. Whether NRF2, an antioxidant transcription factor, is involved is yet to be investigated in the context of pGSN-mediated OVCA chemoresistance. In this thesis, we investigated GSH regulatory role of pGSN in OVCA chemoresistance.

We observed that elevated pGSN expression resulted in increased phosphorylation of NRF2 leading to increased production of GSH. These responses resulted in decreased accumulation of CDDP in the tumour cells (phosphorylation of H2AX) and reduced CDDP-induced death. Our investigation of OVCA public datasets also revealed a significant correlation between pGSN and NRF2 mRNAs as well as its related gene, xCT. These findings could in part explain why most OVCA patients are resistant to platinum-based treatments. Fibroblast-derived GSH also confer CDDP-resistance in OVCA cells[24], suggesting that GSH metabolism plays a key role in OVCA chemoresistance. Our current data is consistent with these findings and advances an intrinsic regulatory mechanism by which GSH is involved in pGSN-mediated OVCA chemoresistance.

8.4 Clinical relevance of tissue pGSN expression and OVCA chemoresistance

Despite the enormous efforts in OVCA research, little success has been seen in terms of reliable prognostic markers, long term treatment and 5-year overall survival[1-3]. Thus, there is an urgent need to discover novel prognostic markers that will provide clinical advantages to OVCA patients regardless of their ethnic backgrounds. We thus, investigated the expression of pGSN in OVCA patients from North America (Canada), Asia (Japan) and public datasets (TCGA cbioportal). Unlike North America, the Asian cohort had unusual patient distribution in histology (high number of non-serous), age (< average age at diagnosis), tumour stage (~60% stage 1), surgical outcomes (> average complete/optimal residual disease) and treatment regimen (increased treatment response). This diversity could impart patient survival and could explain why this cohort of patients had relatively higher PFS compared with patients from North America. These strengthen the point that ethnic differences (e.g. genetic, lifestyle, dietary stc)

may play a possible role in ovarian cancer pathology, management and patient survival, an area which has been overlooked until recently.

Regardless of ethnic differences and histologic subtypes, pGSN expression was highly expressed in malignant tissues compared with normal tissues. Also, increased pGSN expression was significantly associated with increased tumour stage, suboptimal residual disease, recurrence, chemoresistance and poor survival. These findings are not only consistent with previous studies where increased total gelsolin expression in ovarian cancer[11], head-and-neck cancer[10], osteosarcoma[25] and prostate cancer[20] were significantly associated with poor prognosis, tumour recurrence and chemoresistance, but also demonstrate the clinical relevance of this isoform (pGSN) in OVCA patients with different ethnic backgrounds and histological subtypes. This suggests that pGSN is a potential OVCA prognostic marker independent of ethnic and histologic differences.

Aside pGSN expression in the TME, the extracellular matrix (ECM) and vasculature system might also play a role in OVCA chemoresistance[26]. ECM provides structural support and regulates other cellular activities as well. During tumorigenesis, the tumour-associated ECM serves as a gateway for cancer cell invasion and proliferation[26]. Since pGSN has tumorigenic properties and activates the Akt pathway, it is worth investigating if it has a role to play in ECM-mediated cancer cell invasion and proliferation.

8.5 Immuno-regulatory role of pGSN in the ovarian tumor microenvironment

Immunotherapy has achieved significant therapeutic success in haematological cancers and other solid cancer types[27-30]; however, they have achieved modest responses in OVCA patients[4,31]. These include but not limited to anti-CTLA-4 and anti-PD1/PD-L1. Anti-

PDL1 achieved 1 partial response (PR) and disease stabilization (SD) in 2 patients in a phase 1 clinical study involving 17 OVCA patients[27,32]. In another phase I trial, another anti-PDL1 antibody showed 4 PR and 11 SD[32]. These modest responses require further investigations into the ovarian TME to discover novel targets to improve treatment successes. This motivated us to investigate if and how pGSN regulate the anti-tumour functions of T cells and tumour-associated macrophages in the OVCA chemoresistance.

In our clinical tissues, we observed that increased infiltration of CD8+ T cells and M1 macrophages were both significantly associated with prolonged progression-free and overall survivals. Interestingly, the survival benefits of these infiltrated immune cells to OVCA patients were inversely and significantly associated with increased tissue pGSN expression, an observation that was marked by decreased PFS. In addition, we found that most of the CD8+ T cells that stained positive for pGSN were also positive for caspase-3, an indication of apoptosis. Patients with increased caspase-3+ CD8+ T cells were significantly associated with poor survival. Mechanistically, we observed that chemoresistant cell-derived exosomal pGSN induced caspase-3-mediated apoptosis in both CD8+ T cells and M1 macrophages compared with their sensitive counterparts. The reduction of the viability of CD8+ T cells and M1 macrophages were associated with decreased IFNγ and iNOS and TNFα, respectively. These findings are consistent with previous studies where pGSN induced cell death in T cells and NK/T cells as well as reduced pro-inflammatory cytokines (TNFα, IL-6 and IL-10) in macrophages. These suggest that the mere presence of T cells or M1 macrophages do not automatically imply improved survival; however, their functionality and viability determine therapeutic success. This could in part explain why immunotherapies have achieved modest responses in OVCA patients.

The viability of infiltrated T cells is an important determining factor of a patient's response to treatment and improved survival[14,33,34]. Thus, we investigated the reciprocal effects of immuno-suppressed T cells on OVCA cells. We observed that functional CD8+ T cells secreted increased levels of IFNγ which activated the STAT1 pathway in OVCA cancer cells, a mechanism that led to the reduction of GSH production and sensitized OVCA cells to CDDP-induced death. The reverse happened when IFNγ secretion was reduced due to pGSN-mediated CD8+ T cells. A similar mechanism has been demonstrated in fibroblast where IFNγ reduced the production of GSH. For the first time, we have demonstrated how pGSN suppresses the anti-tumour functions of T cells and M1 macrophages in OVCA chemoresistance. Tissue pGSN levels could therefore be used to stratify patients into immunotherapy responsive and non-responsive groups, a strategy which could provide the clinicians an idea about the immunological status of OVCA patients. This approach could provide insight into maximizing the therapeutic efficiencies of immunotherapy which hitherto has provided modest results.

Recently, adoptive T cell transfer (ACT) therapy has received considerable attention as potential alternative treatment for OVCA patients[30]. ACT therapy is when autologous specific tumour infiltrating lymphocytes (TILs) are expanded ex-vivo and re-introduced into the same patient to generate tumour-specific immune response[30]. In a small pilot study with 13 recurrent OVCA patients, administering ACT after surgical resection and chemotherapy resulted in a significantly prolonged PFS and favourable clinical outcomes compared with the control subjects[35]. Our knowledge on the immuno-regulatory role of pGSN could enable one to select highly specific TILs for expansion and immune responses. Engineering T cells to express either pGSN-specific T cell receptors (TCRs) or chimeric pGSN receptors (CPRs) could also offer therapeutic advantages to OVCA patients.

8.6 Early diagnosis and residual disease in ovarian cancer

Tumour stage and residual disease are key prognostic factors with marked impact on OVCA patients' treatment success and survival. Despite considerable efforts to screen for OVCA, minimal progress has been made to date on early detection[36-38]. In this thesis, we investigated the utility of circulatory pGSN as a biomarker for early diagnosis and residual disease. Although circulating pGSN alone had higher test accuracy compared with the conventional marker, CA125, the combination of the two markers provided a more sensitive diagnostic test for both stage 1 OVCA and residual disease. These suggest that including more promising markers such as CA153, LPA, HE4, VEGF, kallikreins and osteopontin in a multi-analyte index assay could further enhance the test accuracy of pGSN[39-42].

Circulating pGSN levels are inversely proportional to the tissue levels with regards to tumor stage. Although the reason(s) for this apparent discordance is not clear, it is possible that increased actin concentration resulting from disease-related tissue destruction facilitates the clearance of pGSN from the blood, thus resulting in decreased circulatory pGSN levels with increased tumour stage[43]. Ovarian tumour progression results in tissue invasion and, in the process, tissue destruction releasing actin into the circulation[44,45]. Whether the inverse correlation seen in the plasma is due to increased urinary excretion of pGSN-actin complex with tumour development is not known and worth investigated.

CHAPTER 9 - FUTURE RESEARCH DIRECTIONS

The current studies provide significant evidence that pGSN plays a key role in epithelial OVCA chemoresistance. Specifically, pGSN promotes tumour recurrence, chemoresistance, poor survival as well as suppress anti-tumour functions of infiltrated immune cells. This presents pGSN as an independent prognostic marker for epithelial OVCA patients. However, despite these major advances made as discussed in the previous section, there remains significant information gap in the current understanding on the molecular and cellular basis of OVCA chemoresistance and how these new principles could be applied in the development of new diagnostic and therapeutic strategies. These information gap includes but not limited to the following and require further investigation: **(a)** establishing the role of pGSN in chemoresistance in OVCA ***in vivo***; **(b)** understanding why pGSN is expressed in higher levels in chemoresistant compared to chemosensitive OVCA cells; **(c)** specificity of immune-modulatory actions of pGSN in OVCA; **(d)** novel strategic approach in diagnostic development; and **(e)** pGSN as a novel target for alternative treatment. These possible future research directions are briefly elaborated hereafter.

A) Establishing the role of pGSN in chemoresistance in OVCA *in vivo*

1. Experimental significance of human primary OVCA cells

In the present studies, *in vitro* experiments were conducted using isogenic OVCA cell lines. We acknowledge the limitation of these cells and thus, propose the use of primary OVCA cells in key future studies to validate the molecular and cellular mechanisms involved. Primary human OVCA cells will be collected from human ovarian tumours as well as ascites with clinical information, such as sex, age, tumor stage, PFS, OS, PFI, histologic subtypes, treatment regimen

and residual disease. This makes it feasible to relate molecular findings with patient clinical outcomes to assess their relative importance to the patients' prognosis, a strategy not achievable with isogenic cell lines. Another advantage of using primary human OVCA cells is that one could treat the cells with chemotherapeutic agent to assess the pre- and post-treatment response *in vitro* from the same tumour, which is difficult to achieve with TMAs. This makes it possible to investigate drug response mechanisms in the context of the clinical outcomes of the patients.

2. Xenograft models

Although cell lines and human clinical samples provide convenient and informative findings, extending the current studies to include xenograft models will further provide insight into the molecular and cellular basis of OVCA chemoresistance and its target therapy *in vivo*[1]. We have shown that pGSN knockdown sensitizes chemoresistant OVCA cells to CDDP in vitro while its forced expression renders sensitive OVCA cells resistant to CDDP. We also observed that pGSN suppresses immune cell function by inducing cell death and increasing Th2/Th1 ratio, suggesting that T cell immunity may play a role in the action of pGSN in the regulation of chemosensitivity of OVCA. Dr. B Vanderhyden (uOttawa) has demonstrated that ID8 murine OVCA cells form tumors that resemble HGSC and has shown that these tumors are infiltrated by T cells. Our preliminary studies also revealed that murine ID8 cells express lower levels of pGSN and are also sensitive to CDDP-induced death **(Fig. 1).** This might explain the T cell infiltration observed by Dr. Vanderhyden in the ID8 tumors. Collaborating with Dr. Vanderhyden to define the role of pGSN in these tumors, ID8-GFP-luc-pGSN-OX murine cells (5×10^6 cells/mouse), which are CDDP resistant after stably overexpressing pGSN (LentiCRISPRv2/cas-9 technology), will be GFP-tagged and injected intrabursally in syngeneic

mice to develop ovarian tumours. ID8-GFP-luc-pGSN-KO cells (LentiCRISPRv2/cas-9 technology; $5x10^6$ cells) tumors will also be developed and ID8-GFP-luc murine cells expressing scrambled sequence used as control. The inclusion of GFP in the expression construct will facilitate whole animal imaging of tumour growth over the experimental period. When the tumour size reaches 0.5 cm in diameter, CDDP (5 mg/kg, i.p.) will be administered and changes in tumour volume will be measured weekly by bio-luminescent imaging. This dose of CDDP proposed to be used in this study is equivalent to the recommended dose used in human treatment. At humane endpoint, tumours will be processed for the assessment of tumour cell proliferation (Ki67; IHC), immune cell infiltration (CD8+, CD4+, TAMs, T regs; IHC/IF), CD8+ apoptosis and immunosuppressive cytokine expression (IFNγ, TNFα, IL-10). We anticipate that increased pGSN will result in decreased tumor burden, poor immune function and worse mice survival regardless of CDDP treatment, outcomes that will be reversed with pGSN KO.

We have observed that pGSN suppressed T cell function and thus we will study the involvement of T cells in the pGSN-mediated response. We will compare CDDP responsiveness of the tumour developed in C57BL/6 mice with B6.129P2-Tcrbtm1Mom/J KO mice (deficient in T cell beta receptor) with and without CDDP treatment. To investigate if T cell responses are key to inhibiting pGSN-mediated tumour growth and CDDP-resistance, we will assess tumour burden and regression (bioluminescent imaging), immune responses, apoptosis and survival (Kaplan-Meier analysis). Since ID8 cells express lower levels of pGSN, we anticipate that tumour growth *in vivo* will be low irrespective of the host immune status and suppressed by CDDP treatment although not significantly affected by pGSN knock-out (LentiCRISPRv2/cas-9 technology).

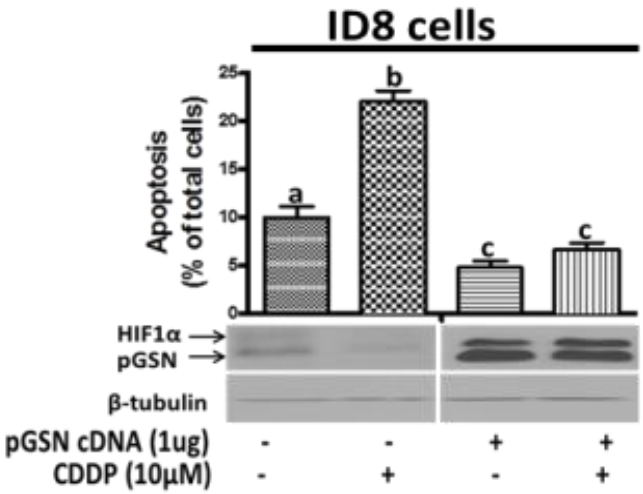

Fig. 9.1. pGSN up-regulation in murine ID8 cells attenuated CDDP-induced apoptosis. Murine ID8 cells were transfected with pGSN cDNA (1 μg; 24 h) and treated with CDDP (10 μM; 24 h). Empty plasmids were used as controls. pGSN and HIF1α contents were assessed by WB and apoptosis examined by Hoechst nuclear staining. Three (3) independent replicates were done and a representative blot shown. *(a; ***p < 0.001vs b, a; *p < 0.05 vs c)*. N=3.

In contrast, pGSN overexpression would enhance tumor growth in normal immune environment (C57BL/6 mice), a response not affected by CDDP. Moreover, the same cells in immune-compromised mouse (B6.129P2-Tcrbtm1Mom/J KO mice) will lead to increased tumor burden and decreased CDDP-induced apoptosis and cancer survival.

Xenograft models are useful in explaining the cellular and molecular basis of OVCA pathology since the pGSN expression in these isogenic cell lines could easily be manipulated using loss- and gain-in-function strategies. However, we also acknowledge the limitations of this model. Isogenic OVCA cell lines used to establish xenograft models upon several passages lose their genetic properties and heterogeneity, changes that affect tumor development. Also, tumours developed using this model may not necessarily be true representation of tumor heterogeneity as observed in OVCA primary tumors. These limit the use of cell line-xenograft models in the investigation of drug and immune responses. In order to circumvent these limitations, PDX model will be established using human primary OVCA cells to complement the findings observed in the cell line-xenograft model.

3. Human primary OVCA cell xenograft model (PDX)

PDX models are established when immuno-deficient mice are implanted with human OVCA primary tumour tissues or ascites-derived tumour cells. This model enables the tumour to grow in a physiologic TME similar to that of patient primary tumours, maintain their genetic and molecular features as well as preserve the heterogeneous population of cells as observed in OVCA primary tumors[2-4]. These features of PDX models are difficult to achieve in isogenic cell line-xenograft models.

Thus, PDX models will be used to investigate the role of pGSN in epithelial OVCA chemoresistance and immunological responses in future studies. Instead of isogenic OVCA cell lines, chemosensitive (PFI > 6 months) and chemoresistant (PFI ≤ 6 months) human primary tumours will be injected intrabursally in syngeneic mice to develop ovarian tumours and extended with the above experimental strategies and endpoints.

B) Understanding why pGSN is expressed in higher levels in chemoresistant compared to chemosensitive OVCA cells

In the current study, we observed that pGSN expression is higher in chemoresistant OVCA cells compared with their sensitive counterparts irrespective of their histologic subtype. Whether this differential expression is as a result of dysregulation upstream of the GSN gene is yet to be investigated. MicroRNAs (miRNAs) are short single-stranded non-coding RNAs that negatively regulate gene expression by inhibiting mRNA expression or protein translation. miRNAs have been implicated in several pathologies including cancers. In a recent study, GSN was identified as a functional target of miR-200a, an action that regulates GSN expression and hepatocellular carcinoma progression[5]. Specifically, miR-200a expression was relatively higher in normal cells compared with malignant cells. MiR-200a overexpression in cancer cells significantly reduced GSN expression suggesting that GSN is a functional target of miR-200a[5]. Our interrogation of public datasets (TCGA, Nature 2011) also revealed a significant ($P = 0.006$) negative correlation between miR-200a and pGSN mRNA expression although the association was weak (Pearson = -0.12) **(Fig. 9.1)**. If and how miR-200a regulates pGSN levels in OVCA chemoresistance, thus contributing to the differential expression observed, needs further investigation.

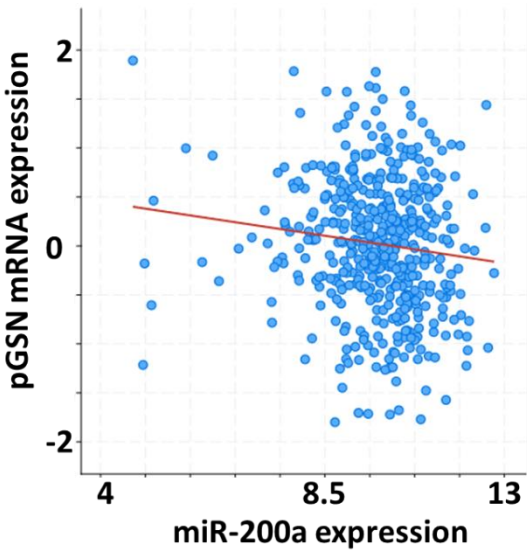

Fig. 9.2. pGSN mRNA expression is inversely correlated with miR-200a expression. 489 ovarian serous cystadenocarcinoma patients were interrogated in public datasets (TCGA, Nature 2011). mRNA levels of pGSN were inversely correlated with miR-200a expression using the Pearson's correlation test. $P = 0.006$; N = 489.

In our future studies, miR-200a and pGSN mRNA abundance and protein content will be examined in both chemosensitive and chemoresistant OVCA cells to determine the relationship between miR-200a and pGSN in the context of chemoresistance. CDDP effect on the expression levels of miR-200a and pGSN will also be assessed. MiR-200a loss- and gain-in-function will be investigated in OVCA cells using miR-200a mimic and inhibitors in chemoresistant and chemosensitive OVCA cells, respectively to establish the role of miR-200a in regulating pGSN levels. Synthetic scrambled non-targeting double-oligonucleotide will be used as a control. To measure the functional effect of miR-200a, pGSN mRNA, protein content and CDDP-induced apoptosis will be assessed and compared between the chemosensitive and chemoresistant OVCA cells.

We expect that the relative basal levels of miR-200a in the chemosensitive OVCA cells will be significantly higher compared with their chemoresistant counterparts. Also, increased levels of miR-200a will sensitize OVCA cells to CDDP-induced apoptosis, a mechanism that may explain the differential expression of pGSN in OVCA chemoresistance as well as provide a promising prognostic tool and target for the treatment of OVCA patients.

C) Specificity of immune-modulatory actions of pGSN in OVCA

We have demonstrated that pGSN attenuates the anti-tumour functions of T cells and M1 macrophages. In addition to T cells and macrophages, natural killer (NK) cells play a key effector role in immune-surveillance in the TME. NK cell suppression in the tumour microenvironment is significantly associated with poor prognosis in OVCA. As to whether pGSN is involved in the suppression of NK cells in OVCA chemoresistance is yet to be investigated. A previous study has demonstrated that pGSN overexpression promoted NK cell

line apoptosis although its clinical implication was not investigated. Thus, we hypothesize that increased tumour expression of pGSN will induce NK cell exhaustion and apoptosis resulting in chemoresistance and reduced patient survival. The immuno-regulatory role of pGSN in NK cells will be assessed using OVCA isogenic cell lines, primary OVCA cells and OVCA tissues.

NK cells densities in the ovarian TME will be analysed by IF and correlated with clinical outcomes such as PFS, OS, PFI, tumour stage and residual disease to determine their prognostic impact. Patients will also be stratified by tissue pGSN levels and NK cells and groups correlated with patient survival. This will provide clinical information whether pGSN expression may hinder the prognostic impact of infiltrated NK cells, as demonstrated in T cells and macrophages. To further demonstrate how the effector functions of NK cells are inhibited in human OVCA tissues, co-culture systems of NK cells with chemosensitive and chemoresistant OVCA cells will be established to investigated how NK cells' function are regulated in relation to chemo-responsiveness. Apoptosis and anti-tumour soluble factors will be measured using annexin V flow cytometry and ELISA, respectively. pGSN loss and gain-in-function studies will be conducted with pGSN siRNA and cDNA respectively to demonstrate the immuno-suppressive role of pGSN in NK cells. We anticipate that increased pGSN will suppress the anti-tumour effects of NK cells contributing to OVCA chemoresistance. The outcome of this study will provide pre-clinical information of the potential role of NK cells in OVCA patient survival as well as enable the stratification of NK cell-based therapy (immunotherapy) responsive and non-responsive patients based on tissue pGSN levels. These novel strategic efforts will not only enhance the therapeutic effects of immunotherapies but also prolong patient survival.

D) Novel strategic approach in diagnostic development

Circulating pGSN has higher test accuracy for the detection of early stage OVCA compared with the conventional marker, CA125. The test accuracy was further enhanced when pGSN and CA125 was combined in a multi-analyte index assay. Although CA125 is used in tandem with transvaginal ultrasound (TVS), their diagnostic accuracy have not yielded much success partly due to the non-specificity of CA125. TVS has a superior ability to image the ovary although its specificity is not sufficient to provide higher test accuracy especially in early stage OVCA. Thus, there is the need to discover biomarkers that could complement the imaging superiority of TVS to successfully detect early stage OVCA. We hypothesize that combining multi-analyte index assay (pGSN/CA125) with TVS will further enhance the diagnostic superiority of pGSN in the detection of early stage OVCA patients.

To investigate this possibility, OVCA patients will be recruited and the image of their ovaries taken using TVS. CA125 and pGSN concentrations will also be measured in the plasma of these patients. The parameters, TVS, CA125 and pGSN will be combined in a multi-analyte index assay as previously demonstrated and dichotomized by their median cut-offs into low and high. The groups (low vs. high) will be correlated with the tumour stages of the patients. Receiving operating characteristic (ROC) curves will be used to assess the performances of multi-analyte index assay over their entire range of values. The area under the curve (AUC) will be used as an index of global test performance to predict early stage. The outcome from this study will provide a highly sensitive and specific diagnostic strategy for the detection of early stage OVCA, an approach that will significantly contribute to a successful treatment of OVCA.

E) pGSN as a novel target for alternative treatments

In our current studies, we have demonstrated that pGSN expression promotes ovarian tumor recurrence, chemoresistant and immune-suppression. Thus, targeting pGSN expression presents as a novel approach to enhancing treatment responses and survival in OVCA patients. Additionally, pGSN targeting could be combined with other tested therapies such as below to maximize therapeutic effects in OVCA.

1. Nanomedicine based pGSN therapy

Nanotechnology has gained significant attention as a potentially alternative approach to cancer treatment due to its unique properties in size, advanced delivery, precise molecular level control of cellular and TME interactions[9]. Our laboratory has previously demonstrated that the C-terminus of the gelsolin protein sensitized chemoresistant OVCA cells to CDDP-induced apoptosis[11]. Thus, packaging the C-terminus in nanoparticles could serve as a novel therapeutic strategy to sensitize chemoresistant OVCA cells to CDDP-induced death.

Encapsulation of therapeutic peptides in biocompatible and biodegradable polymeric nanoparticles is an emerging trend in biopharmaceutic development. In collaboration with Dr. Dar-Bin Shieh (NCKU, Taiwan), we will design and optimize the nanoformulation tailored for the GSN sub-fragment. To effectively transfer the therapeutic GSN sub-fragment into target cancer cells, we will use a polymeric nano-vehicle with cell-penetrating peptide (CPPs) and cancer cell targeting ligand (folate-modified PEG; folate receptor is highly expressed on cancer cells but barely or minimally expressed on normal cells) as the platform **(Fig. 9.2)**. CPP-GSN sub-fragment complex will facilitate trans-membrane delivery of the peptide as guided by folate receptor-mediated cancer cell targeting. The transmembrane delivery of CPP-GSN sub-fragment

will first be validated *in vitro* by Western blotting. To compare the efficacy of the new nano-delivery system, *in vitro* cytotoxicity assays (MTT), cell cycle analysis, G2/M regulators investigation and mitosis and apoptosis evaluation will be performed to compare its mechanism of action. We will also assess and improve the stability, controlled release, and delivery of the complex and prepare pilot scale up for the animal study. Acute, sub-acute and chronic systemic toxicity of CPP-GSN-sub-fragment-PLGA-CDDP will be determined in vivo using 7-week-old BALB/c mice. The outcome from this study will provide the basis for future prospective clinical studies on their safety and effectiveness in chemoresistant OVCA treatment.

2. Immune Checkpoint Blockers (ICBs)

Previous studies on immunotherapies in OVCA have yielded modest positive outcomes. This has resulted in the combination of immunotherapies with other treatment modalities such as radiotherapy, chemotherapy and targeted therapies. These new approaches have shown therapeutic promise and hence, clinical trials are underway to further validate their safety and efficacy. Currently, there are ongoing clinical trials testing the combination of anti-CTLA-4 and PARP inhibitor (NCT02571725) as well as anti-PDL1 and bevacizumab (NCT02659384) in ovarian cancer patients. Pre-clinical studies have demonstrated the efficacy of anti-PDL1 and paclitaxel/carboplatin chemotherapy combination on ovarian cancer cells which has warranted an ongoing phase II clinical trial (NCT02520154) combining paclitaxel/carboplatin chemotherapy and pembrolizumab.

Combining pGSN inhibitors (oligonucleotide sequences that degrades pGSN mRNA) with immune checkpoint blockers (ICBs) could be tested in pre-clinical models, strategies that will generate important clinical information for subsequent clinical trials.

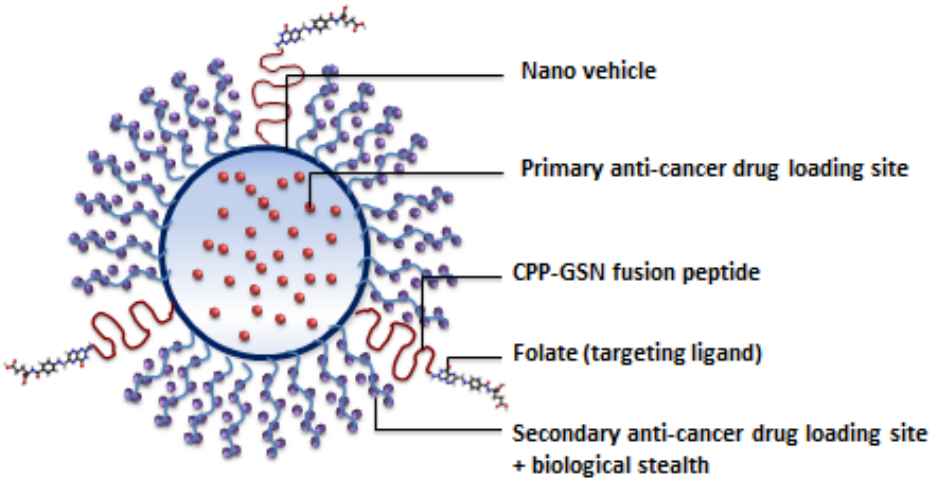

Fig. 9.3. Schematic diagram of therapeutic targeting nanoformulation with GSN sub-fragment. Nano-vehicle with cell-penetrating peptide (CPPs)-GSN complex, anti-cancer drug loading site and cancer cell targeting ligand (folate-modified PEG) as the platform. CPP-GSN sub-fragment complex with a sequence will facilitates trans-membrane delivery of the peptide as guided by folate receptor-mediated cancer cell targeting (Curtesy of Professor Dar-Bin Shieh, National Cheng Kong University, Tainan, Taiwan).

.

OVCA PDX models with chemosensitive and chemoresistant OVCA primary tumors will be established as previously discussed and tumour treated CDDP, pGSN inhibitors and/or anti-CTLA-4 monoclonal antibody intraperitoneally. pGSN inhibitors will suppress the expression and secretion of pGSN, a mechanism that will prevent the autocrine feedback of pGSN in OVCA cells as well as the paracrine suppression of immune cells. To demonstrate the efficacy of pGSN inhibitors in combination with/without the other treatments, tumours will be resected and their volumes measured for tumour growth. Immune cell infiltration and mice survival will be measured as previously discussed. We expect that the combination of pGSN inhibitors and anti-CTLA-4 monoclonal antibody will be associated with lower tumour burden, increased immune cell infiltration and prolonged mice survival.

CHAPTER 10 - CONCLUSION

This thesis delineates the cellular and molecular mechanisms of epithelial OVCA chemoresistance in both Western and Asian cohorts. We have demonstrated that pGSN increased ovarian tumour recurrence, chemoresistance and suppressed anti-tumor functions of immune cells, end points that were significantly associated with poor patient survival. These novel findings include: **a)** pGSN transported by small extracellular vesicles **b)** pGSN upregulated FAK/Akt/HIF1α–mediated pGSN endogenous expression in chemoresistant OVCA cells in an autocrine manner as well as conferred cisplatin resistance in otherwise chemosensitive OVCA cells; **c)** pGSN induced intracellular GSH in OVCA cells which led to decreased accumulation of CDDP (decreased phosphorylation of H2AX) and thus, reduced CDDP-induced apoptosis; **d)** pGSN decreased IFNγ production which was secondary to pGSN-mediated CD8+ T cell death via FLIP downregulation and caspase-8/3 activation; **e)** pGSN polarized CD4+ T cells to type II helper cells and **f)** pGSN induced M1 macrophage apoptosis resulting in decreased production of iNOS and TNFα.

In our clinical investigations of North American, Asian and public OVCA patient cohorts, we found that increased tissue pGSN expressions were significantly associated with advanced tumour stage, suboptimal residual disease, tumour recurrence, chemoresistance and poor survival. Also, increased pGSN was associated with lowered survival benefits of infiltrated CD8+ T cells and M1 macrophages in OVCA patients, outcomes that were associated with reduced PFS. Circulating pGSN presented a better early diagnostic marker and predictor of residual disease for OVCA patients compared with CA125. The test accuracy was further enhanced when circulating pGSN was combined with CA125 in a multivariate assay index.

Our findings provide mechanistic and clinical evidence of pGSN as an inhibitor of immune-surveillance and promoter of chemoresistance in epithelial OVCA. Our efforts provide useful information for OVCA early diagnosis and surgical outcomes as well as maximizing the efficiency of immunotherapy and combinational therapies for chemoresistant OVCA.

CHAPTER 11 - REFERENCES

Chapter 1

1. Bray F, Ferlay J, Soerjomataram I, Siegel RL, Torre LA, Jemal A. Global cancer statistics 2018: GLOBOCAN estimates of incidence and mortality worldwide for 36 cancers in 185 countries. *CA: a cancer journal for clinicians.* 2018;68(6):394-424.
2. Siegel RL, Miller KD, Jemal A. Cancer statistics, 2015. *CA: a cancer journal for clinicians.* 2015;65(1):5-29.
3. Release notice - Canadian Cancer Statistics 2019. *Health Promot Chronic Dis Prev Can.* 2019;39(8-9):255.
4. Noone AM, Cronin KA, Altekruse SF, et al. Cancer Incidence and Survival Trends by Subtype Using Data from the Surveillance Epidemiology and End Results Program, 1992-2013. *Cancer epidemiology, biomarkers & prevention : a publication of the American Association for Cancer Research, cosponsored by the American Society of Preventive Oncology.* 2017;26(4):632-641.
5. Torre LA, Trabert B, DeSantis CE, et al. Ovarian cancer statistics, 2018. *CA: a cancer journal for clinicians.* 2018;68(4):284-296.
6. Prat J. Ovarian carcinomas: five distinct diseases with different origins, genetic alterations, and clinicopathological features. *Virchows Archiv : an international journal of pathology.* 2012;460(3):237-249.
7. Prat J, D'Angelo E, Espinosa I. Ovarian carcinomas: at least five different diseases with distinct histological features and molecular genetics. *Human pathology.* 2018;80:11-27.
8. Lheureux S, Braunstein M, Oza AM. Epithelial ovarian cancer: Evolution of management in the era of precision medicine. *CA: a cancer journal for clinicians.* 2019;69(4):280-304.

9. Jelovac D, Armstrong DK. Recent progress in the diagnosis and treatment of ovarian cancer. *CA: a cancer journal for clinicians.* 2011;61(3):183-203.

10. Hunn J, Rodriguez GC. Ovarian cancer: etiology, risk factors, and epidemiology. *Clin Obstet Gynecol.* 2012;55(1):3-23.

11. Saito T, Katabuchi H. Annual Report of the Committee on Gynecologic Oncology, Japan Society of Obstetrics and Gynecology: Patient Annual Report for 2013 and Treatment Annual Report for 2008. *J Obstet Gynaecol Res.* 2016;42(9):1069-1079.

12. Goldgar DE, Easton DF, Cannon-Albright LA, Skolnick MH. Systematic population-based assessment of cancer risk in first-degree relatives of cancer probands. *J Natl Cancer Inst.* 1994;86(21):1600-1608.

13. Schildkraut JM, Risch N, Thompson WD. Evaluating genetic association among ovarian, breast, and endometrial cancer: evidence for a breast/ovarian cancer relationship. *Am J Hum Genet.* 1989;45(4):521-529.

14. Toss A, Tomasello C, Razzaboni E, et al. Hereditary ovarian cancer: not only BRCA 1 and 2 genes. *BioMed research international.* 2015;2015:341723.

15. Walsh T, Casadei S, Coats KH, et al. Spectrum of mutations in BRCA1, BRCA2, CHEK2, and TP53 in families at high risk of breast cancer. *Jama.* 2006;295(12):1379-1388.

16. Yun MH, Hiom K. Understanding the functions of BRCA1 in the DNA-damage response. *Biochemical Society transactions.* 2009;37(Pt 3):597-604.

17. Cipak L, Watanabe N, Bessho T. The role of BRCA2 in replication-coupled DNA interstrand cross-link repair in vitro. *Nat Struct Mol Biol.* 2006;13(8):729-733.

18. Metcalfe KA, Poll A, Royer R, et al. Screening for founder mutations in BRCA1 and BRCA2 in unselected Jewish women. *Journal of clinical oncology : official journal of the American Society of Clinical Oncology*. 2010;28(3):387-391.

19. Sekine M, Nagata H, Tsuji S, et al. Mutational analysis of BRCA1 and BRCA2 and clinicopathologic analysis of ovarian cancer in 82 ovarian cancer families: two common founder mutations of BRCA1 in Japanese population. *Clinical cancer research : an official journal of the American Association for Cancer Research.* 2001;7(10):3144-3150.

20. Foulkes WD. Inherited susceptibility to common cancers. *The New England journal of medicine.* 2008;359(20):2143-2153.

21. Schrader KA, Hurlburt J, Kalloger SE, et al. Germline BRCA1 and BRCA2 mutations in ovarian cancer: utility of a histology-based referral strategy. *Obstetrics and gynecology.* 2012;120(2 Pt 1):235-240.

22. Zhang S, Royer R, Li S, et al. Frequencies of BRCA1 and BRCA2 mutations among 1,342 unselected patients with invasive ovarian cancer. *Gynecologic oncology.* 2011;121(2):353-357.

23. Pal T, Permuth-Wey J, Betts JA, et al. BRCA1 and BRCA2 mutations account for a large proportion of ovarian carcinoma cases. *Cancer.* 2005;104(12):2807-2816.

24. Jazaeri AA, Lu K, Schmandt R, et al. Molecular determinants of tumor differentiation in papillary serous ovarian carcinoma. *Molecular carcinogenesis.* 2003;36(2):53-59.

25. Bolton KL, Chenevix-Trench G, Goh C, et al. Association between BRCA1 and BRCA2 mutations and survival in women with invasive epithelial ovarian cancer. *Jama.* 2012;307(4):382-390.

26. Tan DS, Kaye SB. Chemotherapy for Patients with BRCA1 and BRCA2-Mutated Ovarian Cancer: Same or Different? *Am Soc Clin Oncol Educ Book.* 2015:114-121.

27. Tan DS, Rothermundt C, Thomas K, et al. "BRCAness" syndrome in ovarian cancer: a case-control study describing the clinical features and outcome of patients with epithelial ovarian cancer associated with BRCA1 and BRCA2 mutations. *Journal of clinical oncology : official journal of the American Society of Clinical Oncology.* 2008;26(34):5530-5536.

28. Vencken PM, Kriege M, Hoogwerf D, et al. Chemosensitivity and outcome of BRCA1- and BRCA2-associated ovarian cancer patients after first-line chemotherapy compared with sporadic ovarian cancer patients. *Annals of oncology : official journal of the European Society for Medical Oncology.* 2011;22(6):1346-1352.

29. Pennington KP, Walsh T, Harrell MI, et al. Germline and somatic mutations in homologous recombination genes predict platinum response and survival in ovarian, fallopian tube, and peritoneal carcinomas. *Clinical cancer research : an official journal of the American Association for Cancer Research.* 2014;20(3):764-775.

30. Lynch HT, Casey MJ, Snyder CL, et al. Hereditary ovarian carcinoma: heterogeneity, molecular genetics, pathology, and management. *Mol Oncol.* 2009;3(2):97-137.

31. Lindor NM, Petersen GM, Hadley DW, et al. Recommendations for the care of individuals with an inherited predisposition to Lynch syndrome: a systematic review. *Jama.* 2006;296(12):1507-1517.

32. Bonadona V, Bonaiti B, Olschwang S, et al. Cancer risks associated with germline mutations in MLH1, MSH2, and MSH6 genes in Lynch syndrome. *Jama.* 2011;305(22):2304-2310.

33. Guillotin D, Martin SA. Exploiting DNA mismatch repair deficiency as a therapeutic strategy. *Experimental cell research.* 2014;329(1):110-115.

34. Ketabi Z, Bartuma K, Bernstein I, et al. Ovarian cancer linked to Lynch syndrome typically presents as early-onset, non-serous epithelial tumors. *Gynecologic oncology.* 2011;121(3):462-465.

35. Ledermann JA, Drew Y, Kristeleit RS. Homologous recombination deficiency and ovarian cancer. *European journal of cancer (Oxford, England : 1990).* 2016;60:49-58.

36. Rojas V, Hirshfield KM, Ganesan S, Rodriguez-Rodriguez L. Molecular Characterization of Epithelial Ovarian Cancer: Implications for Diagnosis and Treatment. *International journal of molecular sciences.* 2016;17(12).

37. Integrated genomic analyses of ovarian carcinoma. *Nature.* 2011;474(7353):609-615.

38. Norquist BM, Harrell MI, Brady MF, et al. Inherited Mutations in Women With Ovarian Carcinoma. *JAMA Oncol.* 2016;2(4):482-490.

39. Shih Ie M, Kurman RJ. Ovarian tumorigenesis: a proposed model based on morphological and molecular genetic analysis. *The American journal of pathology.* 2004;164(5):1511-1518.

40. Karnezis AN, Cho KR, Gilks CB, Pearce CL, Huntsman DG. The disparate origins of ovarian cancers: pathogenesis and prevention strategies. *Nature reviews Cancer.* 2017;17(1):65-74.

41. Prat J. New insights into ovarian cancer pathology. In: *Ann Oncol.* Vol 23 Suppl 10. England2012:x111-117.

42. Salani R, Kurman RJ, Giuntoli R, 2nd, et al. Assessment of TP53 mutation using purified tissue samples of ovarian serous carcinomas reveals a higher mutation rate than

previously reported and does not correlate with drug resistance. *International journal of gynecological cancer : official journal of the International Gynecological Cancer Society.* 2008;18(3):487-491.

43. Bowtell DD. The genesis and evolution of high-grade serous ovarian cancer. In: *Nat Rev Cancer.* Vol 10. England2010:803-808.

44. Kroeger PT, Jr., Drapkin R. Pathogenesis and heterogeneity of ovarian cancer. *Curr Opin Obstet Gynecol.* 2017;29(1):26-34.

45. Tashiro H, Miyazaki K, Okamura H, Iwai A, Fukumoto M. c-myc over-expression in human primary ovarian tumours: its relevance to tumour progression. *International journal of cancer Journal international du cancer.* 1992;50(5):828-833.

46. Piek JM, van Diest PJ, Zweemer RP, et al. Dysplastic changes in prophylactically removed Fallopian tubes of women predisposed to developing ovarian cancer. *The Journal of pathology.* 2001;195(4):451-456.

47. Folkins AK, Jarboe EA, Roh MH, Crum CP. Precursors to pelvic serous carcinoma and their clinical implications. *Gynecologic oncology.* 2009;113(3):391-396.

48. Kurman RJ. Origin and molecular pathogenesis of ovarian high-grade serous carcinoma. *Annals of oncology : official journal of the European Society for Medical Oncology.* 2013;24 Suppl 10:x16-21.

49. Singh N, Gilks CB, Hirshowitz L, Wilkinson N, McCluggage WG. Adopting a Uniform Approach to Site Assignment in Tubo-Ovarian High-Grade Serous Carcinoma: The Time has Come. *Int J Gynecol Pathol.* 2016;35(3):230-237.

50. Auersperg N. Ovarian surface epithelium as a source of ovarian cancers: unwarranted speculation or evidence-based hypothesis? *Gynecologic oncology.* 2013;130(1):246-251.

51. Adler E, Mhawech-Fauceglia P, Gayther SA, Lawrenson K. PAX8 expression in ovarian surface epithelial cells. *Human pathology.* 2015;46(7):948-956.

52. Gourley C, Farley J, Provencher DM, et al. Gynecologic Cancer InterGroup (GCIG) consensus review for ovarian and primary peritoneal low-grade serous carcinomas. *International journal of gynecological cancer : official journal of the International Gynecological Cancer Society.* 2014;24(9 Suppl 3):S9-13.

53. Liliac L, Carcangiu ML, Canevari S, et al. The value of PAX8 and WT1 molecules in ovarian cancer diagnosis. *Rom J Morphol Embryol.* 2013;54(1):17-27.

54. Wong KK, Gershenson D. The continuum of serous tumors of low malignant potential and low-grade serous carcinomas of the ovary. *Dis Markers.* 2007;23(5-6):377-387.

55. Motohara T, Tashiro H, Miyahara Y, Sakaguchi I, Ohtake H, Katabuchi H. Long-term oncological outcomes of ovarian serous carcinomas with psammoma bodies: a novel insight into the molecular pathogenesis of ovarian epithelial carcinoma. *Cancer Sci.* 2010;101(6):1550-1556.

56. Jones S, Wang TL, Kurman RJ, et al. Low-grade serous carcinomas of the ovary contain very few point mutations. *J Pathol.* 2012;226(3):413-420.

57. Singer G, Oldt R, 3rd, Cohen Y, et al. Mutations in BRAF and KRAS characterize the development of low-grade ovarian serous carcinoma. *J Natl Cancer Inst.* 2003;95(6):484-486.

58. Sainz de la Cuesta R, Eichhorn JH, Rice LW, Fuller AF, Jr., Nikrui N, Goff BA. Histologic transformation of benign endometriosis to early epithelial ovarian cancer. *Gynecologic oncology.* 1996;60(2):238-244.

59. Scully RE, Richardson GS, Barlow JF. The development of malignancy in endometriosis. *Clin Obstet Gynecol.* 1966;9(2):384-411.

60. Fukunaga M, Nomura K, Ishikawa E, Ushigome S. Ovarian atypical endometriosis: its close association with malignant epithelial tumours. *Histopathology.* 1997;30(3):249-255.

61. Kobayashi H, Kajiwara H, Kanayama S, et al. Molecular pathogenesis of endometriosis-associated clear cell carcinoma of the ovary (review). *Oncology reports.* 2009;22(2):233-240.

62. Yamaguchi K, Mandai M, Toyokuni S, et al. Contents of endometriotic cysts, especially the high concentration of free iron, are a possible cause of carcinogenesis in the cysts through the iron-induced persistent oxidative stress. *Clinical cancer research : an official journal of the American Association for Cancer Research.* 2008;14(1):32-40.

63. McConechy MK, Ding J, Senz J, et al. Ovarian and endometrial endometrioid carcinomas have distinct CTNNB1 and PTEN mutation profiles. *Mod Pathol.* 2014;27(1):128-134.

64. Wright K, Wilson P, Morland S, et al. beta-catenin mutation and expression analysis in ovarian cancer: exon 3 mutations and nuclear translocation in 16% of endometrioid tumours. *Int J Cancer.* 1999;82(5):625-629.

65. del Carmen MG, Birrer M, Schorge JO. Clear cell carcinoma of the ovary: a review of the literature. *Gynecologic oncology.* 2012;126(3):481-490.

66. Fujiwara K, McAlpine JN, Lheureux S, Matsumura N, Oza AM. Paradigm Shift in the Management Strategy for Epithelial Ovarian Cancer. *Am Soc Clin Oncol Educ Book.* 2016;35:e247-257.

67. Senkel S, Lucas B, Klein-Hitpass L, Ryffel GU. Identification of target genes of the transcription factor HNF1beta and HNF1alpha in a human embryonic kidney cell line. *Biochimica et biophysica acta.* 2005;1731(3):179-190.

68. Tanaka T, Tomaru Y, Nomura Y, Miura H, Suzuki M, Hayashizaki Y. Comprehensive search for HNF-1beta-regulated genes in mouse hepatoma cells perturbed by transcription regulatory factor-targeted RNAi. *Nucleic Acids Res.* 2004;32(9):2740-2750.

69. Komiyama S, Aoki D, Tominaga E, Susumu N, Udagawa Y, Nozawa S. Prognosis of Japanese patients with ovarian clear cell carcinoma associated with pelvic endometriosis: clinicopathologic evaluation. *Gynecologic oncology.* 1999;72(3):342-346.

70. Matsuo Y, Tashiro H, Yanai H, Moriya T, Katabuchi H. Clinicopathological heterogeneity in ovarian clear cell adenocarcinoma: a study on individual therapy practice. *Medical molecular morphology.* 2015;48(3):146-154.

71. Veras E, Mao TL, Ayhan A, et al. Cystic and adenofibromatous clear cell carcinomas of the ovary: distinctive tumors that differ in their pathogenesis and behavior: a clinicopathologic analysis of 122 cases. *The American journal of surgical pathology.* 2009;33(6):844-853.

72. Yamamoto S, Tsuda H, Yoshikawa T, et al. Clear cell adenocarcinoma associated with clear cell adenofibromatous components: a subgroup of ovarian clear cell adenocarcinoma with distinct clinicopathologic characteristics. *The American journal of surgical pathology.* 2007;31(7):999-1006.

73. Itamochi H, Oishi T, Oumi N, et al. Whole-genome sequencing revealed novel prognostic biomarkers and promising targets for therapy of ovarian clear cell carcinoma. *British journal of cancer.* 2017;117(5):717-724.

74. Hashiguchi Y, Tsuda H, Inoue T, Berkowitz RS, Mok SC. PTEN expression in clear cell adenocarcinoma of the ovary. *Gynecologic oncology.* 2006;101(1):71-75.

75. Shibuya Y, Tokunaga H, Saito S, et al. Identification of somatic genetic alterations in ovarian clear cell carcinoma with next generation sequencing. *Genes, chromosomes & cancer.* 2018;57(2):51-60.

76. Seidman JD, Kurman RJ, Ronnett BM. Primary and metastatic mucinous adenocarcinomas in the ovaries: incidence in routine practice with a new approach to improve intraoperative diagnosis. *The American journal of surgical pathology.* 2003;27(7):985-993.

77. Jang JYA, Yanaihara N, Pujade-Lauraine E, et al. Update on rare epithelial ovarian cancers: based on the Rare Ovarian Tumors Young Investigator Conference. *Journal of gynecologic oncology.* 2017;28(4):e54.

78. Zaino RJ, Brady MF, Lele SM, Michael H, Greer B, Bookman MA. Advanced stage mucinous adenocarcinoma of the ovary is both rare and highly lethal: a Gynecologic Oncology Group study. *Cancer.* 2011;117(3):554-562.

79. Park SY, Kim HS, Hong EK, Kim WH. Expression of cytokeratins 7 and 20 in primary carcinomas of the stomach and colorectum and their value in the differential diagnosis of metastatic carcinomas to the ovary. *Human pathology.* 2002;33(11):1078-1085.

80. Heinzelmann-Schwarz VA, Gardiner-Garden M, Henshall SM, et al. A distinct molecular profile associated with mucinous epithelial ovarian cancer. *British journal of cancer.* 2006;94(6):904-913.

81. Hunter SM, Gorringe KL, Christie M, Rowley SM, Bowtell DD, Campbell IG. Pre-invasive ovarian mucinous tumors are characterized by CDKN2A and RAS pathway

aberrations. *Clinical cancer research : an official journal of the American Association for Cancer Research.* 2012;18(19):5267-5277.

82. Ryland GL, Hunter SM, Doyle MA, et al. Mutational landscape of mucinous ovarian carcinoma and its neoplastic precursors. *Genome medicine.* 2015;7(1):87.

83. Anglesio MS, Kommoss S, Tolcher MC, et al. Molecular characterization of mucinous ovarian tumours supports a stratified treatment approach with HER2 targeting in 19% of carcinomas. *The Journal of pathology.* 2013;229(1):111-120.

84. Prat J. FIGO's staging classification for cancer of the ovary, fallopian tube, and peritoneum: abridged republication. *Journal of gynecologic oncology.* 2015;26(2):87-89.

85. Benedet JL, Bender H, Jones H, 3rd, Ngan HY, Pecorelli S. FIGO staging classifications and clinical practice guidelines in the management of gynecologic cancers. FIGO Committee on Gynecologic Oncology. *International journal of gynaecology and obstetrics: the official organ of the International Federation of Gynaecology and Obstetrics.* 2000;70(2):209-262.

86. Silverberg SG. Histopathologic grading of ovarian carcinoma: a review and proposal. *Int J Gynecol Pathol.* 2000;19(1):7-15.

87. Malpica A, Deavers MT, Lu K, et al. Grading ovarian serous carcinoma using a two-tier system. *The American journal of surgical pathology.* 2004;28(4):496-504.

88. Morgado M, Sutton MN, Simmons M, et al. Tumor necrosis factor-alpha and interferon-gamma stimulate MUC16 (CA125) expression in breast, endometrial and ovarian cancers through NFkappaB. *Oncotarget.* 2016;7(12):14871-14884.

89. Jacobs IJ, Skates S, Davies AP, et al. Risk of diagnosis of ovarian cancer after raised serum CA 125 concentration: a prospective cohort study. *Bmj.* 1996;313(7069):1355-1358.

90. Jacobs IJ, Menon U, Ryan A, et al. Ovarian cancer screening and mortality in the UK Collaborative Trial of Ovarian Cancer Screening (UKCTOCS): a randomised controlled trial. *Lancet (London, England).* 2016;387(10022):945-956.

91. Jacobs I, Bast RC, Jr. The CA 125 tumour-associated antigen: a review of the literature. *Human reproduction (Oxford, England).* 1989;4(1):1-12.

92. Arakawa N, Miyagi E, Nomura A, et al. Secretome-based identification of TFPI2, a novel serum biomarker for detection of ovarian clear cell adenocarcinoma. *Journal of proteome research.* 2013;12(10):4340-4350.

93. Bourne TH, Hampson J, Reynolds K, Collins WP, Campbell S. Screening for early ovarian cancer. *British journal of hospital medicine.* 1992;48(8):454-459.

94. Bourne TH, Campbell S, Reynolds KM, et al. Screening for early familial ovarian cancer with transvaginal ultrasonography and colour blood flow imaging. *Bmj.* 1993;306(6884):1025-1029.

95. van Nagell JR, Jr., DePriest PD, Reedy MB, et al. The efficacy of transvaginal sonographic screening in asymptomatic women at risk for ovarian cancer. *Gynecologic oncology.* 2000;77(3):350-356.

96. van Nagell JR, Jr., DePriest PD, Ueland FR, et al. Ovarian cancer screening with annual transvaginal sonography: findings of 25,000 women screened. *Cancer.* 2007;109(9):1887-1896.

97. Jacobs I, Stabile I, Bridges J, et al. Multimodal approach to screening for ovarian cancer. *Lancet (London, England).* 1988;1(8580):268-271.

98. Jacobs IJ, Skates SJ, MacDonald N, et al. Screening for ovarian cancer: a pilot randomised controlled trial. *Lancet (London, England).* 1999;353(9160):1207-1210.

99. Siegel RL, Miller KD, Jemal A. Cancer statistics, 2018. *CA: a cancer journal for clinicians.* 2018;68(1):7-30.

100. Prat J. Staging classification for cancer of the ovary, fallopian tube, and peritoneum. *International journal of gynaecology and obstetrics: the official organ of the International Federation of Gynaecology and Obstetrics.* 2014;124(1):1-5.

101. Harter P, Sehouli J, Lorusso D, et al. A Randomized Trial of Lymphadenectomy in Patients with Advanced Ovarian Neoplasms. *The New England journal of medicine.* 2019;380(9):822-832.

102. Garcia-Soto AE, Boren T, Wingo SN, Heffernen T, Miller DS. Is comprehensive surgical staging needed for thorough evaluation of early-stage ovarian carcinoma? *American journal of obstetrics and gynecology.* 2012;206(3):242.e241-245.

103. du Bois A, Reuss A, Pujade-Lauraine E, Harter P, Ray-Coquard I, Pfisterer J. Role of surgical outcome as prognostic factor in advanced epithelial ovarian cancer: a combined exploratory analysis of 3 prospectively randomized phase 3 multicenter trials: by the Arbeitsgemeinschaft Gynaekologische Onkologie Studiengruppe Ovarialkarzinom (AGO-OVAR) and the Groupe d'Investigateurs Nationaux Pour les Etudes des Cancers de l'Ovaire (GINECO). *Cancer.* 2009;115(6):1234-1244.

104. Chi DS, Eisenhauer EL, Lang J, et al. What is the optimal goal of primary cytoreductive surgery for bulky stage IIIC epithelial ovarian carcinoma (EOC)? *Gynecologic oncology*. 2006;103(2):559-564.

105. Winter WE, 3rd, Maxwell GL, Tian C, et al. Tumor residual after surgical cytoreduction in prediction of clinical outcome in stage IV epithelial ovarian cancer: a Gynecologic Oncology Group Study. *Journal of clinical oncology : official journal of the American Society of Clinical Oncology*. 2008;26(1):83-89.

106. Eisenhauer EL, Abu-Rustum NR, Sonoda Y, Aghajanian C, Barakat RR, Chi DS. The effect of maximal surgical cytoreduction on sensitivity to platinum-taxane chemotherapy and subsequent survival in patients with advanced ovarian cancer. *Gynecologic oncology*. 2008;108(2):276-281.

107. Katsumata N, Yasuda M, Isonishi S, et al. Long-term results of dose-dense paclitaxel and carboplatin versus conventional paclitaxel and carboplatin for treatment of advanced epithelial ovarian, fallopian tube, or primary peritoneal cancer (JGOG 3016): a randomised, controlled, open-label trial. *The Lancet Oncology*. 2013;14(10):1020-1026.

108. Katsumata N, Yasuda M, Takahashi F, et al. Dose-dense paclitaxel once a week in combination with carboplatin every 3 weeks for advanced ovarian cancer: a phase 3, open-label, randomised controlled trial. *Lancet (London, England)*. 2009;374(9698):1331-1338.

109. Komiyama S, Katabuchi H, Mikami M, et al. Japan Society of Gynecologic Oncology guidelines 2015 for the treatment of ovarian cancer including primary peritoneal cancer and fallopian tube cancer. *International journal of clinical oncology*. 2016;21(3):435-446.

110. Armstrong DK, Bundy B, Wenzel L, et al. Intraperitoneal cisplatin and paclitaxel in ovarian cancer. *The New England journal of medicine.* 2006;354(1):34-43.

111. Jaaback K, Johnson N, Lawrie TA. Intraperitoneal chemotherapy for the initial management of primary epithelial ovarian cancer. *The Cochrane database of systematic reviews.* 2016(1):Cd005340.

112. Graybill W, Sood AK, Monk BJ, Coleman RL. State of the science: Emerging therapeutic strategies for targeting angiogenesis in ovarian cancer. *Gynecologic oncology.* 2015;138(2):223-226.

113. Perren TJ, Swart AM, Pfisterer J, et al. A phase 3 trial of bevacizumab in ovarian cancer. *The New England journal of medicine.* 2011;365(26):2484-2496.

114. Burger RA, Brady MF, Bookman MA, et al. Incorporation of bevacizumab in the primary treatment of ovarian cancer. *The New England journal of medicine.* 2011;365(26):2473-2483.

115. du Bois A, Kristensen G, Ray-Coquard I, et al. Standard first-line chemotherapy with or without nintedanib for advanced ovarian cancer (AGO-OVAR 12): a randomised, double-blind, placebo-controlled phase 3 trial. *The Lancet Oncology.* 2016;17(1):78-89.

116. Helleday T, Petermann E, Lundin C, Hodgson B, Sharma RA. DNA repair pathways as targets for cancer therapy. *Nature reviews Cancer.* 2008;8(3):193-204.

117. Cass I, Baldwin RL, Varkey T, Moslehi R, Narod SA, Karlan BY. Improved survival in women with BRCA-associated ovarian carcinoma. *Cancer.* 2003;97(9):2187-2195.

118. Ledermann J, Harter P, Gourley C, et al. Olaparib maintenance therapy in platinum-sensitive relapsed ovarian cancer. *The New England journal of medicine.* 2012;366(15):1382-1392.

119. Ledermann J, Harter P, Gourley C, et al. Olaparib maintenance therapy in patients with platinum-sensitive relapsed serous ovarian cancer: a preplanned retrospective analysis of outcomes by BRCA status in a randomised phase 2 trial. *The Lancet Oncology*. 2014;15(8):852-861.

120. Coleman RL, Sill MW, Bell-McGuinn K, et al. A phase II evaluation of the potent, highly selective PARP inhibitor veliparib in the treatment of persistent or recurrent epithelial ovarian, fallopian tube, or primary peritoneal cancer in patients who carry a germline BRCA1 or BRCA2 mutation - An NRG Oncology/Gynecologic Oncology Group study. *Gynecologic oncology*. 2015;137(3):386-391.

121. Dobrzanski MJ, Rewers-Felkins KA, Samad KA, et al. Immunotherapy with IL-10- and IFN-gamma-producing CD4 effector cells modulate "Natural" and "Inducible" CD4 TReg cell subpopulation levels: observations in four cases of patients with ovarian cancer. *Cancer immunology, immunotherapy : CII*. 2012;61(6):839-854.

122. Leffers N, Lambeck AJ, Gooden MJ, et al. Immunization with a P53 synthetic long peptide vaccine induces P53-specific immune responses in ovarian cancer patients, a phase II trial. *International journal of cancer Journal international du cancer*. 2009;125(9):2104-2113.

123. Ohno S, Kyo S, Myojo S, et al. Wilms' tumor 1 (WT1) peptide immunotherapy for gynecological malignancy. *Anticancer research*. 2009;29(11):4779-4784.

124. Wagner U, Kohler S, Reinartz S, et al. Immunological consolidation of ovarian carcinoma recurrences with monoclonal anti-idiotype antibody ACA125: immune responses and survival in palliative treatment. See The biology behind: K. A. Foon and M. Bhattacharya-Chatterjee, Are solid tumor anti-idiotype vaccines ready for prime time?

Clin. Cancer Res., 7:1112-1115, 2001. *Clinical cancer research : an official journal of the American Association for Cancer Research.* 2001;7(5):1154-1162.

125. Hamanishi J, Mandai M, Ikeda T, et al. Safety and Antitumor Activity of Anti-PD-1 Antibody, Nivolumab, in Patients With Platinum-Resistant Ovarian Cancer. *Journal of clinical oncology : official journal of the American Society of Clinical Oncology.* 2015;33(34):4015-4022.

126. Hamanishi J, Mandai M, Iwasaki M, et al. Programmed cell death 1 ligand 1 and tumor-infiltrating CD8+ T lymphocytes are prognostic factors of human ovarian cancer. *Proceedings of the National Academy of Sciences of the United States of America.* 2007;104(9):3360-3365.

127. Brahmer JR, Tykodi SS, Chow LQ, et al. Safety and activity of anti-PD-L1 antibody in patients with advanced cancer. *The New England journal of medicine.* 2012;366(26):2455-2465.

128. Zamarin D, Burger RA, Sill MW, et al. Randomized Phase II Trial of Nivolumab Versus Nivolumab and Ipilimumab for Recurrent or Persistent Ovarian Cancer: An NRG Oncology Study. *Journal of clinical oncology : official journal of the American Society of Clinical Oncology.* 2020:Jco1902059.

129. Pedersen M, Westergaard MCW, Milne K, et al. Adoptive cell therapy with tumor-infiltrating lymphocytes in patients with metastatic ovarian cancer: a pilot study. *Oncoimmunology.* 2018;7(12):e1502905.

130. Colombo N, Gore M. Treatment of recurrent ovarian cancer relapsing 6-12 months post platinum-based chemotherapy. *Critical reviews in oncology/hematology.* 2007;64(2):129-138.

131. Markman M, Markman J, Webster K, et al. Duration of response to second-line, platinum-based chemotherapy for ovarian cancer: implications for patient management and clinical trial design. *Journal of clinical oncology : official journal of the American Society of Clinical Oncology.* 2004;22(15):3120-3125.

132. Zeng B, Zhou M, Wu H, Xiong Z. SPP1 promotes ovarian cancer progression via Integrin beta1/FAK/AKT signaling pathway. *OncoTargets and therapy.* 2018;11:1333-1343.

133. Page C, Lin HJ, Jin Y, et al. Overexpression of Akt/AKT can modulate chemotherapy-induced apoptosis. *Anticancer research.* 2000;20(1a):407-416.

134. Yang X, Fraser M, Moll UM, Basak A, Tsang BK. Akt-mediated cisplatin resistance in ovarian cancer: modulation of p53 action on caspase-dependent mitochondrial death pathway. *Cancer research.* 2006;66(6):3126-3136.

135. Mitsiades CS, Mitsiades N, Koutsilieris M. The Akt pathway: molecular targets for anti-cancer drug development. *Current cancer drug targets.* 2004;4(3):235-256.

136. Levine AJ. p53, the cellular gatekeeper for growth and division. *Cell.* 1997;88(3):323-331.

137. Lasky T, Silbergeld E. P53 mutations associated with breast, colorectal, liver, lung, and ovarian cancers. *Environmental health perspectives.* 1996;104(12):1324-1331.

138. Fraser M, Leung BM, Yan X, Dan HC, Cheng JQ, Tsang BK. p53 is a determinant of X-linked inhibitor of apoptosis protein/Akt-mediated chemoresistance in human ovarian cancer cells. *Cancer research.* 2003;63(21):7081-7088.

139. Pink RC, Samuel P, Massa D, Caley DP, Brooks SA, Carter DR. The passenger strand, miR-21-3p, plays a role in mediating cisplatin resistance in ovarian cancer cells. *Gynecologic oncology.* 2015;137(1):143-151.

140. Au Yeung CL, Co NN, Tsuruga T, et al. Exosomal transfer of stroma-derived miR21 confers paclitaxel resistance in ovarian cancer cells through targeting APAF1. *Nature communications.* 2016;7:11150.

141. Ying X, Wu Q, Wu X, et al. Epithelial ovarian cancer-secreted exosomal miR-222-3p induces polarization of tumor-associated macrophages. *Oncotarget.* 2016;7(28):43076-43087.

142. Shulga N, Wilson-Smith R, Pastorino JG. Hexokinase II detachment from the mitochondria potentiates cisplatin induced cytotoxicity through a caspase-2 dependent mechanism. *Cell cycle (Georgetown, Tex).* 2009;8(20):3355-3364.

143. Suh DH, Kim MA, Kim H, et al. Association of overexpression of hexokinase II with chemoresistance in epithelial ovarian cancer. *Clinical and experimental medicine.* 2014;14(3):345-353.

144. Gomez-Roman N, Sahasrabudhe NM, McGregor F, Chalmers AJ, Cassidy J, Plumb J. Hypoxia-inducible factor 1 alpha is required for the tumourigenic and aggressive phenotype associated with Rab25 expression in ovarian cancer. *Oncotarget.* 2016;7(16):22650-22664.

145. Tiwari AK, Sodani K, Dai CL, Ashby CR, Jr., Chen ZS. Revisiting the ABCs of multidrug resistance in cancer chemotherapy. *Current pharmaceutical biotechnology.* 2011;12(4):570-594.

146. Morrow CS, Peklak-Scott C, Bishwokarma B, Kute TE, Smitherman PK, Townsend AJ. Multidrug resistance protein 1 (MRP1, ABCC1) mediates resistance to mitoxantrone via glutathione-dependent drug efflux. *Molecular pharmacology.* 2006;69(4):1499-1505.

147. Sodani K, Patel A, Kathawala RJ, Chen ZS. Multidrug resistance associated proteins in multidrug resistance. *Chin J Cancer.* 2012;31(2):58-72.

148. Mo L, Pospichalova V, Huang Z, et al. Ascites Increases Expression/Function of Multidrug Resistance Proteins in Ovarian Cancer Cells. *PLoS One.* 2015;10(7):e0131579.

149. Gee ME, Faraahi Z, McCormick A, Edmondson RJ. DNA damage repair in ovarian cancer: unlocking the heterogeneity. *Journal of ovarian research.* 2018;11(1):50.

150. Rodriguez GM, Galpin KJC, McCloskey CW, Vanderhyden BC. The Tumor Microenvironment of Epithelial Ovarian Cancer and Its Influence on Response to Immunotherapy. *Cancers.* 2018;10(8).

151. Galluzzi L, Buque A, Kepp O, Zitvogel L, Kroemer G. Immunological Effects of Conventional Chemotherapy and Targeted Anticancer Agents. *Cancer cell.* 2015;28(6):690-714.

152. Plooy AC, van Dijk M, Lohman PH. Induction and repair of DNA cross-links in chinese hamster ovary cells treated with various platinum coordination compounds in relation to platinum binding to DNA, cytotoxicity, mutagenicity, and antitumor activity. *Cancer research.* 1984;44(5):2043-2051.

153. Ise T, Shimizu T, Lee EL, Inoue H, Kohno K, Okada Y. Roles of volume-sensitive Cl-channel in cisplatin-induced apoptosis in human epidermoid cancer cells. *J Membr Biol.* 2005;205(3):139-145.

154. Munchausen LL, Rahn RO. Physical studies on the binding of cis-dichlorodiamine platinum (II) to DNA and homopolynucleotides. *Biochimica et biophysica acta.* 1975;414(3):242-255.

155. Perez RP. Cellular and molecular determinants of cisplatin resistance. *European journal of cancer (Oxford, England : 1990).* 1998;34(10):1535-1542.

156. Jamieson ER, Lippard SJ. Structure, Recognition, and Processing of Cisplatin-DNA Adducts. *Chemical reviews.* 1999;99(9):2467-2498.

157. Siddik ZH. Cisplatin: mode of cytotoxic action and molecular basis of resistance. *Oncogene.* 2003;22(47):7265-7279.

158. Zamzami N, Kroemer G. The mitochondrion in apoptosis: how Pandora's box opens. *Nature reviews Molecular cell biology.* 2001;2(1):67-71.

159. Olivero OA, Chang PK, Lopez-Larraza DM, Semino-Mora MC, Poirier MC. Preferential formation and decreased removal of cisplatin-DNA adducts in Chinese hamster ovary cell mitochondrial DNA as compared to nuclear DNA. *Mutation research.* 1997;391(1-2):79-86.

160. Murata T, Hibasami H, Maekawa S, Tagawa T, Nakashima K. Preferential binding of cisplatin to mitochondrial DNA and suppression of ATP generation in human malignant melanoma cells. *Biochemistry international.* 1990;20(5):949-955.

161. Ishida S, Lee J, Thiele DJ, Herskowitz I. Uptake of the anticancer drug cisplatin mediated by the copper transporter Ctr1 in yeast and mammals. *Proceedings of the National Academy of Sciences of the United States of America.* 2002;99(22):14298-14302.

162. Safaei R, Otani S, Larson BJ, Rasmussen ML, Howell SB. Transport of cisplatin by the copper efflux transporter ATP7B. *Molecular pharmacology.* 2008;73(2):461-468.

163. Ozols R. Treatment of gynecologic cancer: the US experience. *Tumori.* 1999;85(3 Suppl 1):S5-11.

164. Patch AM, Christie EL, Etemadmoghadam D, et al. Corrigendum: Whole-genome characterization of chemoresistant ovarian cancer. In: *Nature.* Vol 527. England2015:398.

165. Rabik CA, Dolan ME. Molecular mechanisms of resistance and toxicity associated with platinating agents. *Cancer treatment reviews.* 2007;33(1):9-23.

166. Sodek KL, Murphy KJ, Brown TJ, Ringuette MJ. Cell-cell and cell-matrix dynamics in intraperitoneal cancer metastasis. *Cancer metastasis reviews.* 2012;31(1-2):397-414.

167. Schreiber RD, Old LJ, Smyth MJ. Cancer immunoediting: integrating immunity's roles in cancer suppression and promotion. *Science (New York, NY).* 2011;331(6024):1565-1570.

168. Quail DF, Joyce JA. Microenvironmental regulation of tumor progression and metastasis. *Nature medicine.* 2013;19(11):1423-1437.

169. Drakes ML, Stiff PJ. Regulation of Ovarian Cancer Prognosis by Immune Cells in the Tumor Microenvironment. *Cancers.* 2018;10(9).

170. McMillin DW, Negri JM, Mitsiades CS. The role of tumour-stromal interactions in modifying drug response: challenges and opportunities. *Nature reviews Drug discovery.* 2013;12(3):217-228.

171. Liu X. ABC Family Transporters. *Adv Exp Med Biol.* 2019;1141:13-100.

172. Zhang T, Guan M, Jin HY, Lu Y. Reversal of multidrug resistance by small interfering double-stranded RNAs in ovarian cancer cells. *Gynecologic oncology.* 2005;97(2):501-507.

173. Metzinger DS, Taylor DD, Gercel-Taylor C. Induction of p53 and drug resistance following treatment with cisplatin or paclitaxel in ovarian cancer cell lines. *Cancer letters.* 2006;236(2):302-308.

174. Hipfner DR, Almquist KC, Leslie EM, et al. Membrane topology of the multidrug resistance protein (MRP). A study of glycosylation-site mutants reveals an extracytosolic NH2 terminus. *The Journal of biological chemistry.* 1997;272(38):23623-23630.

175. Bakos E, Hegedus T, Hollo Z, et al. Membrane topology and glycosylation of the human multidrug resistance-associated protein. *The Journal of biological chemistry.* 1996;271(21):12322-12326.

176. Cole SP, Sparks KE, Fraser K, et al. Pharmacological characterization of multidrug resistant MRP-transfected human tumor cells. *Cancer research.* 1994;54(22):5902-5910.

177. Ishikawa T, Wright CD, Ishizuka H. GS-X pump is functionally overexpressed in cis-diamminedichloroplatinum (II)-resistant human leukemia HL-60 cells and down-regulated by cell differentiation. *The Journal of biological chemistry.* 1994;269(46):29085-29093.

178. Ishikawa T, Ali-Osman F. Glutathione-associated cis-diamminedichloroplatinum(II) metabolism and ATP-dependent efflux from leukemia cells. Molecular characterization of glutathione-platinum complex and its biological significance. *The Journal of biological chemistry.* 1993;268(27):20116-20125.

179. Filipits M, Suchomel RW, Dekan G, et al. MRP and MDR1 gene expression in primary breast carcinomas. *Clinical cancer research : an official journal of the American Association for Cancer Research.* 1996;2(7):1231-1237.

180. Wright SR, Boag AH, Valdimarsson G, et al. Immunohistochemical detection of multidrug resistance protein in human lung cancer and normal lung. *Clinical cancer research : an official journal of the American Association for Cancer Research.* 1998;4(9):2279-2289.

181. Nunes SC, Serpa J. Glutathione in Ovarian Cancer: A Double-Edged Sword. *International journal of molecular sciences.* 2018;19(7).

182. Bansal A, Simon MC. Glutathione metabolism in cancer progression and treatment resistance. *The Journal of cell biology.* 2018;217(7):2291-2298.

183. Zhang K, Chew M, Yang EB, Wong KP, Mack P. Modulation of cisplatin cytotoxicity and cisplatin-induced DNA cross-links in HepG2 cells by regulation of glutathione-related mechanisms. *Molecular pharmacology.* 2001;59(4):837-843.

184. Juvekar AS, Adwankar MK, Tongaonkar HB. Effect of cisplatin-based chemotherapy on emergence of cisplatin resistance, and its correlation with intracellular glutathione levels and accumulation of p53 protein in human ovarian cancer. *Cancer Biother Radiopharm.* 2000;15(3):295-300.

185. Hamaguchi K, Godwin AK, Yakushiji M, O'Dwyer PJ, Ozols RF, Hamilton TC. Cross-resistance to diverse drugs is associated with primary cisplatin resistance in ovarian cancer cell lines. *Cancer research.* 1993;53(21):5225-5232.

186. Wang W, Kryczek I, Dostal L, et al. Effector T Cells Abrogate Stroma-Mediated Chemoresistance in Ovarian Cancer. *Cell.* 2016;165(5):1092-1105.

187. Boyd J, Sonoda Y, Federici MG, et al. Clinicopathologic features of BRCA-linked and sporadic ovarian cancer. *Jama.* 2000;283(17):2260-2265.

188. Risch HA, McLaughlin JR, Cole DE, et al. Prevalence and penetrance of germline BRCA1 and BRCA2 mutations in a population series of 649 women with ovarian cancer. *Am J Hum Genet.* 2001;68(3):700-710.

189. Al-Attar A, Gossage L, Fareed KR, et al. Human apurinic/apyrimidinic endonuclease (APE1) is a prognostic factor in ovarian, gastro-oesophageal and pancreatico-biliary cancers. *Br J Cancer.* 2010;102(4):704-709.

190. Selvakumaran M, Pisarcik DA, Bao R, Yeung AT, Hamilton TC. Enhanced cisplatin cytotoxicity by disturbing the nucleotide excision repair pathway in ovarian cancer cell lines. *Cancer research.* 2003;63(6):1311-1316.

191. Abedini MR, Muller EJ, Bergeron R, Gray DA, Tsang BK. Akt promotes chemoresistance in human ovarian cancer cells by modulating cisplatin-induced, p53-dependent ubiquitination of FLICE-like inhibitory protein. *Oncogene.* 2010;29(1):11-25.

192. Abedini MR, Wang PW, Huang YF, et al. Cell fate regulation by gelsolin in human gynecologic cancers. *Proceedings of the National Academy of Sciences of the United States of America.* 2014;111(40):14442-14447.

193. Kandel ES, Hay N. The regulation and activities of the multifunctional serine/threonine kinase Akt/PKB. *Experimental cell research.* 1999;253(1):210-229.

194. Datta SR, Brunet A, Greenberg ME. Cellular survival: a play in three Akts. *Genes & development.* 1999;13(22):2905-2927.

195. Rafalski VA, Brunet A. Energy metabolism in adult neural stem cell fate. *Progress in neurobiology.* 2011;93(2):182-203.

196. Peltier J, O'Neill A, Schaffer DV. PI3K/Akt and CREB regulate adult neural hippocampal progenitor proliferation and differentiation. *Developmental neurobiology*. 2007;67(10):1348-1361.

197. Guertin DA, Stevens DM, Thoreen CC, et al. Ablation in mice of the mTORC components raptor, rictor, or mLST8 reveals that mTORC2 is required for signaling to Akt-FOXO and PKCalpha, but not S6K1. *Developmental cell.* 2006;11(6):859-871.

198. Carpenter CL, Duckworth BC, Auger KR, Cohen B, Schaffhausen BS, Cantley LC. Purification and characterization of phosphoinositide 3-kinase from rat liver. *The Journal of biological chemistry.* 1990;265(32):19704-19711.

199. Cheng JQ, Godwin AK, Bellacosa A, et al. AKT2, a putative oncogene encoding a member of a subfamily of protein-serine/threonine kinases, is amplified in human ovarian carcinomas. *Proceedings of the National Academy of Sciences of the United States of America.* 1992;89(19):9267-9271.

200. Hill MM, Hemmings BA. Inhibition of protein kinase B/Akt. implications for cancer therapy. *Pharmacology & therapeutics.* 2002;93(2-3):243-251.

201. Yang ZZ, Tschopp O, Baudry A, Dummler B, Hynx D, Hemmings BA. Physiological functions of protein kinase B/Akt. *Biochemical Society transactions.* 2004;32(Pt 2):350-354.

202. Rane MJ, Coxon PY, Powell DW, et al. p38 Kinase-dependent MAPKAPK-2 activation functions as 3-phosphoinositide-dependent kinase-2 for Akt in human neutrophils. *The Journal of biological chemistry.* 2001;276(5):3517-3523.

203. Delcommenne M, Tan C, Gray V, Rue L, Woodgett J, Dedhar S. Phosphoinositide-3-OH kinase-dependent regulation of glycogen synthase kinase 3 and protein kinase B/AKT by

the integrin-linked kinase. *Proceedings of the National Academy of Sciences of the United States of America.* 1998;95(19):11211-11216.

204. Balendran A, Casamayor A, Deak M, et al. PDK1 acquires PDK2 activity in the presence of a synthetic peptide derived from the carboxyl terminus of PRK2. *Current biology : CB.* 1999;9(8):393-404.

205. Aman MJ, Lamkin TD, Okada H, Kurosaki T, Ravichandran KS. The inositol phosphatase SHIP inhibits Akt/PKB activation in B cells. *The Journal of biological chemistry.* 1998;273(51):33922-33928.

206. Liu Q, Sasaki T, Kozieradzki I, et al. SHIP is a negative regulator of growth factor receptor-mediated PKB/Akt activation and myeloid cell survival. *Genes & development.* 1999;13(7):786-791.

207. Stambolic V, Suzuki A, de la Pompa JL, et al. Negative regulation of PKB/Akt-dependent cell survival by the tumor suppressor PTEN. *Cell.* 1998;95(1):29-39.

208. Li J, Simpson L, Takahashi M, et al. The PTEN/MMAC1 tumor suppressor induces cell death that is rescued by the AKT/protein kinase B oncogene. *Cancer research.* 1998;58(24):5667-5672.

209. Yuan ZQ, Sun M, Feldman RI, et al. Frequent activation of AKT2 and induction of apoptosis by inhibition of phosphoinositide-3-OH kinase/Akt pathway in human ovarian cancer. *Oncogene.* 2000;19(19):2324-2330.

210. Buttitta F, Marchetti A, Gadducci A, et al. p53 alterations are predictive of chemoresistance and aggressiveness in ovarian carcinomas: a molecular and immunohistochemical study. *British journal of cancer.* 1997;75(2):230-235.

211. Mihara M, Erster S, Zaika A, et al. p53 has a direct apoptogenic role at the mitochondria. *Molecular cell.* 2003;11(3):577-590.

212. Liu MC, Gelmann EP. P53 gene mutations: case study of a clinical marker for solid tumors. *Seminars in oncology.* 2002;29(3):246-257.

213. Honda R, Tanaka H, Yasuda H. Oncoprotein MDM2 is a ubiquitin ligase E3 for tumor suppressor p53. *FEBS Lett.* 1997;420(1):25-27.

214. Kussie PH, Gorina S, Marechal V, et al. Structure of the MDM2 oncoprotein bound to the p53 tumor suppressor transactivation domain. *Science (New York, NY).* 1996;274(5289):948-953.

215. Jung YS, Qian Y, Chen X. Examination of the expanding pathways for the regulation of p21 expression and activity. *Cellular signalling.* 2010;22(7):1003-1012.

216. Peng CY, Graves PR, Thoma RS, Wu Z, Shaw AS, Piwnica-Worms H. Mitotic and G2 checkpoint control: regulation of 14-3-3 protein binding by phosphorylation of Cdc25C on serine-216. *Science (New York, NY).* 1997;277(5331):1501-1505.

217. Chan TA, Hermeking H, Lengauer C, Kinzler KW, Vogelstein B. 14-3-3Sigma is required to prevent mitotic catastrophe after DNA damage. *Nature.* 1999;401(6753):616-620.

218. Park SY, Jeong MS, Jang SB. In vitro binding properties of tumor suppressor p53 with PUMA and NOXA. *Biochemical and biophysical research communications.* 2012;420(2):350-356.

219. Sax JK, Fei P, Murphy ME, Bernhard E, Korsmeyer SJ, El-Deiry WS. BID regulation by p53 contributes to chemosensitivity. *Nature cell biology.* 2002;4(11):842-849.

220. Moroni MC, Hickman ES, Lazzerini Denchi E, et al. Apaf-1 is a transcriptional target for E2F and p53. *Nature cell biology.* 2001;3(6):552-558.

221. Liu X, Yue P, Khuri FR, Sun SY. p53 upregulates death receptor 4 expression through an intronic p53 binding site. *Cancer research.* 2004;64(15):5078-5083.

222. Abedini MR, Qiu Q, Yan X, Tsang BK. Possible role of FLICE-like inhibitory protein (FLIP) in chemoresistant ovarian cancer cells in vitro. *Oncogene.* 2004;23(42):6997-7004.

223. Kong B, Tsuyoshi H, Orisaka M, Shieh DB, Yoshida Y, Tsang BK. Mitochondrial dynamics regulating chemoresistance in gynecological cancers. *Annals of the New York Academy of Sciences.* 2015;1350:1-16.

224. Ali AY, Abedini MR, Tsang BK. The oncogenic phosphatase PPM1D confers cisplatin resistance in ovarian carcinoma cells by attenuating checkpoint kinase 1 and p53 activation. *Oncogene.* 2012;31(17):2175-2186.

225. Tan DS, Lambros MB, Rayter S, et al. PPM1D is a potential therapeutic target in ovarian clear cell carcinomas. *Clinical cancer research : an official journal of the American Association for Cancer Research.* 2009;15(7):2269-2280.

226. Shreeram S, Demidov ON, Hee WK, et al. Wip1 phosphatase modulates ATM-dependent signaling pathways. *Molecular cell.* 2006;23(5):757-764.

227. Carlessi L, Buscemi G, Fontanella E, Delia D. A protein phosphatase feedback mechanism regulates the basal phosphorylation of Chk2 kinase in the absence of DNA damage. *Biochimica et biophysica acta.* 2010;1803(10):1213-1223.

228. Pei D, Zhang Y, Zheng J. Regulation of p53: a collaboration between Mdm2 and Mdmx. *Oncotarget.* 2012;3(3):228-235.

229. Zhang X, Lin L, Guo H, et al. Phosphorylation and degradation of MdmX is inhibited by Wip1 phosphatase in the DNA damage response. *Cancer research.* 2009;69(20):7960-7968.

230. Ghisoni E, Imbimbo M, Zimmermann S, Valabrega G. Ovarian Cancer Immunotherapy: Turning up the Heat. *International journal of molecular sciences.* 2019;20(12).

231. Sun Y. Tumor microenvironment and cancer therapy resistance. *Cancer letters.* 2016;380(1):205-215.

232. Vesely MD, Kershaw MH, Schreiber RD, Smyth MJ. Natural innate and adaptive immunity to cancer. *Annual review of immunology.* 2011;29:235-271.

233. Turner TB, Buchsbaum DJ, Straughn JM, Jr., Randall TD, Arend RC. Ovarian cancer and the immune system - The role of targeted therapies. *Gynecologic oncology.* 2016;142(2):349-356.

234. Mantovani A, Sozzani S, Locati M, Allavena P, Sica A. Macrophage polarization: tumor-associated macrophages as a paradigm for polarized M2 mononuclear phagocytes. *Trends in immunology.* 2002;23(11):549-555.

235. Speiser DE, Ho PC, Verdeil G. Regulatory circuits of T cell function in cancer. *Nature reviews Immunology.* 2016;16(10):599-611.

236. Takaishi K, Komohara Y, Tashiro H, et al. Involvement of M2-polarized macrophages in the ascites from advanced epithelial ovarian carcinoma in tumor progression via Stat3 activation. *Cancer science.* 2010;101(10):2128-2136.

237. Budnik V, Ruiz-Canada C, Wendler F. Extracellular vesicles round off communication in the nervous system. *Nature reviews Neuroscience.* 2016;17(3):160-172.

238. Colombo M, Moita C, van Niel G, et al. Analysis of ESCRT functions in exosome biogenesis, composition and secretion highlights the heterogeneity of extracellular vesicles. *Journal of cell science.* 2013;126(Pt 24):5553-5565.

239. Roma-Rodrigues C, Fernandes AR, Baptista PV. Exosome in tumour microenvironment: overview of the crosstalk between normal and cancer cells. *BioMed research international.* 2014;2014:179486.

240. Crow J, Atay S, Banskota S, Artale B, Schmitt S, Godwin AK. Exosomes as mediators of platinum resistance in ovarian cancer. *Oncotarget.* 2017;8(7):11917-11936.

241. Taylor DD, Gercel-Taylor C. MicroRNA signatures of tumor-derived exosomes as diagnostic biomarkers of ovarian cancer. *Gynecologic oncology.* 2008;110(1):13-21.

242. Xu Y, Zhang Y, Wang L, et al. miR-200a targets Gelsolin: A novel mechanism regulating secretion of microvesicles in hepatocellular carcinoma cells. *Oncology reports.* 2017;37(5):2711-2719.

243. Wieckowski EU, Visus C, Szajnik M, Szczepanski MJ, Storkus WJ, Whiteside TL. Tumor-derived microvesicles promote regulatory T cell expansion and induce apoptosis in tumor-reactive activated CD8+ T lymphocytes. *Journal of immunology (Baltimore, Md : 1950).* 2009;183(6):3720-3730.

244. Burger D, Vinas JL, Akbari S, et al. Human endothelial colony-forming cells protect against acute kidney injury: role of exosomes. *The American journal of pathology.* 2015;185(8):2309-2323.

245. Corcoran C, Rani S, O'Brien K, et al. Docetaxel-resistance in prostate cancer: evaluating associated phenotypic changes and potential for resistance transfer via exosomes. *PLoS One.* 2012;7(12):e50999.

246. Wei Y, Lai X, Yu S, et al. Exosomal miR-221/222 enhances tamoxifen resistance in recipient ER-positive breast cancer cells. *Breast cancer research and treatment.* 2014;147(2):423-431.

247. Chen WX, Liu XM, Lv MM, et al. Exosomes from drug-resistant breast cancer cells transmit chemoresistance by a horizontal transfer of microRNAs. *PLoS One.* 2014;9(4):e95240.

248. Ciravolo V, Huber V, Ghedini GC, et al. Potential role of HER2-overexpressing exosomes in countering trastuzumab-based therapy. *Journal of cellular physiology.* 2012;227(2):658-667.

249. Safaei R, Larson BJ, Cheng TC, et al. Abnormal lysosomal trafficking and enhanced exosomal export of cisplatin in drug-resistant human ovarian carcinoma cells. *Molecular cancer therapeutics.* 2005;4(10):1595-1604.

250. Labani-Motlagh A, Israelsson P, Ottander U, et al. Differential expression of ligands for NKG2D and DNAM-1 receptors by epithelial ovarian cancer-derived exosomes and its influence on NK cell cytotoxicity. *Tumour biology : the journal of the International Society for Oncodevelopmental Biology and Medicine.* 2016;37(4):5455-5466.

251. Bretz NP, Ridinger J, Rupp AK, et al. Body fluid exosomes promote secretion of inflammatory cytokines in monocytic cells via Toll-like receptor signaling. *The Journal of biological chemistry.* 2013;288(51):36691-36702.

252. Peng P, Yan Y, Keng S. Exosomes in the ascites of ovarian cancer patients: origin and effects on anti-tumor immunity. *Oncology reports.* 2011;25(3):749-762.

253. Yin HL, Kwiatkowski DJ, Mole JE, Cole FS. Structure and biosynthesis of cytoplasmic and secreted variants of gelsolin. *The Journal of biological chemistry.* 1984;259(8):5271-5276.

254. Kwiatkowski DJ, Stossel TP, Orkin SH, Mole JE, Colten HR, Yin HL. Plasma and cytoplasmic gelsolins are encoded by a single gene and contain a duplicated actin-binding domain. *Nature.* 1986;323(6087):455-458.

255. Zapun A, Grammatyka S, Deral G, Vernet T. Calcium-dependent conformational stability of modules 1 and 2 of human gelsolin. *The Biochemical journal.* 2000;350 Pt 3:873-881.

256. Sun HQ, Yamamoto M, Mejillano M, Yin HL. Gelsolin, a multifunctional actin regulatory protein. *The Journal of biological chemistry.* 1999;274(47):33179-33182.

257. Wang PW, Abedini MR, Yang LX, et al. Gelsolin regulates cisplatin sensitivity in human head-and-neck cancer. *International journal of cancer Journal international du cancer.* 2014;135(12):2760-2769.

258. Antequera D, Vargas T, Ugalde C, et al. Cytoplasmic gelsolin increases mitochondrial activity and reduces Abeta burden in a mouse model of Alzheimer's disease. *Neurobiology of disease.* 2009;36(1):42-50.

259. Lind SE, Smith DB, Janmey PA, Stossel TP. Role of plasma gelsolin and the vitamin D-binding protein in clearing actin from the circulation. *The Journal of clinical investigation.* 1986;78(3):736-742.

260. Self WH, Wunderink RG, DiNubile MJ, et al. Low Admission Plasma Gelsolin Concentrations Identify Community-acquired Pneumonia Patients at High Risk for Severe Outcomes. *Clin Infect Dis.* 2019;69(7):1218-1225.

261. Spinardi L, Witke W. Gelsolin and diseases. *Sub-cellular biochemistry.* 2007;45:55-69.

262. Lee PS, Waxman AB, Cotich KL, Chung SW, Perrella MA, Stossel TP. Plasma gelsolin is a marker and therapeutic agent in animal sepsis. *Crit Care Med.* 2007;35(3):849-855.

263. Lee PS, Patel SR, Christiani DC, Bajwa E, Stossel TP, Waxman AB. Plasma gelsolin depletion and circulating actin in sepsis: a pilot study. *PLoS One.* 2008;3(11):e3712.

264. Lee PS, Drager LR, Stossel TP, Moore FD, Rogers SO. Relationship of plasma gelsolin levels to outcomes in critically ill surgical patients. *Ann Surg.* 2006;243(3):399-403.

265. Guo XC, Luo BY, Li XF, Yang DG, Zheng XN, Zhang K. Plasma gelsolin levels and 1-year mortality after first-ever ischemic stroke. *Journal of critical care.* 2011;26(6):608-612.

266. Huang S, Rhoads SL, DiNubile MJ. Temporal association between serum gelsolin levels and clinical events in a patient with severe falciparum malaria. *Clin Infect Dis.* 1997;24(5):951-954.

267. Smith DB, Janmey PA, Sherwood JA, Howard RJ, Lind SE. Decreased plasma gelsolin levels in patients with Plasmodium falciparum malaria: a consequence of hemolysis? *Blood.* 1988;72(1):214-218.

268. Marrocco C, Rinalducci S, Mohamadkhani A, D'Amici GM, Zolla L. Plasma gelsolin protein: a candidate biomarker for hepatitis B-associated liver cirrhosis identified by proteomic approach. *Blood transfusion = Trasfusione del sangue.* 2010;8 Suppl 3:s105-112.

269. Chen ZY, Wang PW, Shieh DB, Chiu KY, Liou YM. Involvement of gelsolin in TGF-beta 1 induced epithelial to mesenchymal transition in breast cancer cells. *J Biomed Sci.* 2015;22:90.

270. Wang HC, Chen CW, Yang CL, et al. Tumor-Associated Macrophages Promote Epigenetic Silencing of Gelsolin through DNA Methyltransferase 1 in Gastric Cancer Cells. *Cancer Immunol Res.* 2017;5(10):885-897.

271. Huang GW, Liao LD, Li EM, Xu LY. siRNA induces gelsolin gene transcription activation in human esophageal cancer cell. *Scientific reports.* 2015;5:7901.

272. Ma X, Sun W, Shen J, et al. Gelsolin promotes cell growth and invasion through the upregulation of p-AKT and p-P38 pathway in osteosarcoma. *Tumour biology : the journal of the International Society for Oncodevelopmental Biology and Medicine.* 2016;37(6):7165-7174.

273. Tsai MH, Wu CC, Peng PH, et al. Identification of secretory gelsolin as a plasma biomarker associated with distant organ metastasis of colorectal cancer. *Journal of molecular medicine (Berlin, Germany).* 2012;90(2):187-200.

274. Chen CC, Chiou SH, Yang CL, et al. Secreted gelsolin desensitizes and induces apoptosis of infiltrated lymphocytes in prostate cancer. *Oncotarget.* 2017;8(44):77152-77167.

275. Bohgaki M, Matsumoto M, Atsumi T, et al. Plasma gelsolin facilitates interaction between beta2 glycoprotein I and alpha5beta1 integrin. *Journal of cellular and molecular medicine.* 2011;15(1):141-151.

Chapter 2

1. Release notice - Canadian Cancer Statistics 2019. *Health Promot Chronic Dis Prev Can.* 2019;39(8-9):255.
2. Torre LA, Trabert B, DeSantis CE, et al. Ovarian cancer statistics, 2018. *CA: a cancer journal for clinicians.* 2018;68(4):284-296.
3. Fujiwara K, McAlpine JN, Lheureux S, Matsumura N, Oza AM. Paradigm Shift in the Management Strategy for Epithelial Ovarian Cancer. *Am Soc Clin Oncol Educ Book.* 2016;35:e247-257.
4. Lheureux S, Braunstein M, Oza AM. Epithelial ovarian cancer: Evolution of management in the era of precision medicine. *CA: a cancer journal for clinicians.* 2019;69(4):280-304.
5. Sun Y. Tumor microenvironment and cancer therapy resistance. *Cancer letters.* 2016;380(1):205-215.
6. Ghisoni E, Imbimbo M, Zimmermann S, Valabrega G. Ovarian Cancer Immunotherapy: Turning up the Heat. *International journal of molecular sciences.* 2019;20(12).
7. Wang PW, Abedini MR, Yang LX, et al. Gelsolin regulates cisplatin sensitivity in human head-and-neck cancer. *International journal of cancer Journal international du cancer.* 2014;135(12):2760-2769.
8. Abedini MR, Wang PW, Huang YF, et al. Cell fate regulation by gelsolin in human gynecologic cancers. *Proceedings of the National Academy of Sciences of the United States of America.* 2014;111(40):14442-14447.
9. Chen Z, Li K, Yin X, et al. Lower Expression of Gelsolin in Colon Cancer and Its Diagnostic Value in Colon Cancer Patients. *Journal of Cancer.* 2019;10(5):1288-1296.

10. Rodriguez GM, Galpin KJC, McCloskey CW, Vanderhyden BC. The Tumor Microenvironment of Epithelial Ovarian Cancer and Its Influence on Response to Immunotherapy. *Cancers*. 2018;10(8).

11. Yin J, Yan X, Yao X, et al. Secretion of annexin A3 from ovarian cancer cells and its association with platinum resistance in ovarian cancer patients. *Journal of cellular and molecular medicine.* 2012;16(2):337-348.

12. Peng P, Yan Y, Keng S. Exosomes in the ascites of ovarian cancer patients: origin and effects on anti-tumor immunity. *Oncology reports.* 2011;25(3):749-762.

13. Crow J, Atay S, Banskota S, Artale B, Schmitt S, Godwin AK. Exosomes as mediators of platinum resistance in ovarian cancer. *Oncotarget.* 2017;8(7):11917-11936.

14. Roma-Rodrigues C, Fernandes AR, Baptista PV. Exosome in tumour microenvironment: overview of the crosstalk between normal and cancer cells. *BioMed research international.* 2014;2014:179486.

15. Ying X, Wu Q, Wu X, et al. Epithelial ovarian cancer-secreted exosomal miR-222-3p induces polarization of tumor-associated macrophages. *Oncotarget.* 2016;7(28):43076-43087.

Chapter 3

1. Ferlay J, Soerjomataram I, Dikshit R, et al. Cancer incidence and mortality worldwide: sources, methods and major patterns in GLOBOCAN 2012. *International journal of cancer Journal international du cancer.* 2015;136(5):E359-386.
2. Armstrong DK, Bundy B, Wenzel L, et al. Intraperitoneal cisplatin and paclitaxel in ovarian cancer. *N Engl J Med.* 2006;354(1):34-43.
3. Stefanou DT, Bamias A, Episkopou H, et al. Aberrant DNA damage response pathways may predict the outcome of platinum chemotherapy in ovarian cancer. *PLoS One.* 2015;10(2):e0117654.
4. Fu LJ, Wang B. Investigation of the hub genes and related mechanism in ovarian cancer via bioinformatics analysis. *Journal of ovarian research.* 2013;6(1):92.
5. Yang X, Fraser M, Moll UM, Basak A, Tsang BK. Akt-mediated cisplatin resistance in ovarian cancer: modulation of p53 action on caspase-dependent mitochondrial death pathway. *Cancer research.* 2006;66(6):3126-3136.
6. Kwiatkowski DJ, Stossel TP, Orkin SH, Mole JE, Colten HR, Yin HL. Plasma and cytoplasmic gelsolins are encoded by a single gene and contain a duplicated actin-binding domain. *Nature.* 1986;323(6087):455-458.
7. Sun HQ, Yamamoto M, Mejillano M, Yin HL. Gelsolin, a multifunctional actin regulatory protein. *The Journal of biological chemistry.* 1999;274(47):33179-33182.
8. Abedini MR, Qiu Q, Yan X, Tsang BK. Possible role of FLICE-like inhibitory protein (FLIP) in chemoresistant ovarian cancer cells in vitro. *Oncogene.* 2004;23(42):6997-7004.

9. Abedini MR, Wang PW, Huang YF, et al. Cell fate regulation by gelsolin in human gynecologic cancers. *Proceedings of the National Academy of Sciences of the United States of America.* 2014;111(40):14442-14447.

10. Lee PS, Waxman A. The importance of differentiating gelsolin isoforms. In: *Am J Respir Crit Care Med.* Vol 173. United States2006:685; author reply 685.

11. Lofberg M, Paunio T, Tahtela R, Kiuru S, Somer H. Serum gelsolin and rhabdomyolysis. *Journal of the neurological sciences.* 1998;157(2):187-190.

12. Smith DB, Janmey PA, Herbert TJ, Lind SE. Quantitative measurement of plasma gelsolin and its incorporation into fibrin clots. *The Journal of laboratory and clinical medicine.* 1987;110(2):189-195.

13. Tsai MH, Wu CC, Peng PH, et al. Identification of secretory gelsolin as a plasma biomarker associated with distant organ metastasis of colorectal cancer. *Journal of molecular medicine (Berlin, Germany).* 2012;90(2):187-200.

14. Yin HL, Kwiatkowski DJ, Mole JE, Cole FS. Structure and biosynthesis of cytoplasmic and secreted variants of gelsolin. *The Journal of biological chemistry.* 1984;259(8):5271-5276.

15. Bohgaki M, Matsumoto M, Atsumi T, et al. Plasma gelsolin facilitates interaction between beta2 glycoprotein I and alpha5beta1 integrin. *Journal of cellular and molecular medicine.* 2011;15(1):141-151.

16. Safaei R, Larson BJ, Cheng TC, et al. Abnormal lysosomal trafficking and enhanced exosomal export of cisplatin in drug-resistant human ovarian carcinoma cells. *Molecular cancer therapeutics.* 2005;4(10):1595-1604.

17. Roma-Rodrigues C, Fernandes AR, Baptista PV. Exosome in tumour microenvironment: overview of the crosstalk between normal and cancer cells. *BioMed research international.* 2014;2014:179486.

18. Crow J, Atay S, Banskota S, Artale B, Schmitt S, Godwin AK. Exosomes as mediators of platinum resistance in ovarian cancer. *Oncotarget.* 2017;8(7):11917-11936.

19. Chen WX, Liu XM, Lv MM, et al. Exosomes from drug-resistant breast cancer cells transmit chemoresistance by a horizontal transfer of microRNAs. *PLoS One.* 2014;9(4):e95240.

20. Au Yeung CL, Co NN, Tsuruga T, et al. Exosomal transfer of stroma-derived miR21 confers paclitaxel resistance in ovarian cancer cells through targeting APAF1. *Nature communications.* 2016;7:11150.

21. Budnik V, Ruiz-Canada C, Wendler F. Extracellular vesicles round off communication in the nervous system. *Nature reviews Neuroscience.* 2016;17(3):160-172.

22. Gyorffy B, Lanczky A, Szallasi Z. Implementing an online tool for genome-wide validation of survival-associated biomarkers in ovarian-cancer using microarray data from 1287 patients. *Endocrine-related cancer.* 2012;19(2):197-208.

23. Spinardi L, Witke W. Gelsolin and diseases. *Sub-cellular biochemistry.* 2007;45:55-69.

24. Elattar A, Bryant A, Winter-Roach BA, Hatem M, Naik R. Optimal primary surgical treatment for advanced epithelial ovarian cancer. *The Cochrane database of systematic reviews.* 2011(8):Cd007565.

25. Wefers C, Lambert LJ, Torensma R, Hato SV. Cellular immunotherapy in ovarian cancer: Targeting the stem of recurrence. *Gynecologic oncology.* 2015;137(2):335-342.

26. Quail DF, Joyce JA. Microenvironmental regulation of tumour progression and metastasis. *Nature medicine.* 2013;19(11):1423-1437.

27. Chen CC, Chiou SH, Yang CL, et al. Secreted gelsolin desensitizes and induces apoptosis of infiltrated lymphocytes in prostate cancer. *Oncotarget.* 2017;8(44):77152-77167.

28. Wang PW, Abedini MR, Yang LX, et al. Gelsolin regulates cisplatin sensitivity in human head-and-neck cancer. *International journal of cancer Journal international du cancer.* 2014;135(12):2760-2769.

29. Meng X, Muller V, Milde-Langosch K, Trillsch F, Pantel K, Schwarzenbach H. Diagnostic and prognostic relevance of circulating exosomal miR-373, miR-200a, miR-200b and miR-200c in patients with epithelial ovarian cancer. *Oncotarget.* 2016;7(13):16923-16935.

30. Yin J, Yan X, Yao X, et al. Secretion of annexin A3 from ovarian cancer cells and its association with platinum resistance in ovarian cancer patients. *Journal of cellular and molecular medicine.* 2012;16(2):337-348.

31. Pink RC, Samuel P, Massa D, Caley DP, Brooks SA, Carter DR. The passenger strand, miR-21-3p, plays a role in mediating cisplatin resistance in ovarian cancer cells. *Gynecologic oncology.* 2015;137(1):143-151.

32. Wei Y, Lai X, Yu S, et al. Exosomal miR-221/222 enhances tamoxifen resistance in recipient ER-positive breast cancer cells. *Breast cancer research and treatment.* 2014;147(2):423-431.

33. Ying X, Wu Q, Wu X, et al. Epithelial ovarian cancer-secreted exosomal miR-222-3p induces polarization of tumour-associated macrophages. *Oncotarget.* 2016;7(28):43076-43087.

34. Delcommenne M, Tan C, Gray V, Rue L, Woodgett J, Dedhar S. Phosphoinositide-3-OH kinase-dependent regulation of glycogen synthase kinase 3 and protein kinase B/AKT by the integrin-linked kinase. *Proceedings of the National Academy of Sciences of the United States of America.* 1998;95(19):11211-11216.

35. Bruney L, Liu Y, Grisoli A, Ravosa MJ, Stack MS. Integrin-linked kinase activity modulates the pro-metastatic behavior of ovarian cancer cells. *Oncotarget.* 2016.

36. Zeng B, Zhou M, Wu H, Xiong Z. SPP1 promotes ovarian cancer progression via Integrin beta1/FAK/AKT signaling pathway. *OncoTargets and therapy.* 2018;11:1333-1343.

37. Ata R, Antonescu CN. Integrins and Cell Metabolism: An Intimate Relationship Impacting Cancer. *International journal of molecular sciences.* 2017;18(1).

38. Greijer AE, van der Groep P, Kemming D, et al. Up-regulation of gene expression by hypoxia is mediated predominantly by hypoxia-inducible factor 1 (HIF-1). *The Journal of pathology.* 2005;206(3):291-304.

39. Daponte A, Ioannou M, Mylonis I, et al. Prognostic significance of Hypoxia-Inducible Factor 1 alpha(HIF-1 alpha) expression in serous ovarian cancer: an immunohistochemical study. *BMC cancer.* 2008;8:335.

40. Gomez-Roman N, Sahasrabudhe NM, McGregor F, Chalmers AJ, Cassidy J, Plumb J. Hypoxia-inducible factor 1 alpha is required for the tumourigenic and aggressive phenotype associated with Rab25 expression in ovarian cancer. *Oncotarget.* 2016;7(16):22650-22664.

41. Yu T, Tang B, Sun X. Development of Inhibitors Targeting Hypoxia-Inducible Factor 1 and 2 for Cancer Therapy. *Yonsei medical journal.* 2017;58(3):489-496.

42. Fraser M, Leung BM, Yan X, Dan HC, Cheng JQ, Tsang BK. p53 is a determinant of X-linked inhibitor of apoptosis protein/Akt-mediated chemoresistance in human ovarian cancer cells. *Cancer research.* 2003;63(21):7081-7088.

43. Abedini MR, Muller EJ, Bergeron R, Gray DA, Tsang BK. Akt promotes chemoresistance in human ovarian cancer cells by modulating cisplatin-induced, p53-dependent ubiquitination of FLICE-like inhibitory protein. *Oncogene.* 2010;29(1):11-25.

44. Faridi J, Fawcett J, Wang L, Roth RA. Akt promotes increased mammalian cell size by stimulating protein synthesis and inhibiting protein degradation. *American journal of physiology Endocrinology and metabolism.* 2003;285(5):E964-972.

45. Dai CL, Shi J, Chen Y, Iqbal K, Liu F, Gong CX. Inhibition of protein synthesis alters protein degradation through activation of protein kinase B (AKT). *The Journal of biological chemistry.* 2013;288(33):23875-23883.

46. Chang F, Lee JT, Navolanic PM, et al. Involvement of PI3K/Akt pathway in cell cycle progression, apoptosis, and neoplastic transformation: a target for cancer chemotherapy. *Leukemia.* 2003;17(3):590-603.

47. Liu P, Begley M, Michowski W, et al. Cell-cycle-regulated activation of Akt kinase by phosphorylation at its carboxyl terminus. *Nature.* 2014;508(7497):541-545.

48. Yang ZY, Di MY, Yuan JQ, et al. The prognostic value of phosphorylated Akt in breast cancer: a systematic review. *Scientific reports.* 2015;5:7758.

49. Pal SK, Reckamp K, Yu H, Figlin RA. Akt inhibitors in clinical development for the treatment of cancer. *Expert opinion on investigational drugs.* 2010;19(11):1355-1366.

50. Nitulescu GM, Margina D, Juzenas P, et al. Akt inhibitors in cancer treatment: The long journey from drug discovery to clinical use (Review). *International journal of oncology.* 2016;48(3):869-885.

51. Dengler VL, Galbraith M, Espinosa JM. Transcriptional regulation by hypoxia inducible factors. *Critical reviews in biochemistry and molecular biology.* 2014;49(1):1-15.

52. Andjelkovic M, Alessi DR, Meier R, et al. Role of translocation in the activation and function of protein kinase B. *The Journal of biological chemistry.* 1997;272(50):31515-31524.

53. Alessi DR, Andjelkovic M, Caudwell B, et al. Mechanism of activation of protein kinase B by insulin and IGF-1. *The EMBO journal.* 1996;15(23):6541-6551.

54. Krieg T, Landsberger M, Alexeyev MF, Felix SB, Cohen MV, Downey JM. Activation of Akt is essential for acetylcholine to trigger generation of oxygen free radicals. *Cardiovasc Res.* 2003;58(1):196-202.

55. Ali AY, Abedini MR, Tsang BK. The oncogenic phosphatase PPM1D confers cisplatin resistance in ovarian carcinoma cells by attenuating checkpoint kinase 1 and p53 activation. *Oncogene.* 2012;31(17):2175-2186.

56. Nakka KK, Chaudhary N, Joshi S, et al. Nuclear matrix-associated protein SMAR1 regulates alternative splicing via HDAC6-mediated deacetylation of Sam68. *Proceedings of the National Academy of Sciences of the United States of America.* 2015;112(26):E3374-3383.

57. Burger D, Vinas JL, Akbari S, et al. Human endothelial colony-forming cells protect against acute kidney injury: role of exosomes. *The American journal of pathology.* 2015;185(8):2309-2323.

58. Vinas JL, Burger D, Zimpelmann J, et al. Transfer of microRNA-486-5p from human endothelial colony forming cell-derived exosomes reduces ischemic kidney injury. *Kidney international.* 2016;90(6):1238-1250.

59. Reunov A, Pimenova E, Reunova Y, Menchinskaiya E, Lapshina L, Aminin D. The study of the calpain and caspase-1 expression in ultrastructural dynamics of Ehrlich ascites carcinoma necrosis. *Gene.* 2018;658:1-9.

Chapter 4

1. Tsibulak I, Zeimet AG, Marth C. Hopes and failures in front-line ovarian cancer therapy. Critical reviews in oncology/hematology. 2019;143:14-9.

2. Pogge von Strandmann E, Reinartz S, Wager U, Muller R. Tumor-Host Cell Interactions in Ovarian Cancer: Pathways to Therapy Failure. Trends in cancer. 2017;3(2):137-48.

3. Haanen J. Converting Cold into Hot Tumors by Combining Immunotherapies. Cell. 2017;170(6):1055-6.

4. Lo CS, Sanii S, Kroeger DR, Milne K, Talhouk A, Chiu DS, et al. Neoadjuvant Chemotherapy of Ovarian Cancer Results in Three Patterns of Tumor-Infiltrating Lymphocyte Response with Distinct Implications for Immunotherapy. Clin Cancer Res. 2017;23(4):925-34.

5. Webb JR, Milne K, Kroeger DR, Nelson BH. PD-L1 expression is associated with tumor-infiltrating T cells and favorable prognosis in high-grade serous ovarian cancer. Gynecol Oncol. 2016;141(2):293-302.

6. Santoiemma PP, Powell DJ, Jr. Tumor infiltrating lymphocytes in ovarian cancer. Cancer biology & therapy. 2015;16(6):807-20.

7. Kwiatkowski DJ, Stossel TP, Orkin SH, Mole JE, Colten HR, Yin HL. Plasma and cytoplasmic gelsolins are encoded by a single gene and contain a duplicated actin-binding domain. Nature. 1986;323(6087):455-8.

8. Yin HL, Kwiatkowski DJ, Mole JE, Cole FS. Structure and biosynthesis of cytoplasmic and secreted variants of gelsolin. The Journal of biological chemistry. 1984;259(8):5271-6.

9. Abedini MR, Wang PW, Huang YF, Cao M, Chou CY, Shieh DB, et al. Cell fate regulation by gelsolin in human gynecologic cancers. Proceedings of the National Academy of Sciences of the United States of America. 2014;111(40):14442-7.

10. Wang PW, Abedini MR, Yang LX, Ding AA, Figeys D, Chang JY, et al. Gelsolin regulates cisplatin sensitivity in human head-and-neck cancer. International journal of cancer Journal international du cancer. 2014;135(12):2760-9.

11. Budnik V, Ruiz-Canada C, Wendler F. Extracellular vesicles round off communication in the nervous system. Nature reviews Neuroscience. 2016;17(3):160-72.

12. Roma-Rodrigues C, Fernandes AR, Baptista PV. Exosome in tumour microenvironment: overview of the crosstalk between normal and cancer cells. BioMed research international. 2014;2014:179486.

13. Asare-Werehene M, Nakka K, Reunov A, Chiu CT, Lee WT, Abedini MR, et al. The exosome-mediated autocrine and paracrine actions of plasma gelsolin in ovarian cancer chemoresistance. Oncogene. 2019.

14. Asare-Werehene M, Communal L, Carmona E, Le T, Provencher D, Mes-Masson AM, et al. Pre-operative Circulating Plasma Gelsolin Predicts Residual Disease and Detects Early Stage Ovarian Cancer. Scientific reports. 2019;9(1):13924.

15. Manupati K, Debnath S, Goswami K, Bhoj PS, Chandak HS, Bahekar SP, et al. Glutathione S-transferase omega 1 inhibition activates JNK-mediated apoptotic response in breast cancer stem cells. The FEBS journal. 2019;286(11):2167-92.

16. Bansal A, Simon MC. Glutathione metabolism in cancer progression and treatment resistance. The Journal of cell biology. 2018;217(7):2291-8.

17. Nunes SC, Serpa J. Glutathione in Ovarian Cancer: A Double-Edged Sword. International journal of molecular sciences. 2018;19(7).

18. Shin CS, Mishra P, Watrous JD, Carelli V, D'Aurelio M, Jain M, et al. The glutamate/cystine xCT antiporter antagonizes glutamine metabolism and reduces nutrient flexibility. Nature communications. 2017;8:15074.

19. Lim JKM, Delaidelli A, Minaker SW, Zhang HF, Colovic M, Yang H, et al. Cystine/glutamate antiporter xCT (SLC7A11) facilitates oncogenic RAS transformation by preserving intracellular redox balance. Proceedings of the National Academy of Sciences of the United States of America. 2019;116(19):9433-42.

20. Lu H, Samanta D, Xiang L, Zhang H, Hu H, Chen I, et al. Chemotherapy triggers HIF-1-dependent glutathione synthesis and copper chelation that induces the breast cancer stem cell phenotype. Proceedings of the National Academy of Sciences of the United States of America. 2015;112(33):E4600-9.

21. Li M, Cui F, Cheng Y, Han L, Wang J, Sun D, et al. Gelsolin: role of a functional protein in mitigating radiation injury. Cell biochemistry and biophysics. 2015;71(1):389-96.

22. Labrie M, De Araujo LOF, Communal L, Mes-Masson AM, St-Pierre Y. Tissue and plasma levels of galectins in patients with high grade serous ovarian carcinoma as new predictive biomarkers. Scientific reports. 2017;7(1):13244.

23. Abedini MR, Muller EJ, Bergeron R, Gray DA, Tsang BK. Akt promotes chemoresistance in human ovarian cancer cells by modulating cisplatin-induced, p53-dependent ubiquitination of FLICE-like inhibitory protein. Oncogene. 2010;29(1):11-25.

24. Abedini MR, Qiu Q, Yan X, Tsang BK. Possible role of FLICE-like inhibitory protein (FLIP) in chemoresistant ovarian cancer cells in vitro. Oncogene. 2004;23(42):6997-7004.

25. Provencher DM, Lounis H, Champoux L, Tetrault M, Manderson EN, Wang JC, et al. Characterization of four novel epithelial ovarian cancer cell lines. In Vitro Cell Dev Biol Anim. 2000;36(6):357-61.

26. Letourneau IJ, Quinn MC, Wang LL, Portelance L, Caceres KY, Cyr L, et al. Derivation and characterization of matched cell lines from primary and recurrent serous ovarian cancer. BMC cancer. 2012;12:379.

27. Ali AY, Abedini MR, Tsang BK. The oncogenic phosphatase PPM1D confers cisplatin resistance in ovarian carcinoma cells by attenuating checkpoint kinase 1 and p53 activation. Oncogene. 2012;31(17):2175-86.

28. Burger D, Vinas JL, Akbari S, Dehak H, Knoll W, Gutsol A, et al. Human endothelial colony-forming cells protect against acute kidney injury: role of exosomes. The American journal of pathology. 2015;185(8):2309-23.

29. Turner TB, Buchsbaum DJ, Straughn JM, Jr., Randall TD, Arend RC. Ovarian cancer and the immune system - The role of targeted therapies. Gynecologic oncology. 2016;142(2):349-56.

30. Wang W, Kryczek I, Dostal L, Lin H, Tan L, Zhao L, et al. Effector T Cells Abrogate Stroma-Mediated Chemoresistance in Ovarian Cancer. Cell. 2016;165(5):1092-105.

31. Chen CC, Chiou SH, Yang CL, Chow KC, Lin TY, Chang HW, et al. Secreted gelsolin desensitizes and induces apoptosis of infiltrated lymphocytes in prostate cancer. Oncotarget. 2017;8(44):77152-67.

32. Tsai MH, Wu CC, Peng PH, Liang Y, Hsiao YC, Chien KY, et al. Identification of secretory gelsolin as a plasma biomarker associated with distant organ metastasis of colorectal cancer. Journal of molecular medicine (Berlin, Germany). 2012;90(2):187-200.

33. Wieckowski EU, Visus C, Szajnik M, Szczepanski MJ, Storkus WJ, Whiteside TL. Tumor-derived microvesicles promote regulatory T cell expansion and induce apoptosis in tumor-reactive activated CD8+ T lymphocytes. Journal of immunology (Baltimore, Md : 1950). 2009;183(6):3720-30.

34. Guo Y, Zhang H, Xing X, Wang L, Zhang J, Yan L, et al. Gelsolin regulates proliferation, apoptosis and invasion in natural killer/T-cell lymphoma cells. Biology open. 2018;7(1).

35. Matanes E, Gotlieb WH. Immunotherapy of gynecological cancers. Best Pract Res Clin Obstet Gynaecol. 2019.

36. Doo DW, Norian LA, Arend RC. Checkpoint inhibitors in ovarian cancer: A review of preclinical data. Gynecol Oncol Rep. 2019;29:48-54.

37. Ghisoni E, Imbimbo M, Zimmermann S, Valabrega G. Ovarian Cancer Immunotherapy: Turning up the Heat. International journal of molecular sciences. 2019;20(12).

38. Zepeta-Flores N, Valverde M, Lopez-Saavedra A, Rojas E. Glutathione depletion triggers actin cytoskeleton changes via actin-binding proteins. Genet Mol Biol. 2018;41(2):475-87.

39. Kavanagh JJ, Gershenson DM, Choi H, Lewis L, Patel K, Brown GL, et al. Multi-institutional phase 2 study of TLK286 (TELCYTA, a glutathione S-transferase P1-1 activated glutathione analog prodrug) in patients with platinum and paclitaxel refractory or resistant ovarian cancer. International journal of gynecological cancer : official journal of the International Gynecological Cancer Society. 2005;15(4):593-600.

40. Kirkpatrick DL, Powis G. Clinically Evaluated Cancer Drugs Inhibiting Redox Signaling. Antioxid Redox Signal. 2017;26(6):262-73.

Chapter 5

1. Tsibulak I, Zeimet AG, Marth C. Hopes and failures in front-line ovarian cancer therapy. Critical reviews in oncology/hematology. 2019;143:14-9.

2. Release notice - Canadian Cancer Statistics 2019. Health Promot Chronic Dis Prev Can. 2019;39(8-9):255.

3. Torre LA, Trabert B, DeSantis CE, Miller KD, Samimi G, Runowicz CD, et al. Ovarian cancer statistics, 2018. CA: a cancer journal for clinicians. 2018;68(4):284-96.

4. Bonaventura P, Shekarian T, Alcazer V, Valladeau-Guilemond J, Valsesia-Wittmann S, Amigorena S, et al. Cold Tumors: A Therapeutic Challenge for Immunotherapy. Front Immunol. 2019;10:168.

5. Doo DW, Norian LA, Arend RC. Checkpoint inhibitors in ovarian cancer: A review of preclinical data. Gynecol Oncol Rep. 2019;29:48-54.

6. Ghisoni E, Imbimbo M, Zimmermann S, Valabrega G. Ovarian Cancer Immunotherapy: Turning up the Heat. International journal of molecular sciences. 2019;20(12).

7. Matanes E, Gotlieb WH. Immunotherapy of gynecological cancers. Best Pract Res Clin Obstet Gynaecol. 2019.

8. Takaishi K, Komohara Y, Tashiro H, Ohtake H, Nakagawa T, Katabuchi H, et al. Involvement of M2-polarized macrophages in the ascites from advanced epithelial ovarian carcinoma in tumor progression via Stat3 activation. Cancer Sci. 2010;101(10):2128-36.

9. Mantovani A, Sozzani S, Locati M, Allavena P, Sica A. Macrophage polarization: tumor-associated macrophages as a paradigm for polarized M2 mononuclear phagocytes. Trends in immunology. 2002;23(11):549-55.

10. Drakes ML, Stiff PJ. Regulation of Ovarian Cancer Prognosis by Immune Cells in the Tumor Microenvironment. Cancers. 2018;10(9).

11. Gupta V, Yull F, Khabele D. Bipolar Tumor-Associated Macrophages in Ovarian Cancer as Targets for Therapy. Cancers. 2018;10(10).

12. Wang HC, Chen CW, Yang CL, Tsai IM, Hou YC, Chen CJ, et al. Tumor-Associated Macrophages Promote Epigenetic Silencing of Gelsolin through DNA Methyltransferase 1 in Gastric Cancer Cells. Cancer Immunol Res. 2017;5(10):885-97.

13. Lolo FN, Rius C, Casas-Tinto S. Elimination of classically-activated macrophages in tumor-conditioned medium by alternatively-activated macrophages. Biol Open. 2017;6(12):1897-903.

14. Ying X, Wu Q, Wu X, Zhu Q, Wang X, Jiang L, et al. Epithelial ovarian cancer-secreted exosomal miR-222-3p induces polarization of tumor-associated macrophages. Oncotarget. 2016;7(28):43076-87.

15. Tang M, Liu B, Bu X, Zhao P. Cross-talk between ovarian cancer cells and macrophages through periostin promotes macrophage recruitment. Cancer science. 2018;109(5):1309-18.

16. Feldt J, Schicht M, Garreis F, Welss J, Schneider UW, Paulsen F. Structure, regulation and related diseases of the actin-binding protein gelsolin. Expert reviews in molecular medicine. 2019;20:e7.

17. Sun HQ, Yamamoto M, Mejillano M, Yin HL. Gelsolin, a multifunctional actin regulatory protein. The Journal of biological chemistry. 1999;274(47):33179-82.

18. Spinardi L, Witke W. Gelsolin and diseases. Sub-cellular biochemistry. 2007;45:55-69.

19. Asare-Werehene M, Nakka K, Reunov A, Chiu CT, Lee WT, Abedini MR, et al. The exosome-mediated autocrine and paracrine actions of plasma gelsolin in ovarian cancer chemoresistance. Oncogene. 2019.

20. Roma-Rodrigues C, Fernandes AR, Baptista PV. Exosome in tumour microenvironment: overview of the crosstalk between normal and cancer cells. BioMed research international. 2014;2014:179486.

21. Chen Z, Li K, Yin X, Li H, Li Y, Zhang Q, et al. Lower Expression of Gelsolin in Colon Cancer and Its Diagnostic Value in Colon Cancer Patients. Journal of Cancer. 2019;10(5):1288-96.

22. Chen CC, Chiou SH, Yang CL, Chow KC, Lin TY, Chang HW, et al. Secreted gelsolin desensitizes and induces apoptosis of infiltrated lymphocytes in prostate cancer. Oncotarget. 2017;8(44):77152-67.

23. Xu Y, Zhang Y, Wang L, Zhao R, Qiao Y, Han D, et al. miR-200a targets Gelsolin: A novel mechanism regulating secretion of microvesicles in hepatocellular carcinoma cells. Oncology reports. 2017;37(5):2711-9.

24. Abedini MR, Wang PW, Huang YF, Cao M, Chou CY, Shieh DB, et al. Cell fate regulation by gelsolin in human gynecologic cancers. Proceedings of the National Academy of Sciences of the United States of America. 2014;111(40):14442-7.

25. Wang PW, Abedini MR, Yang LX, Ding AA, Figeys D, Chang JY, et al. Gelsolin regulates cisplatin sensitivity in human head-and-neck cancer. International journal of cancer Journal international du cancer. 2014;135(12):2760-9.

26. Asare-Werehene M, Communal L, Carmona E, Le T, Provencher D, Mes-Masson AM, et al. Pre-operative Circulating Plasma Gelsolin Predicts Residual Disease and Detects Early Stage Ovarian Cancer. Sci Rep. 2019;9(1):13924.

27. Yoshida Y, Kurokawa T, Horiuchi Y, Sawamura Y, Shinagawa A, Kotsuji F. Localisation of phosphorylated mTOR expression is critical to tumour progression and outcomes

in patients with endometrial cancer. European journal of cancer (Oxford, England : 1990). 2010;46(18):3445-52.

28. Provencher DM, Lounis H, Champoux L, Tetrault M, Manderson EN, Wang JC, et al. Characterization of four novel epithelial ovarian cancer cell lines. In Vitro Cell Dev Biol Anim. 2000;36(6):357-61.

29. Letourneau IJ, Quinn MC, Wang LL, Portelance L, Caceres KY, Cyr L, et al. Derivation and characterization of matched cell lines from primary and recurrent serous ovarian cancer. BMC cancer. 2012;12:379.

30. Ali AY, Abedini MR, Tsang BK. The oncogenic phosphatase PPM1D confers cisplatin resistance in ovarian carcinoma cells by attenuating checkpoint kinase 1 and p53 activation. Oncogene. 2012;31(17):2175-86.

31. Abedini MR, Muller EJ, Bergeron R, Gray DA, Tsang BK. Akt promotes chemoresistance in human ovarian cancer cells by modulating cisplatin-induced, p53-dependent ubiquitination of FLICE-like inhibitory protein. Oncogene. 2010;29(1):11-25.

32. Yang X, Fraser M, Moll UM, Basak A, Tsang BK. Akt-mediated cisplatin resistance in ovarian cancer: modulation of p53 action on caspase-dependent mitochondrial death pathway. Cancer research. 2006;66(6):3126-36.

33. Abedini MR, Qiu Q, Yan X, Tsang BK. Possible role of FLICE-like inhibitory protein (FLIP) in chemoresistant ovarian cancer cells in vitro. Oncogene. 2004;23(42):6997-7004.

34. Diskin C, Palsson-McDermott EM. Metabolic Modulation in Macrophage Effector Function. Front Immunol. 2018;9:270.

35. Gordon S, Pluddemann A, Martinez Estrada F. Macrophage heterogeneity in tissues: phenotypic diversity and functions. Immunol Rev. 2014;262(1):36-55.

36. Choi BD, Yu X, Castano AP, Bouffard AA, Schmidts A, Larson RC, et al. CAR-T cells secreting BiTEs circumvent antigen escape without detectable toxicity. Nat Biotechnol. 2019.

37. Wang W, Kryczek I, Dostal L, Lin H, Tan L, Zhao L, et al. Effector T Cells Abrogate Stroma-Mediated Chemoresistance in Ovarian Cancer. Cell. 2016;165(5):1092-105.

38. Wei J, Marisetty A, Schrand B, Gabrusiewicz K, Hashimoto Y, Ott M, et al. Osteopontin mediates glioblastoma-associated macrophage infiltration and is a potential therapeutic target. The Journal of clinical investigation. 2019;129(1):137-49.

39. Honkanen TJ, Tikkanen A, Karihtala P, Makinen M, Vayrynen JP, Koivunen JP. Prognostic and predictive role of tumour-associated macrophages in HER2 positive breast cancer. Scientific reports. 2019;9(1):10961.

40. Zhang F, Parayath NN, Ene CI, Stephan SB, Koehne AL, Coon ME, et al. Genetic programming of macrophages to perform anti-tumor functions using targeted mRNA nanocarriers. Nature communications. 2019;10(1):3974.

41. Wang P, Wang H, Huang Q, Peng C, Yao L, Chen H, et al. Exosomes from M1-Polarized Macrophages Enhance Paclitaxel Antitumor Activity by Activating Macrophages-Mediated Inflammation. Theranostics. 2019;9(6):1714-27.

42. Li B, Song TN, Wang FR, Yin C, Li Z, Lin JP, et al. Tumor-derived exosomal HMGB1 promotes esophageal squamous cell carcinoma progression through inducing PD1(+) TAM expansion. Oncogenesis. 2019;8(3):17.

43. Guo Y, Zhang H, Xing X, Wang L, Zhang J, Yan L, et al. Gelsolin regulates proliferation, apoptosis and invasion in natural killer/T-cell lymphoma cells. Biology open. 2018;7(1).

44. Piktel E, Wnorowska U, Ciesluk M, Deptula P, Pogoda K, Misztalewska-Turkowicz I, et al. Inhibition of inflammatory response in human keratinocytes by magnetic nanoparticles functionalized with PBP10 peptide derived from the PIP2-binding site of human plasma gelsolin. J Nanobiotechnology. 2019;17(1):22.

45. Cheng Y, Hu X, Liu C, Chen M, Wang J, Wang M, et al. Gelsolin Inhibits the Inflammatory Process Induced by LPS. Cell Physiol Biochem. 2017;41(1):205-12.

46. Gupta AK, Parasar D, Sagar A, Choudhary V, Chopra BS, Garg R, et al. Analgesic and Anti-Inflammatory Properties of Gelsolin in Acetic Acid Induced Writhing, Tail Immersion and Carrageenan Induced Paw Edema in Mice. PLoS One. 2015;10(9):e0135558.

Chapter 6

1. Ferlay J, Soerjomataram I, Dikshit R, et al. Cancer incidence and mortality worldwide: sources, methods and major patterns in GLOBOCAN 2012. *International journal of cancer Journal international du cancer.* 2015;136(5):E359-386.
2. Armstrong DK, Bundy B, Wenzel L, et al. Intraperitoneal cisplatin and paclitaxel in ovarian cancer. *N Engl J Med.* 2006;354(1):34-43.
3. Stefanou DT, Bamias A, Episkopou H, et al. Aberrant DNA damage response pathways may predict the outcome of platinum chemotherapy in ovarian cancer. *PLoS One.* 2015;10(2):e0117654.
4. Siegel RL, Miller KD, Jemal A. Cancer statistics, 2015. *CA: a cancer journal for clinicians.* 2015;65(1):5-29.
5. Nossov V, Amneus M, Su F, et al. The early detection of ovarian cancer: from traditional methods to proteomics. Can we really do better than serum CA-125? *American journal of obstetrics and gynecology.* 2008;199(3):215-223.
6. Clarke-Pearson DL. Clinical practice. Screening for ovarian cancer. *The New England journal of medicine.* 2009;361(2):170-177.
7. Coticchia CM, Yang J, Moses MA. Ovarian cancer biomarkers: current options and future promise. *Journal of the National Comprehensive Cancer Network : JNCCN.* 2008;6(8):795-802.
8. Moore RG, McMeekin DS, Brown AK, et al. A novel multiple marker bioassay utilizing HE4 and CA125 for the prediction of ovarian cancer in patients with a pelvic mass. *Gynecologic oncology.* 2009;112(1):40-46.

9. Coleman RL, Herzog TJ, Chan DW, et al. Validation of a second-generation multivariate index assay for malignancy risk of adnexal masses. *American journal of obstetrics and gynecology.* 2016;215(1):82.e81-82.e11.

10. Ueland FR, Desimone CP, Seamon LG, et al. Effectiveness of a multivariate index assay in the preoperative assessment of ovarian tumors. *Obstetrics and gynecology.* 2011;117(6):1289-1297.

11. Elias KM, Guo J, Bast RC, Jr. Early Detection of Ovarian Cancer. *Hematology/oncology clinics of North America.* 2018;32(6):903-914.

12. Chung YW, Bae HS, Song JY, et al. Detection of microRNA as novel biomarkers of epithelial ovarian cancer from the serum of ovarian cancer patients. *International journal of gynecological cancer : official journal of the International Gynecological Cancer Society.* 2013;23(4):673-679.

13. Taylor DD, Gercel-Taylor C. MicroRNA signatures of tumor-derived exosomes as diagnostic biomarkers of ovarian cancer. *Gynecologic oncology.* 2008;110(1):13-21.

14. Ueda Y, Enomoto T, Kimura T, Miyatake T, Yoshino K, Fujita M. Serum biomarkers for early detection of gynecologic cancers. *Cancers.* 2010;2(2):1312-1327.

15. Bristow RE, Tomacruz RS, Armstrong DK, Trimble EL, Montz FJ. Survival effect of maximal cytoreductive surgery for advanced ovarian carcinoma during the platinum era: a meta-analysis. *Journal of clinical oncology : official journal of the American Society of Clinical Oncology.* 2002;20(5):1248-1259.

16. Elattar A, Bryant A, Winter-Roach BA, Hatem M, Naik R. Optimal primary surgical treatment for advanced epithelial ovarian cancer. *The Cochrane database of systematic reviews.* 2011(8):Cd007565.

17. Chang SJ, Bristow RE. Evolution of surgical treatment paradigms for advanced-stage ovarian cancer: redefining 'optimal' residual disease. *Gynecologic oncology.* 2012;125(2):483-492.

18. Soletormos G, Duffy MJ, Othman Abu Hassan S, et al. Clinical Use of Cancer Biomarkers in Epithelial Ovarian Cancer: Updated Guidelines From the European Group on Tumor Markers. *International journal of gynecological cancer : official journal of the International Gynecological Cancer Society.* 2016;26(1):43-51.

19. Bast RC, Jr., Xu FJ, Yu YH, Barnhill S, Zhang Z, Mills GB. CA 125: the past and the future. *The International journal of biological markers.* 1998;13(4):179-187.

20. Tuxen MK, Soletormos G, Dombernowsky P. Serum tumor marker CA 125 for monitoring ovarian cancer during follow-up. *Scandinavian journal of clinical and laboratory investigation.* 2002;62(3):177-188.

21. Tuxen MK, Soletormos G, Dombernowsky P. Tumor markers in the management of patients with ovarian cancer. *Cancer treatment reviews.* 1995;21(3):215-245.

22. Spinardi L, Witke W. Gelsolin and diseases. *Sub-cellular biochemistry.* 2007;45:55-69.

23. Sun HQ, Yamamoto M, Mejillano M, Yin HL. Gelsolin, a multifunctional actin regulatory protein. *The Journal of biological chemistry.* 1999;274(47):33179-33182.

24. Kwiatkowski DJ, Stossel TP, Orkin SH, Mole JE, Colten HR, Yin HL. Plasma and cytoplasmic gelsolins are encoded by a single gene and contain a duplicated actin-binding domain. *Nature.* 1986;323(6087):455-458.

25. Yin HL, Kwiatkowski DJ, Mole JE, Cole FS. Structure and biosynthesis of cytoplasmic and secreted variants of gelsolin. *The Journal of biological chemistry.* 1984;259(8):5271-5276.

26. Abedini MR, Wang PW, Huang YF, et al. Cell fate regulation by gelsolin in human gynecologic cancers. *Proceedings of the National Academy of Sciences of the United States of America.* 2014;111(40):14442-14447.

27. Tsai MH, Wu CC, Peng PH, et al. Identification of secretory gelsolin as a plasma biomarker associated with distant organ metastasis of colorectal cancer. *Journal of molecular medicine (Berlin, Germany).* 2012;90(2):187-200.

28. Kulakowska A, Zajkowska JM, Ciccarelli NJ, Mroczko B, Drozdowski W, Bucki R. Depletion of plasma gelsolin in patients with tick-borne encephalitis and Lyme neuroborreliosis. *Neuro-degenerative diseases.* 2011;8(5):375-380.

29. Guo XC, Luo BY, Li XF, Yang DG, Zheng XN, Zhang K. Plasma gelsolin levels and 1-year mortality after first-ever ischemic stroke. *Journal of critical care.* 2011;26(6):608-612.

30. Smith DB, Janmey PA, Herbert TJ, Lind SE. Quantitative measurement of plasma gelsolin and its incorporation into fibrin clots. *The Journal of laboratory and clinical medicine.* 1987;110(2):189-195.

31. Chen CC, Chiou SH, Yang CL, et al. Secreted gelsolin desensitizes and induces apoptosis of infiltrated lymphocytes in prostate cancer. *Oncotarget.* 2017;8(44):77152-77167.

32. Sorensen SM, Schnack TH, Hogdall C. Impact of residual disease on overall survival in patients with FIGO stage IIIB-IIIC vs. stage IV epithelial ovarian cancer after primary surgery. *Acta obstetricia et gynecologica Scandinavica.* 2018.

33. Nowak M, Janas L, Stachowiak G, Stetkiewicz T, Wilczynski JR. Current clinical application of serum biomarkers to detect ovarian cancer. *Przeglad menopauzalny = Menopause review.* 2015;14(4):254-259.

34. Dupont J, Tanwar MK, Thaler HT, et al. Early detection and prognosis of ovarian cancer using serum YKL-40. *Journal of clinical oncology : official journal of the American Society of Clinical Oncology.* 2004;22(16):3330-3339.

35. Cannistra SA. Cancer of the ovary. *The New England journal of medicine.* 2004;351(24):2519-2529.

36. Gadducci A, Cosio S, Tana R, Genazzani AR. Serum and tissue biomarkers as predictive and prognostic variables in epithelial ovarian cancer. *Critical reviews in oncology/hematology.* 2009;69(1):12-27.

37. Hendrickson MR, Longacre TA, Kempson RL. Clinicopathology of malignant surface epithelial neoplasms of the ovary. *Pathology (Philadelphia, Pa).* 1993;1(2):367-410.

Chapter 7

1. Abedini MR, Wang PW, Huang YF, et al. Cell fate regulation by gelsolin in human gynecologic cancers. *Proceedings of the National Academy of Sciences of the United States of America.* 2014;111(40):14442-14447.
2. Wang PW, Abedini MR, Yang LX, et al. Gelsolin regulates cisplatin sensitivity in human head-and-neck cancer. *International journal of cancer Journal international du cancer.* 2014;135(12):2760-2769.
3. Chen ZY, Wang PW, Shieh DB, Chiu KY, Liou YM. Involvement of gelsolin in TGF-beta 1 induced epithelial to mesenchymal transition in breast cancer cells. *J Biomed Sci.* 2015;22:90.
4. Zeng B, Zhou M, Wu H, Xiong Z. SPP1 promotes ovarian cancer progression via Integrin beta1/FAK/AKT signaling pathway. *OncoTargets and therapy.* 2018;11:1333-1343.
5. Bruney L, Liu Y, Grisoli A, Ravosa MJ, Stack MS. Integrin-linked kinase activity modulates the pro-metastatic behavior of ovarian cancer cells. *Oncotarget.* 2016.
6. Delcommenne M, Tan C, Gray V, Rue L, Woodgett J, Dedhar S. Phosphoinositide-3-OH kinase-dependent regulation of glycogen synthase kinase 3 and protein kinase B/AKT by the integrin-linked kinase. *Proceedings of the National Academy of Sciences of the United States of America.* 1998;95(19):11211-11216.
7. Bohgaki M, Matsumoto M, Atsumi T, et al. Plasma gelsolin facilitates interaction between beta2 glycoprotein I and alpha5beta1 integrin. *Journal of cellular and molecular medicine.* 2011;15(1):141-151.

8. Lind SE, Smith DB, Janmey PA, Stossel TP. Role of plasma gelsolin and the vitamin D-binding protein in clearing actin from the circulation. *The Journal of clinical investigation.* 1986;78(3):736-742.

Chapter 8

1. Release notice - Canadian Cancer Statistics 2019. *Health Promot Chronic Dis Prev Can.* 2019;39(8-9):255.
2. Torre LA, Trabert B, DeSantis CE, et al. Ovarian cancer statistics, 2018. *CA: a cancer journal for clinicians.* 2018;68(4):284-296.
3. Siegel RL, Miller KD, Jemal A. Cancer statistics, 2018. *CA: a cancer journal for clinicians.* 2018;68(1):7-30.
4. Lheureux S, Braunstein M, Oza AM. Epithelial ovarian cancer: Evolution of management in the era of precision medicine. *CA: a cancer journal for clinicians.* 2019;69(4):280-304.
5. Elias KM, Guo J, Bast RC, Jr. Early Detection of Ovarian Cancer. *Hematology/oncology clinics of North America.* 2018;32(6):903-914.
6. Duffy MJ, Bonfrer JM, Kulpa J, et al. CA125 in ovarian cancer: European Group on Tumor Markers guidelines for clinical use. *International journal of gynecological cancer : official journal of the International Gynecological Cancer Society.* 2005;15(5):679-691.
7. Pogge von Strandmann E, Reinartz S, Wager U, Muller R. Tumor-Host Cell Interactions in Ovarian Cancer: Pathways to Therapy Failure. *Trends in cancer.* 2017;3(2):137-148.
8. Gomez-Roman N, Sahasrabudhe NM, McGregor F, Chalmers AJ, Cassidy J, Plumb J. Hypoxia-inducible factor 1 alpha is required for the tumourigenic and aggressive phenotype associated with Rab25 expression in ovarian cancer. *Oncotarget.* 2016;7(16):22650-22664.
9. Nunes SC, Serpa J. Glutathione in Ovarian Cancer: A Double-Edged Sword. *International journal of molecular sciences.* 2018;19(7).

10. Wang PW, Abedini MR, Yang LX, et al. Gelsolin regulates cisplatin sensitivity in human head-and-neck cancer. *International journal of cancer Journal international du cancer.* 2014;135(12):2760-2769.

11. Abedini MR, Wang PW, Huang YF, et al. Cell fate regulation by gelsolin in human gynecologic cancers. *Proceedings of the National Academy of Sciences of the United States of America.* 2014;111(40):14442-14447.

12. Yang X, Fraser M, Moll UM, Basak A, Tsang BK. Akt-mediated cisplatin resistance in ovarian cancer: modulation of p53 action on caspase-dependent mitochondrial death pathway. *Cancer research.* 2006;66(6):3126-3136.

13. Drakes ML, Stiff PJ. Regulation of Ovarian Cancer Prognosis by Immune Cells in the Tumor Microenvironment. *Cancers.* 2018;10(9).

14. Ghisoni E, Imbimbo M, Zimmermann S, Valabrega G. Ovarian Cancer Immunotherapy: Turning up the Heat. *International journal of molecular sciences.* 2019;20(12).

15. McCloskey CW, Rodriguez GM, Galpin KJC, Vanderhyden BC. Ovarian Cancer Immunotherapy: Preclinical Models and Emerging Therapeutics. *Cancers.* 2018;10(8).

16. Feldt J, Schicht M, Garreis F, Welss J, Schneider UW, Paulsen F. Structure, regulation and related diseases of the actin-binding protein gelsolin. *Expert reviews in molecular medicine.* 2019;20:e7.

17. Yin HL, Kwiatkowski DJ, Mole JE, Cole FS. Structure and biosynthesis of cytoplasmic and secreted variants of gelsolin. *The Journal of biological chemistry.* 1984;259(8):5271-5276.

18. Piktel E, Levental I, Durnas B, Janmey PA, Bucki R. Plasma Gelsolin: Indicator of Inflammation and Its Potential as a Diagnostic Tool and Therapeutic Target. *International journal of molecular sciences.* 2018;19(9).

19. Chen Z, Li K, Yin X, et al. Lower Expression of Gelsolin in Colon Cancer and Its Diagnostic Value in Colon Cancer Patients. *Journal of Cancer.* 2019;10(5):1288-1296.

20. Chen CC, Chiou SH, Yang CL, et al. Secreted gelsolin desensitizes and induces apoptosis of infiltrated lymphocytes in prostate cancer. *Oncotarget.* 2017;8(44):77152-77167.

21. Wang HC, Chen CW, Yang CL, et al. Tumor-Associated Macrophages Promote Epigenetic Silencing of Gelsolin through DNA Methyltransferase 1 in Gastric Cancer Cells. *Cancer Immunol Res.* 2017;5(10):885-897.

22. Bansal A, Simon MC. Glutathione metabolism in cancer progression and treatment resistance. *The Journal of cell biology.* 2018;217(7):2291-2298.

23. Li M, Cui F, Cheng Y, et al. Gelsolin: role of a functional protein in mitigating radiation injury. *Cell biochemistry and biophysics.* 2015;71(1):389-396.

24. Wang W, Kryczek I, Dostal L, et al. Effector T Cells Abrogate Stroma-Mediated Chemoresistance in Ovarian Cancer. *Cell.* 2016;165(5):1092-1105.

25. Ma X, Sun W, Shen J, et al. Gelsolin promotes cell growth and invasion through the upregulation of p-AKT and p-P38 pathway in osteosarcoma. *Tumour biology : the journal of the International Society for Oncodevelopmental Biology and Medicine.* 2016;37(6):7165-7174.

26. Sodek KL, Murphy KJ, Brown TJ, Ringuette MJ. Cell-cell and cell-matrix dynamics in intraperitoneal cancer metastasis. *Cancer metastasis reviews.* 2012;31(1-2):397-414.

27. Brahmer JR, Tykodi SS, Chow LQ, et al. Safety and activity of anti-PD-L1 antibody in patients with advanced cancer. *The New England journal of medicine.* 2012;366(26):2455-2465.

28. Sunshine J, Taube JM. PD-1/PD-L1 inhibitors. *Current opinion in pharmacology.* 2015;23:32-38.

29. Hodi FS, Lee S, McDermott DF, et al. Ipilimumab plus sargramostim vs ipilimumab alone for treatment of metastatic melanoma: a randomized clinical trial. *Jama.* 2014;312(17):1744-1753.

30. Pedersen M, Westergaard MCW, Milne K, et al. Adoptive cell therapy with tumor-infiltrating lymphocytes in patients with metastatic ovarian cancer: a pilot study. *Oncoimmunology.* 2018;7(12):e1502905.

31. Fujiwara K, McAlpine JN, Lheureux S, Matsumura N, Oza AM. Paradigm Shift in the Management Strategy for Epithelial Ovarian Cancer. *Am Soc Clin Oncol Educ Book.* 2016;35:e247-257.

32. Turner TB, Buchsbaum DJ, Straughn JM, Jr., Randall TD, Arend RC. Ovarian cancer and the immune system - The role of targeted therapies. *Gynecologic oncology.* 2016;142(2):349-356.

33. Santoiemma PP, Powell DJ, Jr. Tumor infiltrating lymphocytes in ovarian cancer. *Cancer biology & therapy.* 2015;16(6):807-820.

34. Matanes E, Gotlieb WH. Immunotherapy of gynecological cancers. *Best Pract Res Clin Obstet Gynaecol.* 2019.

35. Fujita K, Ikarashi H, Takakuwa K, et al. Prolonged disease-free period in patients with advanced epithelial ovarian cancer after adoptive transfer of tumor-infiltrating

lymphocytes. *Clinical cancer research : an official journal of the American Association for Cancer Research.* 1995;1(5):501-507.

36. Bourne TH, Hampson J, Reynolds K, Collins WP, Campbell S. Screening for early ovarian cancer. *British journal of hospital medicine.* 1992;48(8):454-459.

37. Jelovac D, Armstrong DK. Recent progress in the diagnosis and treatment of ovarian cancer. *CA: a cancer journal for clinicians.* 2011;61(3):183-203.

38. Coticchia CM, Yang J, Moses MA. Ovarian cancer biomarkers: current options and future promise. *Journal of the National Comprehensive Cancer Network : JNCCN.* 2008;6(8):795-802.

39. van Nagell JR, Jr., DePriest PD, Reedy MB, et al. The efficacy of transvaginal sonographic screening in asymptomatic women at risk for ovarian cancer. *Gynecologic oncology.* 2000;77(3):350-356.

40. Soletormos G, Duffy MJ, Othman Abu Hassan S, et al. Clinical Use of Cancer Biomarkers in Epithelial Ovarian Cancer: Updated Guidelines From the European Group on Tumor Markers. *International journal of gynecological cancer : official journal of the International Gynecological Cancer Society.* 2016;26(1):43-51.

41. Moore RG, McMeekin DS, Brown AK, et al. A novel multiple marker bioassay utilizing HE4 and CA125 for the prediction of ovarian cancer in patients with a pelvic mass. *Gynecologic oncology.* 2009;112(1):40-46.

42. Gadducci A, Cosio S, Tana R, Genazzani AR. Serum and tissue biomarkers as predictive and prognostic variables in epithelial ovarian cancer. *Critical reviews in oncology/hematology.* 2009;69(1):12-27.

43. Lind SE, Smith DB, Janmey PA, Stossel TP. Role of plasma gelsolin and the vitamin D-binding protein in clearing actin from the circulation. *The Journal of clinical investigation.* 1986;78(3):736-742.

44. Zeng B, Zhou M, Wu H, Xiong Z. SPP1 promotes ovarian cancer progression via Integrin beta1/FAK/AKT signaling pathway. *OncoTargets and therapy.* 2018;11:1333-1343.

45. Kroeger PT, Jr., Drapkin R. Pathogenesis and heterogeneity of ovarian cancer. *Curr Opin Obstet Gynecol.* 2017;29(1):26-34.

Chapter 9

1. Tentler JJ, Tan AC, Weekes CD, et al. Patient-derived tumour xenografts as models for oncology drug development. *Nat Rev Clin Oncol.* 2012;9(6):338-350.
2. Topp MD, Hartley L, Cook M, et al. Molecular correlates of platinum response in human high-grade serous ovarian cancer patient-derived xenografts. *Mol Oncol.* 2014;8(3):656-668.
3. Hutchinson L, Kirk R. High drug attrition rates--where are we going wrong? *Nat Rev Clin Oncol.* 2011;8(4):189-190.
4. Liu JF, Palakurthi S, Zeng Q, et al. Establishment of Patient-Derived Tumor Xenograft Models of Epithelial Ovarian Cancer for Preclinical Evaluation of Novel Therapeutics. *Clinical cancer research : an official journal of the American Association for Cancer Research.* 2017;23(5):1263-1273.
5. Xu Y, Zhang Y, Wang L, et al. miR-200a targets Gelsolin: A novel mechanism regulating secretion of microvesicles in hepatocellular carcinoma cells. *Oncol Rep.* 2017;37(5):2711-2719.
6. Santoiemma PP, Powell DJ, Jr. Tumor infiltrating lymphocytes in ovarian cancer. *Cancer biology & therapy.* 2015;16(6):807-820.
7. Ghisoni E, Imbimbo M, Zimmermann S, Valabrega G. Ovarian Cancer Immunotherapy: Turning up the Heat. *International journal of molecular sciences.* 2019;20(12).
8. Turner TB, Buchsbaum DJ, Straughn JM, Jr., Randall TD, Arend RC. Ovarian cancer and the immune system - The role of targeted therapies. *Gynecologic oncology.* 2016;142(2):349-356.

9. Engelberth SA, Hempel N, Bergkvist M. Development of nanoscale approaches for ovarian cancer therapeutics and diagnostics. *Critical reviews in oncogenesis.* 2014;19(3-4):281-315.

10. Xiong X, Arvizo RR, Saha S, et al. Sensitization of ovarian cancer cells to cisplatin by gold nanoparticles. *Oncotarget.* 2014;5(15):6453-6465.

11. Abedini MR, Wang PW, Huang YF, et al. Cell fate regulation by gelsolin in human gynecologic cancers. *Proceedings of the National Academy of Sciences of the United States of America.* 2014;111(40):14442-14447.